JSCSEN 75(12)1617–1762(2010)

Journal of the Serbian Chemical Society

VOLUME 75

No 12

BELGRADE 2010

Available on line at

www.shd.org.rs/JSCS/

The full search of JSCS is available through

DOAJ DIRECTORY OF OPEN ACCESS JOURNALS

www.doaj.org

Journal of the Serbian Chemical Society
JSCS-info@shd.org.rs • www.shd.org.rs/JSCS

J. Serb. Chem. Soc. Vol. 75, No. 12 (2010)

CONTENTS

Published by the Serbian Chemical Society
Karnegijeva 4/III, 11000 Belgrade, Serbia
Printed by the Faculty of Technology and Metallurgy
Karnegijeva 4, P.O. Box 35-03, 11120 Belgrade, Serbia

Journal of the Serbian Chemical Society
JSCS-info@shd.org.rs • www.shd.org.rs/JSCS
J. Serb. Chem. Soc. *75* (12) 1617–1623 (2010)
JSCS–4081
UDC 633.888:542.913
Original scientific paper

The total synthesis of cannabisin G

YAMU XIA*, YINGLAN GUO and YANLING WEN

College of Chemical Engineering, Qingdao University of Science and Technology, Qingdao 266042, P. R. China

(Received 26 October 2009, revised 29 June 2010)

Abstract: A convenient method for the synthesis of lignanamide cannabisin G, starting from vanillin, was developed. The convergent synthesis was based on the Stobbe reaction as C–C bond-forming steps to give the skeleton of lignan, which was condensed with a derivative of tyramine to obtain synthetic cannabisin G for the first time.

Keywords: synthesis; lignanamide; stobbe reaction; cannabisin G.

INTRODUCTION

Cannabisin G (**1**) was first isolated from the fruits of *Cannabis sativa* in 1995.[1] *C. sativa* is an annual plant which belongs to the family Cannabaceae from Central Asia.[2] *C. sativa* has been utilized as an anti-asthma, anticonstipation, anthelminthic drug in traditional Chinese medicine, and these uses are still well-rooted in folk medicine today.[3,4] Cannabinoids, flavonoids, stilbenoids, terpenoids, alkaloids and lignanamides are some of the secondary metabolites present in *C. sativa*.[5] Cannabisin G belongs to the lignanamide group and is classified as lignans of the arylnaphthalene derivative type. Natural products of the lignanamide family displayed interesting and diverse biological activities, including feeding deterrent activity and insecticidal effects.[6,7] In 2002, it was first reported that cannabisin G showed cytotoxic activity against human prostate cancer LNCaP cells.[8]

A synthetic approach to the lignanamide family has not hitherto been reported. Herein, full details of the total synthesis of the lignanamide cannabisin G (**1**) are provided.

In the retrosynthetic analysis (Scheme 1), cannabisin G must be developed for the coupling of (*E*,*E*)-**2** with tyramine. The key intermediate (*E*,*E*)-**2** is obtained by the condensation of vanillin with diethyl succinate.

* Corresponding author. E-mail: xiaym@qust.edu.cn
doi: 10.2298/JSC091016128X

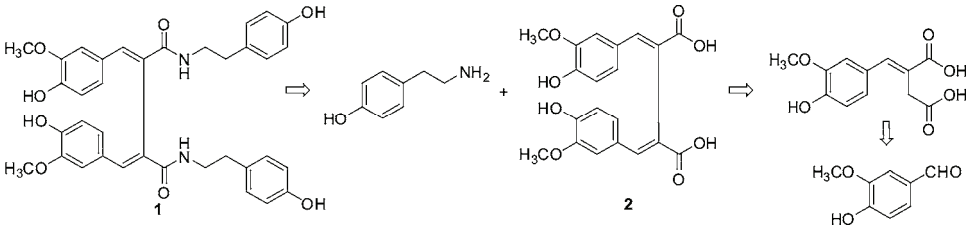

Scheme 1. In the retrosynthetic analysis, cannabisin G must be developed by the coupling of (*E*,*E*)-**2** with tyramine. The key intermediate (*E*,*E*)-**2** was obtained by the condensation of vanillin and diethyl succinate, involving double Stobbe reactions.

As shown in Scheme 2, the synthesis involved the Stobbe reaction to construct the skeleton of lignan (C_6-C_4-C_6), followed by condensation with tyramine to obtain cannabisin G (**1**).

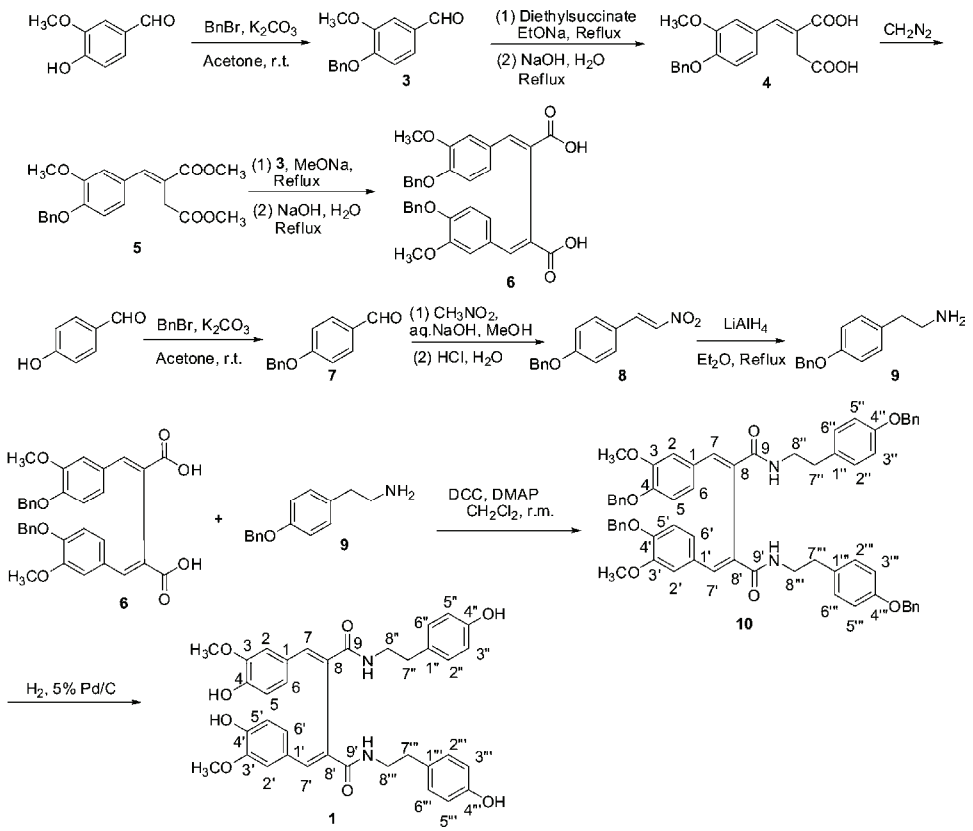

Scheme 2. Reaction scheme for the preparation of cannabisin G starting from vanillin.

EXPERIMENTAL

General

Melting points were taken on a Gallenkamp melting point apparatus and were uncorrected. The infrared spectra were recorded on a Nicolet Nexus 670 FTIR spectrometer. The ^{1}H-NMR and ^{13}C-NMR spectra were recorded on a Bruker AM−500 MHz spectrometer. The mass spectra were recorded on a ZAB−HS spectrometer. HRMS were obtained on a Bruker Daltonics APEXII47e spectrometer. Flash column chromatography was performed on silica gel (200–300 mesh) and TLC inspections on silica gel GF254 plates.

*4-Benzyloxy-3-methoxybenzaldehyde (**3**)*

A mixture of vanillin (60.8 g, 400 mmol), benzyl bromide (68.4 g, 400 mmol) and anhydrous potassium carbonate (55.2 g, 400 mmol) in acetone (200 ml) was stirred overnight at room temperature. The reaction mixture was filtered, and the solvent was removed *in vacuo*. The residue was crystallized from EtOH to give the compound **3** as yellow crystals (92.0 g).

*(E)-2-(4-benzyloxy-3-methoxybenzylidene)succinic acid (**4**)*

Compound **3** (72.6 g, 300 mmol) and diethyl succinate (52.2 g, 300 mmol) were added to a solution of NaOEt (40.8 g, 600 mmol) in EtOH (500 mL). The mixture was heated under N_2 and was refluxed for 4 h, and then the ethanol was removed. The residue was cooled and acidified with HCl (5 mol L^{-1}, 60 ml). This was then extracted with EtOAc (3×70 mL). The EtOAc layer was then re-extracted with saturated $NaHCO_3$ solution (300 mL). Acidification of the aq. $NaHCO_3$ extract with HCl (5 mol L^{-1}, 60 ml) provided an oily layer, which was again extracted with EtOAc (3×70 mL). The combined organic layer was dried over $MgSO_4$ and concentrated *in vacuo*. This residue was added to a solution of 20 % aqueous NaOH (500 mL) and refluxed for 3 h. After cooling to room temperature, the mixture was washed with EtOAc (3×70 mL). After decolorizing with active carbon, the mixture was acidified with HCl (5 mol L^{-1}, 60 ml) whereby a white solid was obtained. The crude product was crystallized from EtOH to give the diacid **4** as a yellow crystal (120.0 g).

*(E)-Dimethyl 2-(4-benzyloxy-3-methoxybenzylidene)succinate (**5**)*

The diacid **4** (68.4 g, 200 mmol) was added to an ice-cold solution containing an excess of CH_2N_2 in Et_2O. The mixture was stirred for 12 h, and concentrated *in vacuo*. Flash column chromatography of the residue gave diester **5** as a yellow oil (71.8 g).

*(E,E)-2,3-bis(4-benzyloxy-3-methoxybenzylidene)succinic acid (**6**)*

Diester **5** (37.0 g, 100 mmol) on Stobbe condensation (following the above-mentioned procedure) with compound **3** (24.2 g, 100 mmol) provided a light-yellow solid which was purified by recrystallization from MeOH to yield product **6** (42.5 g).

*4-Benzyloxybenzaldehyde (**7**)*

A mixture of 4-hydroxybenzaldehyde (24.4 g, 200 mmol), benzyl bromide (34.0 g, 200 mmol) and anhydrous potassium carbonate (27.6 g, 200 mmol) in acetone(100 ml) were stirred overnight at room temperature. The reaction mixture was filtered, and the solvent was removed *in vacuo*. The residue was crystallized from EtOH to give the compound **7** as yellow crystals (39.4 g).

*1-Benzyloxy-4-(2-nitroethenyl)benzene (**8**)*

To a mixture of nitromethane (9.2 g, 150 mmol) and compound **7** (31.8 g, 150 mmol) in MeOH (200 mL) was added dropwise sodium hydroxide (8.0 g, 200 mmol) in water (200 mL) under an ice bath. The reaction mixture was stirred for 5 h and then poured into 500 mL of

HCl (2 M) in water. The mixture was filtered and the yellow crystalline mass was washed with water and crystallized from EtOH to give product **8** as yellow crystals (32.1 g).

o-*Benzyltyramine (**9**)*

Compound **8** (12.8 g, 50 mmol) in dry Et_2O was added to the solution of $LiAlH_4$ (5.0 g, 132 mmol) in Et_2O. The mixture was heated at reflux for 4 h under nitrogen. Then the reaction was quenched with ice water and the resulting mixture filtered. The filtrate was dried over anhydrous $MgSO_4$ and concentrated *in vacuo*. Flash column chromatography of the residue gave product **9** (8.8 g).

*Cannabisin G (**1**)*

A solution of compound **6** (2.8 g, 5 mmol) in dry CH_2Cl_2 (20 mL) was added dropwise to a solution of compound **9** (2.3 g, 10 mmol), *N*,*N*'-dicyclohexylcarbodiimideline, DCC (2.1 g, 10 mmol), and 4-dimethylaminopyridineline, DMAP (1.3 g, 10 mmol), in dry CH_2Cl_2 (100 mL) at 0 °C for 2 h under nitrogen. After stirring the mixture overnight at room temperature, the reaction mixture was filtrated and the solvent was distilled off. Flash column chromatography (petroleumether: ethyl acetate = 6:1) of the residue gave product **10** (4.2 g).

Product **10** (3.0 g, 3.0 mmol) was dissolved in 50 mL MeOH and stirred under a hydrogen atmosphere (1 atm) for 7 h in the presence of 5 % Pd/C (1.5 g). The reaction mixture was filtered through a pad of celite and then the solvent was removed *in vacuo*. Flash column chromatography (petroleumether: ethyl acetate = 5:1) of the residue gave an amorphous powder cannabisin G (**1**) (1.4 g).

RESULTS AND DISCUSSION

The analytic and spectroscopic data of cannabisin G and the intermediate products are given below.

*4-Benzyloxy-3-methoxybenzaldehyde (**3**)*. Yield: 95 %; m.p. 65–67 °C. IR (KBr, cm^{-1}): 3014, 2845, 1679, 1671, 1587, 1505, 1466, 1385, 1276, 1134, 1032. ^{1}H-NMR (500 MHz, DMSO–d_6, δ / ppm): 3.84 (3H, *s*, OCH_3), 5.16 (2H, *s*, $ArCH_2O$), 6.87–7.54 (8H, *m*, ArH), 9.85 (1H, *s*, ArCHO). EI−MS (*m/z*, (%)): 242 (M^+) (12), 214 (7), 151 (2), 91 (100), 67 (13).

*(*E*)-2-(4-Benzyloxy-3-methoxybenzylidene)succinic acid (**4**)*. Yield: 83 %; m.p. 131–133 °C. IR (KBr, cm^{-1}): 3250, 3060, 2912, 1709, 1615, 1497, 1484. ^{1}H-NMR (500 MHz, $CDCl_3$, δ / ppm): 3.57 (2H, *s*, CH_2), 3.86 (3H, *s*, OCH_3), 5.15 (2H, *s*, $ArCH_2O$), 6.68–7.43 (8H, *m*, ArH), 7.87 (1H, *s*, ArCH=C). EI−MS (*m/z*, (%)): 342 (M^+) (26), 324 (12), 297 (27), 175 (16), 91 (100).

*(*E*)-Dimethyl 2-(4-benzyloxy-3-methoxybenzylidene)succinate (**5**)*. Yield: 97 %; IR (KBr, cm^{-1}): 3080, 2908, 1712 (CH_2**C**$OOCH_3$), 1641 (**C**$OOCH_3$), 1503, 1465. ^{1}H-NMR (500 MHz, $CDCl_3$, δ / ppm): 3.69 (3H, *s*, $COOCH_3$), 3.78 (3H, *s*, $COOCH_3$), 3.83 (3H, *s*, OCH_3), 3.56 (2H, *s*, C**H**$_2COOCH_3$), 5.15 (2H, *s*, $ArCH_2O$), 6.68–7.45 (8H, *m*, ArH), 7.88 (1H, *s*, ArCH=C). EI−MS (*m/z*, (%)): 370 (M^+) (36), 338 (18), 307 (14), 175 (23), 91 (100).

*(*E,E*)-2,3-Bis(4-benzyloxy-3-methoxybenzylidene)succinic acid (**6**)*. Yield: 75 %; m.p. 151–153 °C. IR (KBr, cm^{-1}): 3350, 2900, 1740 (2×**C**$OOCH_3$), 1496, 1241, 1042. ^{1}H-NMR (500 MHz, $CDCl_3$, δ / ppm): 3.78 (6H, *s*, 2×OCH_3), 5.16 (4H, *s*,

2×$ArCH_2O$), 6.79 (2H, *d*, ArH, *J* = 8.5 Hz), 7.07 (2H, *dd*, ArH, *J* = 2.0 and 8.5 Hz), 7.19 (2H, *d*, ArH, *J* = 2.0 Hz), 7.28–7.40 (10H, *m*, ArH), 7.96 (2H, *s*, 2×ArCH=C). ^{13}C-NMR ($CDCl_3$, 125 MHz, δ / ppm): 55.7 (2×OCH_3), 70.7 (2×$ArCH_2$), 112.7, 113.1, 123.3, 124.9, 127.2, 127.3, 128.0, 128.6 (2×ArCH=**C**), 136.4 (2×Ar**C**H=C), 144.2, 149.2, 150.1, 172.7 (2×C=O). EI−MS (*m/z*, (%)): 566 (M^+) (2.1), 549 (4.3), 325 (11), 175 (35), 151 (5.2), 91 (100). HRMS Calcd. for $C_{34}H_{31}O_8$ ($M+H^+$): 567.2014, found: 567.2012.

*4-Benzyloxybenzaldehyde (**7**)*. Yield: 93 %; m.p. 72–74 °C. IR (KBr, cm^{-1}): 3034, 2840, 2739, 1690, 1601, 1570, 1510, 1453, 1321, 1262, 1166, 1021. ^{1}H--NMR (500 MHz, $CDCl_3$, δ / ppm): 5.16 (2H, *s*, $ArCH_2O$), 7.05–7.84 (9H, *m*, ArH), 9.88 (1H, *s*, ArCHO). EI−MS (*m/z*, (%)): 212 (M^+) (17), 182 (0.8), 151 (1.8), 121 (1.5), 91 (100), 65 (12).

*1-Benzyloxy-4-(2-nitroethenyl)benzene (**8**)*. Yield: 84 %; m.p. 113–115 °C. IR (KBr, cm^{-1}): 3110, 3042, 2960, 1635, 1607, 1550, 1510, 1346, 1265, 1164. ^{1}H-NMR (500 MHz, $CDCl_3$, δ / ppm): 5.15 (2H, *s*, $ArCH_2O$), 7.04 (2H, *d*, ArH, *J* = 8.5 Hz), 7.35–7.50 (7H, *m*, ArH), 7.52 (1H, *d*, ArCH=C**H**, *J* = 13.5 Hz), 7.98 (1H, *d*, Ar**H**=CH, *J* = 13.5 Hz). EI−MS (*m/z*, (%)): 255 (M^+) 1.4), 238 (2.5), 226 (3.2), 151 (2.8), 121 (5.3), 91 (100), 65 (7.1).

o-*Benzyltyramine (**9**)*. Yield: 78 %; m.p. 203–206 °C. IR (KBr, cm^{-1}): 3285, 3050, 3025, 2932, 2867, 2586, 1615, 1597, 1518, 1460, 1259, 1030. ^{1}H--NMR (500 MHz, $CDCl_3$, δ / ppm): 2.82–2.85 (2H, *m*, Ar**H**$_2$$CH_2$), 2.94–2.98 (2H, *m*, $ArCH_2$C**H**$_2$), 5.08 (2H, *s*, $ArCH_2O$), 6.95 (2H, *d*, ArH, *J* = 8.5 Hz), 7.18 (2H, *d*, ArH, *J* = 8.5 Hz), 7.31–7.45 (5H, *m*, ArH). ^{13}C-NMR (125 MHz, $CDCl_3$, δ / ppm): 32.5 (Ar**C**H_2CH_2), 39.8 ($ArCH_2$**C**H_2), 69.6 ($ArCH_2O$), 115.4, 128.1, 128.3, 128.9, 129.9, 130.2, 137.6, 157.6. EI−MS (*m/z*, (%)): 227 (M^+) (8.7), 198 (1.2), 151 (4.9), 121 (23.6), 91 (100); HRMS Calcd. for $C_{15}H_{18}NO$ ($M+H^+$): 228.1383, found: 228.1389.

*4,4',4",4"'-tetrabenzyloxy cannabisin G (**10**)*. Yield: 85 %. ^{1}H-NMR (500 MHz, $CDCl_3$, δ / ppm): 2.48 (2H, *dt*, H-7"α, H-7"'α, *J* = 13.5, 7.0 Hz), 2.55 (2H, *dt*, H-7"β, H-7"'β, *J* = 13.5 and 7.0 Hz), 3.28 (2H, *dt*, H-8"α, H-8"'α, *J* = 13.5, 7.0 Hz), 3.52 (2H, *dt*, H-8"β, H-8"'β, *J* = 13.5, 7.0 Hz), 3.78 (6H, *s*, 2×OCH_3), 5.15 (4H, *s*, 2×$ArCH_2$), 5.21 (4H, *s*, 2×$ArCH_2$), 6.51–7.48 (34H, *m*, ArH), 7.96 (2H, *s*, 2×ArCH=C). HRMS Calcd. for $C_{64}H_{64}N_3O_8$ ($M+NH_4^+$): 1002.4688, found: 1002.4683.

*Cannabisin G (**1**)*. Yield: 75 %. IR (KBr, cm^{-1}): 3356, 2910, 1659, 1615, 1517, 1194. ^{1}H-NMR (500 MHz, $CDCl_3$, δ / ppm): 2.43 (2H, *dt*, H-7"α, H-7"'α, *J* = 13.6, 6.5 Hz), 2.51 (2H, *dt*, H-7"β, H-7"'β, *J* = 13.6, 6.5 Hz), 3.25 (2H, *dt*, H--8"α, H-8'"α, *J* = 13.6, 6.5 Hz), 3.50 (2H, *dt*, H-8"β, H-8"'β, *J* = 13.6, 6.5 Hz), 3.75 (6H, *s*, 2×OCH_3), 6.82–7.31 (14H, *m*, ArH), 7.89 (2H, *s*, 2×ArCH=C). ^{13}C--NMR (125 MHz, $CDCl_3$, δ / ppm): 35.6 (C-7", C-7"'), 42.7 (C-8"', C-8"'), 56.8 (2×OCH_3), 113.1, 116.2, 125.4, 127.6, 127.8 (C-8, C-8'), 130.2, 130.7, 140.8 (C-7,

C-7'), 148.3, 149.2, 156.5, 166.8 (C-9, C-9'). EI−MS (*m/z*, (%)): 624 (M^+) (0.2), 339 (18), 337 (9), 151 (23), 91 (100); HRMS Calcd. for $C_{36}H_{40}N_3O_8$ ($M+NH_4^+$): 642.2810, found: 642.2814. The data are consistent with the literature.[1]

As is shown in Scheme 2, vanillin was used as the raw material and the 4-hydroxyl group of vanillin was protected with benzyl chloride to afford product **3**. Compound **3** underwent Stobbe condensation with diethyl succinate in the presence of sodium ethoxide in ethanol to produce compound **4**. The (*E*)-configuration of the olefinic double bond was evident from the appearance of the deshielded vinylic proton at δ 7.87 in its ^{1}H-NMR spectrum.[9] Compound **4** was methylated with diazomethane in diethyl ether to yield the diester **5**. The second Stobbe condensation of **5** with **3** in methanol in the presence of sodium methoxide yielded the key intermediate **6**. The deshielded vinylic proton at δ 7.96 in the ^{1}H-NMR spectrum of **6** indicated the (*E*)-configuration for both olefinic double bonds.[10,11]

4-Hydroxybenzaldehyde was protected with benzyl chloride to give product **7**. Condensation of **7** with nitromethane in the presence of sodium hydroxide gave compound **8**, which was followed by reduction with $LiAlH_4$ to afford intermediate **9**.

The intermediate **6** was condensed with compound **9** in CH_2Cl_2 in the presence of DCC and DMAP, followed by hydrogenolysis with 5 % palladium on charcoal catalyst at room temperature to remove the benzyl group and obtain the target product cannabisin G (**1**). Although it is possible to affect cleavage of the benzyl group in the presence of an olefin, in general, the degree of selectivity is dependent upon the substitution pattern and the level of steric hindrance. Good selectivity was achieved for hydrogenolysis of a benzyl group in the presence of a trisubstituted conjugated olefin.[12]

CONCLUSIONS

In summary, an efficient, high-yielding and convergent synthesis of a lignanamide cannabisin G with an overall yield of 22.3 % was developed. The synthesis was based on the Stobbe reaction for the C–C bond-formation steps to give the skeleton of lignan, which afforded the key intermediate diacid, which was condensed with a derivative of tyramine to obtain the natural product cannabisin G for the first time. The present method is a new avenue for the synthesis of a variety of useful and biologically active lignanamides.

Acknowledgements. This work was supported by Shandong Provincial Natural Science Foundation, China (No. ZR2010HM023) and Specialized Research Foundation for the Doctoral Program of Higher Education, China (No. 20093719120004).

И З В О Д

ТОТАЛНА СИНТЕЗА КАНАБИСИНА G

YAMU XIA, YINGLAN GUO и YANLING WEN

College of Chemical Engineering, Qingdao University of Science and Technology, Qingdao 266042, P. R. China

Развијена је погодна синтеза лигнанамида канабисина G, полазећи од ванилина. Конвергентна синтеза заснива се на Стобеовој реакцији, у којој се формира угљеник–угљеник веза скелета лигнана, који је повезан са дериватом тирамина. Овим поступком први пут је добијен синтетички канабисин G.

(Примљено 26. октобра 2009, ревидирано 29. јуна 2010)

REFERENCES

1. I. Sakakibara, Y. Ikeya, K. Hayashi, M. Okada, M. Maruno, *Phytochemistry* **38** (1995) 1003
2. H. Jiang, X. Li, Y. X. Zhao, D. K. Ferguson, F. Hueber, S. Bera, Y. F. Wang, L. C. Zhao, C. J. Liu, C. S. Li, *J. Ethnopharmacol.* **108** (2006) 414
3. R. Mechoulam, N. K. McCallum, S. Burstein, *Chem. Rev.* **76** (1976) 75
4. G. Appendino, S. Gibbons, A. Giana, A. Pagani, G. Grassi, M. Stavri, E. Smith, M. M. Rahman, *J. Nat. Prod.* **71** (2008) 1427
5. I. J. Flores-Sanchez, R. Verpoorte, *Phytochem. Rev.* **7** (2008) 615
6. L. Lajide, P. Escoubas, J. Mizutani, *Phytochemistry* **40** (1995) 1105
7. E. S. Garcia, P. Azambuja, *Toxicon* **44** (2004) 431
8. C. Y. Ma, W. K. Liu, C. T. Che, *J. Nat. Prod.* **65** (2002) 206
9. J. Liu, N. R. Brooks, *Org. Lett.* **4** (2002) 3521
10. P. K. Datta, C. Yau, T. S. Hooper, B. L. Yvon, J. L. Charlton, *J. Org. Chem.* **66** (2001) 8606
11. H. Miyazaki, H. Ohmizu, T. Ogiku, *Org. Process Res. Dev.* **13** (2009) 760
12. D. Caine, T. L. Smith Jr., *J. Am. Chem. Soc.* **102** (1980) 7568.

Journal of the Serbian Chemical Society
JSCS-info@shd.org.rs • www.shd.org.rs/JSCS
J. Serb. Chem. Soc. 75 (12) 1625–1635 (2010)
JSCS–4082
UDC 547.77+547.857.8+547.852+
547–304.4:66.095.3.095.252
Original scientific paper

Synthesis of new derivatives of 1-(3-aminophenyl)-4-benzoyl--5-phenyl-1*H*-pyrazole-3-carboxylic acid

RAHMI KASIMOGULLARI[1]*, BELMA ZENGIN[1], MAKBULE MADEN[1], SAMET MERT[1] and CAVIT KAZAZ[2]

[1]*Department of Chemistry, Art and Science Faculty, Dumlupinar University, Kutahya and* [2]*Department of Chemistry, Science Faculty, Atatürk University, Erzurum, Turkey*

(Received 18 October, revised 6 December 2010)

Abstract: 1-(3-Aminophenyl)-4-benzoyl-5-phenyl-1*H*-pyrazole-3-carboxylic acid (**1**) was synthesized according to the literature.[1] 2-(3-Aminophenyl)-2,6-dihydro-3,4-diphenyl-7*H*-pyrazolo[3,4-*d*]pyridazin-7-one (**5**) was obtained by the cyclocondensation reaction of **1** with hydrazine hydrate. New pyrazole derivatives of compounds **1** and **5** were synthesized by their reaction with *β*-diketones, *β*-ketoesters, *β*-naphthol, phenol and various other reagents. The structures of the synthesized compounds were characterized by ^{1}H-NMR, ^{13}C-NMR, IR and mass spectroscopy, as well as elemental analysis.

Keywords: pyrazole-3-carboxylic acid; pyridazin; diazonium salts; cyclocondensation.

INTRODUCTION

It is known that pyrazole derivatives having heteroaryl groups attached as substituents exhibit significant biological activity and that some pyrazolo-pyridazine compounds containing heteroaryl groups are used to treat many diseases.[2–4] On the other hand, diazonium salts have been the focus of great interest for a long time since they play a crucial role in organic syntheses and are commercially important coloring agents.[5,6]

Arene diazonium groups not only couple to activated aromatic carbon atoms, but may also undergo coupling reactions with aliphatic compounds containing active methylene groups. The facilitated abstraction of the acidic proton in *β*-diketones and *β*-ketoesters leads to the formation of a resonance stable anion, which can, therefore, behave as a good nucleophile. Thus, the coupling of this anion with aryl diazonium chlorides gives 2-arylazo-hydrazo derivatives, from which azo-hydrazo substituted heterocyclic compounds can be obtained. These

* Corresponding author. E-mail: rahmikasimoglu@hotmail.com
doi: 10.2298/JSC101018135K

compounds play a significant role in the dye industry and, in addition, enable the synthesis of heterocyclic compounds with different biological activities. Hence, these coupling products are among the most investigated groups of compounds.[2,7–9]

Commencing from these facts, an attempt was made to expand the research on the preparation of different derivatives of pyrazole carboxylic acid compounds, which are biologically very important and exhibit pharmaceutical activities.[2,5,7]

RESULTS AND DISCUSSION

In this study, first the diazonium salts from compounds **1** and **5**, which contain aromatic primary amine groups, were prepared *in situ* (Schemes 1 and 2).[2,5,6] For this purpose, compounds **1** and **5** were dissolved in an ethanol–water mixture (50 %) containing sodium acetate and the temperature was kept constant (0–5 °C). Three moles of acid were used per mole of the amine compound in the diazotization reaction.[10,11] In the experiments, different pH ranges were tested and the best yield was observed in the pH range 3.5−4.0.

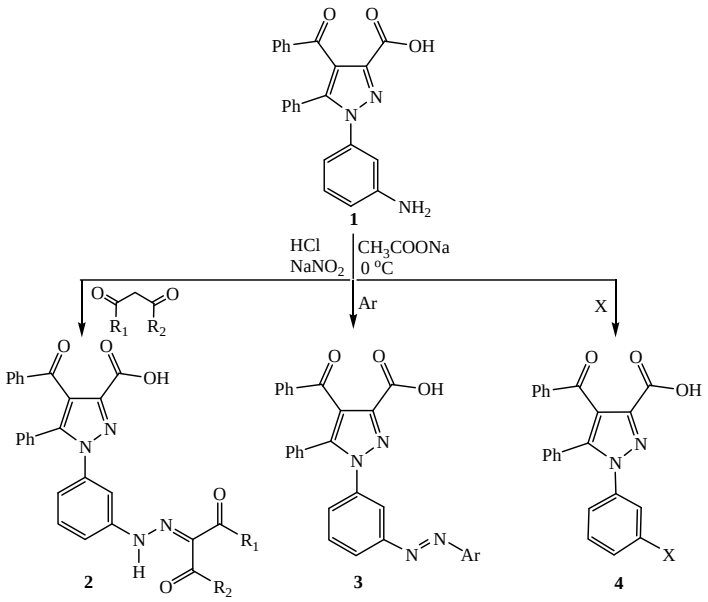

2	R_1	R_2
a	OC_2H_5	C_6H_5
b	CH_3	C_6H_5
c	$OC(CH_3)_3$	CH_3
d	OC_2H_5	CH_3
e	C_6H_5	C_6H_5
f	CH_3	CH_3

3	Ar
a	OH
b	OH

4	X
a	Br
b	CN
c	I
d	OH

Scheme 1. The synthesis of compounds **2a**–**f**, **3a**–**b** and **4a**–**d**.

In this study, as a result of the coupling reactions of **1** with various *β*-dicarbonyl compounds that contained an active aliphatic C–H group, derivatives **2a**–**f** were synthesized in 42−86 % yield. In all these compounds, due to the unpaired electron pairs on the nitrogen atoms, the proton that transferred to the base was subject to resonance. Thus, the products formed may be in the form of azo (–N=N–) or hydrazo (–NH–N=C) tautomeric structures.[12–17] However, in the present study, an examination of the ^{1}H-NMR and IR spectra clearly revealed that the signals belonging to compounds **2a**–**d** at δ 11.90–11.20 ppm and in the range of 3475–3414 cm^{-1} stem from the hydrogen on the nitrogen in the corresponding hydrazo forms (–NH–N=C) (Fig. 1).

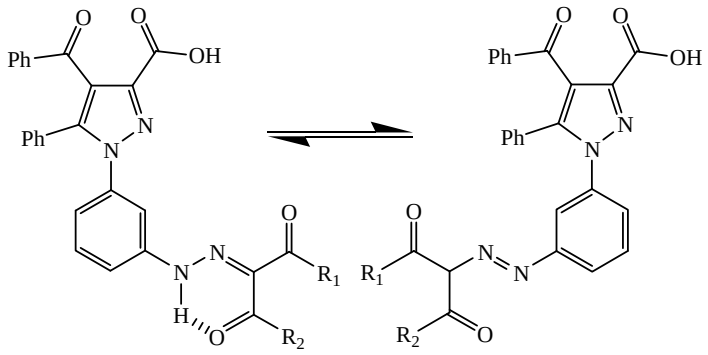

Fig. 1. Possible tautomeric structures for compounds **2a**–**f**.

On reaction of compound **1** with phenol and *β*-naphthol, derivatives **3a** (74 % yield) and **3b** (45% yield) were obtained, respectively. The structures of the compounds were verified by their spectral data (see EXPERIMENTAL). An examination of their resonance structures revealed that although the aryl diazonium ion, bearing partial positive charges on both nitrogen atoms, exhibits weak electrophilic character, it normally formed azo compounds in the diazo coupling reaction with the quite active aromatic compounds phenol and *β*–naphthol, giving the corresponding diazo compounds **3a** and **3b**. The mechanism of coupling reactions is the same as those of electrophilic aromatic replacement reactions. In the first step, the electrophile binds to the carbon of the nucleophilic substrate through a covalent bond and an intermediate product is formed. Subsequently, a proton transfer to the base occurs. In the phenol and *β*-naphthol derivatives, coupling occurs almost exclusively in the para position if the para position is free. If the para position is occupied, then coupling occurs in the ortho position.[18,19]

In the syntheses, the Sandmeyer reaction[20] was employed, in which Cu(I) salts as catalysts together with the potassium salts of Br^- and CN^- were used to obtain derivatives **4a** and **b** in 46 and 88 % yield, respectively.[20] For replacement

by I^-, having a strong nucleophilic character, the KI alone was sufficient without any necessity for a catalyst and thus, compound **4c** was obtained. On heating the diazo compound with H_2O to 100 °C, derivative **4d** was obtained in high yield (85 %). In addition, the cyclocondensation of compound **1** with anhydrous hydrazine hydrate yielded a pyrazolo[3,4-*d*]pyridazin-7-one (**5**).[1,21] During the reaction of intermediary **5** with different *β*-diketones, compounds **6a**–**c** were obtained**.** Derivatives **7a** and **7b** were synthesized by the coupling reactions of **5** with phenol and *β*-naphthol, respectively (Scheme 2).

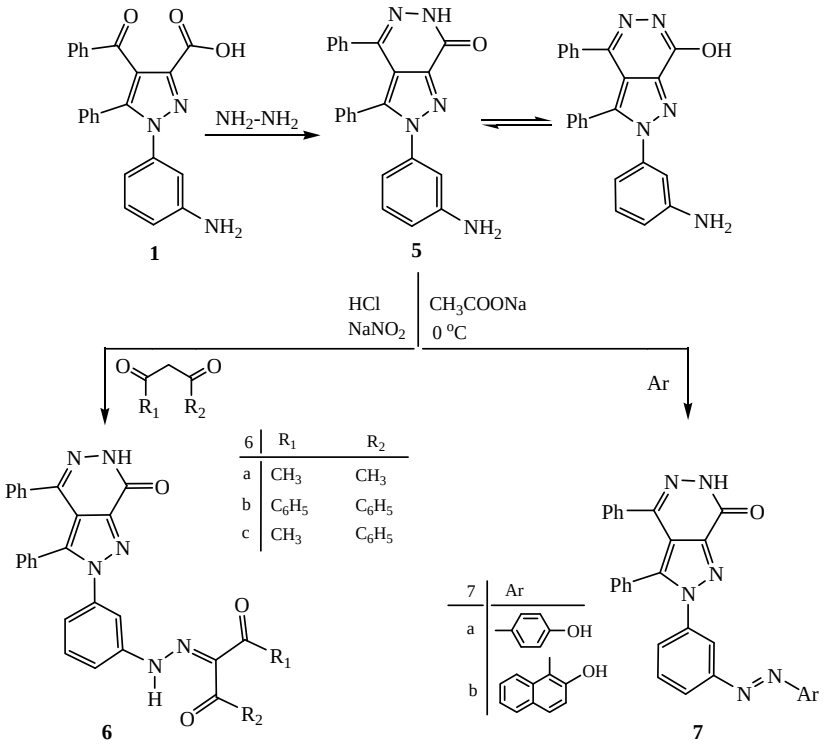

Scheme 2. The synthesis of compounds **6a**–**c** and **7a**–**b**.

The yields, melting points, analytic data and spectral data of the prepared compounds are given below.

*4-Benzoyl-1-(3-(2-(1-benzoyl-2-ethoxy-2-oxoethylidene)hydrazinyl)phenyl)--5-phenyl-1*H*-pyrazole-3-carboxylic acid (**2a**)*. Yield: 42 %; m.p. 147–148 °C. Anal. Calcd. for $C_{34}H_{26}N_4O_6$: C, 69.62; H, 4.47; N, 9.55 %. Found: C, 69.45; H, 4.58; N, 9.50 %. IR (KBr, cm^{-1}): 2500−3500 (COOH), 3060 (Ar CH), 2901 and 2835 (aliphatic CH), 1724 and 1666 (C=O), 1607−1463 (Ar C=C and C=N). ^{1}H-NMR (400 MHz, DMSO–d_6, δ / ppm): 12.70 (1H, *br s*, COOH), 11.90 (1H, *br s*, NH−N=C), 7.20−7.90 (19H, *m*, ArH), 4.30 (2H, *q*, J = 7.1 Hz, OCH_2), 1.30

(3H, *t*, *J* = 7.0 Hz, CH_3). ^{13}C-NMR (100 MHz, DMSO–d_6, δ / ppm): 191.65 and 189.27 (benzoyl C=O), 163.46 (ester C=O), 162.75 (acid C=O), 145.60 (NH−N=C), 142.85 (pyrazole C–3), 61.79 (OCH_2), 14.33 (CH_3), 140.13, 138.34, 137.20, 133.67, 133.08, 130.38, 130.04, 129.83, 129.70, 129.65, 129.57, 129.53, 129.01, 128.96, 128.73, 128.61, 128.36, 128.25, 123.31, 120.35.

*4-Benzoyl-1-(3-(2-(1-benzoyl-2-oxopropylidene)hydrazinyl)phenyl)-5-phenyl-1*H*-pyrazole-3-carboxylic acid (**2b**)*. Yield: 86 %; m.p. 126–128 °C. Anal. Calcd. for $C_{33}H_{24}N_4O_5$: C, 71.21; H, 4.35; N, 10.07 %. Found: C, 69.32; H, 4.65; N, 9.57 %. IR (KBr, cm^{-1}): 2600−3500 (COOH), 3061 (Ar CH), 2950 (aliphatic CH), 1680 and 1665 (C=O), 1601−1461 (Ar C=C and C=N). ^{1}H-NMR (400 MHz, DMSO–d_6, δ / ppm): 13.09 (1H, *br s*, COOH), 11.23 (1H, *br s*, NH−N=C), 6.90−7.90 (19H, *m*, ArH), 2.50 (3H, *s*, CH_3). ^{13}C-NMR (100 MHz, DMSO–d_6, δ / ppm): 196.49 (acetyl C=O), 195.43 and 191.30 (benzoyl C=O), 162.78 (acid C=O), 144.32 (NH−N=C), 143.09 (pyrazole C–3), 25.40 (CH_3), 140.13, 139.97, 138.09, 135.93, 133.93, 130.63, 130.02, 129.81, 129.53, 129.33, 129.21, 129.14, 129.04, 128.98, 128.91, 128.40, 128.28, 127.41, 123.50, 112.19; MS (CI) (*m*/*z*): 557.0 (M+1).

*4-Benzoyl-1-(3-(2-(1-(tert-butoxycaronyl)-2-oxopropylidene)hydrazinyl)phenyl)-5-phenyl-1*H*-pyrazole-3-carboxylic acid (**2c**)*. Yield: 49 %; m.p. 230–231 °C. Anal. Calcd. for $C_{31}H_{28}N_4O_6$: C, 67.38; H, 5.11; N, 10.14 5. Found: C, 67.25; H, 5.15; N, 10.17 %. IR (KBr, cm^{-1}): 2500−3500 (COOH), 3415 (NH), 3059 (Ar CH), 2900 and 2835 (aliphatic CH), 1718 and 1666 (C=O), 1605−1461 (Ar C=C and C=N). ^{1}H-NMR (400 MHz, DMSO–d_6, δ / ppm): 12.70 (1H, *br s*, COOH), 11.20 (1H, *br s*, NH−N=C), 6.90−7.90 (14H, *m*, ArH), 2.60 (9H, *s*, $OC(CH_3)_3$), 1.50 (3H, *s*, CH_3). ^{13}C-NMR (100 MHz, DMSO–d_6, δ / ppm): 195.47 (acetyl C=O), 191.86 (benzoyl C=O), 185.38 (acid C=O), 163.86 (ester C=O), 146.96 (NH−N=C), 145.31 (pyrazole C–3), 82.63 ($O\mathbf{C}(CH_3)_3$), 28.39 ($C(\mathbf{C}H_3)_3$), 21.58 (CH_3), 142.54, 140.18, 138.49, 135.70, 133.52, 130.60, 130.32, 129.97, 129.48, 129.20, 128.95, 128.77, 127.50, 123.19, 121.95, 115.12.

*4-Benzoyl-1-(3-(2-(1-(ethoxycaronyl)-2-oxopropylidene)hydrazinyl)phenyl)-5-phenyl-1*H*-pyrazole-3-carboxylic acid (**2d**)*. Yield: 47 %; m.p. 240–242 °C. Anal. Calcd. for $C_{29}H_{24}N_4O_6$: C, 66.41; H, 4.61; N, 10.68 %. Found: C, 66.29; H, 4.65; N, 10.65 %. IR (KBr, cm^{-1}): 2600−3500 (COOH), 3415 (NH), 3060 (Ar CH), 2883 (aliphatic CH), 1665 (C=O), 1609–1460 (Ar C=C and C=N). ^{1}H-NMR (400 MHz, DMSO–d_6, δ / ppm): 12.80 (1H, *br s*, COOH), 11.60 (1H, *br s*, NH−N=C), 7.80−7.10 (14H, *m*, ArH), 4.30 (2H, *q*, *J* = 7.1 Hz, OCH_2), 2.26 (3H, *s*, CH_3), 1.26 (3H, *t*, *J* = 7.1 Hz, $OCH_2C\mathbf{H}_3$). ^{13}C-NMR (100 MHz, DMSO-d_6, δ / ppm): 195.47 (acetyl C=O), 191.86 (benzoyl C=O), 185.38 (acid C=O), 163.86 (ester C=O), 145.90 (NH−N=C), 144.21 (pyrazole C–3), 60.93 (OCH_2), 24.40 ($O{=}C\mathbf{C}H_3$), 14.20 ($CH_2\mathbf{C}H_3$), 142.35, 139.15, 138.45, 135.50, 134.01, 130.65, 130.40, 130.12, 129.45, 129.32, 128.85, 128.53, 127.60, 123.29, 112.10.

*4-Benzoyl-1-(3-(2-(1-benzoyl-2-oxo-2-phenylethylidene)hydrazinyl)phenyl)-5-phenyl-1*H*-pyrazole-3-carboxylic acid* (***2e***). Yield: 55 %; m.p. 205–206 °C. Anal. Calcd. for $C_{38}H_{26}N_4O_5$: C, 73.78; H, 4.24; N, 9.06 %. Found: C, 73.67; H, 4.30; N, 9.11 %. IR (KBr, cm^{-1}): 2500−3500 (COOH), 3422 (NH), 3059 (Ar CH), 1725 and 1664 (C=O), 1599–1460 (Ar C=C and C=N). ^{1}H-NMR (400 MHz, DMSO–d_6, δ / ppm): 13.70 (1H, *br s*, COOH), 13.20 (1H, *br s*, NH−N=C), 7.75−7.15 (24H, *m*, ArH). ^{13}C-NMR (100 MHz, DMSO–d_6, δ / ppm): 197.46, 196.79 and 191.28 (benzoyl C=O), 162.78 (acid C=O), 143.43 (NH–N=C), 143.21 (pyrazole C–3), 113.60 (pyrazole C–4), 143.12, 142.99, 140.13, 139.96, 138.09, 134.53, 133.94, 130.71, 130.49, 130.11, 130.04, 129.82, 129.57, 129.13, 129.03, 128.97, 128.45, 128.27, 128.18, 123.48, 122.38, 118.30, 116.96.

*1-(3-(2-(1-Acetyl-2-oxo-propylidene)hydrazinyl)phenyl)-4-benzoyl-5-phenyl--1*H*-pyrazole-3-carboxylic acid* (***2f***). Yield: 55 %; m.p. 222–224 °C. Anal. Calcd. for $C_{28}H_{22}N_4O_5$: C, 68.01; H, 4.48; N, 11.33 %. Found: C, 67.89; H, 4.53; N, 11.35 %. IR (KBr, cm^{-1}): 2500−3500 (COOH), 3422 (NH), 3059 (Ar CH), 1725 and 1664 (C=O), 1599−1460 (Ar C=C and C=N); ^{1}H-NMR (400 MHz, DMSO–d_6, δ / ppm): 13.75 (1H, *br s*, COOH), 13.15 (1H, *br s*, NH−N=C), 7.80−7.20 (14H, *m*, ArH), 2.45 and 2.29 (6H, *s*, $2CH_3$). ^{13}C-NMR (100 MHz, DMSO–d_6, δ / ppm): 197.49 and 196.78 (acetyl C=O), 191.25 (benzoyl C=O), 162.70 (acid C=O), 143.43 (NH−N=C), 143.19 (pyrazole C–3), 113.57 (pyrazole C-4), 31.67 and 26.88 (CH_3), 142.99, 140.11, 138.06, 134.59, 133.94, 130.72, 130.02, 129.81, 129.54, 129.13, 129.02, 128.16, 123.48, 122.36, 116.96. MS (CI) (*m*/*z*): 495.0 (M+1).

*4-Benzoyl-1-(3-((4-hydroxyphenyl)diazenyl)phenyl)-5-phenyl-1*H*-pyrazole--3-carboxylic acid* (***3a***). Yield: 74 %; m.p. 286–288 °C. Anal. Calcd. for $C_{29}H_{20}N_4O_4$: C, 71.30; H, 4.13; N, 11.47 %. Found: C, 71.17; H, 4.18; N, 11.45 %. IR (KBr, cm^{-1}): 2700−3600 (COOH), 3416 (NH), 3060 (Ar CH), 1663 (C=O), 1607−1494 (Ar C=C and C=N), 1354 (ArOH); ^{1}H-NMR (400 MHz, DMSO–d_6, δ / ppm): 12.95 (1H, *br s*, COOH), 7.85−7.15 (18H, *m*, ArH), 6.95 (1H, *d*, J = 8.7 Hz, ArOH). ^{13}C-NMR (100 MHz, DMSO–d_6, δ / ppm): 192.38 (benzoyl C=O), 164.92 (acid C=O), 150.13 (C=**C**−OH), 149.50 (Ar**C**−N=N), 145.15 (pyrazole C–3), 96.37 (pyrazole C–4), 143.25, 141.87, 140.34, 138.82, 135.40, 133.24, 130.75, 130.41, 130.15, 129.86, 129.44, 129.18, 128.97, 128.82, 128.40, 122.99, 116.74.

*4-Benzoyl-1-(3-((2-hydroxynaphthalen-1-yl)diazenyl)phenyl)-5-phenyl-1*H*--pyrazole-3-carboxylic acid* (***3b***). Yield: 45 %; m.p. 261–263 °C. Anal. Calcd. for $C_{33}H_{22}N_4O_4$: C, 73.60; H, 4.12; N, 10.40 %. Found: C, 73.48; H, 4.19; N, 10.47 %. IR (KBr, cm^{-1}): 2500−3600 (COOH), 3415 (NH), 3064 (Ar CH), 1665 (C=O), 1609–1493 (Ar C=C and C=N), 1354 (ArOH). ^{1}H-NMR (400 MHz, DMSO–d_6, δ / ppm): 15.54 (1H, *s*, ArOH), 13.30 (1H, *br s*, COOH), 8.26−6.86 (20H, *m*, ArH). ^{13}C-NMR (100 MHz, DMSO–d_6, δ / ppm): 191.27 (benzoyl C=O), 171.37

(acid C=O), 162.77 (Ar**C**−OH), 145.47 (pyrazole C–3), 143.47, 143.37, 141.33, 140.28, 138.12, 133.96, 132.93, 130.87, 130.15, 129.92, 129.90, 129.62, 129.35, 129.33, 129.14, 129.05, 128.31, 128.29, 126.67, 124.63, 124.50, 123.64, 121.99, 119.83, 114.90. MS (CI) (*m*/*z*): 539.0 (M+1).

*4-Benzoyl-1-(3-bromophenyl)-5-phenyl-1*H-*pyrazole-3-carboxylic acid (**4a**)*. Yield: 46 %; m.p. 273–274 °C. Anal. Calcd. for $C_{23}H_{15}BrN_2O_3$: C, 61.76; H, 3.38; N, 6.26 %. Found: C, 61.55; H, 3.45; N, 6.22 %. IR (KBr, cm^{-1}): 2500−3500 (COOH), 3062 (Ar CH), 1666 (C=O), 1611–1448 (Ar C=C and C=N). ^{1}H-NMR (400 MHz, DMSO–d_6, δ / ppm): 13.20 (1H, *br s*, COOH), 7.82––7.21 (14H, *m*, ArH). ^{13}C-NMR (100 MHz, DMSO–d_6, δ / ppm): 190.52 (benzoyl C=O), 165.28 (acid C=O), 144.47 (pyrazole C–3), 142.55, 141.30, 139.67, 138.25, 137.64, 134.06, 130.85, 130.26, 129.60, 129.30, 129.25, 129.08, 126.27, 123.75, 123.40, 122.50.

*4-Benzoyl-1-(3-cyanophenyl)-5-phenyl-1*H-*pyrazole-3-carboxylic acid (**4b**)*. Yield: 88 %; m.p. 255–256 °C. Anal. Calcd. for $C_{24}H_{15}N_3O_3$: C, 73.27; H, 3.84; N, 10.68 %. Found: C, 73.15; H, 3.87; N, 10.74 %. IR (KBr, cm^{-1}): 2800−3600 (COOH), 3061 (Ar CH), 2130 (CN), 1661 (C=O), 1601–1426 (Ar C=C and C=N). ^{1}H-NMR (400 MHz, DMSO–d_6, δ / ppm): 13.80 (1H, *br s*, COOH), 7.95−6.70 (14H, *m*, ArH). ^{13}C-NMR (100 MHz, DMSO–d_6, δ / ppm): 190.52, (benzoyl C=O), 165.35, (acid C=O), 144.48 (pyrazole C–3), 116.13 (CN), 143.25, 141.12, 139.68, 138.82, 137.63, 134.06, 130.53, 130.27, 129.62, 129.30, 129.08, 128.97, 127.88, 126.26, 123.07, 122.92.

*4-Benzoyl-1-(3-iodophenyl)-5-phenyl-1*H-*pyrazole-3-carboxylic acid (**4c**)*. Yield: 70 %; m.p. 265–266 °C. Anal. Calcd. for $C_{23}H_{15}IN_2O_3$: C, 55.89; H, 3.06; N, 5.67 %. Found: C, 55.78; H, 3.11; N, 5.64 %. IR (KBr, cm^{-1}): 2500−3500 (COOH), 3059 (Ar CH), 1664 (C=O), 1608−1427 (Ar C=C and C=N). ^{1}H-NMR (400 MHz, DMSO–d_6, δ / ppm): 13.10 (1H, *br s*, COOH), 7.80−7.17 (14H, *m*, ArH). ^{13}C-NMR (100 MHz, DMSO–d_6, δ / ppm): 191.28 (benzoyl C=O), 162.79 (acid C=O), 143.38 (pyrazole C–3), 95.20 (Ar**C**–I), 139.96, 138.09, 133.92, 130.49, 130.10, 129.80, 129.56, 129.12, 128.97, 128.28, 127.10, 124.95, 123.44, 118.66, 107.62. MS (CI) (*m*/*z*): 495.0 (M+1).

*4-Benzoyl-1-(3-hydroxyphenyl)-5-phenyl-1*H-*pyrazole-3-carboxylic acid (**4d**)*. Yield: 85 %; m.p. 235–237 °C. Anal. Calcd. for $C_{23}H_{16}N_2O_4$: C, 71.87; H, 4.20; N, 7.29 %. Found: C, 71.79; H, 4.26; N, 7.32 %. IR (KBr, cm^{-1}): 2700−3600 (COOH), 3059 (Ar CH), 1665 (C=O), 1607−1428 (Ar C=C and C=N). ^{1}H-NMR (400 MHz, DMSO–d_6, δ / ppm): 12.70 (1H, *br s*, COOH), 10.15 (1H, *br s*, Ar––OH) 7.74−7.15 (14H, *m*, ArH). ^{13}C-NMR (100 MHz, DMSO–d_6, δ / ppm): 190.52 (benzoyl C=O), 165.30 (acid C=O), 152.13 (Ar**C**−OH), 144.48 (pyrazole C–3), 143.22, 139.70, 137.61, 134.07, 130.55, 130.26, 129.89, 129.77, 129.62, 129.08, 128.91, 127.89, 127.41, 123.08, 114.96.

*2-(3-(2-(1-Acetyl-2-oxopropylidene)hydrazinyl)phenyl)-2,6-dihydro-3,4-diphenyl-7*H*-pyrazolo[3,4-*d*]pyridayin-7-one (**6a**)*. Yield: 79 %; m.p. 214–216 °C. Anal. Calcd. for $C_{28}H_{22}N_6O_3$: C, 68.56; H, 4.52; N, 17.13 %. Found: C, 68.39; H, 4.54; N, 17.13 %. IR (KBr, cm^{-1}): 3456 and 3155 (NH), 3021 (Ar–CH), 2969 (aliphatic CH), 1740 (acetyl C=O), 1663 (amide C=O), 1608−1476 (Ar C=C and C=N). ^{1}H-NMR (400 MHz, DMSO–d_6, δ / ppm): 7.31 (1H, *br s*, NH), 7.56−6.92 (14H, *m*, ArH), 2.41 and 2.26 (6H, *s*, $2CH_3$). ^{13}C-NMR (100 MHz, DMSO–d_6, δ / / ppm): 197.67 and 196.95 (tautomeric acetyl C=O), 156.79 (amide C=O), 144.28 (Ar**C**−NH−N), 143.16 (pyrazole C–3), 140.58 (pyrazole C–5), 31.82 and 27.07 (tautomeric CH_3), 134.92, 131.20, 131.17, 129.66, 129.61, 128.96, 128.81, 128.77, 128.52, 128.47, 128.41, 128.38, 128.01, 123.17, 117.37, 117.35, 114.30.

*2-(3-(2-(1-Benzoyl-2-oxo-2-phenylethylidene)hydrazinyl)phenyl)-2,6-dihydro-3,4-diphenyl-7*H*-pyrazolo[3,4-*d*]pyridayin-7-one (**6b**)*. Yield: 88 %; m.p. 234––236 °C. Anal. Calcd. for $C_{38}H_{26}N_6O_3$: C, 74.25; H, 4.26; N, 13.67 %. Found: C, 74.12; H, 4.28; N, 13.65 %. IR (KBr, cm^{-1}): 3461 and 3156 (NH), 3023 (Ar CH), 1740 (benzoyl C=O), 1670 (amide C=O), 1601−1475 (Ar C=C and C=N). ^{1}H-NMR (400 MHz, DMSO–d_6, δ / ppm): 11.60 (1H, *br s*, NH), 8.15−6.82 (24H, *m*, ArH). ^{13}C-NMR (100 MHz, DMSO–d_6, δ / ppm): 186.02 (benzoyl C=O), 156.81 (amide C=O), 144.47 (Ar**C**−NH−N), 144.27 (NH−N=C), 142.78 (pyrazole C–3), 140.88 (pyrazole C–5), 140.32, 135.29, 134.92, 133.69, 133.15, 131.15, 130.76, 130.61, 129.73, 129.61, 129.52, 129.29, 129.17, 128.94, 128.89, 128.79, 128.47, 128.40, 128.31, 128.09, 128.01, 117.37, 93.97.

*2-(3-(2-(1-Benzoyl-2-oxopropylidene)hydrazinyl)phenyl)-2,6-dihydro-3,4-diphenyl-7*H*-pyrazolo[3,4-*d*]pyridayin-7-one (**6c**)*. Yield: 50 %; m.p. 256–257 °C. Anal. Calcd. for $C_{33}H_{24}N_6O_3$: C, 71.73; H, 4.38; N, 15.21 %. Found: C, 71.58; H, 4.41; N, 15.22 %; IR (KBr, cm^{-1}): 3393−3241 (NH), 3067 and 3028 (Ar CH), 1666 (C=O), 1608−1477 (Ar C=C and C=N). ^{1}H-NMR (400 MHz, DMSO–d_6, δ / / ppm): 12.61 (1H, *br s*, NH), 7.45−6.92 (19H, *m*, ArH), 2.47 (3H, *s*, CH_3). ^{13}C--NMR (100 MHz, DMSO–d_6, δ / ppm): 199.50 (acetyl C=O), 188.25 (benzoyl C=O), 156.81 (amide C=O), 144.28 (Ar**C**−NH−N), 142.78 (pyrazole C–3), 140.89 (pyrazole C–5), 20.24 (CH_3), 140.33, 134.92, 131.33, 131.17, 130.77, 130.61, 129.61, 129.43, 129.09, 128.94, 128.78, 128.54, 128.47, 128.41, 128.01, 127.60, 123.86, 122.57, 117.37, 95.27.

*2,6-Dihydro-2-(3-((4-hydroxyphenyl)diazenyl)phenyl)-3,4-diphenyl-7*H*-pyrazolo[3,4-*d*]pyridazin-7-one (**7a**)*. Yield: 68 %; m.p. 278–279 °C. Anal. Calcd. for $C_{29}H_{20}N_6O_2$: C, 71.89; H, 4.16; N, 17.35 %. Found: C, 71.78; H, 4.16; N, 17.37 %. IR (KBr, cm^{-1}): 3622 (OH), 3446−3160 (NH), 3062 and 3024 (Ar CH), 1662 (amide C=O), 1608−1476 (Ar C=C and C=N). ^{1}H-NMR (400 MHz, DMSO–d_6, δ / ppm): 12.54 (1H, *br s*, NH), 10.31 (1H, *s*, OH), 7.84−6.91 (18H, *m*, ArH). ^{13}C-NMR (100 MHz, DMSO–d_6, δ / ppm): 162.28 (Ar**C**−OH), 156.82 (amide C=O), 153.00 and 145.70, (Ar**C**−N=N), 144.29, 142.90, 141.07, 140.39,

134.91, 131.29, 130.55, 129.72, 128.98, 128.82, 128.56, 128.38, 128.18, 128.01, 125.86, 124.35, 119.31, 117.41, 116.74.

*2,6-Dihydro-2-(3-((2-hydroxynaphthalen-1-yl)diazenyl)phenyl)-3,4-diphenyl-7*H*-pyrazolo[3,4-*d*]pyridazin-7-one (**7b**)*. Yield: 70 %; m.p. 234–235 °C. Anal. Calcd. for $C_{33}H_{22}N_6O_2$: C, 74.14; H, 4.15; N, 15.72 %. Found: C, 73.98; H, 4.18; N, 15.73 %. IR (KBr, cm^{-1}): 3362 and 3170 (NH and OH), 3061 and 3027 (Ar CH), 1665 (amide C=O), 1606−1476 (Ar C=C and C=N). ^{1}H-NMR (400 MHz, DMSO–d_6, δ / ppm): 8.25 (1H, *br s*, NH), 5.56−5.23 (1H, *br s*, OH), 7.31−6.90 (20H, *m*, ArH). ^{13}C-NMR (100 MHz, DMSO–d_6, δ / ppm): 156.80 (amide C=O), 156.68 (Ar**C**−OH), 156.59 and 144.09 (Ar**C**−N=N), 142.54 (pyrazole C–3), 140.66 (pyrazole C–5), 140.29, 140.08, 134.80, 134.67, 131.08, 130.94, 130.87, 130.41, 130.15, 129.75, 129.49, 129.41, 129.23, 128.73, 128.58, 128.26, 128.18, 127.81, 121.95, 122.30, 117.15, 116.84, 113.80.

EXPERIMENTAL

The chemical compounds used in this research were of analytical grade purity and the solvents were purified using appropriate purifying agents and distillation. All melting points were measured using a Barnstead Electrothermal 9200 apparatus, and are reported uncorrected. The IR spectra of the compounds in KBr pellets were recorded on a Mattson 1000 FT–IR spectrometer. The ^{1}H-NMR and ^{13}C-NMR spectra were recorded on Bruker DPX–400, (400 MHz), and high performance digital FT–NMR (100 MHz) spectrometers. The mass spectra were obtained using Varian Mat III 80 eV spectrometer. At the end of the each experiment, TLC was performed using DC Alufolien Kieselgel 60F/254 Merck and a Camag TLC device. The elemental analyses were performed on a Leco CHNS–932 instrument.

*General procedure for the syntheses of compounds **2a–f**, **3a,b**, **6a–c** and **7a,b***

To an aqueous solution of sodium acetate (3.0 g, 37 mmol) was added 2 ml HCl and then 1 mmol the required amine compound. Subsequently, ethanol was added until complete dissolution. The prepared solution was cooled to 0 °C on an ice bath. To this solution, a solution of 1.2 mmol $NaNO_2$ in 2 ml water was slowly added taking care that the temperature did not exceed 5 °C. Thus, the diazonium salt solution was prepared.

An aromatic or *β*-dicarbonyl compound (1 mmol) was dissolved in a sufficient amount of ethanol, then cooled and added dropwise into the prepared diazonium salt solution. The resulting colored precipitate was filtered under vacuum and the crude product purified by crystallization from an ethanol–water mixture.

*Synthesis of 4-benzoyl-1-(3-bromophenyl)-5-phenyl-1*H*-pyrazole-3-carboxylic acid (**4a**)*

CuBr solution was prepared according to the procedure given in literature[22] and was slowly added by stirring continuously into the diazonium salt solution of compound **1** (prepared as described in the general procedure). The resulting colored precipitate was filtered and purified by crystallization from ethanol–water mixture (9:1).

*Synthesis of 4-benzoyl-1-(3-cyanophenyl)-5-phenyl-1*H*-pyrazole-3-carboxylic acid (**4b**)*

A CuCN + KCN solution, which had been prepared in accordance with a procedure given in the literature,[22] was cooled to 0 °C and added dropwise under continuous stirring into a diazonium salt solution of compound **1** (prepared as described in the general procedure). Following the addition, the cold mixture is allowed to warm up to room temperature. When

the temperature reached about 15 °C, the formation of nitrogen gas began. Then the solution was placed on a steam bath and heated at 50 °C for 15 min to complete the decomposition. The pH was adjusted to 3–4 and left for 12 h at room temperature; the resulting precipitate was filtered under vacuum and dried. The residue was purified by crystallization from an ethanol–water mixture (8:2).

*Synthesis of 4-benzoyl-1-(3-iodophenyl)-5-phenyl-1*H*-pyrazole-3-carboxylic acid (**4c**)*

KI (0.166 g, 1 mmol) was dissolved in 10 ml water and the solution was cooled to 0 °C. Then, it was added dropwise under continuous stirring into a diazonium salt solution of compound **1**, which had been prepared in accordance with the general procedure. The pH was adjusted to 3–4 and after standing for 12 h at room temperature, the resulting colored precipitate was filtered under vacuum and purified by crystallization from an ethanol–water mixture (8:2).

*Synthesis of 4-benzoyl-1-(3-hydroxyphenyl)-5-phenyl-1*H*-pyrazole-3-carboxylic acid (**4d**)*

A diazonium salt solution of **1** was prepared according to the general procedure. This solution was brought to room temperature and then heated in a steam bath at 100 °C to allow for the release of nitrogen gas (approximately 15 min). Then some more water was added to the mixture and the pH adjusted to 4. The solution was kept for about 24 h. The formed yellow-colored precipitate was collected by filtration and purified by crystallization from an ethanol–water mixture (9:1).

Acknowledgements. This study was funded by The Scientific and Research Council of Turkey (TUBITAK) and Dumlupinar University, Scientific Research and Project Department. In addition, the authors would like to thank the Faculty of Science of Atatürk University, Turkey, for spectral analysis.

ИЗВОД

СИНТЕЗА НОВИХ ДЕРИВАТА 1-(3-АМИНО-ФЕНИЛ)-4-БЕНЗОИЛ-5-ФЕНИЛ-1*H*-ПИРАЗОЛ-3-КАРБОКСИЛНЕ КИСЕЛИНЕ

RAHMI KASIMOGULLARI[1], BELMA ZENGIN[1], MAKBULE MADEN[1], SAMET MERT[1] и CAVIT KAZAZ[2]

[1]*Department of Chemistry, Art and Science Faculty, Dumlupinar University, Kutahya и* [2]*Department of Chemistry, Science Faculty, Atatürk University, Erzurum, Turkey*

Синтеза 4-бензоил-1-(3-аминофенил)-5-фенил-1*H*-пиразол-3-карбоксилне киселине (**1**) извршена је према поступку описаном у литератури.[1] Производ 2-(3-аминофенил)-3,4-дифенил-2*H*-пиразол[3,4-*d*]пиридазин-7(6*H*)-он (**5**) добијен је циклокондензационом реакцијом киселине **1** и хидразин-хидрата. Нови пиразолски деривати добијени су реакцијом **1** и **5** са *β*-дикетонима, *β*-кетоестрима, *β*-нафтолом, фенолом и другим реагенсима. Добијена једињења окарактерисана су ^{1}H-NMR, ^{13}C-NMR, ИСи MS спектрима и микроанализом.

(Примљено 18. октобра, ревидирано 6. децембра 2010)

REFERENCES

1. A. Şener, R. Kasımoğulları, M. K. Şener, I. Bildirici, Y. Akçamur, *J. Heterocycl. Chem*. **39** (2002) 869
2. R. Kasımoğulları, M. Bülbül, H. Günhan, H. Güleryüz, *Bioorg. Med. Chem.* **17** (2009) 3295
3. D. K. Dodiya, A. R. Trivedi, S. H. Jarsania, S. J. Vaghasia, V. H. Shah, *J. Serb. Chem. Soc*. **73** (2008) 683

4. P. T. Chovatia, J. D. Akabari, P. K. Kachhadia, P. D. Zalavadia, H. S. Joshi, *J. Serb. Chem. Soc.* **71** (2007) 713
5. R. Kasımoğulları, M. Bülbül, B. S. Arslan, B. Gökçe, *Eur. J. Med. Chem.* **45** (2010) 4769
6. R. Kumar, Y. C. Joshi, *J. Serb. Chem. Soc.* **73** (2008) 937
7. M. Bülbül, R. Kasımoğulları, Ö. İ. Küfrevioğlu, *J. Enzyme Inhib. Med. Chem.* **23** (2008) 895
8. B. K. Kaymakçıoğlu, S. Rollas, *Farmaco* **57** (2002) 595
9. N. Ergenç, B. Durgun, G. Otuk, *Pharmazie* **47** (1992) 495
10. H. A. J. Schoutissen, *Rec. Trav. Chim. Pays-Bas* **40** (1921) 763
11. G. Çapan, *PhD. Thesis*, *İ.Ü. Sağlık Bil. Enst*, İstanbul, Turkey, 1990, p. 7 (in Turkish)
12. C. J. Lestina, T. H. Regan, *J. Org. Chem.* **34** (1969**)** 1685
13. H. Yashuda, H. Midorikawa, *J. Org. Chem.* **31** (1966) 1722
14. M. F. Abdel Megeed, *Spectrosc. Lett.* **20** (1987) 291
15. L. Antonov, S. Stoyanov, *Dyes Pigm.* **5** (1995) 83
16. H. Zollinger, *Color Chemistry*, Wiley–VCH, New York, 1991, p. 135
17. J. Kelemen, S. Moss, S. Glitsch, *Dyes Pigm.* **5** (1984) 83
18. I. Wawer, V. Koleva, *Magn. Reson. Chem.* **31** (1993) 375
19. A. Lycka, H. Murstroph, *J. Prakt. Chem./Chem-Ztg.* **331** (1989) 11
20. A. R. Katritzky, P. Barczynski, D. L. Ostercamp, *J. Chem. Soc. Perk. Trans. 2* (1987) 1214
21. Y. Akçamur, A. Şener, A. M. İpekoğlu, G. Kollenz, *J. Heterocycl. Chem.* **34** (1997) 221
22. A. I. Vogel, *Vogel's Textbook of Practical Organic Chemistry*, Longman, London, 1989, p. 428.

Journal of the Serbian Chemical Society
JSCS-info@shd.org.rs • www.shd.org.rs/JSCS
J. Serb. Chem. Soc. *75* (12) 1637–1640 (2010)
JSCS–4083
UDC *Kindbergia*+631.445.1:582.32:581.184+543
Short communication

SHORT COMMUNICATION

Preliminary analysis of fatty acid chemistry of *Kindbergia praelonga* and *Kindbergia stokesii* (Brachytheciaceae)

BORIS PEJIN[1]*#, LJUBODRAG VUJISIĆ[2#], MARKO SABOVLJEVIĆ[3], ANETA SABOVLJEVIĆ[3], VELE TEŠEVIĆ[1#] and VLATKA VAJS[2#]

[1]*Department of Organic Chemistry, Faculty of Chemistry, University of Belgrade, Studentski trg 16, 11000 Belgrade* [2]*Center of Chemistry, Institute of Chemistry, Technology and Metallurgy, Njegoševa 12, 11000 Belgrade and* [3]*Institute of Botany and Garden, Faculty of Biology, University of Belgrade, Takovska 43, 11000 Belgrade, Serbia*

(Received 9 February, revised 5 September 2010)

Abstract: Moss species of the family Brachytheciaceae, *Kindbergia praelonga* (Hedw.) Ochyra and *Kindbergia stokesii* (Turn.) Ochyra, were preliminarily analysed for their fatty acid composition with the aim of studying the chemical relationship of these two entities. Fatty acid methyl esters were examined by GC and GC–MS in their methanol extracts. Thirteen fatty acids were identified. It is likely that the mosses are chemically distinguishable and should be treated as separate entities. However, additional chemical constituents of various moss samples, such as phenolic acids, their derivatives and flavonoids, must be also analyzed in order to support the re-examination of the relationship between these two species.

Keywords: bryophytes; mosses; *Kindbergia*; fatty acids; chemotaxonomy.

INTRODUCTION

Kindbergia praelonga (Hedw.) Ochyra (typified by *Hypnum praelongum* Hedw.) and *Kindbergia stokesii* (Turn.) Ochyra (typified by *Hypnum stokesii* Turn.) belong to the subgenus *Oxyrrhynchium*. The latter species is now usually considered as a synonym for or variety of *K. praelonga*. The genus *Kindbergia* Ochyra was recently treated as a separate genus from the *Eurhynchium* Schimp.[1,2] According to Hill *et al.*,[1] in Europe only one species is present within the genus: *K. praelonga* (Hedw.) Ochyra (syn. *Eurhynchium praelongum* (Hedw.) Schimp.). The same authors classified *Eurhynchium praelongum* var. *stokesii* (Turner) Dixon and *Eurhynchium stokesii* (Turner) Schimp. as a syno-

* Corresponding author. E-mail: borispejin@yahoo.com
# Serbian Chemical Society member.
doi: 10.2298/JSC100209129P

nym for *K. praelonga*. These two entities were separated into the genus *Stokesiella* (Kindb.) H. Rob., which was later considered as an incorrect homonym of the algal generic name *Stokesiella* Lemmerm. Ochyra renamed the genus *Kindbergia* Ochyra. Now molecular results support this generic independence.[3]

Worldwide, eleven taxa found at various locations are known, namely *K. africana* (Herz.) Ochyra, *K. altaica* Ignatov, *K. arbuscula* (Broth.) Ochyra, *K. brittoniae* (Grout) Ochyra, *K. dumosa* Mitt., *K. kenyae* (Dix. Ex Tosco & Piovano) O'Schea *et* Ochyra, *K. oedogonium* (C. Müll.) Ochyra, *K. oregana* (Sull.) Ochyra, *K. praelonga*, *K. stokesii* and *K. squarrifolia* Broth. *ex* Iishiba.

The main reason for the repeated nomenclatural confusion and the resulting complications surrounding *Oxyrrhynchium* is that the name *E. praelongum* was widely used with two different meanings. Schimper employed it for *E. hians* (syn. *Hypnum hians*, *Oxyrrhynchium hians* (Hedw.) Loeske) including the conspecific *E. swartzii* Turn. (syn. *Hypnum swartzii* Turn.) and several closely related elements) for varietal synonymy, whereas his *Eurhynchium stokesii* corresponded to *E. praelongum*, or following the recent nomenclature *K. praelonga*. Although many bryologists knew of the problem, frequently the use of the name *E. praelongum*, instead of *E. hians*, continued.[4] Thus, *K. stokesii* was often easily overlooked.

Analyses were performed to test if chemotaxonomy can be helpful in the assignment of the two entity species, *K. praelonga* and *K. stokesii*.

EXPERIMENTAL

Both moss species, which were available as fresh material, were collected in Germany in December 2007: *Kindbergia praelonga* (Hedw.) Ochyra (BEOU4701) in Kologne and *Kindbergia stokesii* (Turn.) Ochyra (BEOU4703) in the surroundings of Bonn. Voucher specimens were deposited in the Herbarium of the Institute of Botany, University of Belgrade, Serbia (bryophyte collection – BEOU).

The moss samples were carefully selected and cleaned from soil and other contaminants. The gametophyte tips were used for the extraction. Air-dried parts of both mosses were ground (1 g) and extracted 3 times with 90 % MeOH for 1 h at room temperature. The extracts were evaporated to dryness and were further transesterified with 5 % H_2SO_4 in MeOH (v/v) for 4 h at 80 °C. The resulting methyl esters of the fatty acids were analysed by comparing their GC-FID chromatograms with the chromatogram of a standard mixture (Supelco 37) obtained under the same conditions, and/or by analysis of GC–MS data using NIST 5 and Wiley 7 libraries.

The GC analyses were performed on an Agilent 7890A GC system equipped with a 5975C MSD and an FID, using a DB-23 column (30 m×0.25 mm×0.25 μm). The injection volume was 1 μL and injector temperature was 220 °C with 10:1 split ratio. The carrier gas was He at a flow rate 0.9 ml min^{-1}, while the column temperature was linearly programmed in the range of 150–240 °C at a rate of 4 °C min^{-1} and held at 240 °C for 10 min. The transfer line was maintained at 240 °C. The FID detector temperature was 300 °C. The EI mass spectra (70 eV) were acquired in the *m*/*z* range 40–500.

RESULTS

For *K. stokesii*, 13 fatty acids were identified (Fig. 1): palmitic acid (C16:0, 25.04 %), arachidonic acid (C20:4,*n*-6, 18.29 %), linolelaidic acid (C18:2,*n*-6*t*, 14.57 %), *α*-linolenic acid (C18:3,*n*-3, 11.13 %), *cis*-5,8,11,14,17-eicosapentaenoic acid (C20:3,*n*-6, 8.94 %), elaidic acid (C18:1,*n*-9*t*, 6.32 %), behenic acid (C22:0, 3.04 %), lignoceric acid (C24:0, 2.90 %), palmitoleic acid (C16:1, 2.76 %), stearic acid (C18:0, 2.31 %), myristic acid (C14:0, 1.31 %), oleic acid (C18:1,*n*-9*c*, 1.30 %) and arachidic acid (C20:0, 1.28 %). *K. praelongum* showed less variety in these constituents: only two fatty acid constituents were found (Fig. 2), palmitic acid (C16:0, 88.58 %) and stearic acid (C18:0, 11.42 %).

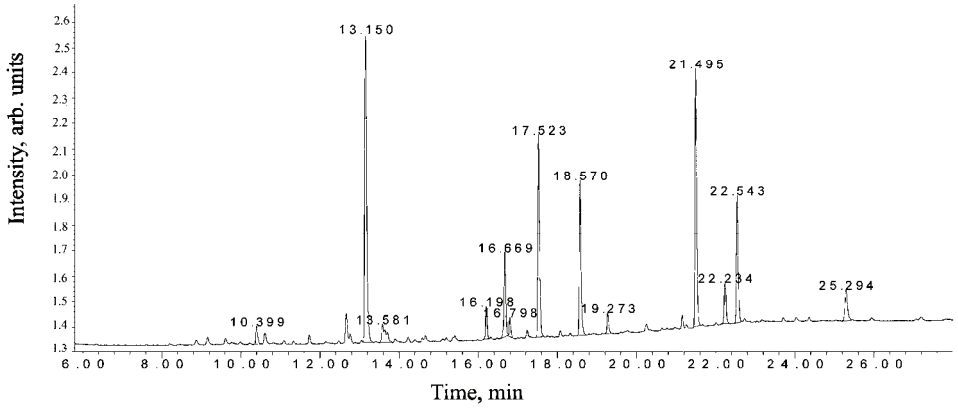

Fig. 1. Fatty acid methyl ester chromatogram for *K. stokesii*; myristic acid (*RT* 10.399 min); palmitic acid (*RT* 13.150 min); palmitoleic acid (*RT* 13.581 min); stearic acid (*RT* 16.198 min); elaidic acid (*RT* 16.669 min); oleic acid (*RT* 16.798 min); linolelaidic acid (*RT* 17.523 min); *α*-linolenic acid (*RT* 18.570 min); arachidic acid (*RT* 19.273 min); arachidonic acid (*RT* 21.495 min); behenic acid (*RT* 22.234 min); *cis*-5,8,11,14,17-eicosapentaenoic acid (*RT* 22.543 min) and lignoceric acid (*RT* 25.294 min).

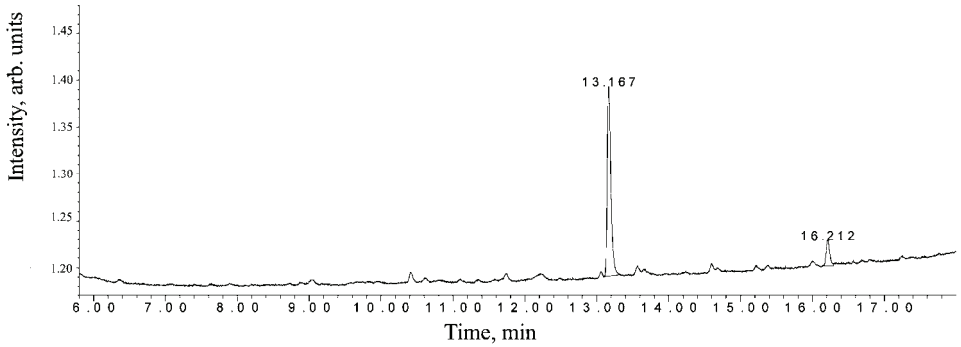

Fig. 2. Fatty acid methyl ester chromatogram for *K. praelongum*; palmitic acid (*RT* 13.167 min) and stearic acid (*RT* 16.212 min).

CONCLUSIONS

The fatty acid composition of the two related and often synonymized *Kindbergia* species strongly suggested that they are chemically distinguishable and, thus, could be treated as separate entities. This, however, has still to be confirmed by the analyses of additional chemical constituents, such as phenolic acids and their derivatives as well as flavonoids,[5] of various moss samples in order to support a re-examination of the relationship between them. For a general consideration of the quality of fatty acid profiling for chemotaxonomy, more replicates and additional species would have to be included in a follow-up study.

Acknowledgment. This work was supported by the Ministry of Science and Technological Development of the Republic of Serbia (Research grants No. 142053 and 143015).

И З В О Д

ПРЕЛИМИНАРНА АНАЛИЗА ХЕМИЈЕ МАСНИХ КИСЕЛИНА ВРСТА *Kindbergia praelonga* И *Kindbergia stokesii* (BRACHYTHECIACEAE)

БОРИС ПЕЈИН[1], ЉУБОДРАГ ВУЈИСИЋ[2], МАРКО САБОВЉЕВИЋ[3], АНЕТА САБОВЉЕВИЋ[3], ВЕЛЕ ТЕШЕВИЋ[1] и ВЛАТКА ВАЈС[2]

[1]Катедра за органску хемију, Хемијски факултет, Универзитет у Београду, Студентски трг 16, 11000 Београд, [2]Центар за хемију, Институт за хемију, технологију и металургију, Његошева 12, 11000 Београд и [3]Институт за ботанику и ботаничка башта, Биолошки факултет, Универзитет у Београду, Таковска 43, 11000 Београд

Прелиминарно је испитиван састав виших масних киселина две маховине из фамилије Brachytheciaceae, *Kindbergia praelonga* (Hedw.) Ochyra и *Kindbergia stokesii* (Turn.) Ochyra, са хемотаксономским циљем. Укупно је идентификовано 13 виших масних киселина GC и GC–MS анализом. На основу добијених експерименталних резултата се може закључити да се наведене биљне врсте значајно хемијски разликују и да би се могле сматрати засебним ентитетима уколико се то потврди и додатним анализама.

(Примљено 9. фебруара, ревидирано 5. септембра 2010)

REFERENCES

1. M. O. Hill, N. Bell, M. A. Bruggemann-Nannenga, M. Brugues, M. J. Cano, J. Enroth, K. I. Flatberg, J.-P. Frahm, M. T. Gallego, R. Garilleti, J. Guerra, L. Hedenäs, D. T. Holyoak, J. Hyvönen, M. S. Ignatov, F. Lara, V. Mazimpaka, J. Munoz, L. Söderström, *J. Bryol.* **28** (2006) 198
2. M. Sabovljević, R. Natcheva, G. Dihoru, E. Tsakiri, S. Dragićević, A. Erdag, B. Papp, *Phytol. Balcan.* **14** (2008) 159
3. M. S. Ignatov, S. Huttunen, *Arctoa* **11** (2002) 245
4. M. Ignatov, P. Isoviita, *Taxon* **52** (2003) 352
5. N. Jocković, P. B. Andrade, P. Valentao, M. Sabovljević, *J. Serb. Chem. Soc.* **73** (2008) 1161.

Journal of the Serbian Chemical Society
JSCS-info@shd.org.rs • www.shd.org.rs/JSCS
J. Serb. Chem. Soc. 75 (12) 1641–1652 (2010)
JSCS–4084
UDC 547.56:634.84:581.48:
547.972.3(497.11)
Original scientific paper

Polyphenolic compounds in seeds from some grape cultivars grown in Serbia

DEJAN GOĐEVAC[1*#], VELE TEŠEVIĆ[2#], MILOVAN VELIČKOVIĆ[3], LJUBODRAG VUJISIĆ[2], VLATKA VAJS[1#] and SLOBODAN MILOSAVLJEVIĆ[2#]

[1]*Institute of Chemistry, Technology and Metallurgy, Njegoševa 12, 11000 Belgrade*
[2]*Faculty of Chemistry, Studentski trg 16, 11000 Belgrade and* [3]*Faculty of Agriculture, Nemanjina 6, 11080 Zemun, Serbia*

(Received 19 May, revised 26 July 2010)

Abstract: Seed extracts from eight grape cultivars (*Vitis vinifera*) growing in Serbia were screened for their polyphenolic composition by means of HPLC/ /PDA/ESI/MS analysis. The study revealed 34 phenolic compounds belonging to the following groups: flavan-3-ol monomers, proanthocyanidins, flavonols, hydroxycinnamic acid and hydroxybenzoic acid derivatives. The quantities of the main constituents were determined using PDA/HPLC. Qualitative and quantitative differences among the cultivars were observed.

Keywords: *Vitis vinifera*; grape seeds; HPLC/PDA/ESI/MS; flavanol monomers; proanthocyanidins; flavonols; hydroxycinnamic acid; hydroxybenzoic acid derivatives.

INTRODUCTION

Many agricultural by-products are composed of plant tissues rich in phytochemicals, with valuable chemical and biological properties. Examples are by--products from wine processing,[1–3] such as marcs, stems, dregs (a sludgy residue deposited on the bottom of fermentation vats) and grape-seeds, which represent rich sources of polyphenolics.

Phenols represent the third most abundant constituent in grapes after carbohydrates and fruit acids.[4] The composition of phenolics depends on whether the extraction is performed on whole grape, pulp, skin or seeds. The total extractable phenolics in grapes are present at only about 10 % or less in pulp, 60–70 % in the seeds and 28–35 % in the skin. The phenol content of seeds may range from 5 to 8 % by weight.[5]

* Corresponding author. E-mail: dgodjev@chem.bg.ac.rs
# Serbian Chemical Society member.
doi: 10.2298/JSC100519131G

The phenolic compounds in grapes can be divided into two main groups: phenolic acids (localized mainly in the skin and pulp) and flavonoids. The most common phenolic acids in grape include cinnamic and benzoic acid derivatives. Flavonoids include colorless flavan-3-ols, flavonols and red and blue anthocyanins.[5] The most abundant phenolics isolated from grape seeds and skins are flavan-3-ols (catechin and epicatechin) and their oligomers and polymers (proanthocyanidins). The outer seed coat contains the majority of both the monomeric and polymeric flavan-3-ols (2 to 5 times more than the endosperm).[6] Grape skins also contain anthocyanins which contribute to their red or blue color.[7,8]

Various conditions (time, solvent, and the manner) for the extraction of polyphenols from grape seeds are described in the literature. Due to the acidic lability of interflavan linkages within proanthocyanidins and the susceptibility of polyphenols to oxidation, a valid extraction method should provide for the complete as possible extraction of the polyphenolics while limiting their degradation.[9] Methanol/water[10,11] or acetone/water systems[12] are the common solvents used for extracting polyphenols from grape seeds. In particular, lower molecular weight polyphenols, such as phenolic acids, anthocyanins, and flavanol monomers and oligomers, are well extracted with methanol, while the higher molecular weight flavanols are better extracted with aqueous acetone than with methanol.[13–16]

Several methods for the analysis of polyphenols have been proposed in the literature. Most of them are based on high performance liquid chromatography (HPLC) coupled with either a photodiode array (PDA) detector or a mass spectrometer (MS). Reverse phase columns are favorable, using acetonitrile and acidic water solutions as eluents.[17] Since UV detection depends upon the chemical structure of a molecule, several wavelengths could be selected for monitoring. Red-colored anthocyanins show an absorbance maximum at around 520 nm; yellow-colored flavonols display an absorbance maximum at around 360 nm; hydroxycinnamic acids can be specifically detected by their high absorbance around 320 nm. Flavan-3-ols show no specific absorbance and have a maximum around 280 nm, as do all the above-mentioned phenolics.[18]

Many studies proved that procyanidins and other polyphenolics from grape seed could be the key compounds responsible for various beneficial effects for human health.[19,20] These effects are mainly associated with the antioxidant activity of the phenolic compounds, which act as reducing agents by trapping free radicals, by acting as chelators, by donating hydrogen, and by quenching singlet oxygen. These highly reactive species are present in biological systems and may oxidize lipids, proteins, nucleic acids, which may initiate degenerative heart disease. In addition, grape seed polyphenolics possess various potent biological effects, such as antitumor, antibacterial, antiviral, anti-inflammatory, enzyme-inhibiting effects.[21–24] Waste products of the winery and grape juice industry derived from grape seeds represent a rich source of polyphenols.[5,25] It is well

known that the concentration of polyphenolic compounds in grapes depends on the grape cultivar,[26,27] and other factors, such as ripening time, climate, soil and location of growth.[28]

The aim of this study was to determine the polyphenolic composition of grape seed extracts from *Vitis vinifera* L. cv., Smederevka, Prokupac, Serbian original varieties, and Italian Riesling, Traminer, Black Burgundy, Gamay Noir, Muscat Hamburg and Gamay Bojadiser, all grown in the same geographical area and vintage. Two grape cultivars, Italian Riesling and Traminer, have a yellow--green colored grape berry used for production of high-quality white wines. The cultivar Smederevka is an autochthonous grape cultivar of Serbia, with lightly yellow and green colored berries. This cultivar is used for production of quality white wines as well as for all kinds of blending, because the grapes accumulate a high level of acids. Since the grape is well transportable and the pulp is crispy, it is also used fresh. Black Burgundy and Gamay Noir are purple-colored grape cultivars, used in production of high-quality red wines. Muscat Hamburg is the most widespread table grape in Serbia. This grape can be used fresh as well as for wine and grape brandy production. Prokupac is also an autochthonous grape cultivar of Serbia. Its berries are navy-blue colored with plenty of dots, and it is used for the production of quality rosé wines. Gamay Bojadiser grapes are full of colored materials, and it is mostly used for blending. An HPLC/PDA/MS method was used for the polyphenols analysis. The similarities and differences between the polyphenolic compositions of grape seed extracts from different cultivars are discussed.

EXPERIMENTAL

Plant material

Seeds from eight grape cultivars, including Italian Riesling, Traminer, Smederevka, Black Burgundy, Gamay Noir, Muscat Hamburg, Prokupac and Gamay Bojadiser were examined. All studied cultivars were grown in the vicinity of Belgrade (experimental orchard of Radmilovac, property of Faculty of Agriculture, University of Belgrade). The experimental vineyard was raised in 1995 (cultivars Smederevka and Gamay Noir), and 1996 (cultivars Italian Riesling, Traminer, Black Burgundy, Muscat Hamburg, Prokupac and Gamay Bojadiser). The distance of sowing was 3×1 m, with two rows support, and the training system was a "double-branched asymmetrical cordone",[29] the tree being 90 cm high. Approximately 20 clusters (about 5 kg of grape) were collected in late summer 2008, from 10 different plants. All the samples were collected when the Brix values were in range 22.5–24.5°.

Chemicals

Gallic acid, catechin, epicatechin, caffeic acid, ellagic acid, and rutin were purchased from Sigma Aldrich (St. Louis, MO, USA). All chemicals and solvents were of analytical grade. The HPLC water was purified by a Milli-Q System.

Sample preparation

The seeds from the berries were manually separated from pulp and dried on filter paper. The samples of whole, dried seeds (20 g) were macerated in 120 mL of 50 % MeOH, and 1

mL of rutin solution (2.78 mg mL^{-1} in MeOH, internal standard) was added. The mixtures were sonicated in an ultrasonic bath for 8 h. The extracts were filtered through filter paper, evaporated (to 1 mL) at 45 °C under reduced pressure and filtered through a 0.45 mm cellulose filter (Millipore). The filtrate was then transferred into a vial and filled up with 50 % MeOH to a volume of 1.5 mL.

HPLC/PDA Analysis

HPLC analysis of extracts was performed using an Agilent 1200 chromatograph equipped with a PDA model G1315B, a Bin pump model G1312A, an autosampler model G1313A and a RR Zorbax Eclipse Plus C18 column (1.8 μm, 150 mm×4.6 mm). The mobile phase A was 0.2 % formic acid in water and the mobile phase B was acetonitrile. Elution was performed at 0.95 mL min^{-1} with the following gradient program of solvent B: 0–20 min, 5–16 %; 20–28 min, 16–40 %; 28–32 min, 40–70 %; 32–36 min, 70–99 %; 36–45 min, 99 % and 45–46, min. 99–5 %.[30] The injection volume was 10 μL. Wavelengths of 280 nm (for flavan-3-ols and benzoic acid derivatives) and 360 nm (for flavonols and cinnamic acid derivatives) were selected for detection.

Quantification of the compounds was realized using calibration curves obtained by HPLC of pure standards: gallic acid, caffeic acid, (+)-catechin, (-)-epicatechin, and ellagic acid. Rutin was used as an internal standard. Some compounds were quantified as equivalents of the most similar chemical structures: gallic acid for gallic acid glucoside, gentisic acid glucoside, protocatechuic acid, *p*-hydroxybenzoic acid and methyl gallate; caftaric acid as caffeic acid; (+)--catechin for proanthocyanidin dimers and trimers and their monogallates; (–)-epicatechin for epicatechin gallate; ellagic acid for ellagic acid pentoside.

LC/MS analysis

LC/MS analysis was performed on an Agilent MSD TOF coupled to an Agilent 1200 series HPLC, using the same column and gradient program as were employed for the HPLC/ /PDA analysis. Mass spectra were acquired using an Agilent ESI-MSD TOF. The drying gas (N2) flow was 12 L min^{-1}; the nebulizer pressure was 310.264 kPa and the drying gas temperature was 350 °C. For ESI analysis, the parameters were: capillary voltage, 4000 V; fragmentor, 140 V; skimmer, 60 V; Oct RF V 250 V, for negative modes. The mass range was from 100 to 2000 *m*/*z*. Data processing was realized with the software Molecular Feature Extractor and Mass Profiler.

Statistical analysis

All the experiments were performed in triplicate. Significant differences between the means were separated by analysis of variance (ANOVA) followed by Tukey's test. Computations were realized using Origin software package version 7.0.

RESULTS AND DISCUSSION

The rapid resolution HPLC column and the appropriate gradient program afforded the separation of some 34 phenolic compounds in less than 30 min. Identification of the compounds was based on the UV spectra and molecular formula obtained from accurate mass measurements, both measured on the HPLC/ /PDA/ESI/MS equipment, which also involved comparison of these data with those of the metabolites previously reported for grape seed extracts.[23,31] The identified phenolic compounds could be classified into the following groups: flavanol monomers (catechin and epicatechin), proanthocyanidins, flavonols,

hydroxycinnamic acids, and hydroxybenzoic acid derivatives (Table I, Fig. 1.). However, owing to the unavailability of authentic compounds, with exception of gallic acid, ellagic acid, catechin and epicatechin, the peaks could be tentatively assigned but without determination of stereochemistry.

TABLE I. LC/MS Data of grape seed extracts (GSEs)

Peak	t_R min	Compound	Class of compound[a]	λ_{max} nm	Species	Mass	Molecular formula
1	3.2	Gallic acid	HB	220, 272	M–H, 2M–H	170.0215	$C_7H_6O_5$
2	4.0	Proanthocyanidin trimer	PC	200, 218, 228*sh*, 236*sh*, 280	M–2H, M–H	866.2058	$C_{45}H_{38}O_{18}$
3	4.3	Gallic acid glucoside	HB	218, 256	M–H, 2M–H	332.0744	$C_{13}H_{16}O_{10}$
4	5.0	Gentisic acid glucoside	HB	216, 252	M–H, 2M–H	316.0794	$C_{13}H_{16}O_9$
5	5.8	Protocatechuic acid	HB	218, 260, 292*sh*	M–H, 2M–H	154.0266	$C_7H_6O_4$
6	7.3	Caftaric acid	HC	300*sh*, 324	M–H, 2M–H	312.0481	$C_{13}H_{12}O_9$
7	8.2	*p*-Hydroxybenzoic acid	HB	278, 312	M–H, 2M–H	138.0317	$C_7H_6O_3$
8	8.3	Proanthocyanidin dimer	PC	200, 216, 228*sh*, 280	M–H, 2M–H	578.1424	$C_{30}H_{26}O_{12}$
9	9.5	Proanthocyanidin dimer	PC	200, 216, 228*sh*, 280	M–H, 2M–H	578.1424	$C_{30}H_{26}O_{12}$
10	9.8	Methyl gallate	HB	220, 272	M–H, 2M–H	184.0372	$C_8H_8O_5$
11	10.1	(+)-Catechin	FM	200, 218, 226*sh*, 278	M–H, 2M–H	290.0790	$C_{15}H_{14}O_6$
12	10.9	Proanthocyanidin trimer	PC	200, 218, 228*sh*, 236*sh*, 280	M–2H, M–H	866.2058	$C_{45}H_{38}O_{18}$
13	11.3	Proanthocyanidin trimer	PC	200, 218, 228*sh*, 236*sh*, 280	M–2H, M–H	866.2058	$C_{45}H_{38}O_{18}$
14	11.7	Proanthocyanidin dimer	PC	200, 216, 228*sh*, 280	M–H, 2M–H	578.1424	$C_{30}H_{26}O_{12}$
15	11.8	Caffeic acid	HC	246, 298*sh*, 326	M–H	180.0423	$C_9H_8O_4$
16	12.7	Proanthocyanidin dimer	PC	200, 216, 228*sh*, 280	M–H, 2M–H	578.1424	$C_{30}H_{26}O_{12}$
17	13.9	Proanthocyanidin trimer monogallate	PC/HB	200, 218, 278	M–2H, M–H	1018.2168	$C_{52}H_{42}O_{22}$
18	14.3	(–)-Epicatechin	FM	200, 218, 226*sh*, 278	M–H, 2M–H	290.0790	$C_{15}H_{14}O_6$
19	15.4	Proanthocyanidin dimer monogallate	PC/HB	200, 218, 278	M–H, 2M–H	730.1534	$C_{37}H_{30}O_{16}$
20	15.8	Proanthocyanidin trimer	PC	200, 218, 228*sh*, 236*sh*, 280	M–2H, M–H	866.2058	$C_{45}H_{38}O_{18}$

TABLE I. Continued

Peak	t_R min	Compound	Class of compound[a]	λ_{max} nm	Species	Mass	Molecular formula
21	16.5	Proanthocyanidin trimer	PC	200, 218, 228*sh*, 236*sh*, 280	M–2H, M–H	866.2058	$C_{45}H_{38}O_{18}$
22	17.4	Proanthocyanidin dimer monogallate	PC/HB	200, 218, 278	M–H, 2M–H	730.1534	$C_{37}H_{30}O_{16}$
23	17.5	Syringic acid	HB	276	M–H, 2M–H	198.0528	$C_9H_{10}O_5$
24	20.6	Ellagic acid pentoside	HB	254, 300*sh*, 360	M–H, 2M–H	434.0485	$C_{19}H_{14}O_{12}$
25	21.9	Ellagic acid	HB	254, 298*sh*, 368	M–H	302.0063	$C_{14}H6O_8$
26	21.9	(–)-Epicatechin gallate	FM/HB	200, 218, 278	M–H, 2M–H	442.0900	$C_{22}H_{18}O_{10}$
27	22.0	Taxifolin	FL	232, 254, 290, 330*sh*	M–H, 2M–H	304.0583	$C_{15}H_{12}O_7$
28	22.7	Quercetin-3-*O*-glucuronide	FL	256, 264*sh*, 356	M–H, 2M–H	478.0747	$C_{21}H_{18}O_{13}$
29	23.1	Astilbin	FL	292, 326*sh*	M–H, 2M–H	450.1162	$C_{21}H_{22}O_{11}$
30	22.9	Quercetin-3-*O*-glucoside	FL	256, 268*sh*, 300*sh*, 360	M–H, 2M–H	464.0955	$C_{21}H_{20}O_{12}$
31	23.8	Kaempferol rutinoside	FL	266, 320*sh*, 350	M–H	594.1585	$C_{27}H_{30}O_{15}$
32	24.7	Isorhamnetin-3-*O*-glucoside	FL	256, 266*sh*, 302*sh*, 350	M–H, 2M–H	478.1111	$C_{22}H_{22}O_{12}$
33	24.3	Quercetin 3-*O*-rhamnoside	FL	256, 266*sh*, 302*sh*, 350	M–H, 2M–H	448.1006	$C_{21}H_{20}O_{11}$
34	27.4	Quercetin	FL	256, 268*sh*, 300*sh*, 370	M–H, 2M–H	302.0427	$C_{15}H_{10}O_7$

[a]HB – hydroxybenzoic acid derivative, FM – flavanol monomers, PC – proanthocyanidins, FL – flavonols, HC – hydroxycinnamic acids

All the identified compounds exhibited quasi-molecular ion $[M–H]^–$, as the dominant ion species in the mass spectrum. The exception were procyanidin trimers, where doubly charged $[M–2H]^{2–}$ species were dominant. Cluster ions, such as $[2M–H]^–$, were also observed for most of the compounds.

The amounts of phenolic compounds are presented in Tables II and III. The range of free gallic acid varied from 4 to 23 mg per 100 g of grape seeds. While white grape cultivars (Italian Riesling, Traminer and Smederevka) showed high gallic acid contents (over 17 mg per 100 g), the colored cultivars possessed significantly lower contents (below 10 mg per 100 g). This is in accordance with data published for some white and red grape varieties from Spain.[32] Except in Italian Riesling, glucosides of gallic acid were found in all the studied cultivars. In addition, protocatechuic acid was detected in the white grape cultivars and Gamay Noir. The presence of ellagic acid or ellagic acid glycoside was con-

firmed in Muscat Hamburg and Prokupac seeds. This finding is surprising because it was hitherto believed that the presence of ellagic acid is unique for muscadine grapes (*Vitis rotundifolia*) among the *Vitis* varieties.[33,34]

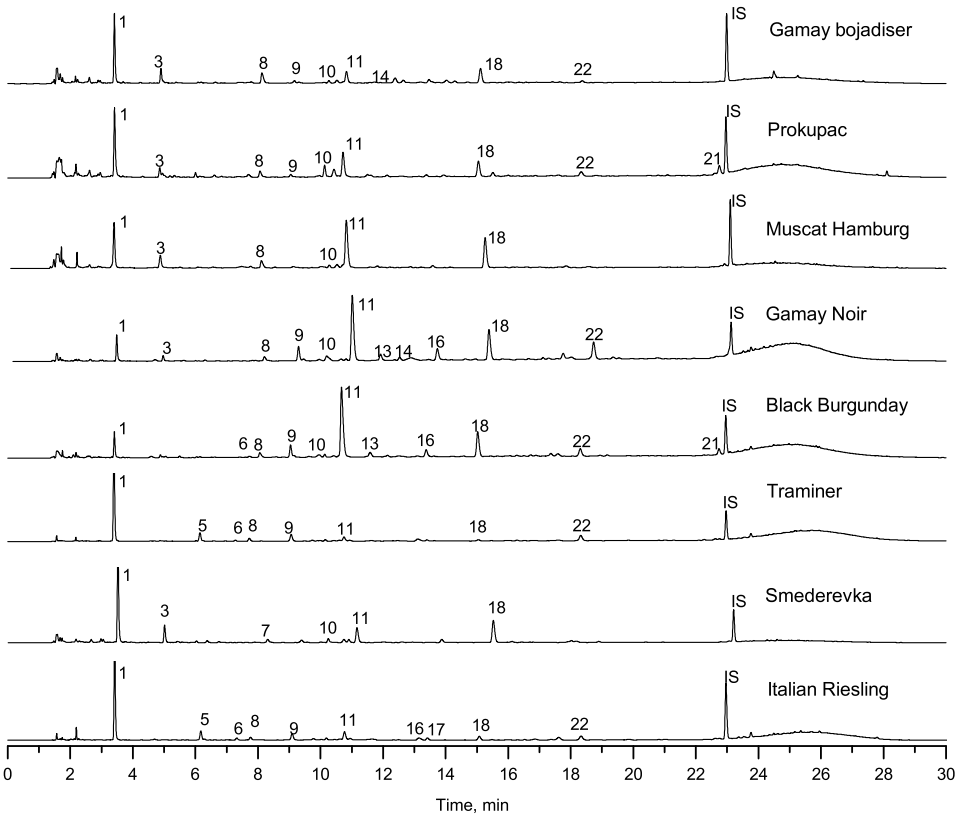

Fig. 1. LC/UV Chromatograms of grape seed extracts (λ = 280 nm).

In comparison with other classes of polyphenolic compounds, hydroxycinnamic acid derivatives were present in lower amounts in the seeds. This is in accordance with data from the literature claiming that hydroxycinnamic acids are localized mainly in the skin and pulp.[5] No hydroxycinnamic acids derivatives were detected in the cultivar Smederevka, while caftaric acid (ester of caffeic acid with tartaric acid) was found in the remaining cultivars. Underivatized caffeic acid was only found in the seeds of Traminer.

The presence of taxifolin (dihydroquercetin) and its glycoside astilbin was confirmed in Italian Riesling and Traminer cultivars, while in Black Burgundy only astilbin was detected. It should be noted that the presence of such types of flavonols is very rare in grape extracts.[35] Kaempferol rutinoside, quercetin or their glycosides were found in all the studied cultivars. Isorhamnetin-3-*O*-gluco-

TABLE II. Hydroxybenzoic acid, hydroxycinnamic acids derivatives and flavonols content in GSEs (IR - Italian Riesling, SM – Smederevka, TR – Traminer, BB - Black Burgundy, GN - Gamay Noir, MH - Muscat Hamburg, PR – Prokupac, GB - Gamay Bojadiser)

Peak	t_R min	Compound	IR		SM		TR		BB		GN		MH		PR		GB	
			Value[a]	*SD*	Value	*SD*	Value	*SD*	Value	*SD*	Value	*SD*	Value	*SD*	Value	*SD*	Value	*SD*
1	3.2	Gallic acid	17.67	0.23	18.62	0.35	22.48	0.41	4.30	0.10	5.15	0.05	5.84	0.05	8.12	0.10	9.45	0.05
3	4.3	Gallic acid glucoside	nd	–	3.51	0.10	0.59	0.04	1.04A*	0.06	1.54B*	0.05	4.50	0.10	1.29AB*	0.10	5.10	0.10
4	5.0	Gentisic acid glucoside	nd	–	0.76A	0.03	nd	–	nd	–	0.64AB	0.06	nd	–	0.54B	0.05	1.25	0.05
5	5.8	Protocatechuic acid	1.96A	0.05	0.78	0.10	2.44	0.03	nd	–	0.84A	0.05	nd	–	nd	–	nd	–
6	7.3	Caftaric acid	1.04A	0.04	nd	–	0.81A	0.01	2.67B	0.15	2.90B	0.10	7.04	0.05	1.87	0.08	6.62	0.11
7	8.2	*p*-Hydroxybenzoic acid	nd	–	1.43	0.15	nd	–	0.24	0.05	nd	–	nd	–	nd	–	nd	–
10	9.8	Methyl gallate	nd	–	1.49	0.10	Traces	–	1.44	0.05	1.42	0.08	3.06	0.06	2.10	0.10	1.35	0.05
15	11.8	Caffeic acid	nd	–	nd	–	2.04	0.03	nd	–	nd	–	nd	–	nd	–	nd	–
23	17.5	Syringic acid	Traces	–	nd	–	Traces	–	nd	–	nd	–	nd	–	nd	–	nd	–
24	20.6	Ellagic acid pentoside	nd	–	nd	–	nd	–	nd	–	nd	–	nd	–	1.24	0.05	nd	–
25	21.9	Ellagic acid	nd	–	nd	–	nd	–	nd	–	nd	–	2.36	0.05	1.26	0.05	nd	–
27	22.0	Taxifolin	Traces	–	nd	–	Traces	–	nd	–	nd	–	nd	–	nd	–	nd	–
28	22.7	Quercetin-3-*O*-glucuronide	Traces	–	nd	–	Traces	–	Traces	–	Traces	–	nd	–	Traces	–	nd	–
29	23.1	Astilbin	Traces	–	nd	–	Traces	–	Traces	–	nd	–	nd	–	nd	–	nd	–
30	22.9	Quercetin-3-*O*-glucoside	Traces	–	nd	–	nd	–	nd	–	nd	–	Traces	–	Traces	–	Traces	–
31	23.8	Kaempferol rutinoside	Traces	–	Traces	–	Traces	–	nd	–	Traces	–	Traces	–	Traces	–	Traces	–
32	24.7	Isorhamnetin-3-O--glucoside	nd	–	nd	–	nd	–	nd	–	nd	–	nd	–	nd	–	Traces	–
33	24.3	Quercetin 3-*O*--rhamnoside	Traces	–	nd	–	nd	–	nd	–	nd	–	nd	–	nd	–	nd	–
34	27.4	Quercetin	nd	–	nd	–	nd	–	nd	–	Traces	–	Traces	–	Traces	–	nd	–

[a]Expressed in mg/100g of dry grape seeds. Values with the same letters within the row are not significantly different ($p < 0.05$, without asterisk or $p < 0.01$, with asterisk)

TABLE III. Flavanol monomers and Proanthocyanidins content in GSEs (IR – Italian Riesling, SM – Smederevka, TR – Traminer, BB – Black Burgundy, GN – Gamay Noir, MH – Muscat Hamburg, PR – Prokupac, GB – Gamay Bojadiser)

Peak	t_R min	Compound	IR		SM		TR		BB		GN		MH		PR		GB	
			Value[a]	*SD*	Value	*SD*	Value	*SD*	Value	*SD*	Value	*SD*	Value	*SD*	Value	*SD*	Value	*SD*
2	4	Proanthocyanidin trimer	4.48	0.08	Traces	–	Traces	–	2.45	0.05	3.34	0.05	nd	–	1.40	0.10	nd	–
8	8.3	Proanthocyanidin dimer	29.50	0.59	0.75	0.05	6.85	0.09	11.27A	0.25	10.42A	0.33	17.38	0.13	5.25	0.05	15.29	0.10
9	9.5	Proanthocyanidin dimer	5.22	0.06	Traces	–	2.18	0.07	7.76	0.08	17.34	0.15	1.56	0.06	4.24	0.05	8.65	0.05
11	10.1	(+)-Catechin	42.41	0.52	6.85	0.10	17.21	0.01	134.82	1.11	145.04	1.00	107.81	1.41	26.14	0.15	37.26	0.64
12	10.9	Proanthocyanidin trimer	nd	–	nd	–	5.14	0.12	nd	–	nd	–	nd	–	4.35	0.05	17.28	0.20
13	11.3	Proanthocyanidin trimer	14.08	0.37	0.96	0.05	Traces	–	6.37	0.08	13.06	0.08	nd	–	nd	–	nd	–
14	11.7	Proanthocyanidin dimer	10.37	0.55	1.52	0.08	Traces	–	8.82	0.08	22.04	0.05	23.25	0.15	5.45	0.05	15.46	0.15
16	12.7	Proanthocyanidin dimer	21.35	0.56	2.90	0.10	8.36	0.05	10.40	0.20	16.69	0.10	29.30	0.19	6.11	0.10	32.74	0.25
17	13.9	Proanthocyanidin trimer monogallate	14.38	0.54	0.78	0.11	nd	–	nd	–	8.00	0.11	nd	–	Traces	–	25.98	0.43
18	14.3	(–)-Epicatechin	29.47	0.50	39.18	0.76	9.83	0.06	60.39	0.54	91.67	0.59	86.31	0.16	23.49	0.50	57.65	0.48
19	15.4	Proanthocyanidin dimer monogallate	14.49	0.50	0.88	0.08	nd	–	4.36	0.05	5.75	0.05	16.25	0.13	traces	–	nd	–
20	15.8	Proanthocyanidin trimer	nd	–	nd	–	nd	–	4.05	0.05	5.65	0.05	nd	–	traces	–	nd	–
21	16.5	Proanthocyanidin trimer	50.59	1.28	Traces	–	Traces	–	8.27	0.11	13.24	0.25	Traces	–	4.27	0.08	27.68	0.16
22	17.4	Proanthocyanidin dimer monogallate	50.77	1.15	1.35	0.05	20.24	0.20	16.70	0.10	40.62	0.78	nd	–	12.15	0.15	32.08	0.11
26	21.9	(–)-Epicatechin gallate	21.56	0.51	1.07	0.08	Traces	–	15.54	0.25	9.80	0.19	7.90	0.10	12.85	0.31	nd	–
		C+E	71.88	1.02	46.03	0.86	27.04	0.06	195.21	1.63	236.72	1.58	194.13	1.56	49.63	0.65	94.91	1.05
		C/E	1.44	0.01	0.17	0.00	1.75	0.01	2.23	0.00	1.58	0.00	1.25	0.01	1.11	0.02	0.65	0.01
		Proanthocyanidin dimer	66.45	1.73	5.17	0.23	17.39	0.21	38.25	0.60	66.49	0.63	71.49	0.52	21.05	0.25	72.13	0.55
		Galloylated proantocyanidins	101.20	2.71	4.07	0.31	20.24	0.20	36.59	0.40	64.18	1.13	24.15	0.23	24.99	0.46	58.06	0.54

[a]Expressed in mg/100g of dry grape seeds. Values with the same letters within the row are not significantly different ($p < 0.05$, without asterisk or $p < 0.01$, with asterisk)

side was detected only in Gamay Bojadiser (Table II). Such flavonols have been already reported in grapes extracts.[32,36]

The most abundant phenolic compounds in the grape seed extracts were monomeric flavan-3-ols and proanthocyanidins, as found by other authors.[26,32,37] Generally, the content of flavan-3-ol monomers (catechin and epicatechin) was higher in the colored than in the white grape cultivars (Table III). Only Smederevka and Gamay Bojadiser possessed greater amounts of epicatechin than catechin, while the catechin/epicatechin ratio for most cultivars was between 1 and 2. The exception was Black Burgundy which contained more than two times more catechin than epicatechin. Muscat Hamburg, Gamay Bojadiser, Italian Riesling and Gamay Noir were the richest in proanthocyanidin dimers, while Italian Riesling possessed a high amount of galloylated proantocyanidins. On the other hand, Smederevka possessed a very low amount of proanthocyanidin dimers and galloylated proanthocyanidins.

CONCLUSIONS

Statistically significant difference in the contents of some polyphenolic compounds between the studied cultivars was noticed. From these findings, it may be concluded that the amounts and distribution of various phenolic compounds in grape seeds depend directly on the cultivar, as the other factors, such as ripening time, climate, soil and location of growth, were the same for all the studied cultivars. This is the first time the presence of ellagic acid or ellagic acid glycoside in some *Vitis vinifera* cultivars was evidenced. The variation of the composition of the phenolic compounds from certain cultivar could be used in industry to make specific food additives or dietary supplements.

И З В О Д

ПОЛИФЕНОЛНА ЈЕДИЊЕЊА ИЗ СЕМЕНКИ ОСАМ СОРТИ ГРОЖЂА ГАЈЕНИХ У СРБИЈИ

ДЕЈАН ГОЂЕВАЦ[1], ВЕЛЕ ТЕШЕВИЋ[2], МИЛОВАН ВЕЛИЧКОВИЋ[3], ЉУБОДРАГ ВУЈИСИЋ[2], ВЛАТКА ВАЈС[1] и СЛОБОДАН МИЛОСАВЉЕВИЋ[2]

[1]Институт за хемију, технологију и металургију, Његошева 12, 11000, Београд, [2]Хемијски факултет, Студентски трг 16, 11000, Београд и [3]Пољопривредни факултет, Немањина 6, 11080, Земун

Помоћу HPLC/PDA/ESI/MS анализе је испитан полифенолни састав екстраката семенки осам сорти грожђа (*Vitis vinifera*) гајених у Србији. Утврђено је присуство 34 фенолна једињења која припадају следећим групама: флаванолски мономери, проантоцијанидини, флавоноли, деривати хидроксициметне и деривати хидроксибензоеве киселине. Квантитативни садржај главних састојака је одређен уз помоћ PDA/HPLC. Примећене су квалитативне и квантитативне разлике између појединих сорти.

(Примљено 19. маја, ревидирано 26. јула 2010)

REFERENCES

1. F. Bonilla, M. Mayen, J. Merida, M. Medina, *Food Chem.* **66** (1999) 209
2. J. L. Torres, R. Bobet, *J. Agric. Food Chem.* **49** (2001) 4627
3. J. L. Torres, B. Varela, M. T. García, J. Carilla, C. Matito, J. J. Centelles, M. Cascante, X. Sort, R. Bobet, *J. Agric. Food Chem.* **50** (2002) 7548
4. V. L. Singleton, in *Proceedings of the University of California, Davis, Grape and Wine Centenary Symposium*, University of California, Davis, CA, 1980, p. 215
5. J. Shi, J. Yu, J. E. Pohorly, Y. Kakuda, *J. Med. Food* **6** (2003) 291
6. J. H. Thorngate, V. L. Singleton, *Am. J. Enol. Viticult.* **45** (1994) 259
7. R. C. Silva, J. Rigaud, V. Cheynier, A. Chemina, *Phytochemistry* **30** (1991) 1259
8. C. Prieur, J. Rigaud, V. Cheynier, M. Moutounet, *Phytochemistry* **36** (1994) 781
9. H. Zou, P. Kilmartin, M. Inglis, A. Frost, *Aust. J. Grape Wine Res.* **8** (2002) 163
10. C. F.-A. E. M. Santos-Buelga, M. T. Escribano-Bailon, *Food Chem.* **53** (1995) 197
11. D. Rusjan, Z. Korosec-Korusa, *Acta Chim. Slov.* **54** (2007) 114
12. G. Spagna, R. N. Barbagallo, P. G. Pifferi, *J. Agric. Food Chem.* **48** (2000) 4619
13. L. Foo, L. Porter, *J. Sci. Food Agric.* **32** (1981) 711
14. R. Hemingway, G. McGraw, *J. Wood Chem. Technol.* **3** (1983) 421
15. I. McMurrough, D. Madigan, M. R. Smyth, *J. Agric. Food Chem.* **44** (1996) 1731
16. S. Guyot, N. Marnet, D. Laraba, P. Sanoner, J. F. Drilleau, *J. Agric. Food Chem.* **46** (1998) 1698
17. S. Muñoz, M. Mestres, O. Busto, J. Guasch, *Anal. Chim. Acta* **628** (2008) 104
18. S. Gómez-Alonsoa, E. García-Romeroa, I. Hermosín-Gutiérrez, *J. Food Comp. Anal.* **20** (2007) 618
19. P. M. Aron, J. A. Kennedy, *Mol. Nutr. Food Res.* **52** (2008) 79
20. S. E. Rasmussen, H. Frederiksen, K. S. Krogholm, L. Poulsen, *Mol. Nutr. Food Res.* **49** (2005) 159
21. X. Terra, J. Valls, X. Vitrac, J. M. Merrillon, L. Arola, A. Ardevol, C. Blade, J. Fernandez-Larrea, G. Pujadas, J. Salvado, M. Blay, *J. Agric. Food Chem.* **55** (2007) 4357
22. C. Agarwal, R. Veluri, M. Kaur, S. C. Chou, J. A. Thompson, R. Agarwal, *Carcinogenesis* **28** (2007) 1478
23. M. Stanković, V. Tešević, V. Vajs, N. Todorović, S. Milosavljević, D. Gođevac, *Planta Med.* **74** (2008) 730
24. N. Nair, S. Mahajan, R. Chawda, C. Kandaswami, T. C. Shanahan, S. A. Schwartz, *Clin. Diagn. Lab. Immunol.* **9** (2002) 470
25. I. S. Arvanitoyannis, D. Ladas, A. Mavromatis, *Int. J. Food Sci. Techol.* **41** (2006) 475
26. E. Bakkalbaşı, O. Yemiş, D. Aslanova, N. Artık, *Eur. Food Res. Technol.* **221** (2005) 792
27. T. Fuleki, J. M. R. da Silva, *J. Agric. Food Chem.* **45** (1997) 1156
28. J. A. Kennedy, M. A. Matthews, A. L. Waterhouse, *Phytochemistry* **55** (2000) 77
29. A. Nakalamić, *Jugoslovensko vinogradarstvo i vinarstvo* **4** (1991) 7 (in Serbian)
30. D. Gođevac, V. Tešević, V. Vajs, S. Milosavljević, M. Stanković, *Food Chem. Toxicol.* **47** (2009) 2853
31. E. Cantos, J. C. Espin, F. A. Tomas-Barberan, *J. Agric. Food Chem.* **50** (2002) 5691
32. R. Rodriguez Montealegre, R. Romero Peces, J. L. Chacon Vozmediano, J. Martinez Gascueña, E. Garcia Romero, *J. Food Compos. Anal.* **19** (2006) 687
33. S. U. Mertens-Talcott, J. H. Lee, S. S. Percival, S. T. Talcott, *J. Agric. Food Chem.* **54** (2006) 5336

34. J. H. Lee, J. V. Johnson, S. T. Talcott, *J. Agric. Food Chem.* **53** (2005) 6003
35. C. Cavaliere, P. Foglia, R. Gubbiotti, P. Sacchetti, R. Samperi A. Lagana, *Rapid Commun. Mass Spectrom*. **22** (2008) 3089
36. E. Obreque-Slier, A. Pena-Neira, R. Lopez-Solis, F. Zamora-Marin, J. M. Ricardo-da Silva, O. Laureano, *J. Agric. Food Chem.* **58** (2010) 3591
37. A. I. Mandić, S. M. Đilas, G. S. Ćetković, J. M. Čanadanović-Brunet, V. T. Tumbas, *Int. J. Food Prop.* **11** (2008) 713.

Journal of the Serbian Chemical Society
JSCS-info@shd.org.rs • www.shd.org.rs/JSCS
J. Serb. Chem. Soc. *75* (12) 1653–1660 (2010)
JSCS–4085
UDC *Pleurospermum austriacum*: 541.18.045:665.52
Original scientific paper

Volatiles of *Pleurospermum austriacum* (L.) Hoffm. (Apiaceae)

NIKO S. RADULOVIĆ*, NEVENKA D. ĐORĐEVIĆ and RADOSAV M. PALIĆ#

Department of Chemistry, Faculty of Science and Mathematics, University of Niš, Višegradska 33, 18000 Niš, Serbia

(Received 23 March, revised 12 May 2010)

Abstract: This work presents the first results of detailed GC and GC–MS analyses of the volatile constituents from the fresh leaves, fruits and stalks of an endangered plant species *Pleurospermum austriacum* (L.) Hoffm. (Apiaceae). Sesquiterpene hydrocarbons made up *ca.* 4/5 of the oils obtained in low yield (0.003–0.086 %, w/w). The major volatiles detected were germacrene D (66.5, 62.4 and 49.0 % in fruits, leaves and stalks, respectively), β-caryophyllene (3.1–5.7 %), δ-cadinene (3.6–5.0 %) and (*E*)-β-farnesene (1.0–1.5 %).

Keywords: *Pleurospermum austriacum*; Apiaceae; essential oil; germacrene D.

INTRODUCTION

Pleurospermum Hoffm. (Apiaceae) is a widespread, heterogeneous genus of complex and controversial taxonomy.[1–3] Russian authors[3] delimit *Pleurospermum sensu stricto* by only two species, *P. austriacum* (that is according to the *Flora Europaea* a sub-boreal Euroasian floral element[1,2]), and *P. uralense*, referring the other species to *Aulacospermum*, *Hymenidium*, *Hymenolaena*, *Physospermopsis* and *Pterocyclus*. Other morphologically similar genera, where generic boundaries become indistinct, include *Trachydium* and *Pseudotrachydium* Pimenov and Kljuykov.[3] As yet, this rather radical classification has not gained widespread acceptance, and the proponents admit that this is a taxonomic hypothesis, and (particularly for some groups) a more natural classification will only be possible following critical revision in the field, herbarium[3] and possibly a more general approach, including the use of chemical markers as *principium divisionis*.

Phytochemically speaking, *Pleurospermum* taxa were investigated on a few occasions. The chemistry regarding the volatile compounds of these taxa has been neglected (essential oil investigations), and only *P. lindleyanum* was studied

* Corresponding author. E-mail: vangelis0703@yahoo.com
# Serbian Chemical Society member.
doi: 10.2298/JSC100323127R

in this sense.[4] Most of the phytochemical work realized in this field resulted in the isolation of a number of coumarins (mono-, di-, and trimers) and related phenylpropanoids and concerned only the non-volatile compounds. Some of these molecules were found for the first time as naturally occurring metabolites.[5–14] Surprisingly, the previously mentioned analyses[4] of the oil of *P. lindleyanum* resulted in the identification of certain anthropogenic compounds as oil constituents.

The aim of this work was to provide the very first and detailed GC and GC–MS analyses of the volatile constituents from the leaves, fruits and stalks of the endangered plant species *Pleurospermum austriacum* (L.) Hoffm.[15]

EXPERIMENTAL

Plant material

Fresh plants (fruits, leaves and stalks) were collected in July, 2007 at the mountain Stara planina (Babin zub), at an altitude of 1707 m above sea level. The plant was identified by Niko Radulović. A voucher specimen (number 200705) is deposited at the Herbarium of the Faculty of Science and Mathematics, Niš.

Extraction of essential oils

Fresh plant material (three batches of about 250 g of each sample) was subjected to hydrodistillation with *ca*. 2 L of distilled water for 2.5 h using an original Clevenger-type apparatus. Due to the small sample size of the isolated essential oils, which were not completely liquid, the volume of the oils was not measured, and hence the yields are expressed as weight of essential oils per weight of plant material. The obtained oils were separated by extraction with freshly distilled diethyl ether (Merck, Germany) and dried over anhydrous magnesium sulfate (Aldrich, USA). The solvent was evaporated under a gentle stream of nitrogen at room temperature, in order to exclude any loss of the essential oils, and stored at 4 °C until analyzed. When the oil yields were determined, after the bulk of the ether had been removed under a stream of N_2, the residue was exposed to vacuum at room temperature for a short period to eliminate the solvent completely. The pure oil was then measured on an analytical balance and multiple gravimetric measurements were taken during 24 h to ensure that all of the solvent had evaporated.

GC–MS

The chemical composition of the oils was investigated by GC and GC–MS. The GC–MS analyses (three repetitions) were realized using a Hewlett-Packard 6890N gas chromatograph equipped with a fused silica capillary column HP-5MS (5 % phenylmethylsiloxane, 30 m×0.25 mm, film thickness 0.25 μm, Agilent Technologies, USA) and coupled with a 5975B mass selective detector from the same company. The injector and interface operated at 250 °C and 300 °C, respectively. The oven temperature was increased from 70–290 °C at a heating rate of 5.0 °C min^{-1} and then isothermally held for 10 min. Helium at a flow rate of 1.0 ml min^{-1} was used as the carrier gas. The sample, 1 μl of the oil solution in diethyl ether (1:100), was injected in a pulsed split mode (the flow was 1.5 ml min^{-1} for the first 0.5 min and then set to 1.0 ml min^{-1} throughout the remainder of the analysis; split ratio 40:1). The MS conditions were as follows: ionization voltage of 70 eV, acquisition mass range 35–500, scan time 0.32 s.

Gas chromatographic analyses were performed using an HP 5890 gas chromatograph equipped with a flame ionization detector (FID) and a split/splitless injector (Agilent Technologies, USA). The separation was achieved using a HP-5 (5 % diphenyl- and 95 % dimethylpolysiloxane) fused silica capillary column, 30 m×0.25 mm i.d., 0.25 μm film thickness. The GC oven temperature was programmed from 70 to 290 °C at a rate of 5.0 °C/min. Hydrogen was used as the carrier gas at a flow rate of 1.6 mL min^{-1} at 45 °C. The injector temperature was 250 °C and the detector temperature: 280 °C; the injection mode was splitless. The percentage composition of the oils was computed from the GC (FID) peak areas without any corrections. The relative standard deviation (*RSD*) of repeated measurements (independent sample preparation and GC–FID) was for all substances below 1 %. The only exceptions which had higher *RSD* were minor components such as methyl salicylate, α-cubebene, 1-hexyl isovalerate, bicycloelemene and germacrene A, for the *RSD* was 2, 3, 5, 9 and 10 %, respectively.

Oil constituents were identified by comparison of their linear retention indices (relative to C_7–C_{29} alkanes[16] on the HP-5MS column) with literature values[17] and their mass spectra with those of authentic standards, as well as those from Wiley 6, NIST02, MassFinder 2.3, and a homemade MS library with the spectra corresponding to pure substances and components of known oils, and wherever possible, by co-injection with an authentic sample.

RESULTS AND DISCUSSION

Hydrodistillation of fresh plant material yielded 0.003 % (w/w, based on weight of fresh plant material) of essential oil in the stalks, 0.012 % (w/w) in the leaves and 0.086 % (w/w) in the fruits. The chemical compositions of the essential oils from different parts of *P. austriacum* are reported in Table I, together with a summation of the compounds according to their respective compound class (percentage and number of detected constituents). Two hundred and five different constituents were identified in the volatile fraction of *P. austriacum* (156 in fruits, 116 in leaves, 117 in stalks) amounting to 94.5–98.6 % of the total oils. In all samples, the sesquiterpenoid fractions were the most abundant (85.7––90.5 %). About one half of all the identified components belonged to this class, with hydrocarbons in a greater number compared to the oxygenated derivatives. Within this class, the germacranes and related sesquiterpenoids (SGE) were the major ones (71.9 % in the fruits, 63.2 % in the leaves and 52.2 % in the stalks). The major components detected were germacrene D (66.5 % in the fruits, 62.4 % in the leaves and 49.0 % in the stalks), β-caryophyllene (3.1–5.7 %), δ-cadinene (3.6–5.0 %) and (*E*)-β-farnesene (1.0–1.5 %). Additional worth mentioning constituents were: (*Z*)-3-hexen-1-ol (8.8 %), 1-hexanol (1.3 %) and *epi*-cubebol (2.4 %) in the leaf oil, β-phellandrene (2.3 %), bicyclogermacrene (3.3 %) in the fruit oil and humulene (1.4 %), α-cadinol (3.0 %) and hexadecanoic acid (5.2 %) in the stalk oil. Shyobunol (0.3 %), α-phellandrene (0.3 %), *cis*-muurola-3,5-diene (0.1 %), aristolone (0.1 %) and cinnamyl valerate (0.1 %) were found only in the fruit oil, while 1-phenylethyl 3-methylbutanoate (0.2 %) was only detected in the leaf oil. γ-Muurolene (0.8 %), gossonorol (0.3 %), *cis*-calamenen-10-ol (0.5 %), α-bisabolol (0.9 %), tetradecanoic acid (0.5 %) and 14-hydroxy-δ-cadinene (0.4 %) were present only in the stalk oil and were completely absent from the other

two oils. An additional dissimilarity between these oils was the content of "green leaf"[18] (G) volatiles (volatile aliphatic aldehydes, alcohols, and their esters formed through the hydroperoxide lyase pathway of oxylipin metabolism, plants start to form Gs after disruption of their tissues and after suffering biotic or abiotic stresses), being predominant in the leaf oil (10.9 %), as expected.

TABLE I. Percentage composition of *Pleurospermum austriacum* oils[a]

RI[b]	Component	Fruit oil	Leaf oil	Stalk oil	Class	Method[c]
861	(*Z*)-3-Hexen-1-ol	0.2	8.8	1.4	G	a, b
863	1-Hexanol	tr[d]	1.3	0.4	G	a, b, c
1034	*β*-Phellandrene	2.3	tr	–	M	a, b
1383	*α*-Copaene	1.0	1.0	0.7	SCO	a, b
1428	*β*-Caryophyllene	3.1	5.7	4.9	SC	a, b, c
1460	(*E*)-*β*-Farnesene	1.0	1.2	1.5	SA	a, b
1462	Humulene	0.4	0.6	1.4	SC	a, b, c
1498	Germacrene D	66.5	62.4	49.0	SGE	a, b, c
1504	*epi*-Cubebol	tr	2.4	tr	SCA	a, b
1507	Bicyclogermacrene	3.3	tr	2.3	SGE	a, b
1511	(*E*,*E*)-*α*-Farnesene	0.6	1.3	1.7	SA	a, b
1514	*β*-Bisabolene	–	0.5	1.0	SBI	a, b, c
1532	*δ*-Cadinene	3.9	3.6	5.0	SCA	a, b
1650	*τ*-Muurolol (syn.[e] *epi*-*α*-muurolol)	0.5	0.3	1.0	SCA	a, b
1664	*α*-Cadinol	1.4	0.9	3.0	SCA	a, b
1962	Hexadecanoic acid	tr	–	5.2	O	a, b, c
2027	Isopropyl hexadecanoate	0.3	–	1.0	O	a, b, c
Total identified		95.1	98.6	94.5		
Number of identified comounds		156	116	117		
Monoterpenoids		2.8 (27)[f]	tr (8)	tr (5)		
Hydrocarbons		2.8 (15)	tr (6)	tr (3)		
Oxygenated derivatives		tr (12)	tr (2)	tr (2)		
Sesquiterpenoids		90.5 (66)	85.7 (58)	85.7 (67)		
Hydrocarbons		85.8 (40)	79.5 (37)	72.6 (36)		
Oxygenates derivatives		4.7 (26)	6.2 (21)	13.1 (31)		
Acyclic sesquiterpene (SA)		1.8 (7)	2.6 (7)	4.1 (8)		
Bisabolanes (SBI)		0.5 (5)	2.0 (7)	4.3 (10)		
Caryophyllanes and related (SC)		3.8 (3)	6.8 (3)	7.2 (3)		
Cadinanes and related (SCA)		8.1 (25)	8.6 (19)	14.6 (24)		
Copaanes and related (SCO)		1.3 (3)	1.3 (3)	1.1 (3)		
Germacranes and related (SGE)		71.9 (5)	63.2 (5)	52.2 (3)		
Other unclassified sesquiterpenes (S)		3.1 (18)	1.2 (14)	2.2 (16)		
Diterpenes (DT)		0.1 (2)	0.9 (5)	tr (2)		
"Green leaf" volatiles (G)		0.7 (27)	10.9 (24)	1.8 (16)		
Others (O)		1.0 (34)	1.1 (21)	7.0 (27)		

[a]The remainder of the identified constituents (minor, that have not reached 1 % in any of the samples) of the investigated essential oils are summarized in the following format bellow: *RI*, Component name, Relative percentage of the component in the fruit oil, Leaf oil and stalk oil, Class of the constituent, Method of identification; -743, pyridine, -, tr[d], -, O, a, b, c; 744, (*E*)-2-pentenal, -, tr, -, G, a, b; 762, 1-pentanol, -, -, tr, G, a, b, c; 765, (*Z*)-

2-penten-1-ol, tr, 0.2, tr, G, a, b; 780, (±)-2,3-butandiol, -, -, tr, O, a, b; 785, *meso*-2,3-butandiol, -, -, tr, O, a, b; 801, hexanal, tr, tr, tr, G, a, b; 834, furfural, tr, tr, tr, O, a, b, c; 852, (*E*)-3-hexen-1-ol, -, 0.1, tr, G, a, b; 885, 2--butylfuran, tr, tr, tr, G, a, b; 895, (2*E*,4*Z*)-2,4-hexadienal, tr, -, -, G, a; 900, nonane, tr, -, tr, O, a, b, c; 903, cyclohexanone, -, tr, -, O, a, b, c; 913, (2*E*,4*E*)-2,4-hexadienal, -, tr, -, G, a, b; 930, α-thujene, tr, -, -, M, a, b; 939, *α*-pinene, 0.1, -, tr, M, a, b, c; 955, camphene, tr, -, -, M, a, b, c; 957, (*E*)-2-heptenal, tr, tr, -, G, a, b; 967, benzaldehyde, tr, tr, tr, O, a, b, c; 978, sabinene, 0.1, tr, tr, M, a, b; 984, *β*-pinene, tr, -, -, M, a, b, c; 993, myrcene, tr, -, -, M, a, b, c; 995, 2-pentylfuran, tr, tr, tr, G, a, b; 999, 2,4,6-trimethylpyridine, -, tr, -, O, a, b, c; 1001, mesitylene, tr, -, -, O, a, b, c; 1005, octanal, tr, tr, tr, G, a, b; 1008, (*E*)-3-hexenyl acetate, 0.1, 0.2, tr, G, a, b; 1010, *α*-phellandrene, 0.3, -, -, M, a, b; 1013, 1-hexyl acetate, -, tr, -, G, a, b, c; 1014, (2*E*,4*E*)-2,4-heptadienal, -, tr, tr, G, a, b; 1021, *α*-terpinene, tr, -, -, M, a, b, c; 1029, *p*-cymene, tr, tr, tr, M, a, b, c; 1033, limonene, tr, tr, -, M, a, b, c; 1044, *β*-isophorone, tr, -, -, O, a, b, c; 1048, phenylacetaldehyde, tr, 0.2, tr, O, a, b, c; 1048, (*E*)-*β*-ocymene, tr, -, -, M, a, b; 1059, (*Z*)-2-octenal, tr, -, -, G, a, b; 1062, *γ*-terpinene, tr, tr, -, M, a, b; 1062, artemisia ketone, tr, -, -, M, a, b, c; 1070, 1-octanol, -, tr, -, G, a, b, c; 1072, acetophenone, -, -, tr, O, a, b, c; 1077, *cis*-linalool oxide (furanoid), tr, -, -, M, a, b, c; 1094, terpinolene, tr, -, -, M, a, b; 1094, *trans*-linalool oxide (furanoid), tr, -, -, M, a, b, c; 1098, 3-isopropyl-2-methoxypyrazine, tr, -, -, O, a, b; 1100, undecane, tr, tr, tr, O, a, b, c; 1103, linalool, tr, tr, tr, M, a, b, c; 1107, nonanal, 0.1, 0.1, -, G, a, b; 1107, hotrienol, tr, -, -, M, a, b; 1109, 2-methylbutyl isovalerate, tr, -, -, O, a, b; 1118, 3-methyl-3-butenyl 3-methylbutanoate, tr, -, -, O, a, b; 1120, *endo*-fenchol, tr, -, -, M, a, b; 1127, dehydrosabina ketone, tr, -, -, M, a, b; 1127, α-isophorone, tr, -, -, O, a, b; 1162, (*E*)-2-nonenal, tr, -, -, G, a, b; 1184, terpinen-4-ol, tr, -, -, M, a, b, c; 1191, naphthalene, tr, -, -, O, a, b, c; 1194, cryptone, tr, -, -, M, a, b; 1199, (*Z*)-4-decenal, tr, -, -, G, a, b; 1201, methyl salicylate, tr, 0.2, tr, O, a, b, c; 1208, decanal, tr, tr, -, G, a, b, c; 1225, *endo*-fenchyl acetate, tr, tr, -, M, a, b; 1227, *β*-cyclocitral, -, tr, -, O, a, b, c; 1227, (2*E*,4*E*)-2,4-nonadien-1-ol, tr, -, -, G, a, b; 1234, (*Z*)-3-hexenyl 2-methylbutanoate, tr, tr, -, G, a, b; 1238, (Z)-3-hexenyl 3-methylbutanoate, 0.1, 0.2, tr, G, a, b; 1238, 1-hexyl 2-methylbutanoate, tr, -, -, G, a, b; 1238, methyl thymol , tr, -, -, M, a, b, c; 1243, 1-hexyl isovalerate, 0.2, tr, tr, G, a, b; 1248, methyl carvacrol, tr, -, -, M, a, b, c; 1265, (*E*)-2-decenal, tr, -, -, G, a, b; 1294, 1-tridecene, tr, -, -, O, a, b; 1297, (2*E*,4*Z*)-2,4-decadienal, tr, -, -, G, a, b; 1300, tridecane, tr, tr, -, O, a, b, c; 1300, 2-methylnaphtalene, tr, -, -, O, a, b; 1309, undecanal, tr, -, -, G, a, b; 1317, (*E*)-3-hexenyl tiglate, tr, tr, -, G, a, b; 1319, *p*-vinylguaiacol, -, tr, -, O, a, b; 1321, (2*E*,4*E*)-2,4-decadienal, tr, tr, tr, G, a, b; 1323, 1-hexyl senecioate (hexyl 2-methyl-2-butenoate), tr, tr, -, G, a, b; 1325, (*E*)-9-undecenal, -, -, tr, G, a, b; 1343, bicycloelemene, 0.1, tr, -, S, a, b; 1355, *α*-cubebene, 0.1, tr, tr, S, a, b; 1374, cyclosativene, tr, -, -, S, a, b; 1378, *α*-ylangene, tr, tr, tr, S, a, b; 1390, geranyl acetate, tr, tr, tr, M, a, b, c; 1392, *β*-bourbonene, tr, tr, tr, S, a, b; 1397, *β*-cubebene, 0.6, 0.8, 0.6, S, a, b; 1398, *β*-elemene, 0.5, tr, tr, S, a, b; 1411, dodecanal, tr, tr, tr, G, a, b; 1419, *α*-gurjunene, 0.2, tr, -, S, a, b; 1421, *cis*-*α*-bergamotene, -, -, tr, SBI, a, b; 1437, *β*-copaene, 0.3, 0.3, 0.4, SCO, a, b; 1441, *trans*-*α*-bergamotene, -, tr, tr, SBI, a, b; 1443, *β*--gurjunene, 0.8, tr, tr, S, a, b; 1448, aromadendrene, tr, tr, -, S, a, b; 1454, *cis*-muurola-3,5-diene, 0.1, -, -, SCA, a, b; 1472, *cis*-muurola-4(14),5-diene, 0.3, 0.2, 0.3, SCA, a, b; 1484, *γ*-muurolene, -, -, 0.8, SCA, a, b; 1485, *γ*--curcumene, -, -, tr, SBI, a, b; 1488, herbertene, -, -, tr, SBI, a, b; 1496, 1-phenylethyl 3-methylbutanoate, -, 0.2, -, O, a, b; 1498, 10,11-epoxy-calamenene, -, -, tr, SCA, a, b; 1500, *β*-selinene, tr, -, 0.2, S, a, b; 1502, *α*-zingiberene, tr, 0.4, -, SBI, a, b; 1503, *trans*-muurola-4(14),5-diene, 0.4, tr, 0.6, SCA, a, b; 1507, *α*-muurolene, tr, tr, tr, SCA, a, b; 1511, *α*-cuprenene, tr, tr, tr, SBI, a, b; 1515, germacrene A, 0.6, tr, -, SGE, a, b; 1515, *δ*-amorphene, tr, -, -, SCA, a, b; 1517, *β*-curcumene, 0.2, 0.4, 0.8, SBI, a, b; 1523, *γ*-cadinene, 0.5, 0.3, 0.5, SCA, a, b; 1524, cubebol, tr, tr, -, SCA, a, b; 1538, (*E*)-*γ*-bisabolene, 0.2, 0.4, 0.7, SBI, a, b; 1540, *trans*-cadina-1,4-diene, 0.1, tr, tr, SCA, a, b; 1546, *α*-cadinene, 0.1, tr, tr, SCA, a, b; 1552, *α*-calacorene, tr, tr, 0.2, SCA, a, b; 1557, *cis*--muurola-5-en-4*β*-ol, tr, -, -, SCA, a, b; 1557, dodecanoic acid, -, -, tr, O, a, b, c; 1564, *cis*-cadinene ether, tr, -, -, SCA, a, b; 1565, *cis*-muurola-5-en-4*α*-ol, tr, -, -, SCA, a, b; 1568, (*E*)-nerolidol, 0.1, 0.1, 0.5, SA, a, b; 1571, *β*--calacorene, tr, tr, tr, SCA, a, b; 1574, *γ*-undecalactone, tr, -, -, O, a, b; 1576, mint oxide, 0.1, 0.1, 0.3, S, a, b; 1582, (*E*)-dendrolasin, tr, tr, tr, SA, a, b; 1584, germacrene D-4-ol, 0.9, 0.3, -, SGE, a, b; 1587, spathulenol, tr, 0.1, 0.2, S, a, b, c; 1590, 10-*epi*-junenol, -, -, tr, S, a, b; 1593, caryophyllene oxide, 0.3, 0.5, 0.9, SC, a, b, c; 1595, β-copaen-4*α*-ol, tr, -, -, SCO, a, b; 1597, *cis*-*β*-elemenone, -, -, tr, S, a, b; 1603, salvial-4(14)-en-1-one, 0.1, tr, tr, S, a, b; 1610, 3-phenylpropyl 2-methylbutanoate, tr, -, -, O, a, b; 1611, rosifoliol, -, -, tr, S, a, b; 1613, 3-phenylpropyl 3-methylbutanoate, tr, -, -, O, a, b; 1615, tetradecanal, 0.1, 0.3, 0.3, O, a, b, c; 1623, 1,10-di-*epi*--cubenol, tr, tr, 0.5, SCA, a, b; 1629, junenol, 0.2, 0.1, 0.6, S, a, b; 1630, α-corocalene, -, -, tr, SCA, a, b; 1632, *nor*-copaanone, -, tr, tr, SCO, a, b; 1637, 1-*epi*-cubenol, 0.1, 0.2, 0.2, SCA, a, b; 1645, gossonorol, -, -, 0.3, S, a, b; 1650, *τ*-cadinol (syn.[e] *epi*-*α*-cadinol), 0.5, 0.3, 0.9, SCA, a, b; 1650, *τ*-muurolol (syn. *epi*-*α*-muurolol), 0.5, 0.3, 1.0, SCA, a, b; 1655, *α*-muurolol, 0.2, 0.2, 0.7, SCA, a, b; 1667, *cis*-calamenen-10-ol, -, -, 0.5, SCA, a, b;

1678, *trans*-calamenen-10-ol, tr, 0.2, tr, SCA, a, b; 1688, cinnamyl valerate (correct isomer not determined), 0.1, -, -, O, a; 1690, *epi*-*α*-bisabolol, 0.1, 0.3, 0.9, SBI, a, b; 1692, *α*-bisabolol, -, -, 0.9, SBI, a, b, c; 1696, germacra-4(15),5,10(14)-trien-1*α*-ol, 0.6, 0.5, 0.9, SGE, a, b; 1701, shyobunol, 0.3, -, -, S, a, b; 1701, 3-phenylpropyl hexanoate (correct isomer not determined), tr, -, -, O, a; 1705, (2*Z*,6*Z*)-farnesol, -, -, tr, SA, a, b; 1713, amorpha-4,9-dien-2*α*-ol, tr, -, tr, SCA, a, b; 1717, pentadecanal, tr, -, tr, O, a, b; 1720, (2*E*,6*Z*)-farnesal, tr, tr, tr, SA, a, b; 1727, (2*Z*,6*E*)-farnesol, 0.1, tr, 0.4, SA, a, b; 1747, (2*E*,6*E*)-farnesal, tr, tr, tr, SA, a, b; 1749, mint sulfide, tr, 0.1, tr, S, a, b; 1763, tetradecanoic acid, -, -, 0.5, O, a, b, c; 1772, aristolone, 0.1, -, -, S, a, b; 1782, 14-hydroxy-*α*-muurolene, tr, tr, tr, SCA, a, b; 1811, 14-hydroxy-*δ*-cadinene, -, -, 0.4, SCA, a, b; 1818, hexadecanal, tr, tr, tr, O, a, b, c; 1841, neophytadiene, isomer II, 0.1, 0.8, tr, DT, a, b; 1862, pentadecanoic acid, -, -, tr, O, a, b; 1900, nonadecane, tr, -, -, O, a, b, c; 1928, methyl hexadecanoate, -, -, tr, O, a, b, c; 1944, (*Z*)-9--hexedecenoic acid (palmitoleic acid), -, -, tr, O, a, b, c; 1950, isophytol, -, tr, -, DT, a, b; 1971, (*Z*,*Z*)-geranyl linalool, -, tr, -, DT, a, b; 1996, ethyl hexadecanoate, -, -, tr, O, a, b, c; 2000, eicosane, tr, -, -, O, a, b, c; 2034, (*E*,*E*)-geranyl linalool, tr, 0.1, tr, DT, a, b; 2083, 1-octadecanol, -, -, tr, O, a, b, c; 2100, heneicosane, 0.1, tr, -, O, a, b, c; 2117, (*E*)-phytol, -, tr, -, DT, a, b; 2200, docosane, tr, tr, -, O, a, b, c; 2281, 1-eicosanol, tr, -, -, O, a, b, c; 2300, tricosane, 0.2, 0.1, tr, O, a, b, c; 2396, 1-tetracosene, -, tr, tr, O, a, b; 2400, tetracosane, tr, tr, tr, O, a, b, c; 2500, pentacosane, 0.2, 0.1, tr, O, a, b, c; 2600, hexacosane, -, -, tr, O, a, b, c; 2700, heptacosane, -, tr, -, O, a, b, c; 2833, (all *E*)-squalene, -, -, tr, O, a, b.; [b]experimentally determined retention indices by co-injection of a homologous series of *n*-alkanes (C_7–C_{29}); [c]a – constituent identified by mass spectra comparison, b – constituent identified by retention index matching, c – constituent identity confirmed by co-injection of an authentic sample; [d]trace (<0.05 %); [e]synonym; [f]the value in brackets represents the number of identified compounds belonging to this specific class; M – monoterpenoids; SA – acyclic sesquiterpenes; SBI – bisabolanes; SC – caryophyllanes and related sesquiterpenoids; SCA – cadinanes and related sesquiterpenoids; SCO – copaanes and related sesquiterpenoids; SGE – germacranes and related sesquiterpenoids; S – other unclassified sesquiterpenes; DT – diterpenes; G – "green leaf" volatiles (aliphatic aldehydes, alcohols, and their esters formed as the plants response after suffering biotic or abiotic stresses); O – other unclassified constituents

The only previously published investigated essential oil from a *Pleurospermum* species was the one from *P. lindleyanum* (according to Pimenov and Kljuykov,[3] this taxon is transferred to the genus *Hymenidium* (*H. stellatum*)).[4] The authors state that 73 oil constituents were identified, and among them were: 1-propoxy-2-propanol, myristicin, 1,2,3-trimethoxy-5-(2-propenyl)-benzene, *cis*--asarone, *n*-hexane, apiol, dimethyl ether, 1,2-dimethoxy-4-(2-propenyl)benzene, ethyl acetate, spathulenol, *α,α*',4-trimethyl-benzenemethanol, *trans*-methyl *iso*-eugenol, and *β*-phellandrene. Apparently a number of the listed compounds represent either misidentifications or identification of a solvent contaminant introduced during the work-up of the essential oil sample (1-propoxy-2-propanol, dimethyl ether, *n*-hexane, ethyl acetate). Apart from this, the authors refer to the content (20.77 %) of cycloserine "as the highest" in conjunction with the essential oil.[4] The compounds in common with the present *P. austriacum* oil were spathulenol and *β*-phellandrene.

The sesquiterpenoid fraction of the oils of *P. austriacum* was mostly comprised of germacranes and highly related types of compounds (Table I) that are the first steps in the biosynthesis pathway of sesquiterpenes from farnesyl diphosphate. Sesquiterpene biosynthesis seems to be complex since the formation *via* either pathway (mevalonic or methylerythrytol) or a combination of both has been reported.[19] However, these appear to be omnipresent in plant taxa and some insects, and is related to the cytosol–mitochondria. A previous investigation showed

a direct correlation between the amount and chemical composition of the essential oils.[18] The results of these statistical analyses strongly suggest that the main volatiles of essential oil-poor species (yields less than 0.1 %) are fatty acid- and carotenoid-derived compounds, while the essential oil rich taxa (essential oil yields much higher than 0.1 %) are generally characterized by the specific production of monotepenoids and/or phenylpropanoids.[18] Two facts, the monoterpenes that accounted only for 0.0–2.8 % and that the yield of each oil was quite low (0.003–0.086 %, w/w), corroborate the previously introduced hypothesis concerning a possible link between the oil yield and the corresponding oil composition. It is, then, directly possible to conclude that if some plant is rich in oil, it will probably have a big portion of monoterpenes, or the phenylpropanoids are predominant. A related hypothesis concerning a possible link between oil yield and composition was already proposed.[20] Lawrence suggested that the oil-poor species of the family Lamiaceae produce essential oils rich in hydrocarbons, with germacrene D often being one of the predominant components.[20] This does not seem to stand for the Lamiaceae alone. For example, in the oil-poor (0.18–0.57 %) aerial parts of *Tamarix boveana* (Tamaricaceae), germacrene D (7.69–31.43 %) with its congeners represented the predominant class of volatile compounds.[21] In some previous investigations of *Lippia alba* (Verbenaceae), possible connections between the morphological characteristics and chemotypes were discussed, and a large content of germacrene D was a feature of one of the chemotypes.[22] More strikingly, a study on *Artemisia annua* showed that the glandless leaves were estimated to contain more than twice as much total sesquiterpenes per unit of fresh weight as the glanded leaves. In this way, the absence of monoterpenes in the steam-distilled oil of the glandless biotype is a good indication that the monoterpenes accumulate exclusively in specialized tissue structures, the glandular trichomes.[23] Thus, one may expect to find germacrene D and/or its hydrocarbon congeners as major constituents of essential oil in plant species not possessing an elaborate biosynthetic apparatus for the production of volatile monoterpenes or phenylpropanoids, as *P. austriacum*.

Acknowledgements. The financial support of this work by the Ministry of Science and Technological Development of the Republic of Serbia is gratefully acknowledged (Project No. 172061).

И З В О Д

ИСПАРЉИВИ САСТОЈЦИ БИЉНЕ ВРСТЕ *Pleurospermum austriacum* (L.) Hoffm. (APIACEAE)

НИКО С. РАДУЛОВИЋ, НЕВЕНКА Д. ЂОРЂЕВИЋ и РАДОСАВ М. ПАЛИЋ

Одсек за хемију, Природно-математички факултет, Универзитет у Нишу, Вишеградска 33, 18000 Ниш

Резултати детаљних GC и GC–MS анализа испарљивих састојака свежих листова, стабљика и плодова угрожене биљне врсте *Pleurospermum austriacum* (L.) Hoffm. (Apiaceae) приказани су у овом раду по први пут. Око 4/5 уља, добијених у ниском приносу (0,003–0,086

mas. %), је било сачињено од сесквитерпенских угљоводоника. Главне компоненте, идентификоване у уљима, су гермакрен Д (66,5 % у плоду, 62,4 % у лишћу и 49,0 % у стабљици), *β*-кариофилен (3,1–5,7 %), *δ*-кадинен (3,6–5,0 %) и (*E*)-*β*-фарнезен (1,0–1,5 %).

(Примљено 23. марта, ревидирано 12. маја 2010)

REFERENCES

1. 1. T. G. Tutin, in *Flora Europaea 2*, T. G. Tutin, V. H. Heywood, N. A. Burges, D. M. Moore, D. H. Valentine, S. M. Walters, D. A. Webb, Eds., Cambridge University Press, London, 1968, p. 343.
2. P. Zehui, F. M. Watson, *Flora Chn.* **14** (2005) 40
3. M. G. Pimenov, E. V. Kljuykov, *Feddes Rep*. **111** (2000) 517
4. H. A. Aisa, Q. Y. Lu, *Tianran Chanwu Yanjiu Yu Kaifa (Nat. Prod. Res. Dev.)* **14** (2002) 46
5. J. J. Tan, C. H. Tan, Y. Q. Wang, S. H. Jiang, D. Y. Zhu, *Helv. Chim. Acta* **89** (2006) 117
6. J. J. Tan, S. H. Jiang, D. Y. Zhu, *Tianran Chanwu Yanjiu Yu Kaifa (Nat. Prod. Res. Dev.)* **17** (2005) 267
7. Y. G. Luo, B. G. Li, G. L. Zhang, *J. Asian Nat. Prod. Res*. **4** (2002) 155
8. M. Taniguchi, Y. Hada, K. Baba, Y. Q. Xiao, in *Proceeding of 42nd Symposium on the Chemistry of Natural Products*, (2000), Okinawa, Japan, 2000, p. 529.
9. M. Taniguchi, Y. Q. Xiao, X. H. Liu, A. Yabu, Y. Hada, K. Baba, *Chem. Pharm. Bull*. **46** (1998) 1946
10. M. Taniguchi, Y. Q. Xiao, K. Baba, *Chem. Pharm. Bull*. **48** (2000) 1246
11. M. Taniguchi, Y. Q. Xiao, X. H. Liu, A. Yabu, Y. Hada, L. Q. Guo, Y. Yamazoe, K. Baba, *Chem. Pharm. Bull*. **47** (1999) 713
12. M. Shibano, H. Naito, M. Taniguchi, N. H. Wang, K. Baba, *Chem. Pharm. Bull*. **54** (2006) 717
13. U. Mahmood, S. B. Singh, R. S. Thakur, *Phytochemistry* **22** (1983) 774
14. U. Mahmood, R. S. Thakur, *Indian J. Pharm. Sci.* **43** (1981) 157
15. O. Gerdjikov, *Biological diversity act*, National Assembly, Republic of Bulgaria, Promulgated, *State gazette* no. 77/9.08.2002
16. H. Van Den Dool, P. D. Kratz, *J. Chromatogr*. **11** (1963) 463
17. R. P. Adams, *Identification of Essential Oil Components by Gas Chromatography and Mass Spectrometry*, 4th ed., Allured Publishing Corporation, Carol Stream, IL, 2007
18. N. S. Radulović, P. D. Blagojević, R. M. Palić, *Nat. Prod. Commun.* **4** (2009) 405
19. D. Umlauf, J. Zapp, H. Becker, K. P. Adam, *Phytochemistry* **65** (2004) 2463
20. B. M. Lawrence, *Essential Oil 1988-1991*, Allured Publishing Corporation, Carol Stream, IL, 1992, p. 194
21. D. Saïdana, M. A. Mahjoub, O. Boussaada, J. Chriaa, I. Chéraif, M. Daami, Z. Mighri, A. N. Helal, *Microbiol. Res.* **163** (2008) 445
22. T. Hennebelle, S. Sahpaz, C. Dermont, H. Joseph, F. Bailleul, *Chem. Biodivers.* **3** (2006) 1116
23. R. M. Tellez, C. Canel, M. A. Rimando, O. S. Duke, *Phytochemistry* **52** (1999) 1035.

Journal of the Serbian Chemical Society
JSCS-info@shd.org.rs • www.shd.org.rs/JSCS
J. Serb. Chem. Soc. 75 (12) 1661–1669 (2010) UDC *Levisticum officinale*:665.52:615.281–188
JSCS–4086 *Original scientific paper*

The composition and antibacterial activity of the essential oil of *Levisticum officinale* Koch flowers and fruits at different developmental stages

MOHAMMAD HOSSEIN MIRJALILI[1]*, PEYMAN SALEHI[1], ALI SONBOLI[1], JAVAD HADIAN[1], SAMAD NEJAD EBRAHIMI[1] and MORTEZA YOUSEFZADI[2]

[1]*Medicinal Plants and Drugs Research Institute, Shahid Beheshti University, G. C., Evin, Tehran and* [2]*Department of Marine Biology, Faculty of Science, Hormozgan University, Bandar Abbas, Iran*

(Received 24 May, revised 9 July 2010)

Abstract: The composition and antibacterial activity of the essential oil of *Levisticum officinale* Koch at different developmental stages (flower, immature fruit, green mature fruit and ripened fruit) is reported. The essential oils were obtained by hydrodistillation of air-dried samples and their antibacterial activities were tested against seven bacteria. The yield of oil (w/w %) in different stages was in the order: immature fruit (1.5 %) > green mature fruit (1.0 %) > > ripened fruit (0.6 %) > flower (0.1 %). The essential oils were analyzed by GC and GC–MS. In total, 27, 31, 28 and 26 constituents were identified and quantified in the mentioned samples, respectively. Monoterpene hydrocarbons were the main group of compounds in the green mature fruit (79.2 %), immature fruit (78.4 %), ripened fruit (75.2 %) and flower (44.0 %). The antibacterial activity of the oils was evaluated by the disk diffusion method using Müller–Hinton agar and determination of inhibition zones. The results of the bioassays showed some variations between the three tested oils in their inhibitory activity against the tested bacteria at a 10 µl disc^{-1} concentration. The oils from mature and ripened fruit exhibited potent antibacterial activity against *Bacillus subtilis*, with minimum inhibitory concentration (*MIC*) values of 0.90 mg ml^{-1} in mature and ripened fruits.

Keywords: Levisticum officinale Koch; Apiaceae; essential oil; antibacterial activity; reproductive stage.

INTRODUCTION

Lovage (*Levisticum officinale* Koch) is a perennial herbaceous plant from the Apiaceae family with origins in Iran and Afghanistan; it can now be found throughout the world.[1–4] The plant has been alternatively classified as *Ligus-*

* Corresponding author. E-mail: m-mirjalili@sbu.ac.ir
doi: 10.2298/JSC100524126M

ticum levisticum L., *Hipposelinum levisticum* Britt. and *Angelica levisticum* Baillon.[5] The essential oil of roots, seeds and leaves of lovage are used in a wide variety of applications including food flavoring, medicinal preparations, aromatherapy, perfumery and industrial fragrances.[2,6,7] Moreover, the plant is used in Iranian folk medicine for the treatment of several gastrointestinal, nervous and rheumatic disorders.[2,8] The essential oil composition of the plant was previously studied in different countries and more than 190 compounds were reported in its root, seed or leaf oil.[9] It was found that the chemical compositions of the essential oils distilled from separate botanical parts of this plant are rather different.[10–12] The chemical constituents of lovage root oil are mainly phthalides including *n*-butylidene phthalide and *n*-butyl-phthalide, sedanonic anhydride, terpenoids such as α-terpineol, carvacrol, phenylpropanoids such as eugenol and volatile acids.[5,13,14] Polyacetylenes as antimycobacterial compounds have also been reported from the plant.[15] The effect of harvesting time, plant age, cutting frequency and the method of plantation establishment on the essential oil yield and components in different parts of *L. officinale* was investigated previously.[7,11,16,17] It was found that the flowers and seeds produced the highest yields of the oil with β-phellandrene (40.8 and 61.5 %, respectively) as the main constituent, while α-terpinyl acetate (≈70.0 %) was reported as the principal constituent of the leaves and stems oils.[7] In another study, the oil of lovage fruits contained β-phellandrene (69.3 %), α-terpinenyl acetate (4.2 %) and α-terpineol (2.1 %) as the major components.[12] It was reported that the essential oil content was similar in roots, stems, petioles, leaves and inflorescence, while the highest content was found in seeds (1.9 %).[18] Seasonal variations in the composition of headspace volatiles were also determined,[10] of which, β-phellandrene was the most abundant component in all plant parts except for root. Samiee *et al*. reported terpinyl acetate (40.5 %) and β-phellandrene (16.7 %) as the main constituents in the essential oil and β-phellandrene (23.0 %), naphthalene (20.6 %) and γ-terpinene (12.1 %) as the major components in the methanol extract of the plant from Iran.[19] Recently, (*Z*)-falcarinol, *n*-octanal, palmitic acid, (*Z*)-ligustilide, (*Z*)--3-butylidenephthalide, *trans*-β-farnesene have been reported as the main compounds of the essential oil of hairy root cultures of *L. officinale*.[20–22] Variations in the essential oil composition of roots and leaves of *L. officinale* from different European countries have also been studied. Ten compounds, including *trans*-*p*--mentha-2,8-dien-1-ol, *iso*-thujyl alcohol, *p*-mentha-1,5-dien-8-ol, bicyclo[3.2.0]-heptan-3-ol, 2-methylene-6,6-dimethyl, *trans*-carveol, perillaldehyde, sabinyl acetate, perillyl alcohol, the methyl ester of methylpentadecanoic acid and methylhexadecadienoic acid, were introduced for the first time.[23] To the best of our knowledge, there is no previous report on the essential oil analysis and antibacterial activity of *L. officinale* at different developmental stages. Thus, in this pa-

per, the composition and antibacterial activity of the essential oils of this plant at different stages of its development are reported.

EXPERIMENTAL

Plant material

These experiments were conducted during 2007–2009 at the field of the Medicinal Plants and Drugs Research Institute of Shahid Beheshti University, located in Evin (35°48' N, 51°23' E at an altitude of 1785 m) in the north of Tehran, Iran. The plant seeds were obtained from the seed bank of the Medicinal Plants and Natural Products Research Institute, Iranian Academic Center for Education, Culture and Research (ACECR) and were sown in a greenhouse in the last week of February, 2007. Nine-week-old seedlings were transplanted at 50 cm row-to-row and 30 cm plant-to-plant spacing in the experimental field in May, 2007. The sampling was realized from a 2-year-old cultivated population by the random collection of 10 individuals for each developmental stage. For the collection of the flowers, all of them on the inflorescence were opened. The samples at the fruiting stage were collected at three different times of fruit maturation, *i.e*. immature (infructescence with young fruits 15 days after flowering), mature (infructescence with solid and dark green colored fruit) and ripened (infructescence with yellowish fruits just in the deciduous time). Voucher specimens (No. 200364-7) representative of each sample were deposited at the Medicinal Plants and Drugs Research Institute Herbarium (MPH), Shahid Beheshti University of Tehran.

Essential oil isolation procedure

The essential oil of air-dried samples (100 g) of each stage was isolated by hydrodistillation for 3 h, using a Clevenger-type apparatus according to the method recommended in British Pharmacopoeia (1993).[24] The isolated oils were dried over anhydrous sodium sulfate and stored in dark tightly closed vials at 4 °C until analysis.

Essential oil analysis procedure

GC analysis was conducted using a Varian CP-3800 instrument equipped with a DB-1 fused silica capillary column (25 m×0.25 mm i.d., film thickness 0.25 μm). Nitrogen was used as the carrier gas at a constant flow rate of 1.1 ml min^{-1}. The oven temperature was held at 60 °C for 1 min, then programmed to 250 °C at a rate of 4 °C min^{-1}, and then held for 10 min. The injector and detector (FID) temperatures were kept at 250 and 280 °C, respectively. GC/MS analysis was realized on a Thermoquest-Finnigan Trace GC/MS instrument equipped with a DB-1 fused silica column (60 m×0.25 mm i.d., film thickness 0.25 μm). The oven temperature was raised from 60 to 250 °C at a rate of 5 °C min^{-1} and then held at 250 °C for 10 min; the transfer line temperature was 250 °C. Helium was used as the carrier gas at a flow rate of 1.1 ml min^{-1}; the split ratio was 1/50. The quadrupole mass spectrometer was scanned over the 45–465 amu range with an ionizing voltage of 70 eV and an ionization current of 150 μA.

Identification and quantification of the oil components

The constituents of the essential oils were identified by calculation of their retention indices under temperature-programmed conditions for *n*-alkanes (C6–C24) and the oil on a DB-1 column under the same chromatographic condition. Identification of individual compounds was made by comparison of their mass spectra with those of the internal reference mass spectra library or with authentic compounds and confirmed by comparison of their retention indices with authentic compounds (purchased from Sigma-Aldrich and Merck) or with those reported in the literature.[25] For quantification purpose, the relative area percentages obtained by FID were used without the use of correction factors.

Antibacterial activity

The antibacterial activity of the oils was evaluated by the disk diffusion method using Müller-Hinton agar[26] and determination of the inhibition zones. The essential oils were tested at a concentration of 10 μl per disk. The microorganisms used were as follows: *Bacillus subtilis* ATCC 9372, *Enterococcus faecalis* ATCC 15753, *Staphylococcus aureus* ATCC 25923, *Staphylococcus epidermidis* ATCC 12228, *Escherichia coli* ATCC 25922, *Pseudomonas aeruginosa* ATCC 27852, and *Klebsiella pneumoniae* ATCC 3583. For the determination of the minimum inhibitory concentration (*MIC*), a microdilution broth susceptibility assay was used, as recommended by NCCLS.[27] The technical data were described previously.[28] Ampicillin was used as the standard reference for the positive control.

RESULTS AND DISCUSSION

Essential oil analysis

The essential oils had a light yellow color with distinct sharp odor. The yield of the essential oils (w/w %) of the plant at different developmental stages were in the order: immature fruit (1.5 %) > green mature fruit (1.0 %) > ripened fruit (0.6 %) > flower (0.1 %). The qualitative and quantitative analytical results are listed in Table I together with the retention indices of the identified compounds, where all the constituents are arranged in order of their elution on the DB-1 column. In total 27, 31, 28 and 26 constituents, respectively, were identified and quantified in the studied samples representing 95.9, 99.9, 98.7 and 92.7 % of the total oil, respectively. A comparison among the composition of the essential oils revealed both quantitative and qualitative differences. The GC and GC–MS analyses showed that the distribution of saturated hydrocarbons of the oil from flower was remarkably different from that of the oils at the fruiting stage. The results revealed that the saturated hydrocarbons from the flower (12.3 %) were present in higher amount than in the other samples. Heneicosane (6.0 %) and tricosane (3.0 %) were found only in the oil of the flower. The major constituent of the oil of the flower was *β*-pinene (17.7 %), but it was found that this compound decreased gradually in subsequent developmental stages. The *β*-pinene and *α*-pinene contents were highest in the essential oil of the first harvest and decreased with progressive maturation of the fruit. On the contrary, *β*-phellandrene was found as the principal component of the oil after fruit initiation, *i.e.*, it constituted 11.7 % of the oil of the flower but increased remarkably in the fruit oils, constituting 62.4, 60.5 and 56.4 % of the green mature, immature and ripened fruit oils, respectively. *β*-Phellandrene has already been reported as the main constituent in the essential oil from the flowers and fruits in previous reports.[7,10,12] *β*-Gurjunene (2.8 %), globulol (0.7 %) and geranyl acetate (3.3 %) were found only in the oil of the flower. *α*-Phellandrene, *δ*-elemene and germacrene-D were absent completely in the oil of flower but were present in trace or low amounts in the other samples. The essential oil obtained from immature fruit contained the highest contents of sabinene (2.3 %), isomenthol (5.6 %), *cis*-dihydrocarvon (0.6

%), germacrene-D (0.6 %), elemol (0.5 %) and *trans*-nerolidol (1.6 %) compared with the other samples.

TABLE I. Composition of the essential oil of *Levisticum officinale* at different developmental stages

RI[a]	Compound	From flowers %	In fruiting stages, %			Identification methods
			Immature	Mature	Ripened	
0935	*α*-Pinene	5.3	4.6	4.3	2.9	RI, MS[b], CoI[c]
0969	Sabinene	1.7	2.3	1.5	1.1	RI, MS
0976	*β*-Pinene	17.7	11.5	4.1	2.9	RI, MS, CoI
0982	Myrcene	1.3	t[d]	t	t	RI, MS
1002	*α*-Phellandrene	–	t	t	t	RI, MS
1010	*δ*-3-Carene	3.0	2.8	5.7	6.8	RI, MS
1017	*ortho*-Cymene	1.4	t	t	t	RI, MS
1026	*β*-Phellandrene	11.7	56.4	62.4	60.5	RI, MS
1038	*cis*-Ocimene	1.9	0.8	0.8	0.8	RI, MS
1083	Terpinolene	–	–	0.4	0.2	RI, MS, CoI
1111	*cis*-*p*-Menth-2-en-1-ol	–	0.3	–	0.2	RI, MS
1162	Isomenthol	1.8	5.6	3.9	2.1	RI, MS
1166	4-Terpineol	0.5	0.6	–	–	RI, MS
1168	*cis*-Dihydrocarvone	–	0.6	–	–	RI, MS
1217	Cuminyl aldehyde	–	0.5	t	–	RI, MS
1265	*p*-Cymene-7-ol	–	0.4	t	–	RI, MS
1339	*δ*-Elemene	–	0.4	0.3	0.3	RI, MS
1358	Geranyl acetate	3.3	–	–	–	RI, MS, CoI
1385	*α*-Copaene	1.3	0.3	0.3	0.2	RI, MS
1392	*β*-Elemene	1.0	1.2	1.3	1.3	RI, MS
1433	*α*-Humulene	0.9	0.4	0.3	0.2	RI, MS
1436	*β*-Gurjunene	2.8	–	–	–	RI, MS
1446	(*Z*)-*β*-Farnesene	4.3	0.2	0.2	0.2	RI, MS
1473	*γ*-Curcumene	8.0	0.2	0.2	0.3	RI, MS
1484	Germacrene-D	–	0.6	0.3	t	RI, MS
1489	Zingiberene	0.8	0.5	0.8	t	RI, MS
1500	Germacrene-B	0.8	1.6	t	1.2	RI, MS
1503	*β*-Bisabolene	1.6	0.8	1.8	–	RI, MS
1518	*β*-Sesquiphellandrene	2.1	1.2	2.4	5.1	RI, MS
1541	Elemol	–	0.5	–	–	RI, MS
1548	*trans*-Nerolidol	0.8	1.6	–	–	RI, MS
1562	*γ*-Elemene	–	0.8	0.8	1.2	RI, MS
1574	Spathulenol	8.9	1.1	1.9	2.7	RI, MS
1593	Globulol	0.7	–	–	–	RI, MS
1601	Hexadecane	3.3	2.1	2.5	2.2	RI, MS
1691	3-*iso*-Thujopsanone	–	–	2.5	0.3	RI, MS
2097	Heneicosane	6.0	–	–	–	RI, MS
2301	Tricosane	3.0	–	–	–	RI, MS
–	Monoterpene hydrocarbons	44.0	78.4	79.2	75.3	–

TABLE I. Continued

RI[a]	Compound	From flowers %	In fruiting stages, %			Identification methods
			Immature	Mature	Ripened	
–	Oxygenated monoterpenes	8.9	8.0	3.5	2.3	
–	Sesquiterpene hydrocarbons	20.3	9.0	9.1	10.7	
–	Oxygenated sesquiterpenes	10.4	2.4	4.4	2.2	
–	Other	12.3	2.1	2.5	2.2	
Total identified		95.9	99.9	98.7	92.7	

[a]Retention indices relative to C_6–C_{24} *n*-alkanes on a DB-1 column; [b]mass spectroscopy; [c]co-injection with authentic compounds; [d]trace, less than 0.1 %

The classification of the identified compounds based on functional groups is summarized at the end of Table I and shows that monoterpene hydrocarbons were the main group of compounds in all samples. The monoterpene hydrocarbons content was the lowest in the flower and increased with subsequent harvesting times to reach maximum in the mature fruit and then decreased in the ripened fruit. In this study, the oil from green mature fruit contained β-phellandrene in higher amount (62.4 %) than the oils from ripened fruit (60.5 %), immature fruit (56.4 %) and flower (11.7 %). The other major monoterpene hydrocarbons which were found in all samples were β-pinene, α-pinene and δ-3-carene, while in another study, α-terpinenyl acetate, α-terpineol, limonene and myrcene were reported as the major monoterpenes.[12] Monoterpene hydrocarbons identified in the oil of flower were present in lower amount than in the oil of other stages. On the other hand, in the essential oil of flower, sesquiterpenes were one of the dominant fraction with spathulenol (8.9 %) as the major compound and their percentage decreased with progressive fruit maturation.

Antibacterial activity

The disk diffusion method, used in preliminary screening of the antibacterial activity, showed that the oils from the three different fruiting stages of *L. officinale* were active against all the tested bacteria. Moreover, the oils proved to be highly active against the tested Gram-positive bacteria, especially *B. subtilis* that was more sensitive than others, and the Gram-negative bacterium, *E. coli* (Table II). The oils were moderately active against *K. pneumoniae* and *P. aeruginosa*. The antibacterial activities of the oils were also determined using the microtiter 96-well dilution method, by measuring the minimal inhibitory concentration (*MIC*) against the tested bacteria (Table II). The essential oils of mature and ripened fruits exhibited the highest activity against *B. subtilis* with an *MIC* value of 0.90 mg ml^{-1}. In addition, the highest activity of the oil of mature fruit was observed against *S. epidermidis*, with an *MIC* value of 0.90 mg ml^{-1}. The oils showed the

lowest activity against *K. pneumoniae* and *P. aeruginosa*, with the *MIC* values ranging from 14.4 to 15.2 mg ml^{-1}.

TABLE II. Antibacterial activity of *L. officinale* essential oil at different fruiting stages

Microorganism	Essential oil[a]						Ampicillin[b]
	Immature		Mature		Ripened		
	DD[c]	*MIC*[d]	*DD*	*MIC*	*DD*	*MIC*	*DD*
B. subtilis	25.0±0.9	3.8	36.0±0.5	0.9	35.0±0.4	0.9	14.0±0.7
E. faecalis	19.0±0.7	15.2	17.0±0.4	7.5	13.0±0.4	7.2	11.0±0.4
S. aureus	17.0±0.5	3.8	21.0±0.5	3.7	16.0±0.5	3.6	13.0±0.6
S. epidermidis	23.0±0.7	1.9	26.0±0.5	0.9	25.0±0.6	1.8	19.0±0.5
E. coli	19.0±0.6	15.2	18.0±0.4	7.2	15.0±0.7	7.2	12.0±0.5
K. pneumoniae	10.0±0.8	>15.2	10.0±0.7	>14.4	9.0±0.4	>14.4	–
P. aeruginosa	11.0±0.7	>15.2	8.0±0.6	>14.4	9.0±0.5	>14.4	9.7±0.7

[a]Tested at a concentration of 10 µl disc^{-1}; [b]tested at a concentration of 10 µg disc^{-1}; [c]diameter of inhibition zone (mm) including disk diameter of 6 mm: inactive (–), moderately active (7–14) and highly active (>14); [d]minimum inhibitory concentration, values as mg ml oil^{-1}

CONCLUSIONS

The study of a plant as a source of aromatic and flavoring compounds requires the analysis of not only the whole plant but also its individual parts at their different developmental stages. While the best harvesting time of lovage to obtain sharp odorant compounds such as α- and β-pinene is the flowering stage, β-phellandrene as the main compound of the plant with a peppery-minty and slightly citrusy odor was achieved at the fruiting stage. Chemical characterization and antibacterial screening studies on the plant-based essential oils could also lead to the discovery of new natural antibacterial agents. In addition to perfume and tobacco products, the essential oil of lovage is used as a flavor agent in major food products, such as beverages, frozen dairy desserts, candy, gelatins and pudding, and meat and its products. Although the antimycobacterial activity of polyacetylenes, such as falcarinol and falcarindiol, from the plant has recently been studied,[15] the present study is the first report on the antibacterial activity of the essential oil from fruits of *L. officinale* at different developmental stages. The oils showed promising antibacterial activity against, *B. subtilis* and *S. epidermidis*. The present results revealed that the essential oils tested represent an inexpensive source of natural antibacterial substances for use in pathogenic systems to prevent the growth of bacteria and extend the shelf life of processed food.

Acknowledgement. We are grateful to Shahid Beheshti University Research Council for financial support of this work.

ИЗВОД

САСТАВ И АНТИБАКТЕРИЈСКА АКТИВНОСТ ЕТАРСКОГ УЉА ЦВЕТА И ПЛОДА БИЉКЕ *Levisticum officinale* Koch У РАЗЛИЧИТИМ РАЗВОЈНИМ ФАЗАМА

MOHAMMAD HOSSEIN MIRJALILI[1], PEYMAN SALEHI[1], ALI SONBOLI[1], JAVAD HADIAN[1], SAMAD NEJAD EBRAHIMI[1] и MORTEZA YOUSEFZADI[2]

[1]*Medicinal Plants and Drugs Research Institute, Shahid Beheshti University,G. C., Evin, Tehran и* [2]*Department of Marine Biology, Faculty of Science, Hormozgan University, Bandar Abbas, Iran*

Одређиван је састав и антибактеријска активност етарског уља биљке *Levisticum officinale* Koch у различитим развојним фазама: цвет, незрео плод, зелени зрео плод и потпуно зрео плод. Етарско уље је добијено из сувих узорака дестилацијом воденом паром, а антибактеријска активност је одређивана спрам седам врста бактерија. Принос уља (масени %) у различитим фазама је био следећи: незрео плод (1,5 %) > зелени зрео плод (1,0 %) > потпуно зрео плод (0,6 %) > цвет (0,1 %). Састав етарског уља је одређиван методама GC и GC–MS. У ова четири узорка је идентификовано и квантификовано редом 27, 31, 28 и 26 састојака. Монотерпенски угљоводоници су чинили главну групу једињења: 79,2 % у зеленом зрелом плоду, 78,4 % у незрелом плоду, 75,2 % у потпуно зрелом плоду и 44,0 % у цвету. Антибактеријска активност уља је одређивана методом прстенасте дифузије у Милер-Хинтоновом агару мерећи зону инфибиције. Коришћено је 10×10 µl уља за инхибицију и резултати су били различити за уља добијена из биљке у различитим развојним фазама. Најјача антибактеријска активност је испољена спрам *Bacillus subtilis*. *MIC* вредност је била 0,90 mg ml^{-1} са уљем потпуно зрелог плода.

(Примљено 24. маја, ревидирано 9. јула 2010)

REFERENCES

1. K. H. Rechinger, in *Flora Iranica*, K. H. Rechinger, Ed., Akademische Drucku Verlagsanstalt, Graz, 1987
2. M. H. Mirjalili, J. Javanmardi, in *Handbook of Herbs and Spices*, K. V. Peter, Ed., Woodhead Publishing Ltd., Abington, 2006
3. V. Mozaffarian, *A Dictionary of Iranian plant names*, Farhang Moaser, Tehran, 1996
4. E. Daukšas, R. P. Venskutonis, B. Sivik, *J. Supercrit. Fluids* **22** (2002) 201
5. J. E. Simon, A. F. Chadwick, L. E. Craker, *The Scientific Literature on Selected Herbs, Aromatic and Medicinal Plants of the Temperate Zone*, Archon Books, Hamden, CT, 1984
6. B. Toulemonde, I. Noleau, *Dev. Food Sci.* **18** (1988) 641
7. E. Bylaite, R. P. Venskutonis, J. P. Roozen, *J. Agric. Food Chem.* **46** (1998) 3735
8. A. Zargari, *Medicinal plants*, Tehran University Publications, Tehran, 1990
9. E. Daukšas, R. P. Venskutonis, B. Sivik, T. Nilson, *J. Supercrit. Fluids* **15** (1999) 51
10. E. Bylaite, J. P. Roozen, A. Legger, R. P. Venskutonis, M. A. Posthumus, *J. Agric. Food Chem.* **48** (2000) 6183
11. I. Novak, E. Nemeth, *Acta Hort.* **576** (2002) 311
12. J. Dyduch, A. Najda, T. Wolski, S. Kwiatkowski, *Folia Hort.* **15** (2003) 141
13. M. J. M. Gijbels, J. J. C. Scheffer, A. B. Svendsen, *Planta Med.* **44** (1982) 207
14. M. E. Ibrahim, *Egypt. J. Hort.* **26** (1999) 177
15. A. Schinkovitz, M. Stavri, S. Gibson, F. Bucar, *Phytother. Res.* **22** (2008) 681
16. C. Rohricht, *Z. Arznei-Gewurzpflanzen* **14** (2009) 105
17. S. Andruszczak, *Acta Sci. Pol.-Hortoru.* **6** (2007) 21

18. K. Seidler-Lozykowska, K. Kazmierczak, *Herba Polonica* **44** (1998) 11
19. K. Samiee, M. R. Akhgar, A. Rustaiyan, S. Masoudi *J. Essent. Oil Res.* **18** (2006) 19
20. S. Nunes, J. M. S. Faria, A. C. Figueiredo, L. G. Pedro, H. Trindade, J. G. Barroso *Planta Med.* **75** (2009) 387
21. M. Costa, A. C. Figueiredo, J. G. Barroso, L. G. Pedro, S. G. Deans, J. J. C. Scheffer *Biotechol. Lett.* **30** (2008) 1265
22. P. A. G. Santos, A. C. Figueiredo, M. M. Oliviera, J. G. Baroso, L. G. Pedro, S. G. Deans, J. J. C. Scheffer, *Plant Sci*. **168** (2005) 1089
23. A. Raal, E. Arak, A. Orav, T. Kailas, M. Müürisepp, *J. Essent. Oil Res.* **20** (2008) 318
24. *British pharmacopoeia*, HMSO, London, 1993
25. T. Shibamoto, in *Capillary Gas Chromatography in Essential Oil Analysis*, P. Sandra, C. Bicchi. Eds., Hüthig Verlag, New York, 1987, p. 259
26. E. J. Baron, S. M. Finegold, *Bailey and Scott's Diagnostic Microbiology*, 8th ed., C.V. Mosby Co., St. Louis, MO, 1990
27. National Committee for Clinical Laboratory Standards, *Performance standards for antimicrobial susceptibility testing*, 9th international supplement, M100-S9, National Committee for Clinical Laboratory Standards, Wayne, PA, 1999
28. D. Azaz, F. Demirci, F. Satil, M. Kurkcuoglu, K. H. C. Baser, *Z. Naturforsch.* **57c** (2002) 817.

Journal of the Serbian Chemical Society
JSCS-info@shd.org.rs • www.shd.org.rs/JSCS
J. Serb. Chem. Soc. *75* (12) 1671–1683 (2010)
JSCS–4087
UDC 547.979.733:539.194:532.14
Original scientific paper

Consistent force field for metalloporphyrins

LJUBICA ANDJELKOVIĆ[1], SONJA GRUBIŠIĆ[1#], IVANA DJORDJEVIĆ[1], MATIJA ZLATAR[1], SVETOZAR NIKETIĆ[1#] and MAJA GRUDEN-PAVLOVIĆ[2*#]

[1]*Center for Chemistry, Institute of Chemistry, Technology and Metallurgy, University of Belgrade, Njegoševa 12, 11001 Belgrade and* [2]*Faculty of Chemistry, University of Belgrade, Studentski Trg 12–16, 11001 Belgrade, Serbia*

(Received 1 July 2010)

Abstract: Molecular mechanics (MM) calculations to analyze the puckering of metalloporphyrins isolated and adsorbed on a graphite layer (0001) as a function of metal ion size and the peripheral substitution are presented. The Consistent Force Field (CFF) program was used with new parameters for metalloporphyrins, which included an out-of-plane bending function. Normal-coordinate structural decomposition (NSD) analysis was performed on the equilibrium structures obtained by the MM calculations. The conformers were also stereochemically characterized and compared with available experimental data and with conformers obtained in a previous MM study.

Keywords: porphyrins; graphite (0001) surface; molecular mechanics; non-planar conformations.

INTRODUCTION

Metalloporphyrins not only have important biological functions, but they can also be applied in many different industries. Among other applications, they were successfully employed for olefin epoxidation and alkane hydroxylation reactions as remarkably effective catalysts.[1]

It is well known that the porphyrins macrocycle displays a range of distorted non-planar shapes.[2–5] The non-planarity of the porphyrin core has profound consequences on the spectral, electrochemical and other properties of porphyrins, including functionality.[6] It was revealed that factors which induce non-planarity can be divided into at least four categories: peripheral substitution, the central metal, axial ligation and the environment of the porphyrin.[7] Previous studies showed that the type and degree of non-planar deformation can be controlled by the peripheral substitution pattern, the steric bulkiness of substituents and the size

* Corresponding author. E-mail: gmaja@chem.bg.ac.rs
# Serbian Chemical Society member.
doi: 10.2298/JSC100701095A

of central metal ion of the macrocycle.[8,9] Furthermore, it was also shown that adsorption of metalloporphyrins on a graphite layer influences conformational changes of the porphyrin core.[10]

Theoretically, the complete set of normal coordinates for a macrocycle forms a basis for describing any distortion of a porphyrin core. For a porphyrin of D_{4h} symmetry, the distortion can be divided into in-plane and out-of-plane deformations. Only a few of the lowest frequency modes are required to adequately describe the out-of-plane distortions.[11] These are: ruffing (*ruf*, B_{1u}), saddling (*sad*, B_{2u}), doming (*dom*, A_{2u}), two wavings (*wav*$_x$, *wav*$_y$, E_g) and propellering (*pro*, A_{1u}), which are shown in Fig. 1. Many experimental techniques have been used for distinguishing the magnitude of non-planar distortion, although distinguishing the different types of distortion (*ruf*, *sad*, *dom*, *wav* and *pro*) has proved to be more challenging.[12] Molecular modeling, developed for the investigation of non-planar porphyrins, provides information about the energetics of non-planar distortions, as well as, additional structural information.[13] In this work, molecular mechanics (MM) calculations were used to study the effects of peripheral substitution, the nature of the central metal atom and the influence of the graphite (0001) surface on the non-planar distortions of metalloporphyrins. Although, some of the porphyrin molecules mentioned in this paper have already been analyzed, recently force field was supplemented with a new function and hence, all parameters were reoptimized in order to improve their reliability, in other words, to improve their accuracy in producing a physically meaningful potential energy surface.

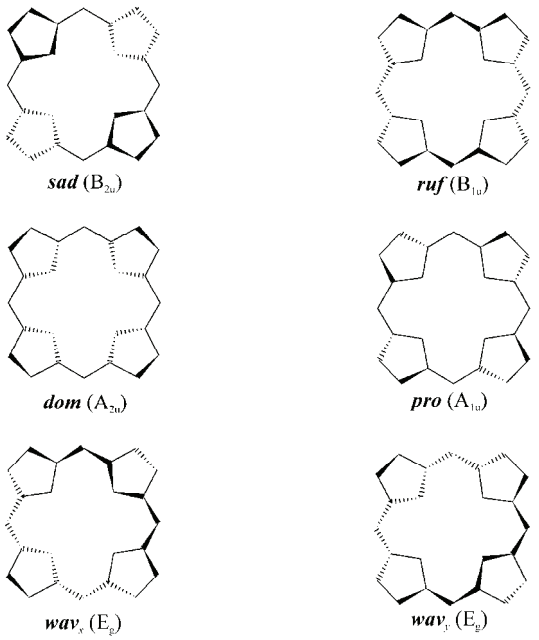

Fig. 1. Non-planar porphyrin-core conformations. Bold and dashed lines represent core fragments lying below and above the mean plane, respectively.

COMPUTATIONAL DETAILS

Molecular mechanics calculations were performed with the 2007/PC version of the Consistent force field (CFF) conformational program.[14] Conformational energy was defined in the usual way as given in Eq. (1):

$$E_{\text{tot}} = \sum E_{\text{b}} + \sum E_{\theta} + \sum E_{\varphi} + \sum E_{\text{nb}}^{(\text{intramol.+intermol.})} + \sum E_{\text{e}}^{(\text{intramol.+intermol.})} + \sum E_{\text{oop}} \qquad (1)$$

where the terms on the right-hand side represent bond-stretching, angle-bending, torsional, non-bonded, Coulomb, and out-of-plane bending contributions, respectively. Bond-stretching and angle-bending contributions were treated with simple harmonic functions (Eq. (2)). Torsional contributions were represented as Fourier series that accounts for all four torsions involving a double bond, or nine torsions involving a single bond.

Non-bonded intramolecular van der Waals interactions were modeled using the Lennard--Jones "12-6" potential function with parameters which were chosen by extrapolation based on the available parameter sets, imposing their consistency with the original force field.[15,16]

Non-bonded intramolecular electrostatic contributions were modeled with the Coulomb function.

Point charges were obtained from *ab-initio* calculations (Gaussian 98).[17]

Out-of-plane bending was defined by using the height of the pyramid formed by the four atoms (Fig. 2, Eq. (2)). This function was added to the CFF conformational program where *h*oop is the perpendicular distance of atom *i* from the plane defined by atoms *jkl*, and *k*oop is the force constant.[18]

$$E_{\text{tot}} = \sum_{r}\frac{1}{2}k_r(r-r^0)^2 + \sum_{\theta}\frac{1}{2}k_\theta(\theta-\theta^0)^2 + \sum_{\varphi}\frac{1}{2}(1+\cos n\varphi) + \sum_{ij}\left[\frac{2}{3}\varepsilon\left(\frac{r^*}{r}\right)^{12} - \varepsilon\left(\frac{r^*}{r}\right)^{6}\right] + \\ + \sum_{ij}\frac{q_i q_j}{\varepsilon_{ij} r_{ij}} + \sum k_{\text{oop}} h_{\text{oop}}^2 + \sum_i \sum_j \frac{1}{r_{ij}^3} q_i \left(e^T \theta_j e\right) \qquad (2)$$

Intermolecular van der Waals interactions between the porphyrin macrocycle and the graphite C atoms were treated with the Lennard-Jones "12-6" type function, with the same parameters as for intramolecular potential.

Modeling of the graphite layer was described in a previous paper.[10]

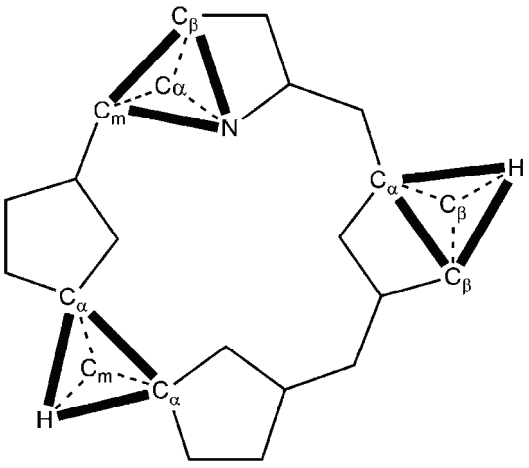

Fig. 2. Out-of-plane bending functions: $NC_mC_\beta C_\alpha$, $C_\alpha HC_\beta C_\beta$ and $C_\alpha HC_\alpha C_m$. Atom types used in defining the force field parameters for the molecular mechanics calculation.

Intermolecular electrostatic interactions were treated as monopole–quadrupole interactions between point charges located on the atomic positions of all metalloporphyrin atoms and uniaxial quadrupoles defined on each C atom of the graphite layer:

$$E^{(e,Q)} = \sum_i \sum_j \frac{1}{r_{ij}^3} q_i \left(e^T \theta_j e \right) \quad (3)$$

where q_i is the point charge on the *i*-th porphyrin atom; r_{ij} is the interatomic distance; e is the unit vector along r_{ij}; θ_j is the quadrupole moment tensor of the j-th C atom on the graphite layer (Eq. (3)).[10]

Non-bonded cut-off was treated with a cubic spline switching function with the spline-on distance of 7 Å and the spline width of 2 Å.

Geometry optimizations were realized using combinations of the steepest-descent, Davidon–Fletcher–Powell and Newton–Raphson methods.[14] Geometry optimizations were performed to the energy rms gradient of $< 10^{-6}$ kJ mol^{-1} Å^{-1}.

For each of the equilibrium structures obtained by the energy minimization procedure, normal-coordinate structural decomposition (NSD) analysis was performed using the software available at http://jasheln.unm.edu/. The NSD method provides a unique way for characterizing the distortions of the macrocycle and gives detailed analysis of the type of deformations present in the calculated porphyrin structures.

Force field parametrization

In this work, new function which describes out-of-plane bending interaction was added in the CFF conformational program for the first time and hence all the force field parameters on the available X-ray structures of Ni(II)porphyrin, Ni(II)mono-*tert*-butylporphyrin, Ni(II)di--*tert*-butylporphyrin, Ni(II)tetraphenylporphyrin and Ni(II)octaethyl-tetraphenylporphyrin were reoptimized by adjusting the appropriate parameters on a trial-and-error basis until the RMSD values between the calculated and crystallographically observed bond lengths and valence angels were ≤ 0.03 Å and $\leq 3°$, respectively.

The force field was parametrized based the four different types of carbon atoms (α and β pyrrole carbons, *meso* carbon of the porphyrin ring, aromatic carbon of the phenyl substituents and sp^3-hybridized C atom of the alkyl substituents), one type of hydrogen and of nitrogen, central metal atoms and the halogen substituents (chlorine and bromine).

The aim of involving the out-of-plane bending function was to assure persistency of planarity of selected fragments of metalloporphyrins in the optimized structures, as is indicated in Fig. 2. In earlier works, higher values of the torsional parameters were used in order to keep planarity of selected fragments in the porphyrin molecules, giving better agreement with the X-ray data. Hence, there was a need to introduce a new function in the CFF conformational program so that the torsional parameters could approach more realistic lower values.

The conformers obtained by MM calculations were stereochemically characterized, compared with available X-ray crystal structures, analyzed by the NSD method and also compared to the results obtained in a previous MM study without the out-of-plane bending function. Comparison of selected structural data for the molecules used in parametrization are given in Table I. These results indicate better agreement between calculated and X-ray structures, in comparison with previous results, establishing the reliability of the present force field, but did not affect any of previous conclusions.

A list of all force field parameters is given in Table S-I in the Supplementary material.

TABLE I. Selected average bond lengths (Å), valence and torsion angles (°) for the equilibrium metalloporphyrins structures and for available crystal structures. Missing values are not reported (–) in the cited sources

Method	Ni–N	C_β–C_β	C_α–C_m	N–C_α	N–Ni–N	C_α–N–C_α	N–C_α–C_β–C_β	N–C_α–C_m–C_α
NiP								
X-Ray[a]	1.951	1.347	1.371	1.379	179.3	104.3	0.3	0.8
MM[b]	1.912	1.336	1.366	1.377	179.9	103.8	0.02	0.0
MM	1.945	1.340	1.375	1.375	180.0	105.5	0.9	1.2
NiMtBuP								
X-Ray[c]	1.901	1.342	1.380	1.380	178.9	106.3	3.0	11.1
MM[d]	1.917	1.338	1.372	1.377	177.3	105.2	4.5	14.3
MM	1.944	1.338	1.377	1.376	177.3	103.5	0.86	1.19
NiDtBuP								
X-Ray[e] (αα)	1.900	1.353	1.394	1.383	177.0	106.2	2.9	14.8
MM[d]αα	1.900	1.341	1.379	1.373	177.6	106.0	5.4	25.1
MMαα	1.934	1.338	1.380	1.376	176.8	106.3	8.8	23.6
MM[d]αβ	1.910	1.337	1.378	1.377	179.9	103.9	6.1	19.1
MMαβ	1.934	1.340	1.379	1.375	177.2	103.3	18.26	21.02
NiTPP								
X-Ray[f]	1.931	1.340	1.383	1.377	180.0	104.9	2.6	9.6
MM[b]	1.930	1.337	1.370	1.377	180.0	104.9	1.4	11.8
MM	1.964	1.334	1.376	1.378	176.2	106.3	4.2	8.7
NiOEtTPP								
X-ray[g]	1.906	1.365	1.395	1.381	90.6	105.9	–	–
MM[h]	1.875	1.341	1.375	1.375	90.4	106.3	–	–
MM	1.924	1.347	1.348	1.376	90.6	108.2	–	–

[a]W. Jentzen, I. Turowska-Tyrk, W. R. Scheidt, J. A. Schelnutt, *Inorg. Chem.* **35** (1996) 3559; [b]M. Gruden-Pavlović, S. Grubišić, S. R. Niketić, *J. Inorg. Biochem.* **98** (2004) 1293; [c]X.-Z. Song, W. Jentzen, L. Jaquinod, R. G. Khoury, C. J. Medforth, S.-L. Jia, J.-G. Ma, K. M. Smith, J. A. Shelnutt, *Inorg. Chem.* **37** (1998) 2117; [d]M. Gruden, S. Grubišić, A. G. Coutsolelos, S. R. Niketić, *J. Mol. Struct.* **595** (2001) 209; [e]X. Z. Song, W. Jentzen, S. L. Jia, L. Jaquinod, D. J. Nurco, C. J. Medforth, K. M. Smith, J. A. Shelnutt, *J. Am. Chem. Soc.* **118** (1996) 12975; [f]A. L. MacLean, G. J. Foran, B. J. Kennedy, P. Turner, T. W. Hambley *Austral. J. Chem.* **49** (1996) 1273; [g]K. M. Barkigia, M. W. Renner, L. R. Furenlid, C. J. Medforth, K. M. Smith, J. Fajer, J. *Am. Chem. Soc.* 115 (1993) 3627; [h]Unpublished work

RESULTS AND DISCUSSION

The effects of peripheral substitution of various substituents, coordination of central metal ions of different radii and adsorption of molecules on the graphite layer (0001) on the conformations of porphyrin macrocycle of octa- and tetrahalogenated (chloro and bromo) tetraphenylporphyrin (TPP) derivates with Ni(II) an Tb(III) metal ions were studied. Ni(II) metal ion and Tb(III) metal ion were chosen to represent central metal atoms with a relatively small and large radius, respectively. As in a previous study, the initial structures for tetrahalogeno TPP were chosen based on the most symmetrical substitution pattern of the halogens and comprised: 2,8,12,18-tetrahalogeno-TPP (trans-trans, or tt)

isomer; 2,3,12,13-tetrahalogeno-TPP (cis-trans, or ct); 2,7,12,17-tetrahalogeno-TPP (windmill, or wm) isomer.

All the stable conformers for the series of porphyrins were obtained by energy minimization starting from five (plan, sad, ruf, dom, wav) initial structures. Furthermore, for the porphyrin macrocycles adsorbed on the graphite surface, two different positions of the metal (one with the metal atom directly above a given graphite carbon atom and the other with the metal located above the hole of the graphite hexagon) and various intermolecular distances (3–8 Å, in steps of 0.5 Å) were considered.

It is noteworthy that the geometrical optimization resulted in one unique equilibrium conformation for all the investigated porphyrin structures, regardless of the initial structures that were started with.

Isolated structures

The structural parameters for the energy-minimized conformers, as well as a comparison with the available crystal structures, are given in Table II; the

TABLE II. Selected average bond lengths (Å), valence and torsion angles (°) for the equilibrium, isolated metalloporphyrins structures and for crystal structures

Method	M–N	N–C_α	C_β–C_β	C_α–C_m	X[a]–C_β	N–M–N	C_α–N–C_α
			Ni(II)Br_xTPP				
X-Ray[b]	1.900	1.380	1.340	1.380	1.870	168.5	106.6
Br_8	1.924	1.374	1.349	1.384	1.911	166.5	108.7
ct-Br_4	1.951	1.337	1.334	1.379	1.903	90.8	105.3
tt-Br_4	1.944	1.376	1.340	1.380	1.898	90.4	106.7
wm-Br_4	1.948	1.376	1.339	1.379	1.896	90.5	107.6
			Ni(II)Cl_xTPP				
X-Ray[c]	1.904	1.384	1.348	1.394	1.705	90.3	107.3
Cl_8	1.932	1.376	1.345	1.383	1.737	90.7	108.3
ct-Cl_4	1.953	1.378	1.338	1.378	1.733	90.6	105.8
tt-Cl_4	1.947	1.376	1.338	1.379	1.730	90.4	107.3
wm-Cl_4	1.950	1.377	1.338	1.379	1.730	90.4	107.5
			Tb(III)Br_xTPP				
Br_8	2.311	1.377	1.342	1.386	1.899	86.1	105.2
ct-Br_4	2.309	1.378	1.340	1.386	1.902	86.7	105.9
tt-Br_4	2.307	1.376	1.341	1.387	1.901	85.6	106.6
wm-Br_4	2.308	1.377	1.340	1.386	1.896	86.1	107.3
			Tb(III)Cl_xTPP				
Cl_8	2.304	1.376	1.346	1.388	1.738	85.1	107.1
ct-Cl_4	2.308	1.376	1.342	1.386	1.733	85.3	108.4
tt-Cl_4	2.308	1.377	1.340	1.387	1.732	85.7	106.8
wm-Cl_4	2.308	1.377	1.340	1.386	1.729	86.1	107.3

[a]Br,Cl; [b]X-Ray data of Ni(II)Br_8TPP, L. M. Henling, W. P. Schaefer, J. A. Hodge, M. E. Hughes, H. B. Gray, *Acta Cryst. C* **49** (1993) 1743; [c]X-Ray data of Ni(II)Cl_8TPP Ni, G. A. Spyroulias, A. P. Despotopoulos, C .P. Raptopoulou, A. Terzis, D. de Montauzon, R. Poilblance, A. G. Coutsolelos, *Org. Chem.* **41** (2002) 2648

calculated energy distributions are listed in Table III and the results of the NSD analysis for all the optimized molecules are presented in Table IV.

TABLE III. Energy contributions (in kcal mol^{-1}) for the isolated, equilibrium TPP conformations

Species	E_{tot}	E_{bond}	E_{angle}	$E_{torsion}$	E_{oop}	E_{vdw}	E_c	E_{nb}
				Ni(II)Br$_x$TPP				
Br_8	55.28	4.72	15.55	18.83	1.39	26.53	–11.74	14.79
ct-Br_4	35.83	1.97	9.99	16.14	1.32	17.95	–11.55	6.40
tt-Br_4	35.51	1.90	8.56	16.71	1.42	18.68	–11.76	6.93
wm-Br_4	33.81	1.80	8.90	14.83	1.51	18.48	–11.72	6.76
				Ni(II)Cl$_x$TPP				
Cl_8	54.09	3.05	12.36	17.83	1.61	23.53	–4.29	19.24
ct-Cl_4	36.32	1.68	8.64	14.90	1.25	18.59	–8.73	9.86
tt-Cl_4	34.64	1.70	8.11	15.98	1.37	19.19	–11.70	7.48
wm-Cl_4	32.91	1.61	8.36	14.51	1.49	18.84	–11.90	6.95
				Tb(III)Br$_x$TPP				
Br_8	75.17	5.20	22.30	38.21	4.55	13.83	–8.92	4.91
ct-Br_4	56.07	4.97	20.1	21.97	2.06	15.73	–8.75	6.98
tt-Br_4	61.21	5.39	24.18	18.59	2.61	19.25	–8.79	10.45
wm-Br_4	57.48	4.92	23.01	19.08	2.52	16.74	–8.78	7.96
				Tb(III)Cl$_x$TPP				
Cl_8	84.93	6.83	31.06	19.59	2.94	25.31	–0.81	24.50
ct-Cl_4	64.69	5.30	25.7	16.10	2.51	20.25	–5.16	15.09
tt-Cl_4	60.08	5.11	23.56	17.46	2.49	19.7	–8.24	11.46
wm-Cl_4	56.7	4.79	22.59	17.98	2.38	17.33	–8.36	8.97

The NSD analysis revealed that the structure of Ni(II)Br8TPP is pure saddle and it shows the largest deviation from planarity (Table IV). The ct--isomer of Ni(II)Br4TPP is a mixture of sad and dom non-planar deformations, the tt-isomer is almost pure saddle with a minor contribution of the pro mode, while the optimized structure of the wm-isomer indicated that it consisted of sad and a small amount of ruf deformations. For the tetrabromo-TPP–Ni(II) complexes, the wm-isomer is the most stable one (Table III).

The Ni(II)Cl8TPP complex is also highly puckered, and the NSD analysis indicated an almost pure saddled macrocycle. All three isomers of Ni(II)Cl4TPP possess sad as the dominant deformation, with contributions of dom, pro and ruf distortions for ct-, tt- and wm-isomer, respectively.

For the octa- and tetrabromo substituted structures with the very large Tb(III) ion, the dom deformation was present in all structures as was expected (Table IV). The NSD analysis revealed that the structure of the Tb(III)Br8TPP complex is a mixture of dom, sad, ruf and pro deformations. In the case of the ct-isomer of Tb(III)Br4TPP, the metal ion favors dom distortion, and saddling is favored by the substituents. An almost equal ratio of sad and dom deformations

was found in the tt-isomer and in the case of wm-isomer, the sad distortion dominates. The ct-isomer is the most stable one, but the difference between total energy of the ct- and wm-isomer is not so significant (Table III).

TABLE IV. Results of the normal-coordinate structural decomposition (NSD) analysis for the equilibrium, isolated TPP conformations. D_{oop} is the total out-of-plane distortion (in Å)

Species	D_{oop}	*sad*	*ruf*	*dom*	*wav(x)*	*wav(y)*	*pro*
			Ni(II)Br$_x$TPP				
Br_8	3.7365	3.7365	0.0083	0.0057	0.0057	0.0084	0.0030
ct-Br_4	2.5544	2.3495	0.0171	1.0021	0.0153	0.0144	1.0100
tt-Br_4	2.4576	2.4426	0.0058	0.0105	0.0091	0.0143	0.2704
wm-Br_4	2.3550	2.3236	0.3825	0.0164	0.0080	0.0162	0.0028
			Ni(II)Cl$_x$TPP				
Cl_8	3.3397	3.3397	0.0065	0.0057	0.0059	0.0080	0.0037
ct-Cl_4	2.2829	2.1277	0.0141	0.8270	0.0115	0.0121	0.0079
tt-Cl_4	2.3360	2.3253	0.0053	0.0102	0.0084	0.0138	0.2219
wm-Cl_4	2.1913	2.1475	0.4354	0.0147	0.0074	0.0151	0.0022
			Tb(III)Br$_x$TPP				
Br_8	2.2838	1.4672	0.5068	1.6167	0.0446	0.0322	0.4353
ct-Br_4	1.8914	0.7306	0.0156	1.7440	0.0311	0.0225	0.0206
tt-Br_4	1.9571	1.4579	0.0341	1.2637	0.0121	0.0027	0.3263
wm-Br_4	3.0589	2.7552	0.0416	1.3281	0.0139	0.0033	0.0088
			Tb(III)Cl$_x$TPP				
Cl_8	3.0589	2.7552	0.0416	1.3281	0.0139	0.0033	0.0088
ct-Cl_4	1.5314	0.9842	0.0115	1.1732	0.0087	0.0066	0.0053
tt-Cl_4	2.9150	2.1099	0.5525	1.1933	0.5995	1.3628	0.3152
wm-Cl_4	3.0589	2.7552	0.0416	1.3281	0.0139	0.0033	0.0088

In optimized structure of the Tb(III)Cl8TPP complex, sad and dom normal modes were observed (Table IV). The NSD analysis of the ct-isomer of Tb(III)Cl4TPP shows an almost equal ratio of dom and sad distortions. The shape of optimized conformation of the tt-isomer is a combination of the five most commonly observed distortions, with domination of the sad deformation mode. In the case of the wm-isomer, the ratio of the sad and dom deformations is almost the same as for the wm-isomer of Tb(III)Br4TPP. As in the case of the tetrachloro substituted TPP isomers, the wm isomer is the most stable (Table III).

Adsorbed structures

The structural parameters for the energy-minimized conformers are presented in Table V, the calculated energy distributions are listed in Table VI and the results of NSD analysis for all the investigated porphyrins adsorbed on a graphite layer are listed in Table VII.

TABLE V. Selected average bond lengths (Å), valence and torsion angles (°) for the equilibrium, adsorbed metalloporphyrins structures

Species	M–N	N–C_α	C_β–C_β	C_α–C_m	X[a]–C_β	N–M–N	C_α–N–C_α
			Ni(II)Br_xTPP				
Br_8	1.925	1.375	1.348	1.385	1.911	166.7	108.80
ct-Br_4	1.962	1.379	1.338	1.378	1.902	90.02	107.54
tt-Br_4	1.968	1.376	1.335	1.376	1.901	90.42	106.80
wm-Br_4	1.971	1.376	1.334	1.374	1.899	89.98	107.54
			Ni(II)Cl_xTPP				
Cl_8	1.945	1.378	1.341	1.384	1.739	90.6	108.60
ct-Cl_4	1.972	1.379	1.334	1.376	1.733	89.98	106.89
tt-Cl_4	1.965	1.376	1.334	1.374	1.735	90.51	106.82
wm-Cl_4	1.971	1.380	1.334	1.372	1.738	90.23	106.72
			Tb(III)Br_xTPP				
Br_8	2.300	1.377	1.344	1.392	1.899	86.5	108.9
ct-Br_4	2.303	1.376	1.340	1.392	1.901	86.8	109.7
tt-Br_4	2.303	1.375	1.339	1.388	1.902	86.2	109.8
wm-Br_4	2.302	1.378	1.340	1.388	1.899	86.3	109.7
			Tb(III)Cl_xTPP				
Cl_8	2.300	1.382	1.343	1.396	1.740	86.6	112.3
ct-Cl_4	2.303	1.379	1.343	1.389	1.737	85.9	109.6
tt-Cl_4	2.300	1.378	1.339	1.390	1.731	85.5	108.5
wm-Cl_4	2.302	1.379	1.342	1.388	1.740	85.6	109.2

[a]Br,Cl

NSD Pattern for structure of Ni(II)Br8TPP adsorbed on graphite surface is almost the same as for isolated molecule, because there is no significant intermolecular interaction (Table VI).

Distance of Ni(II) ion from graphite is approximately 6 Å. Large distance is explained by the presence of bulky groups and repulsive interaction between negative charges, hence the porphyrin macrocycle can not approach more closely to the graphite layer. Geometry optimization for three isomers of Ni(II)Br4TPP leads to parallel orientation of porphyrin macrocycle on graphite, where in all cases the metal ion is above the center of C–C bond. In comparison to the isolated structures, all three isomers adsorbed on a graphite layer are less puckered (Tables IV and VII). In the ct-isomer, an almost equal ratio of dom and sad distortions is observed (Table VII). The ruf and dom deformations dominate in the tt-isomer, with presence of the pro deformation mode, while the wm-isomer can be described with dom deformation and a small contribution of pro distortion.

After geometry optimization of the various initial conformations of the adsorbed molecule Ni(II)Cl8TPP, starting from the various distances from the graphite layer and different initial positions of metal ion in relation to graphite, the end result was a unique conformation, very similar to the isolated structure, with the sad mode as dominant, and with a small contribution of the dom dis-

tortion. Final position of the metal ion is exactly above center of the C–C bond of the graphite layer. The position of the metal ion in relation to the graphite layer of the three isomers of Ni(II)Cl4TPP is the same as in the case of the tetrabromo derivatives. NSD analysis revealed that all three isomers are more planar in comparison to the isolated structures (Tables IV and VII), which enhance the flattening π-stacking interactions. NSD analysis shows that in the ct-isomer, dom and sad deformations dominate. Almost all of the five most commonly observed distortions occur in the equilibrium conformation of the tt-isomer with domination of the ruf and dom modes. In the case of the wm-isomer, dom deformation is the dominant one, with a small contribution of pro distortion (Table VII).

TABLE VI. Energy contributions (in kcal mol^{-1}) for the equilibrium, adsorbed metalloporphyrins conformations

Species	E_{tot}	E_{bond}	E_{angle}	$E_{torsion}$	E_{oop}	E_{vdw}	E_c	E_{nb}	$E_{intervdw}$	E_{interc}	$E_{internb}$
Ni(II)Br$_x$TPP											
Br_8	46.33	4.61	16.15	18.36	1.26	27.11	–11.74	15.37	–5.83	–3.59	–9.42
ct-Br_4	–3.80	2.94	9.94	20.01	2.20	24.29	–11.11	13.17	–19.72	–32.33	–52.06
tt-Br_4	2.32	2.50	12.36	24.62	2.31	21.58	–11.28	10.29	–18.64	–31.12	–49.77
wm-Br_4	–5.40	2.22	11.83	19.67	2.09	20.92	–11.17	9.76	–20.41	–32.71	–53.11
Ni(II)Cl$_x$TPP											
Cl_8	23.48	3.65	16.54	17.44	1.40	32.53	–4.00	28.52	–29.81	–14.28	–44.09
ct-Cl_4	–16.41	2.58	10.35	19.16	2.12	23.16	–7.58	15.58	–20.07	–46.13	–66.21
tt-Cl_4	–15.74	2.26	12.08	25.1	2.13	27.76	–10.54	10.22	–18.25	–49.29	–67.55
wm-Cl_4	–17.69	2.09	13.24	22.42	1.88	20.81	–10.79	10.01	–19.7	–47.65	–67.35
Tb(III)Br$_x$TPP											
Br_8	12.66	6.2	24.28	35.49	3.03	13.81	–8.66	5.15	–29.81	–31.67	–61.48
ct-Br_4	16.84	10.35	29.84	19.09	1.48	20.51	–8.87	11.65	–19.55	–36.02	–55.57
tt-Br_4	16.04	7.59	25.64	21.26	2.02	14.68	–8.84	5.84	–17.68	–28.64	–46.32
wm-Br_4	12.28	9.23	30.76	17.01	1.28	17.5	–8.94	8.56	–19.88	–34.68	–54.56
Tb(III)Cl$_x$TPP											
Cl_8	36.32	8.81	36.07	23.57	2.89	35.05	–0.08	35.07	–19.71	–50.39	–70.09
ct-Cl_4	–4.48	5.32	30.33	22.05	3.15	19.01	–3.81	15.19	–17.88	–62.65	–80.54
tt-Cl_4	–4.84	5.00	32.45	25.5	2.94	17.29	–6.89	10.39	–17.24	–63.89	–81.14
wm-Cl_4	–7.54	4.82	31.75	24.44	2.77	16.17	–7.11	9.06	–18.37	–62.02	–80.39

NSD Analysis of the adsorbed octa- and tetra-halogeno TPP derivates with the Tb(III) ion indicates that all the optimized porphyrin macrocycle conformations are less puckered in comparison to the isolated structures, with domination of the dom distortion mode, as is expected from the metal ion size (Tables IV and VII). In all cases of tetrahalogeno substituted Tb(III) complexes, the metal is located exactly above the hole of the graphite hexagon, at a very small distance, which is explained by the strong attractive M–π interactions.

TABLE VII. Results of the normal-coordinate structural decomposition (NSD) analysis for the equilibrium, adsorbed metalloporphyrins conformations. D_{oop} is the total out-of-plane distortion (in Å)

Species	D_{oop}	*sad*	*ruf*	*dom*	*wav(x)*	*wav(y)*	*pro*
			Ni(II)Br$_x$TPP				
Br_8	3.7438	3.7419	0.0109	0.1210	0.0046	0.0070	0.0037
ct-Br_4	0.9487	0.6100	0.0244	0.7253	0.0212	0.0258	0.0120
tt-Br_4	1.0535	0.0218	0.8121	0.5954	0.0085	0.0072	0.3083
wm-Br_4	0.7426	0.0140	0.0250	0.6912	0.0251	0.0144	0.2683
			Ni(II)Cl$_x$TPP				
Cl_8	3.2494	3.2282	0.0127	0.3700	0.0077	0.0145	0.0035
ct-Cl_4	0.8474	0.5568	0.0264	0.6379	0.0138	0.0122	0.0152
tt-Cl_4	1.0333	0.0812	0.7823	0.6282	0.0145	0.0109	0.2326
wm-Cl_4	0.7060	0.0142	0.0331	0.6283	0.0279	0.0129	0.3186
			Tb(III)Br$_x$TPP				
Br_8	1.7730	0.4255	0.2486	1.6281	0.3444	0.2889	0.2185
ct-Br_4	1.0064	0.3849	0.0166	0.9108	0.0140	0.1859	0.0043
tt-Br_4	1.1030	0.0035	0.3914	1.0310	0.0146	0.0138	0.0067
wm-Br_4	1.0332	0.0081	0.0173	1.0159	0.0161	0.0086	0.1865
			Tb(III)Cl$_x$TPP				
Cl_8	0.9799	0.3491	0.0067	0.8116	0.4237	0.0078	0.0112
ct-Cl_4	1.1660	0.3334	0.0179	1.1171	0.0101	0.0057	0.0127
tt-Cl_4	1.2808	0.0147	0.4852	1.1894	0.0092	0.0077	0.0223
wm-Cl_4	0.7344	0.0382	0.0075	0.7097	0.0147	0.0074	0.1841

Again, the octahalogeno derivates of Tb(III) cannot approach close to the graphite surface, resulting in a similar conformation of the porphyrin core in comparison to the isolated structures.

CONCLUSIONS

The main goal of this study was the development of a new force field for metalloporphyrins using the CFF conformational program. This means that the previous force field was supplemented with a new function which describes the deviation of the atoms from planarity, i.e., an out-of-plane bending function. This function was parameterized and all other parameters were reoptimized in order to improve the consistency of the entire force field. The force field was parameterized on planar and highly puckered complexes, whereby the obtained structural results are in good agreement with the published MM results and with the available crystal structures.8–10 The very good agreement between the calculated and experimental structures is the best indicator of the successful augmentation of the new function and the valid reoptimization of the force field. With essentially the same force field, the effects of the peripheral substitution and the nature of the central metal atom as well as the influence of a presence of graphite (0001) surface on the non-planar distortions of octa- and tetrahalogeno

TPP derivates with Ni(II) and Tb(III) ions were analyzed. It was shown that both metallation and peripheral substitution determine the type and degree of non-planar deformations of porphyrin macrocycle, as a result of various strain-relieving mechanisms. An increase of the radius of the central metal atom enhances the doming of the porphyrin macrocycle, thus dom deformation is present in all of the isomers of the Tb(III) ion. Dodeca-substituted porphyrins showed a large deviation from planarity and relieved their strain predominantly by saddling of the porphyrin core, irrespective of the size of the central metal atom and the nature of the halogeno substituents. The position of the four halogeno atoms in the tetrahalogeno TPP structures has profound consequences on the mode and amount of normal distortions. In almost all cases, the wm isomer is the most stable one, except for the tetrabromo TPP Tb(III) species, when the ct isomer was found to be the most stable, but the energy difference between this and the wm isomer is small. Octahalogeno TPP derivates of Ni(II) and Tb(III) adsorbed on a graphite layer have similar conformations of porphyrin core in comparison to the isolated structures, because they cannot approach close to the graphite surface. All tetrahalogeno TPP structures are more planar in comparison to the isolated structures, as the result of π-stacking interactions. NSD analysis revealed that dom distortion is present in almost all of the structures adsorbed on a graphite layer and the origin of this distorsion can be explained by M–π interactions. If an analyzed molecule is closer to the substrate, doming is more significant. These results indicate that changes of physical and chemical properties of porphyrin adsorbed on a surface (in the present case a graphite layer) can be explained not only by the adsorption process, but also by specific conformational changes.

SUPPLEMENTARY MATERIAL

CFF parameters for metalloporphyrins are available electronically from http://www.shd.org.rs/JSCS/, or from the corresponding author on request.

Acknowledgements. This work was financially supported by the Ministry of Science and Technological Development of the Republic of Serbia.

ИЗВОД

КОНЗИСТЕНТНО ПОЉЕ СИЛА ЗА МЕТАЛОПОРФИРИНЕ

ЉУБИЦА АНЂЕЛКОВИЋ[1], СОЊА ГРУБИШИЋ[1], ИВАНА ЂОРЂЕВИЋ[1], МАТИЈА ЗЛАТАР[1], СВЕТОЗАР НИКЕТИЋ[1] и МАЈА ГРУДЕН-ПАВЛОВИЋ[2]

[1]Центар за хемију, Институт за хемију, технологију и металургију, Универзитет у Београду, Његошева 12, 11001 Београд и [2]Хемијски факултет, Универзитет у Београду, 11001 Београд

Конзистентно поље сила (CFF) за молекулско моделирање металопорфирина, које укључује новоуведену *out-of-plane* функцију, параметризовано је на основу кристалних структура Ni(II)-порфирина, никал(II)-моно-терцбутилпорфирина, никал(II)-ди-терцбутилпорфирина, никал(II)-тетрафенилпорфирина и никал(II)-октаетил-тетрафенилпорфирина. Оно је употребљено за проучавање утицаја величине централног металног јона, периферне супсти-

туције као и утицаја присутног супстрата на конформације порфиринског језгра код окта- и тетрахалогено-тетрафенилпорфирина са Ni(II) и Tb(III). Јединствене равнотежне структуре, добијене на основу молекулско-механичких прорачуна великог броја почетних структура, показују добро слагање са кристалним структурама, као и са претходно публикованим резултатима, не само у метричким подацима, већ и у начину набирања порфиринског језгра. Метод нормалне-координатне структурне декомпозиције (NSD) омогућава да се на једнозначан начин опише свака оптимизована конформација добијена молекулско-механичким прорачунима.

(Примљено 1. јула 2010)

REFERENCES

1. I. D. Kostas, A. G. Coutsolelos, G. Charalambidis, A. Skondra, *Tetrahedron Lett.* **48** (2007) 6688
2. Y. Higuchi, M. Kusunoki, N. Yasuoka, M. Kakudo, *J. Mol. Biol.* **172** (1984) 109
3. G. Fermi, M. F. Perutz, B. Shaanan, R. Fourme, *J. Mol. Biol.* **175** (1984) 159
4. B. C. Finzel, T. L. Poulos, J. Kraut, *J. Biol. Chem.* **259** (1984) 13027
5. G. V. Louie, G. D. Brayer, *J. Mol. Biol.* **214** (1990) 527
6. M. O. Senge, in *The Porphyrin Handbook*, Vol. 1, K. M. Kadish, K. M. Smith, R. Guilard, Eds., Academic Press, New York, 2000, p. 239
7. X. Song, W. Jentzen, L. Jaquinod, R. G. Khoury, C. J. Medforth, S. L. Jia, J. G. Ma, K. M. Smith, J. A. Shelnutt, *Inorg. Chem.* **37** (1998) 2117
8. M. Gruden, S. Grubišić, A. G. Coutsolelos, S. R. Niketić, *J. Mol. Struct.* **595** (2001) 209
9. M. Gruden-Pavlović, S. Grubišić, S. R. Niketić, *J. Inorg. Biochem.* **98** (2004) 1293
10. M. Gruden-Pavlović, S. Grubišić, M. Zlatar, S. R. Niketić, *Int. J. Mol. Sci.* **8** (2007) 810
11. W. Jentzen, X. Z. Song, J. A. Shelnutt, *J. Phys. Chem. B* **101** (1997) 1684
12. J. A. Shelnutt, X. Z. Song, J. G. Ma, S. L. Jia, W. Jentzen, C. J. Medforth, *Chem. Soc. Rev.* **27** (1998) 31
13. M. Zimmer, *Coord. Chem. Rev.* **253** (2009) 817
14. S. R. Niketić, K. Rasmussen, *The Consistent Force Field: A Documentation, Lecture Notes in Chemistry*, Springer, Berlin, 1977
15. K. Rasmussen, *Potential Energy Functions in Conformational Analysis, Lecture Notes in Chemistry*, Springer, Berlin, 1985
16. N. Raos, S. R. Niketić, V. Simeon, *J. Inorg. Biochem.* **16** (1982) 1
17. *Gaussian 98 Pople, Revision A.6*, Gaussian Inc., Pittsburgh, PA, 1998
18. A. K. Rappé, C. J. Casewit, *Molecular Mechanics across Chemistry*, University Science Books, South Orange, NJ, 1997, p. 37.

Journal of the Serbian Chemical Society
JSCS@tmf.bg.ac.rs • www.shd.org.rs/JSCS
J. Serb. Chem. Soc. 75 (12) S1–S3 (2010) *Supplementary material*

SUPPLEMENTARY MATERIAL TO

Consistent force field for metalloporphyrins

LJUBICA ANDJELKOVIĆ[1], SONJA GRUBIŠIĆ[1#], IVANA DJORDJEVIĆ[1], MATIJA ZLATAR[1], SVETOZAR NIKETIĆ[1#] and MAJA GRUDEN-PAVLOVIĆ[2*#]

[1]*Center for Chemistry, Institute of Chemistry, Technology and Metallurgy, University of Belgrade, Njegoševa 12, 11001 Belgrade and* [2]*Faculty of Chemistry, University of Belgrade, Studentski Trg 12–16, 11001 Belgrade, Serbia*

J. Serb. Chem. Soc. 75 (12) (2010) 1671–1683

CFF PARAMETERS FOR METALLOPORPHYRINS

TABLE S-I. Bond stretching parameters

Bond	k_r / kcal mol^{-1} Å^{-2}	r_0 / Å	Bond	k_r / kcal mol^{-1} Å^{-2}	r_0 / Å
Ni–N	359.50	1.940	C_β–Cl	487.48	1.720
Tb–N	359.50	2.360	C_β–Br	355.86	1.881
N–C_α	1594.74	1.375	C_p–C_p	1380.48	1.394
C_α–C_β	1380.48	1.337	C_p–H	661.80	1.084
C_β–H	661.00	1.101	C_p–C_m	632.72	1.497
C_{sp3}–C_{sp3}	633.72	1.523	C_m–C_α	1409.24	1.370
C_{sp3}–H	661.48	1.113	C_β–C_{sp3}	1409.29	1.470

TABLE S-II. Angle bending parameters

Angle	k_θ / kcal mol^{-1} rad^{-2}	θ_0 / *rad*	Angle	k_θ / kcal mol^{-1} rad^{-2}	θ_0 / *rad*
N–M–N(cis)	5.00	1.571	C_{sp3}–C_{sp3}–H	20.84	1.902
N–M–N(trans)	30.32	3.146	H–C_{sp3}–H	46.08	1.902
M–N–C_α	129.60	2.182	C_α–N– C_α	61.92	1.832
C_α–C_β–H	129.60	2.182	C_p–C_p–H	51.84	2.094
C_β–C_β–H	129.60	2.182	C_p–C_p–C_m	61.92	2.094
N–C_α–C_β	129.60	2.182	C_α–C_m–C_α	61.92	2.120
C_α–C_β–C_β	129.60	2.182	N–C_α–C_m	61.92	2.175
C_m–C_α–C_β	129.60	2.182	C_α–C_β–Cl	134.00	2.094
C_β–C_β–Cl	129.60	2.182	C_p–C_p–C_p	61.92	2.094
C_α–C_m–C_p	129.60	2.182	C_β–C_β–Br	109.90	2.094
C_α–C_β–Br	109.90	2.094	C_β–C_β–C_{sp3}	134.00	2.094
C_{sp3}–C_{sp3}–C_{sp3}	61.92	2.094	C_β–C_{sp3}–C_{sp3}	80.80	1.902

* Corresponding author. E-mail: gmaja@chem.bg.ac.rs
# Serbian Chemical Society member.

TABLE S-III. Torsion angle parameters

Angle	k_Φ / kcal mol^{-1}	n	Angle	k_Φ / kcal mol^{-1}	n
C_m–C_α–N–M	1.57	–2.0	C_β–C_β–C_α–C_m	10.00	–2.0
C_α–C_β–C_β–C_α	3.00	–2.0	H–C_β–C_β–H	3.00	–2.0
H–C_β–C_β–C_α	3.00	–2.0	C_p–C_m–C_α–C_β	10.00	–2.0
C_p–C_p–C_m–C_α	0.50	–2.0	C_p–C_p–C_p–C_p	7.50	–2.0
C_m–C_p–C_p–H	7.50	–2.0	H–C_p–C_p–H	7.50	–2.0
Cl–C_β–C_β–Cl	3.00	–2.0	Cl–C_β–C_β–C_α	3.00	–2.0
Cl–C_β–C_β–H[a]	3.00	–2.0	H–C_β–C_β–C_α	3.00	–2.0
C_α–N–C_α–C_m	3.00	–2.0	H–C_{sp3}–C_{sp3}–C_m	0.50	3.0
H–C_{sp3}–C_{sp3}–C_{sp3}	0.00	0.0	Cl–C_β–C_β–Cl[a]	3.00	–2.0
H–C_{sp3}–C_{sp3}–C_β	0.50	3.0	H–C_{sp3}–C_β–C_β	0.24	6.0

[a]If the substituent is Br, the torsion angle parameters are the same

TABLE S-IV. Out-of-plane bending parameters

Conformation	k_ω / kcal mol^{-1}
N–C_β–C_m.C_α	10
C_α–H–C_α.C_m	90
C_β–H–C_α.C_β	10
C_α– C_p–C_α.C_m	90
C_α–C_{sp3}–C_α.C_m	90
C_β–X–C_α.C_β	10

TABLE S-V. Van der Waals parameters (all types of C atoms in C–Br)

Bond	ε / kcal mol^{-1}	r^* / Å	Bond	ε / kcal mol^{-1}	r^* / Å
M–C_β	0.130	3.24	M–H	0.134	2.70
M–C_m	0.130	3.24	M–Cl	0.115	3.28
M–C_p	0.130	3.24	N–H	0.051	3.32
N–C_β	0.049	3.76	N–C_α	0.049	3.76
M–C_m	0.049	3.76	H–H	0.047	3.00
C_α–C_β	0.044	3.88	C_α–C_α	0.044	3.88
C_β–C_β	0.044	3.88	C_m–H	0.046	3.34
C_m–C_α	0.046	3.88	C_m–C_β	0.046	3.88
C_p–C_p	0.044	3.88	N–Cl	0.115	3.85
H–C_β	0.046	3.34	H–C_α	0.046	3.34
Cl–C_β	0.103	3.97	Cl–C_α	0.103	3.97
Cl–Cl	0.240	4.00	H–Cl	0.106	3.53
Cl–C_m	0.103	3.97	N–N	0.055	3.64
H–C_p	0.046	3.34	C_p–C_p	0.044	3.88
C_p–C_m	0.044	3.88	C_p–C_α	0.044	3.88
C_p–C_β	0.044	3.88	C_p–N	0.049	3.74
C_p–Cl	0.103	3.97	C[a]–Br	0.119	4.12
Br–Br	0.320	4.36	M–Br	0.349	3.38
N–Br	0.133	4.00	H–Br	0.122	3.68
C_{sp3}–H	0.046	3.34	C_{sp3}–C_{sp3}	0.044	3.88
C_{sp3}–C_m	0.044	3.88	C_{sp3}–C_β	0.044	3.88
C_{sp3}–M	0.131	3.10	C_{sp3}–N	0.049	3.72

TABLE S-VI. Electrostatic parameters

Species	*Esu*
M	0.543
Cl	–0.315
C_α	0.285
C_p	–0.080
Br	0.032
N	–0.665
C_m	0.334
C_β	0.285
H	0.285
H[a]	0.070

[a]This value was used for CFF calculation of Br-substituted TPP molecules

Journal of the Serbian Chemical Society
JSCS-info@shd.org.rs • www.shd.org.rs/JSCS
J. Serb. Chem. Soc. 75 (12) 1685–1699 (2010)
JSCS–4088
UDC 547.857.5+547.269.3:543.552+541.135.5–033.5
Original scientific paper

Voltammetric determination of dopamine in the presence of uric acid using a 2-hydroxy-1-(1-hydroxynaphthyl-2-azo)--naphthalin-4-sulfonic acid modified glassy carbon electrode

ALI ASGHAR ENSAFI*, SAMIRA DADKHAH-TEHRANI and BEHZAD REZAEI

Department of Chemistry, Isfahan University of Technology, Isfahan 84156-83111, Iran

(Received 11 March, revised 30 July 2010)

Abstract: A polymerized film of 2-hydroxy-1-(1-hydroxynaphthyl-2-azo)-naphthalin-4-sulfonic acid (HHNANSA) was prepared at the surface of a glassy carbon electrode by electropolymerization. The modified electrode was used for the simultaneous determination of dopamine (DA) and uric acid (UA). The electrochemical behaviors of the compounds at the surface of the modified electrode were studied using cyclic voltammetry, chronoamperometry, and square wave voltammetry (SWV). The experimental results indicated that the modified electrode exhibited an efficient electrocatalytic activity towards the oxidation of DA and UA, with a peak separation of about 140 mV at pH 5.0. Using chronoamperometry, the catalytic reaction rate constant was measured and found to equal to 1.23×10^4 mol^{-1} L s^{-1}. At pH 5.0, the catalytic peak currents linearly depended on the DA and/or UA concentrations in the range of 1.0–300 μmol L^{-1} DA (two linear segments with different slopes) and 6.7–20 μmol L^{-1} UA, using SWV. The detection limits for DA and UA were 0.25 and 1.17 μmol L^{-1}, respectively. The *RSD* % for 40.0 and 140.0 μmol L^{-1} DA were 1.9 and 2.2 %, respectively, whereas for 10.0 and 20.0 μmol L^{-1} UA, they were 1.8 and 1.2 %, respectively. The modified electrode showed good sensitivity, selectivity, and stability. It was successfully applied for the determination of DA and UA in real samples, such as drugs and urine.

Keywords: 2-hydroxy-1-(1-hydroxynaphthyl-2-azo)-naphthalin-4-sulfonic acid; simultaneous determination; dopamine and uric acid; voltammetry.

INTRODUCTION

Dihydroxyphenylethylamine, also commonly known as dopamine (DA), is one of the most significant catecholamines and is an important neurotransmitter in the mammalian central nervous system. It is currently the subject of intensive research by neuroscientists and chemists and rapid and simple methods for the

* Corresponding author. E-mail: ensafi@cc.iut.ac.ir
doi: 10.2298/JSC100311134E

determination of its concentration are sought.[1–3] It has also been suggested that DA plays a role in drug addiction and some manifestations of HIV.[4–6] Dopamine is not just a precursor of norepinephrine (noradrenaline) and epinephrine (adrenaline) but a neurotransmitter as well. Therefore, the determination of this compound is very necessary.

Uric acid (2,6,8-trihydroxypurine, UA) is a compound of great biomedical interests and has important roles in human metabolism. UA, the end metabolic product of purine[7] *via* the liver, is present in blood and urine. Monitoring UA in blood or urine can be used as an indicator for an early warning sign of kidney diseases. Abnormal UA level in a human body could be caused by several diseases, such as hyperuricemia, gout, cardiovascular disorder, Lesch–Nyan syndrome, and chronic renal disease. DA and UA are co-present in biological fluids, such as urine and blood. Therefore, it is important to develop new techniques for the selective detection of DA in the presence of UA in a routine assay. The direct electro-oxidation of DA and UA at bare electrodes requires high overpotentials. In addition, they have overlapped signals because the oxidation peaks of DA and UA at a bare electrode are at nearly the same potential, making their discrimination very difficult.[8,9]

Several papers have reported using modified electrodes for the simultaneous determination of DA and UA.[10–17,21] Recently, polymer film modified electrodes have been used as electrochemical sensors in the wide application fields of chemical sensors and biosensors.[18–21] Comparisons of the proposed method with the similar electrochemical methods are presented in Table I. Although, previous studied based on poly(3-(5-chloro-2-hydroxyphenylazo)-4,5-dihydroxynaphthalene-2,7-disulfonic acid[17] and sulfonazo III film[21] modified electrodes have better limits of detection, the proposed modified electrode based on 2-hydroxy-1-(1-

TABLE I. A comparison of the efficiency of some modified electrodes in the determination of DA and UA

Sensitivity μA μmol^{-1} L		Limit of detection μmol L^{-1}		Linear dynamic range μmol L^{-1}		Ref.
DA	UA	DA	UA	DA	UA	
0.3316	0.0929	0.075	0.021	0.2–45.8	0.06–166.0	10
1.0728	0.0910	0.02	1.0	0.1–200	10.0–130.0	11
Not reported	17.00	0.0027	0.2	0.0–6.0	0.5–100.0	12
Not reported	Not reported	1.0	1.0	2.0–1500	2.0–220	13
1.0	Not reported	0.5	Not reported	2.0–10.0	Not reported	14
1.741	0.7360	0.12	0.6	0.2–80.8	1.2–100.0	15
Not reported	Not reported	Not reported	5.0	Not reported	5.0–53.0	16
0.0808	0.1013	0.03	0.11	0.05–470	0.2–100	17
0.0572	0.3533	0.29	0.016	5.0–280	0.1–18.0	21
1.5659	1.1707	0.25	1.17	1.0–20	6.7–20	This work
0.0856	–	–	–	20–300	–	This work

-hydroxynaphthyl-2-azo)-naphthalin-4-sulfonic acid has a longer linear dynamic range and is free from interference by aspirin.

To the best of our knowledge, no work has been reported on the use of 2-hydroxy-1-(1-hydroxynaphthyl-2-azo)-naphthalin-4-sulfonic acid (HHNANSA, Scheme 1) modified glassy carbon electrode (HHNANSA–GCE) for the electrocatalytic determination of DA and UA. Consequently, in this study, a GCE was modified with a HHNANSA polymer film and then the electrochemical behavior of DA and UA at the surface of the modified electrode was studied. Using the modified electrode, a sensitive and selective method was established for the simultaneous determination of DA and UA.

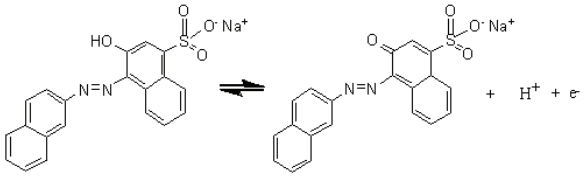

Scheme 1. Structure of 2-hydroxy-1-(1-hydroxynaphthyl-2-azo)-naphthalin-4-sulfonic acid.

EXPERIMENTAL

Chemicals

All chemicals were of analytical reagent grade and used without further purification. Doubly distilled water was used throughout the experiments. Uric acid was purchased from Sigma-Aldrich. Dopamine was obtained from Merck.

Phosphate buffer solutions (PBS) with different pH values were prepared by mixing 0.10 mol L^{-1} Na_2HPO_4 and 0.10 mol L^{-1} NaH_2PO_4. The pH values were adjusted by addition of 1.0 mol L^{-1} H_3PO_4 and/or NaOH solution.

A stock solution of dopamine (0.010 mol L^{-1}) was prepared daily by dissolving dopamine in water. Uric acid solution (0.010 mol L^{-1}) was prepared by dissolving the solid in a small volume of 0.1 mol L^{-1} NaOH solution and diluted with water to obtain the desired concentration. Other dilute standard solutions were prepared by appropriate dilution of the stock solutions in PBS, pH 5.0.

Apparatus

A Corning pH-meter, Model 140, with a glass electrode (conjugated with an Ag/AgCl reference electrode, Model 6.0232.100) was used to determine the pH of the solutions.

Voltammograms were obtained using an EG & G instrument, Model 384B processor, with three electrodes consisting of a platinum wire as the auxiliary electrode, a HHNANSA––GCE as the working electrode and Ag/AgCl (3 mol L^{-1} KCl) as the reference electrode.

Preparation of the poly-2-hydroxy-1-(1-hydroxynaphthyl-2-azo)-naphthalin-4-sulfonic acid film-modified GC electrode

Prior to each experiment, the glassy carbon electrode (GCE) was polished with 0.05 μm alumina in a water surrey using a polishing cloth. The GCE was subsequently sonicated in a mixture of water/ethanol (90/10 v/v) after each polishing step to be electrochemically pretreated later by cycling at a scan rate of 100 mV s^{-1} 10 times in 0.1 mol L^{-1} H_2SO_4 solution in the potential range of –0.40 to 1.50 V, to obtain a stable background current. Subsequently,

the electrode was placed in a solution containing 0.2 mol L^{-1} NaOH and 10.0 mmol L^{-1} 2-hydroxy-1-(1-hydroxynaphthyl-2-azo)-naphthalin-4-sulfonic acid (HHNANSA) and a cyclic potential sweep was applied in the range of –0.10 to 1.00 at a scan rate of 33 mV s^{-1} for 30 times (the anodic peak potential and current tended to be stable after 25 scans). After the polymerization, the modified electrode was washed with water and scan cycled 5 times at pH 5.0 (PBS) between 0.00 and 1.00 V to eliminate untreated HHNANSA monomer, and thus increase its reproducibility and stability.

Procedure

Five milliliters of the buffer solution (pH 5.0) were transferred into the electrochemical cell using the three-electrode system. Then, the SW voltammogram was recorded from 0.00 to 1.00 V at a frequency of 100 Hz and a pulse height of 20 mV with a potential scan rate of 33 mV s^{-1}. The peak current was measured and recorded as the blank signal (I_{pb}). After the background voltammogram had been obtained, aliquots of the sample solution containing DA, and/or UA were introduced into the cell. Then, the SW voltammogram was recorded as described above to give the sample peak current. The peak current was measured and recorded as the sample signal (I_{ps}). All the data were obtained at room temperature. The difference in the currents ($I_{ps} - I_{pb}$) was considered as a net signal (ΔI_p) for each of the experiments. Calibration graphs were prepared by plotting the net peak currents *vs.* the DA and/or UA concentrations in the solution.

Real sample preparation

Dopamine hydrochloride injection solution (40 mg mL^{-1}) was analyzed directly after diluting 100 times with water. 0.10 mL of the diluted solution was injected into a 10-mL volumetric flask and made up to volume with buffer solution (pH 5.0). The test solution was then transferred into the electrochemical cell and the DA content was measured according to the recommended procedure.

Urine samples were analyzed directly after diluting 25 times with buffer solution (pH 5.0) without any further pretreatment. Then, 5 mL of this test solution was transferred into the electrochemical cell and the DA and UA contents were determined according to the recommended procedure.

RESULTS AND DISCUSSION

Electrochemical properties of the poly (2-hydroxy-1-(1-hydroxynaphthyl-2-azo)--naphthalin-4-sulfonic acid) film-modified GCE

The behavior of poly(2-hydroxy-1-(1-hydroxynaphthyl-2-azo)-naphthalin-4--sulfonic acid) (PHHNANSA) at the surface of a GCE is shown in Fig. 1. As can be seen in the cyclic voltammograms, an anodic peak appeared at about 0.10 V due to the oxidation of HHNANSA monomer with cycles, whereas on the reversed scan, a cathodic wave formed at a potential of –0.10 V. These anodic and cathodic peak potentials tended to be stable after 25 scans. This suggest that the initially-formed PHHNANSA film underwent a leaching process during the scan cycles up to 25 cycles, which may imply a self-adjustment of the polymer film thickness at the GCE.

The electrochemical properties of the modified electrode were studied by cyclic voltammetry (CV) in the buffer solution (pH 5.0). The CVs of the mo-

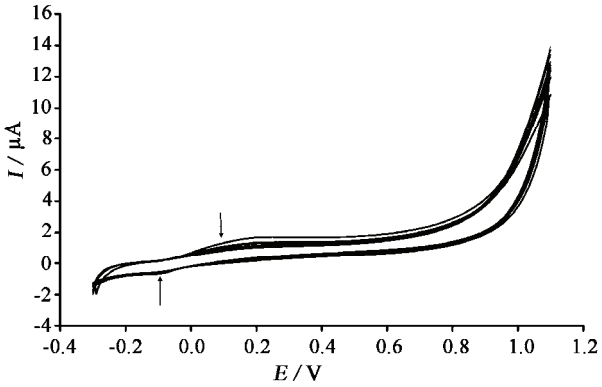

Fig. 1. Electropolymerization graph of HHNANSA in 0.2 mol L^{-1} NaOH and 10 mmol L^{-1} HHNANSA at a scan rate of 100 mV s^{-1}.

dified electrode at various scan rates (10–100 mV s^{-1}) are shown in the inset to Fig. 2. The experimental results show well-defined and reproducible anodic and cathodic peaks, with a peak separation potential of about ΔE_p ($E_{pa} - E_{pc}$) = 200 mV. These CVs were used to examine the variation of the peak currents *vs.* potential scan rates. The plot of the anodic peak currents was linearly dependent on υ with a correlation coefficient of 0.9966 at all scan rates (Fig. 2A). Therefore, the peak current must be related to the surface concentration of electroactive species, Γ, by:

$$I_P = n^2F^2A\Gamma v/4RT \quad (1)$$

where n represents the number of electrons involved in the reaction (n = 1), A is the surface area of the electrode (0.031 cm^2), I_P is the peak current, Γ represents the surface coverage concentration (mol cm^{-2}), and v is the scan rate. From the slope of the anodic peak currents *vs.* the scan rate, the calculated surface concentration of 2-hydroxy-1-(1-hydroxynaphthyl-2-azo)-naphthalin-4-sulfonic acid was 4.46×10^{-8} mol cm^{-2}. The cyclic voltammograms of the bare GCE in PBS (pH 5.0) at various scan rates (between 10 to 110 mV s^{-1}) are shown in Fig. 2B.

The electrochemical response of the HHNANSA–GCE depended on the pH value of the supporting electrolyte solution. By increasing the pH of the supporting electrolyte (from 2.0 to 7.0), the redox and oxidation peak potentials shifted negatively and the anodic peak potential (E_{pa}) depended linearly on the pH value.

Electro-oxidation of DA and UA at the surface of the HHNANSA–GCE

The oxidations of DA and UA at the surface of a bare GCE and HHNANSA––GCE in two different concentrations are shown in Fig. 3. The results showed that both compounds were oxidized with well-defined and distinguishable sharp peaks potential at the HHNANSA–GCE. On the other hand, the indistinguishable

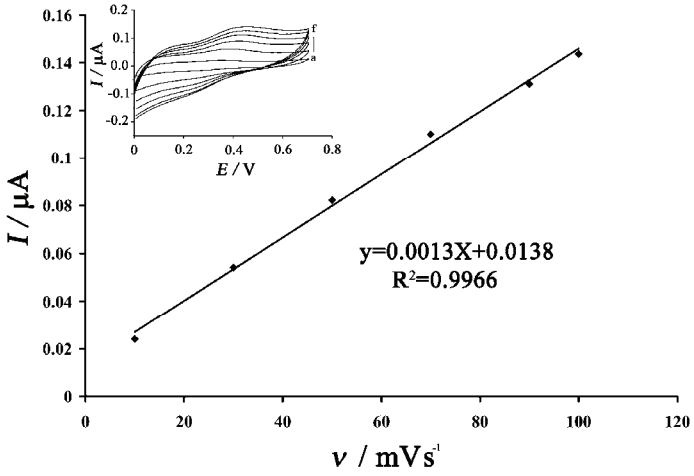

(A)

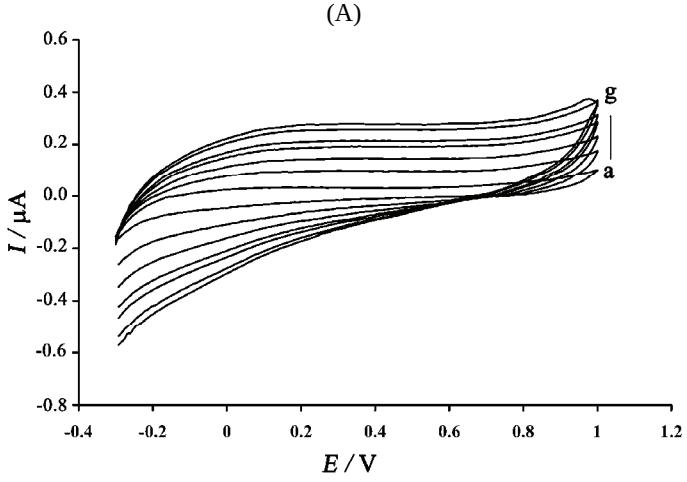

(B)

Fig. 2. A) Dependence of peak current on the scan rate for the poly(HHNANSA)-modified GCE in PBS (pH 5.0). Inset: cyclic voltammograms of the poly(HHNANSA)-modified GCE in PBS (pH 5.0) at various scan rates: a) 10; b) 30; c) 50; d) 70; e) 90; f) 100 mV s^{-1}; B) Cyclic voltammograms of the bare GCE in PBS (pH 5.0) at various scan rates: a) 10; b) 30; c) 50; d) 70; e) 80; f) 100; g) 110 mV s^{-1}.

and broad peak potentials at the bare GCE indicate slow kinetics of electron transfer. The oxidation peak potentials of DA and UA at the modified electrode separated completely into two well-defined peaks at 0.32 and 0.46 V *vs.* Ag/AgCl, respectively, whereas at the bare GCE, the oxidation peak potentials were at about 0.40 and 0.50 V for DA and UA, respectively at pH 5.0. In addition, both the two peaks potential at the HHNANSA–GCE exhibited negative potential shifts. These shifts in the oxidation peaks potential and enhanced currents of the

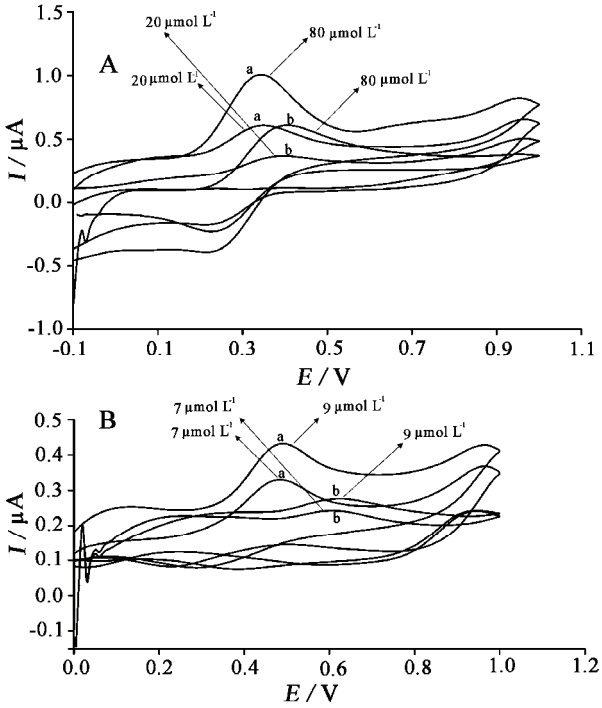

Fig. 3. Cyclic voltammograms of: A) 20.0 and 80.0 μmol L^{-1} DA; B) 7.0 and 9.0 μmol L^{-1} UA at the surface of a) the modified and b) a bare glassy carbon electrode.

oxidation peaks potential with the HHNANSA–GCE indicate that the modified electrode had a catalytic effect on the oxidation of DA and UA. Moreover, the oxidation current of DA increased linearly with the square root of the scan rate, which demonstrates a diffusion controlled electrochemical process (Fig. 4).

The influence of solution pH on the DA and UA peaks current were studied with 50.0 μmol L^{-1} DA and 50.0 μmol L^{-1} UA. The results showed that the UA peak current increased when the solution pH increased from 2.0 to 5.0, whereas at higher pH values, the peak current decreased. For DA, the peak current increased sharply on increasing the pH to 5.0, then leveled off up to pH 7.0 and then decreased at higher pH values. As is known, the pK_a values of R–SO_3H (R = aryl group) are usually about 4; therefore, the –SO_3Na of the poly(2-hydroxy-1-(1-hydroxynaphthyl-2-azo)-naphthalin-4-sulfonic acid) film could dissociate favorably into the negatively charged –SO_3^- group under alkaline conditions. The alkaline –NH_2 group of DA (pK_a 8.9) could obtain a proton and form positive DA ions. These have a great affinity toward the poly(2-hydroxy-1--(1-hydroxynaphthyl-2-azo)-naphthalin-4-sulfonic acid) film.

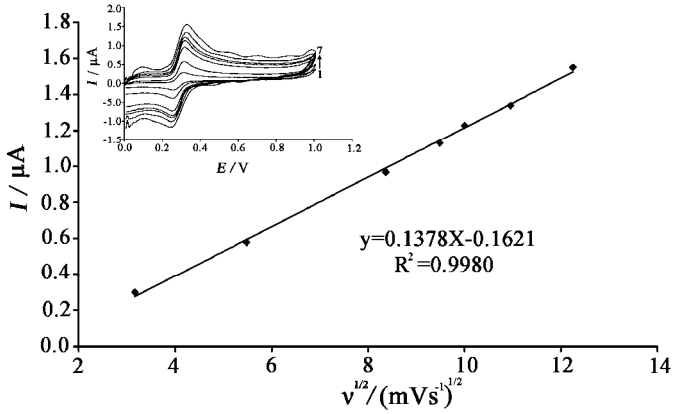

Fig. 4. Variation of electrocatalytic current (I_p) with square scan rate. Inset: cyclic voltammograms of poly(HHNANSA) modified GCE in PBS (pH 5.0) containing 100.0 μmol L^{-1} DA at different scan rates. The number of 1 to 7 corresponds to 10, 30, 70, 90, 100, 120 and 150 mV s^{-1}, respectively.

Chornoamperometric studies

For the determination of the diffusion coefficient of DA, single potential step chronoamperometry was used with the HHNANSA–GCE. The current–time curves of the HHNANSA–GCE obtained by setting the electrode potential at 270 mV (*vs.* Ag|AgCl|KCl_{sat}) for different concentrations of DA are shown in Fig. 5. The linearity of the electrocatalytic current *vs.* $v^{1/2}$ showed that the current is controlled by diffusion of DA from the bulk solution toward the surface of the

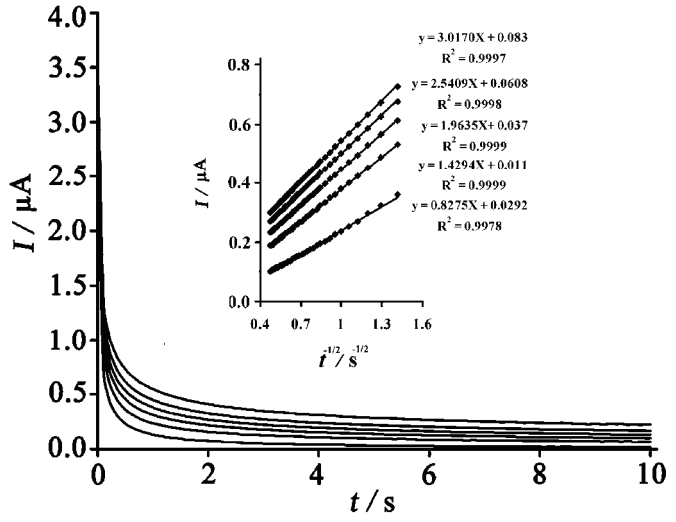

Fig. 5. Chronoamperograms of the poly(HHNANSA) modified GCE in PBS (pH 5.0) in the presence of (in direction of *I*-axis): 0.0; 60.0; 100.0; 160.0; 260.0 and 300.0 μmol L^{-1} of DA. Inset shows Cottrell plots derived from the chronoamperometric data.

electrode, which caused near Cottrellian behavior. The slope of the linear region of a Cottrell plot can be used to estimate the diffusion coefficients. A plot of I *vs.* $t^{-1/2}$ at the HHNANSA–GCE in the presence of DA gave a straight line, the slope of which can be used to estimate the diffusion coefficient (D) of DA in the range of 60 to 300 μmol L^{-1}. The mean value of the D for DA was found to be 1.30×10^{-5} cm^2 s^{-1} (Fig. 5, inset A). This value is different to the previously obtained value of 6.40×10^{-6} cm^2 s^{-1}).[17] This is due to difference in the solution pH, which affects the net charge of DA in the solutions and hence affects the diffusion coefficient.

In addition, chronoamperometry can be performed to evaluate the rate of an electrocatalyzed oxidation. The rate constant for the chemical reaction between DA and redox cites of 2-hydroxy-1-(1-hydroxynaphthyl-2-azo)-naphthalin-4-sulfonic acid can be evaluated according to the method of Galus:[22]

$$I_C/I_L = \gamma^{1/2}(\pi^{1/2} \text{ erf } (\gamma^{1/2}) + \exp(-\gamma)/\gamma^{1/2}) \quad (2)$$

where I_C is the catalytic current of the HHNANSA–GCE in the presence of DA, I_L is the limited current in the absence of DA and $\gamma = k_h C_b t$ (C_b is the bulk concentration of DA, mol L^{-1}) is the argument of the error function. In cases where γ exceeds 2, the error function is almost equal to 1 and Eq. (2) can be reduced to:

$$I_C/I_L = \pi^{1/2}\gamma^{1/2} = \pi^{1/2} (k_h C_b t)^{1/2} \quad (3)$$

where k_h and t are the catalytic rate constant (mol^{-1} L s^{-1}) and time elapsed, respectively. Equation (3) can be used to calculate the rate constant of the catalytic process, k_h. From the slope of I_C/I_L *vs.* $t^{1/2}$, the value of k_h can be simply calculated for a given concentration of the substrate. The calculated value of k_h was equal to 1.23×10^4 mol^{-1} L s^{-1}. This value of k_h explains the sharp feature of the catalytic peak observed for the catalytic oxidation of DA at HHNANSA–GCE. These methods have already been used for an estimation of D and k_h for some compounds.[23–26]

Simultaneous determination of DA and UA

As the obtained results showed, the HHNANSA–GCE possessed excellent electrocatalytic activity for the oxidation of DA and UA. The difference in the oxidation peak potentials for DA–UA was 140 mV, which is large enough to allow for the simultaneous determination of DA and UA in a mixture. The electro-oxidation processes of DA and UA in the mixture were evaluated by varying the concentration of the individual analytic species. The result showed two linear segments with different slopes for the DA concentration; namely, for 1.0–20.0 μmol L^{-1} DA with a regression equation of I_p (μA) = (1.566±0.050)c_{DA} – – (0.4211±0.0080) (r^2 = 0.9944, n = 8) (Fig. 6A), while for 20.0–300.0 μmol L^{-1} DA, the regression equation was I_p (μA) = (0.0856±0.0050)c_{DA} + (31.019±

±0.090) (r^2 = 0.9897, n = 7) (Fig. 6B). In addition, for 6.7–20.0 μmol L^{-1} UA, the regression equation was I_p (μA) = (1.1707±0.05021)c_{UA} – (3.3652±0.07010) (r^2 = 0.9920, n = 5) (Fig. 6C), where c is the concentration of the substance (μmol L^{-1}) and I_p is the net peak current (the sample peak current minus the blank peak current).

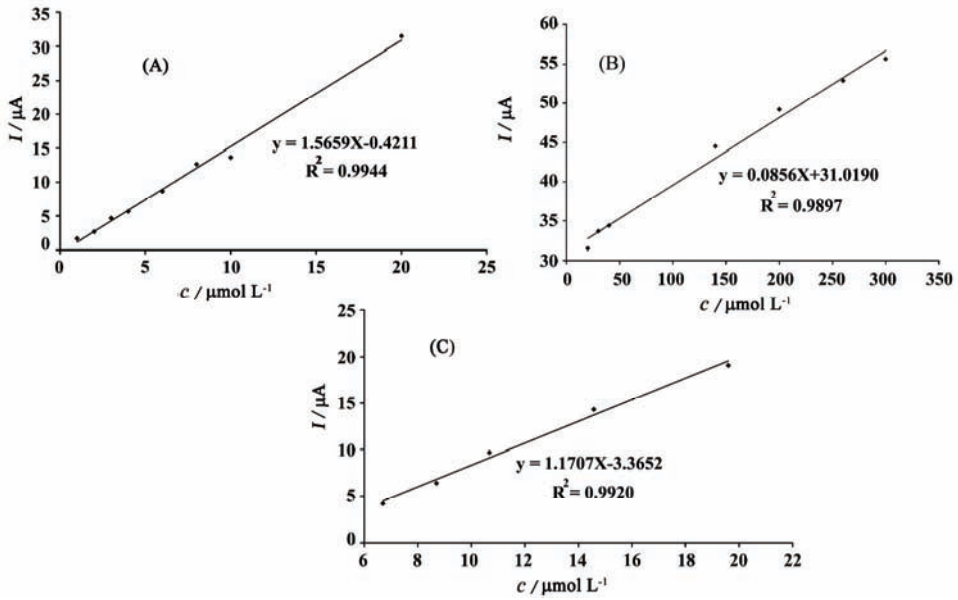

Fig. 6. A) Plot of the oxidation current *vs.* the concentration of DA in the range of 1.0–20.0 μmol L^{-1}; B) as a (A), in the range of 20–300 μmol L^{-1} using SWV; C) calibration curve for UA in the range of 6.7–20.0 μmol L^{-1} using SWV.

The detection limits were determined at 0.25 and 1.17 μmol L^{-1} for DA and UA, respectively, according to the definition of $Y_{LOD} = Y_B + 3\sigma$.[27]

In order to check for the presence of any intermolecular effects between DA and UA, two different experiments were performed under the optimum conditions at pH 5.0. In each experiment, the concentration of one of the two compounds was changed while the concentration of the other compound was kept constant. The results are shown in Figs. 7A and 7B. The results showed no any intermolecular interactions during the oxidation of the compounds at the surface of the HHNANSA–GCE.

The sensitivities towards DA in the absence and presence of UA were found to be 0.0856±0.005 μA μmol L^{-1} (in the absence of UA) and 0.0960±0.006 μA μmol L^{-1} (in the presence of UA) (Fig. 8A). However, for UA, the obtained sensitivities were 1.1707±0.0901 (in the absence of DA) and 1.1691±0.0240 μA μmol L^{-1} (in the presence of DA) (Fig. 8B). It is interesting to note that the

sensitivities of the HHNANSA–GCE to DA and UA in the absence and presence of the other compound were very similar, which indicates that the oxidation processes of DA and UA at the HHNANSA-GCE were independent. Therefore, the simultaneous or independent measurements of the two analytes are possible without any interference.

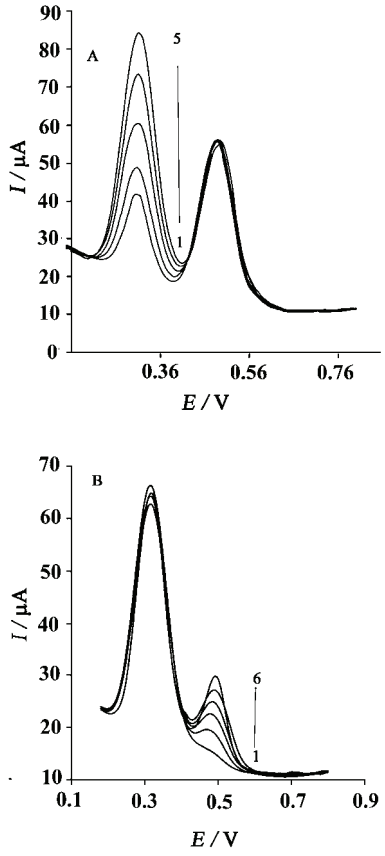

Fig. 7. A) SWV of: 1) 20.0; 2) 50.0; 3) 110.0; 4) 160.0; 5) 220.0 μmol L^{-1} DA in the presence of 60.0 μmol L^{-1} UA; B) SWV of: 1) 8.0; 2) 10.0; 3) 12.0; 4) 15.0; 5) 17.0; 6) 19.0 μmol L^{-1} UA in the presence of 100.0 μmol L^{-1} DA.

Interference study

The influence of various substances as compounds that could potentially interfere with the determination of DA and UA were studied under the optimum conditions with 100.0 μmol L^{-1} DA and 14.0 μmol L^{-1} UA at pH 5.0. The potentially interfering substances were chosen from substances commonly found with DA and UA in pharmaceuticals and/or in biological fluids. The tolerance limit was defined as the maximum concentration of the interfering substance that caused an error of less than ±5 % for the determination of DA and UA. The results are presented in Table II. These results showed the high selectivity of the HHNANSA–GCE for the determination of DA and UA.

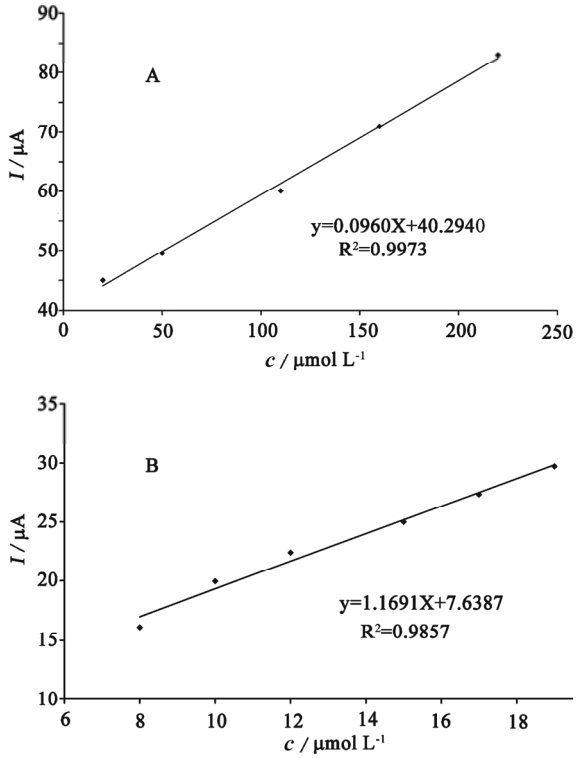

Fig. 8. A) Plot of different concentrations of DA in the presence of a fixed amount of UA; B) Plot of different concentrations of UA in the presence of a fixed amount of DA.

Table II. Interference of some foreign substances on the determination of 100.0 μmol L^{-1} DA and 14.0 μmol L^{-1} UA under the optimized conditions

Species	*w*(substance)/*w*(DA)	*w*(substance)/*w*(UA)
Glucose, sucrose, urea, fructose	400	1000
Citric acid	100	1000
Ca^{2+}, Mg^{2+}, F^{-}, Cl^{-}, Na^{+}, K^{+}, SO_4^{2-}	100	800
Carbonate	200	600
Tryosin, aspirin	20	100
Histidine, cysteine, ascorbic acid	2	100

Real sample analysis

In order to evaluate the applicability of the proposed method for the determination of DA and UA in real samples, the utility of the developed method was tested by analysis of these compounds in mixed synthetic and in real samples using standard addition methods. The results are summarized in Table III. The good recoveries of the mixture samples indicate the successful application of the proposed method for the simultaneous determination of DA and UA. For further

investigation, the recovery of DA was determined for dopamine injection. The dopamine injection solution (specified content of DA was 40.0 mg mL^{-1}) was diluted to 100 mL with water, then a different amount of the diluted solution was transferred into each of a series of 10-mL volumetric flasks and diluted to the mark with phosphate buffer. Then, 10 mL aliquot of this test solution was placed in the electrochemical cell and the DA content was measured by the proposed method. This procedure was repeated five times and the relative standard deviation was found as 1.6 %. Different standard concentrations of DA were added to the diluted DA injection solution, with recoveries between 96.5 and 103.2 % for five measurements (Table III).

Table III. Determination of DA and UA in human urine and DA injection samples

Sample	Added, μmol L^{-1}		Found, μmol L^{-1}		Recovery, %	
	DA	UA	DA	UA	DA	UA
1	20.0	10.0	20.9±0.8	9.9±0.2	104.6	99.0
2	50.0	14.0	51.6±0.6	13.4±0.5	103.1	96.1
3	70.0	20.0	67.9±0.7	19.4±0.4	97.1	97.1
DA injection						
4	10.0	–	9.6±0.5	–	96.5	–
5	15.0	–	15.1±0.7	–	100.8	–
6	50.0	–	51.6±0.6	–	103.2	–

CONCLUSIONS

In this study, the electrochemical behavior of DA and UA at a glassy carbon electrode modified with a polymerized film of 2-hydroxy-1-(1-hydroxynaphthyl--2-azo)-naphthalin-4-sulfonic acid was investigated using cyclic voltammetry and square wave voltammetry. The modified electrode separated the anodic oxidation peak potential of DA and UA with a well-defined peak separation in the presence of each other to measure DA and/or UA separately or simultaneously without any intermolecular effects. The catalytic reaction rate constant, k_h was calculated (1.23×10^4 mol^{-1} L s^{-1}) using chronoamperometry. The sensitivity of the proposed material was higher than those of reported results.[10,11,14,17,21] Moreover, the proposed method was successfully applied for the determination of these compounds in real samples.

Acknowledgements. The authors gratefully acknowledge support of this work by the Research Council of the Isfahan University of Technology (IUT) and the Center of Excellence in Sensor and Green Chemistry.

ИЗВОД

ВОЛТАМЕТРИЈСКО ОДРЕЂИВАЊЕ ДОПАМИНА У ПРИСУСТВУ МОКРАЋНЕ КИСЕЛИНЕ НА ЕЛЕКТРОДИ ОД СТАКЛАСТОГ УГЉЕНИКА МОДИФИКОВАНОГ 2-ХИДРОКСИ-1(1-ХИДРОКСИ НАФТИЛ-2-АЗО)-НАФТАЛИН-4-СУЛФОНСКОМ КИСЕЛИНОМ

ALI ASGHAR ENSAFI, SAMIRA DADKHAH-TEHRANI и B. REZAEI

Department of Chemistry, Isfahan University of Technology, Isfahan 84156-83111, Iran

Полимерни филм 2-хидрокси-(1-хидроксинафтил-2-азо)-нафталин-4-сулфонске киселине је формиран на електроди од стакластог угљеника поступком електрохемијске полимеризације. Тако модификована електрода је коришћена за истовремено одређивање допамина (ДА) и мокраћне киселине (МК). Електрохемијско понашање ових једињења на модификованој електроди је испитивано цикличном волтаметријом, хроноамперометријом и волтаметријом са правоугаоним сигналом. Експериментални резултати показују да модификована електрода представља ефикасан катализатор за оксидацију ДА и МК уз сепарацију пикова од око 140 mV при pH 5,0. Константа брзине катализоване реакције одређена је методом хроноамперометрије и износи $1{,}23\times10^4$ mol^{-1} L s^{-1}. У мерењима волтаметријом са правоугаоним сигналом у раствору pH 5,0 струјни пикови су показали линеарну зависност од концентрације ДА и/или МК у опсегу 1,0–300 μmol L^{-1} ДА (две линеарне области са различитим нагибима) и 6,7–20 μmol L^{-1} МК. Границе детекције за ДА и МК су биле 0,25 и 1,17 μmol L^{-1}, редом. Стандардна девијација за 140,0 μmol L^{-1} ДА је износила 1,9 и 2,2%, а за 10,0 и 20,0 μmol L^{-1} МК 1,8 и 1,2%, редом. Модификована електрода је показала високу осетљивост, селективност и стабилност. Такође је успешно примењена и за одређивање ДА и МК у реалним узорцима као што су лекови и урин.

(Примљено 11. марта, ревидирано 30. јула 2010)

REFERENCES

1. N. Q. Jia, Z. Y. Wang, G. F. Yang, H. B. Shen, L. Z. Zhu, *Electrochem Commun*. **9** (2007) 233
2. J. W. Mo, B. Ogorevc, *Anal. Chem.* **73** (2001) 1196
3. R. M. Wightman, C. Amatorh, R. C. Engstrom, P. D. Hale, E. W. Kristensen, W. G. Kuhr, L. J. May, *Neuroscience* **25** (1998) 513
4. R. M. Wightman, L. J. May, A. C. Michael, *Anal. Chem.* **60** (1988) 769
5. A. Heinz, H. Przuntek, G. Winterer, A. Pietzcker, *Nervenarzt* **66** (1995) 662
6. F. M. Benes, *Trends Pharmacol. Sci.* **22** (2001) 46.
7. J. K. Baillie, M. G. Bates, A. A. Thompson, W. S. Waring, R. W. Partridge, M. F. Schnopp, A. Simpson, F. Gulliver-Sloan, S. R. Maxwell, D. J. Webb, *Chest* **131** (2007) 1473
8. Y. Y. Sun, K. B. Wu, S. S. Hu, *Chem. J. Chin. Universities* **23** (2002) 2067
9. M. Mazloum-Ardakani, H. Beitollahi, B. Ganjipour, H. Naeimi, M. Nejati, *Bioelectrochem.* **75** (2009) 1
10. A. A. Ensafi, M. Taei, T. Khayamian, *Int. J. Electrochem. Sci.* **5** (2010) 116
11. H. Yao, Y. Sun, X. Lin, Y. Tang, L. Huang, *Electrochim. Acta* **52** (2007) 6165
12. J. M. Zen, P. J. Chen, *Anal. Chem.* **69** (1997) 5087
13. A. Safavi, N. Maleki, O. Moradlou, F. Tajabadi, *Anal. Biochem*. **359** (2006) 224
14. A. Balamurugan, S. M. Chen, *Anal. Chim. Acta* **596** (2007) 92
15. P. Wang, Y. Li, X. Huang, L. Wang, *Talanta* **73** (2007) 431

16. P. Ramesh, S. Sampath, *Electroanalysis* 16 (2004) 866
17. A. A. Ensafi, M. Taei, T. Khayamian, A. Arabzadeh, *Sens. Actuators B* **147** (2010) 213
18. J. B. Raoof , R. Ojani, S. Rashid-Nadimi, *Electrochim. Acta* **50** (2005) 4694
19. H. Zhao, Y. Zhang, Y. Yuan, *Analyst* **126** (2001) 358
20. T. Selvaraju, R. Ramaraj, *Electrochem. Comm.* **5** (2003) 667
21. A. A. Ensafi, M. Taei, T. Khayamian, *J. Electroanal. Chem.* **633** (2009) 212
22. Z. Galus, *Fundumentals of Electrochemical Analysis*, Ellis Horwood, New York, 1999
23. E. Mirmomtaz, A. A. Ensafi, H. Karimi-Maleh, *Electroanalysis* **20** (2008) 1973
24. H. Karimi-Maleh, A. A. Ensafi, H. R. Ensafi, *J. Braz. Chem. Soc.* **20** (2009) 880
25. H. Karimi-Maleh, A. A. Ensafi. A. R Allafchian, *J. Solid State Electrochem.* **14** (2010) 9
26. H. Yghoubian, H. Karimi-Maleh, M. A. Khalilzadeh, F. Karimi, *J. Serb. Chem. Soc.* **74** (2009) 1443
27. J. N. Miller, J. C. Miller, *Statistics and Chemometrics for Analytical Chemistry*, 4th ed., Pearson Education Ltd., Harlow, Essex, 2000.

Journal of the Serbian Chemical Society
JSCS-info@shd.org.rs • www.shd.org.rs/JSCS
J. Serb. Chem. Soc. 75 (12) 1701–1709 (2010)
JSCS–4089
UDC 663.2+543.421:546.72+546.56+546.47(497.11)
Original scientific paper

The concentrations of Fe, Cu and Zn in selected wines from South-East Serbia

DANIJELA KOSTIĆ#, SNEŽANA MITIĆ#, GORDANA MILETIĆ, SAŠA DESPOTOVIĆ and ALEKSANDRA ZARUBICA*#

Department of Chemistry, Faculty of Science, University of Niš, 18000 Niš, Serbia

(Received 4 January, revised 30 July 2010)

Abstract: Fruits and vegetables constitute the cheapest source of essential trace elements for the majority of people living in developing countries. The Cu, Fe and Zn contents in twenty selected wine samples produced in the South-East region of Serbia were determined by flame atomic absorption spectrometry. The Cu concentrations varied from 0.07 to 0.57 ppm in wines, and the Fe concentrations fluctuated from 2.93 to 36.2 ppm, while the Zn levels were in the range from 0.21 to 0.67 ppm. The established contents of Cu and Zn showed that wines from this part of the world could serve as good dietary sources of the essential trace metals, and the determined values were within the allowed metals levels in wines for human consumption.

Keywords: AAS; Fe, Cu and Zn contents; South-East Serbian wines; wine analysis.

INTRODUCTION

Several spectroscopy techniques can be commonly used for the evaluation of food and/or drink quality[1] as well as of pharmaceutical samples.[2] Wine is a popular and worldwide consumed alcoholic beverage, which has been well-known since the early periods of civilization. The moderate consumption of wine, especially red wines, was shown to improve health and longevity.[3,4] From an analytical chemical point of view, wine is referred to as a complex matrix with a varying content of inorganic compounds (*e.g.*, traces of dissolved alkaline and alkaline earth elements, and transition metals), as well as organic substances (*e.g.*, polyphenols, polyhydroxy alcohols, proteins, amino acids, and polysaccharides) dissolved and/or dispersed in an aqueous solution of ethanol.[5]

* Corresponding author. E-mail: zarubica2000@yahoo.com
# Serbian Chemical Society member.
doi: 10.2298/JSC100104133K

Scientific discussions concerning human exposure to the trace metals contents of various beverages and dietary products, including wines, have received raising attention, since the consumption of wines, especially reasonably large volumes, may significantly contribute to the daily dietary intake of trace elements by humans.[5] Moreover, some of these trace elements (*e.g.*, Cu, Fe, and Mn) have an organoleptic effect, and also contribute to the haze and taste of wines.[6] The regional variations of the content trace metal in wines can also be used for identification purposes, *i.e.* to verify authenticity.[7] Considering all the above points, the determination of toxic (*e.g.*, As, Cd and Pb) and essential trace elements (*e.g.*, Cu) in wines appears to be an important and challenging analytical task, which requires multi-element methods of good selectivity, sensitivity, and robustness. The origin of Cu in wines is associated with copper-based vineyard sprays, whereas the As, Cd and Pb contents reflect differences in grape variety, environmental factors (*e.g.*, soil and climate), and the wine-processing method (an anthropogenic impact).[5]

However, nutritional metals such as Cu and Zn occur naturally in fruits and vegetables, as essential trace elements necessary for good health, but they could be toxic when their concentrations exceed limits of safe exposure.[3,4,8] In addition to toxicity problems, Cu and Zn deficiency may also be experienced; hence, as stated earlier,[3] knowledge of heavy metal contents in crops is important for the identification of adequate, sub-adequate and marginal intake levels for humans and animals, so that diseases related to trace element deficiency can be overcome. A large number of symptoms/ailments, comprising anemia, depressed growth, dermatitis, dwarfism, electrolyte-imbalance, gastro-intestinal and neurological disorders, lethargy and nausea, have been associated with Cu and Zn deficiency in humans, as well as with toxicity due to excessive intake.[6,8–11] Furthermore, the presence of trace elements in fruits and vegetables has been ascribed to their absorption from the soil and sources such as fertilizer, agricultural chemicals and contaminants.[8,12] Other sources of heavy metals contamination of most foodstuffs may also include agricultural mechanization procedures, sprays, seed preservatives,[13] and components from the global pollution process. Hence, the need to determine and/or monitor the Cu and Zn contents of fruits and vegetables have become imperative due to their principal role as essential or detrimental trace elements. A survey of the literature indicates that such a study is scarce, particularly in the southeast region of Serbia.

Trace elements in wine samples can be measured by different techniques, such as stripping voltammetry,[4–6,8–13] instrumental neutron activation analysis,[14] ICP–AES, ICP–MS[15–17] and/or UV–Vis spectrophotometry.[18–21]

However, the official methods for the determination of heavy metals in wine established by the Office International de la Vigne et du Vin and the American Society of Enologists are essentially based on atomic absorption spectrometry

(AAS).[22] Similarly, Flame-AAS is the official method of analysis for the determination of Na, K, Mg, Ca, Fe, Ag and Zn in wine according to EU regulations.[1] Some elements with relatively high concentrations in wine could be analyzed by flame atomic absorption spectrometry (FAAS).[23–25] However, for some elements present in wine in low concentrations, hydride generation techniques using FAAS (HG–AAS)[26–28] or mostly electrothermal atomic absorption spectrometry (ETAAS)[29–31] are used. The ETAAS method was applied in order to directly determine some trace elements (or using simple dilution) in wine.[32,33]

Flame-AAS is largely employed in wine analysis mainly due to the low cost of instrumentation, which makes the technique easily accessible to most oenological laboratories. Considering the compromise between the cost and sensitivity required, flame-AAS can be considered as the technique of choice for determination for alkaline and alkali-earth metal in wine. It is also well suited for Cu, Fe, Mn and Zn determinations, with respect to the concentration ranges of these metals in wines. On the other hand, it is not suitable for the determination of toxic or undesirable elements, such as As, Cd, Cr, and Hg and Pb, with the exception of highly contaminated samples and/or application of preconcentration procedures.

The analysis precision was usually very good, being on average above 1 % for all the elements considered at the mg L^{-1} concentration level.[14,15]

In the present study, a scheme was developed for the determination of Fe, Cu and Zn in different wine fractions. Flame and electrothermal (ET) atomic absorption spectrometry were used for the quantitative determination of the metals, depending on their levels.[4–6,8–13,34]

EXPERIMENTAL

Reagents and materials

All reagents used were of analytical grade (Merck, Germany). Stock standard solutions were prepared daily by the appropriate dilution of Titrisol standards (Merck) containing 1000 mg L^{-1} Fe, Cu or Zn. High purity water from a Milli-Q apparatus was used to prepare the standard solutions.

Sample preparation

Several types of wine samples were investigated: Serbian wine samples were given from vineries and only filtered in the further procedure. Several other commercially bottled wines (Serbian wines) were purchased from the market. Labels descriptions of the analyzed wine samples are presented in Table I. In each case, aliquots of samples were withdrawn with a glass pipette 10 cm below surface level of the liquid.

An aliquot of 5 ml of wine sample was mixed with 1.0 mL of 2 M HCl solution and further diluted to 10 mL with distilled water, and then directly nebulized in an air–acetylene flame under the optimal instrumental parameters (background correction for zinc was required). Fe, Cu and Zn were determined by AAS in the air-acetylene flame using standard calibration curves. All determinations were performed on untreated wine samples; only nitric

acid was added to lower the pH (1.0 mL of concentrated acid to 100 mL sample, the resulting pH being 1.5).

TABLE I. Label description of the wine samples

Sample No.	Sample label	Year	Vinery
1	Vranac	2001	Župa
2	Rubinova ružica	2002	Rubin
3	Cabernet Sauvignon	2001	Rubin
4	As	2003	Župa
5	Merlot	2005	Navip
6	Car Lazar	2001	Rubin
7	Medveđa krv	2006	Rubin
8	Pinot Noir	2006	Rubin
9	Kratošija	2003	Župa
10	Međaš crni	2004	Župa
11	Župski rizling	2006	Župa
12	Međaš beli	2001	Župa
13	Vranac	2004	Rubin
14	Navipovo crno Rojal	2001	Navip
15	Rubinovo crno	2003	Rubin
16	Graševina	2005	Rubin
17	Pinot Noir	2001	Navip
18	Terra Lazarica	2006	Navip
19	Jagodinska Ružica	2004	Navip
20	Rose	2002	Župa

Apparatus/analysis

The atomic absorption measurements were realized with a Varian Spectra A 10 atomic absorption spectrometer equipped with a deuterium background corrector and single element hollow cathode lamp of Cu, Fe and Zn. An air–acetylene flame was utilized for all the elements. The calibration range, wavelengths and slit values are reported in Table II.

TABLE II. Calibration range, wavelength and slit value

Characteristics of analysis	Fe	Zn	Cu
Wavelength, nm	248.3	213.9	324.8
Slit, nm	0.2	1.0	0.5
Calibration range, mg L^{-1}	0.06–15.0	0.01–2.0	0.03–10.0

RESULTS AND DISCUSSION

The determined concentrations of heavy metals in the examined wine samples originating from the southeast region of Serbia are reported in Table III.

The measured concentrations of iron (Table III) show that these varied in range from 2.93 (“Cabernet Sauvignon”) to 11.21 mg L^{-1} (“Rose”) with the exception being the wine sample named as “As”. This wine sample had an iron content of 36.2 mg L^{-1}. The concentrations of copper in the different wines also differed a lot, *i.e.*, from 0.07 mg L^{-1} (Graševina and Župski rizling) to 0.57 mg

L^{-1} (“Merlot”), while the zinc concentrations covered a somewhat narrower range, from 0.21 (“Navipovo crno Royal”) to 0.67 mg L^{-1} (“Cabernet Sauvignon”).

TABLE III. Average content of Fe, Cu and Zn in the examined wine samples (*ia* – inaccuracy of measurement (standard deviation at the 95 % confidence level))

Sample No.	Sample label	*c*±*ia* / mg L^{-1}		
		Fe(III)	Cu(II)	Zn(II)
1	Vranac	6.40±0.19	0.40±0.008	0.48±0.03
2	Rubinova ružica	5.84±0.17	0.39±0.007	0.65±0.04
3	Cabernet Sauvignon	2.93±0.09	0.11±0.002	0.67±0.01
4	As	36.2±1.08	0.14±0.003	0.57±0.03
5	Merlot	6.62±0.19	0.57±0.011	0.62±0.04
6	Car Lazar	4.69±0.14	0.12±0.002	0.61±0.04
7	Medveđa krv	3.17±0.09	0.10±0.001	0.54±0.03
8	Pinot Noir	4.62±0.14	0.17±0.003	0.55±0.03
9	Kratošija	9.78±0.29	0.12±0.002	0.55±0.03
10	Međaš crni	5.03±0.15	0.10±0.001	0.57±0.03
11	Župski rizling	5.37±0.16	0.07±0.001	0.38±0.02
12	Međaš beli	6.82±0.20	0.08±0.001	0.52±0.03
13	Vranac	3.69±0.11	0.16±0.003	0.49±0.03
14	Navipovo crno Royal	4.17±0.12	0.19±0.004	0.21±0.01
15	Rubinovo crno	3.53±0.10	0.22±0.004	0.57±0.03
16	Graševina	4.75±0.14	0.07±0.001	0.47±0.03
17	Pinot Noir	4.22±0.13	0.44±0.009	0.35±0.02
18	Terra Lazarica	6.60±0.19	0.32±0.006	0.64±0.04
19	Jagodinska Ružica	5.51±0.16	0.26±0.005	0.31±0.02
20	Rose	11.21±0.34	0.26±0.005	0.49±0.03

The allowed levels of metal in wines are defined by standards. The established allowed values of the standards differ from country to country, even though there are common standards prescribed by the International Office for Grapes and Wines.[3] An insight into the accepted limits of the content of metals in wines in different countries and also those given by the Office International de la Vigne et du Vin (OIV) are listed in Table IV.

TABLE IV. The accepted limits of the metals content, mg L^{-1}, in wines in different countries

Country	Al	As	Cd	Cu	Na	Pb	Ti	Zn
Australia	–	0.10	0.05	5.00	–	0.20	–	5.00
Germany	8.00	0.10	0.01	5.00	–	0.30	1.00	5.00
Italy	–	–	–	10.00	–	0.30	–	5.00
OIV	–	0.20	0.01	1.00	60.00	0.20	–	5.00

The results obtained in the current study are comparable with previously reported values showing high degree of agreement.[8] Here, the estimated data (Table III) demonstrate that the contents of the major metal, *i.e.*, Fe, and the

selected trace elements, *i.e.*, Cu and Zn, in wine samples from different parts of Serbia are considerably smaller than the maximum concentrations allowed according to the OIV, Tables III and IV. In addition, the contents of these trace metals in the studied Serbian wines were significantly lower than in some European wines, but similar to those found in some Slovenian and Hungarian wines.[34,35] Namely, it was reported earlier that the contents of Cu and Zn in some selected Slovenian red wine labels are up to 1.0 and 0.6 mg L^{-1}, respectively.[35] It is obvious that determined metal levels in the present study are completely comparable to the ones in the Slovenian wine samples, whereby the contents of Zn are especially similar, Table III. The estimated concentrations of Zn in Serbian wines are also analogous to those discussed formerly in literature data.[36]

The Hungarian national legislation according to OIV recommendations allows a maximum level of 1 mg L^{-1} Cu in wines and other food products.[34] The corresponding Cu contents varied in the range from 0.02 to 0.64 mg L^{-1} being greatly below the cited limit in all the studied Hungarian wine samples.[34] The results of the present study evidenced fluctuation of Cu contents over a similar range as in Hungarian wines, whereas these contents reported to be a bit higher in the case of later wines. On the contrary, in German red wines,[37] the Cu content was found to be even five times higher than the highest concentration of this element in Hungarian wines and almost the same as in Serbian wines. Similarly, for Australian wines,[38] but white ones, the Cu content ranged within limits almost four times higher than in the selected Serbian wines. Unexpectedly, the Cu level ranged from 0.03 to 0.17 mg L^{-1} in Russian and Italian red and white wines, as well,[39] being noticeably lower than the Cu content in wines originating from other European countries, including Serbian wines. On the other hand, in Russian and Italian wines,[39] the Zn content was reported to be between 0.14 and 0.76 mg L^{-1}, which is completely in accordance to values found in wines produced from other European regions. Opposed to other papers, one review article[1] reported very wide ranges of the Fe, Cu and Zn contents in Italian wines. Somewhat curious is/are the highest/higher value/values of the Fe content/s in selected Serbian wines (Table III), being even higher than all reported values in the review article concerning Canadian wines.

Wine samples from Jordan show relatively high values of metal contents,[40] especially the maximal determined levels, but most of the estimated values were below the toxic limit in food (Swiss Standard, 1993). This may be explained by the homemade production procedure applied.

The presence of some other trace metals, such as: lead, manganese, cadmium and nickel, was not detected in the examined wine samples.

The concentration of metals in alcoholic beverages may vary widely depending on the plant origin and the technology used (home-made or by an official producer). Moreover, it was recently reported that some home-produced alcoholic

beverages and spirits contain rather high concentrations of metals.[8] In addition; it was observed that alcoholic beverages from Africa, India and Canada possess higher metal concentrations, *i.e.*, 58, 68 and 245 mg L^{-1} of Cu, Zn and Fe, respectively.[41]

The concentrations of metals and trace metals in wines depend on the metal content in the vineyard soil, which primarily determines the degree of metal uptake by the grape plant. In addition, anthropogenic impact plays a vital role in determining the metal content in wines. Namely, as was stated above before, some home-made wines showed a higher trace element content, probably due to contamination during the wine-making process and/or the mixing/storage procedure, and also additives used.

It is worth emphasizing that the allowed limits for metal contents in alcoholic beverages are higher than those imposed for water envisaged for human consumption.[8] This may be related to the lower predicted intake of alcoholic beverages.

The variation of the discussed levels of metals concentrations in the present study as well as those reported earlier by other authors suggest a necessity for the establishment of common limits.

CONCLUSIONS

Different metals occur in wines at the mg L^{-1} and/or μg L^{-1} level not directly influencing the taste of the end product. Nevertheless, their content should be determined because excess is undesirable due to potential toxicity and risks to human health, consequently imposing the maximal allowed values and/or prohibited limits. The contents of the investigated metals (Fe, Cu and Zn) in wine samples from different areas of Serbia are considerably lower than the maximum concentrations allowed according to the OIV. The contents of selected trace metals were significantly lower than those of some European wines, but similar to the values found in some Slovenian and Hungarian wines. Additionally, these contents were compared with known literature values. Somewhat curious is the relatively high Fe content in the selected Serbian wines (“As” and “Rose”). The variation in the metal content in the studied Serbian wines may be related to the metal content in the vineyard soil, *i.e.*, soil type, and/or an anthropogenic impact arising from the wine-making process and/or storage procedure.

Acknowledgement. The financial support of the Ministry of Science and Technological Development of the Republic of Serbia (Project No. ON 142051) is highly appreciated.

ИЗВОД

КОНЦЕНТРАЦИЈА Fe, Cu И Zn У ОДАБРАНИМ ВИНИМА ЈУГОИСТОЧНЕ СРБИЈЕ

ДАНИЈЕЛА КОСТИЋ, СНЕЖАНА МИТИЋ, ГОРДАНА МИЛЕТИЋ, САША ДЕСПОТОВИЋ и АЛЕКСАНДРА ЗАРУБИЦА

Природно-математички факултет, Универзитет у Нишу, 18000 Ниш

Воће и поврће представљају најјефтинији извор есенцијалних метала, који се јављају у траговима, за највећи део становништва развијеног света. Садржај Cu, Fe и Zn је одређен пламеном атомско апсорпционом спектрометријом у двадесет узорака одабраних вина, пореклом из региона Југоисточне Србије. Концентрација Cu варира од 0,07 до 0,57 ppm у испитиваним винима, гвожђа од 2,93 до 36,2 ppm, док је ниво Zn у интервалу од 0,21 до 0,67 ppm. Установљен садржај Cu и Zn показује да вина из овог дела света могу бити добар дијететски извор есенцијалних метала, заступљених у траговима; одређени садржаји метала су у границама дозвоњених вредности у људској исхрани.

(Примљено 4. јануара, ревидирано 30. јула 2010)

REFERENCES

1. M. Aceto, O. Abollino, M. C. Bruzzoniti, E. Mentasti, C. Sarzanini, M. Malandrino, *Food Addit. Contam.* **19** (2002) 126
2. S. Mitić, J. Vučetić, S. Miletić, D. Kostić, *J. Serb. Chem. Soc.* **65** (2000) 595
3. B. Zoecklein, K. Fugelsang, B. Gump, F. Nury, *Wine Analysis and Production*, Chapman & Hall, New York, 1994
4. J. Wang, S. Mannino, *Analyst* **114** (1989) 643
5. C. Marin, P. Ostapczuk, *Fresenius J. Anal. Chem.* **343** (1992) 881
6. H. Eschnauer, P. Ostapczuk, *Wein-Wiss.* **47** (1992) 206
7. S. Ražić, Dj. Čokeša, S. Sremac, *J. Serb. Chem. Soc.* **72** (2007) 1487
8. J. Ibanez, A. Carreon-Alvarez, M. Barcena-Soto, N. Casillas, *J. Food Composition Anal.* **21** (2008) 672
9. M. Arcos, M. Ancin, J. Echeverria, A. Gonzales, J. Garrido, *J. Agric. Food Chem.* **41** (1993) 2333
10. P. Ostapczuk, *Anal. Chim. Acta* **273** (1993) 35
11. E. Zakharova, V. Pichugina, T. Tolmacheva, *Zh. Anal. Khim.* **51** (1996) 918
12. S. Sanllorente, O. Cruz, M. J. Arcos, *Analyst* **123** (1998) 513
13. O. Domingez, S. Sanllorente, M. Arcos, *Electroanalysis* **1** (1999) 1273
14. S. May, J. Leroy, D. Piccot, G. Pinte, *J. Radioanal. Chem.* **72** (1982) 305
15. H. Eschnauer, L. Jakob, H. Meierer, R. Neeb, *Microchim. Acta* **3** (1989) 291
16. J. Goossens, T. De Smaele, L. Moens, R. Dams, *Fresenius J. Anal. Chem.* **347** (1993) 119
17. S. Augagneur, B. Medina, J. Bernard, Szpunar, R.Lobinski, *J. Anal. At. Spectrom.* **11** (1996) 713
18. G. Weber, G. Schwedt, *Anal. Chim. Acta* **134** (1982) 81
19. C. Garcia-Jahres, M. Lage-Yusty, J. Simal-Lozano, *Fresenius J. Anal. Chem.* **338** (1990) 703
20. K. Ohzeki, I. Nukatsuka, K. Ichimura, F. Kumagai, M. Kogawa, *Microchem. J.* **49** (1994) 256
21. S. Cherubin, S. Buiatti, F. Battistutta, R. Zironi, *Wein-Wiss.* **49** (1994) 78
22. T. Stafilov, J. Cvetkovic, S. Arpadjan, I. Karadjova, *BAÜ Fen Bil. Enst. Dergisi* **4.2** (2002) 90
23. R. Farre, M. Lagarda, *J. Micronutr. Anal.* **2** (1986) 201

24. J. Korkisch, A. Sorio, I. Steffan, *Talanta* **23** (1976) 289
25. U. Anders, G. Hailer, *Fresenius J. Anal. Chem.* **278** (1976) 203
26. D. Siemer, R. Vitek, P. Koteel, H. Prabhakaran, W. Houser, *Anal. Lett.* **10** (1977) 357
27. J. Sanz, P. Basterra, J. Galban, J. R. Castillo, *Mikrochim. Acta* **1** (1989) 271
28. M. Segura, Y. Madrid, C. Camara, *J. Anal. At. Spectrom.* **14** (1999) 131
29. M. Segura, J. Grgic, Z. Grgic, B. Segura, *Dtsch. Lebensm.-Rundsch*. **94** (1998) 336
30. E. Lendinez, M. Lopez, C. Cabrera, M. Lorenzo, *J. AOAC Int.* **81** (1998) 1043
31. C. Cabrera-Vigne, P. Teissedre, M. Cabanis, J. Cabanis, *Am. J. Enol. Vitic.* **51** (2000) 103
32. B. Kildahl, W. Lund, *Fresenius J. Anal. Chem.* **354** (1996) 93
33. C. Cabrera-Vique, P.-L. Teissedre, M.-T. Cabanis, J. Cabanis, *J. Agric. Food Chem*. **45** (1997) 1808
34. Z. Ajtony, S. Zoboszlai, E. Klaudia Susko, P. Mezei, K. Gyorgy, L. Bencs, *Talanta* **76** (2008) 627
35. J. Kristl, M. Veber, M. Slekovec, *Acta Chim. Slov*. **50** (2003) 123
36. K. Bauer, S. Hinkel, R. Neeb, R. Eicher, H. Eschnauer, *Vitic. Enol. Sci*. **49** (1994) 209
37. C. Wiese, G. Schwedt, *Fresenius J. Anal. Chem.* **358** (1997) 718
38. L. Sauvage, D. Frank, J. Stearne, M. B. Millikan, *Anal. Chim. Acta* **458** (2002) 223
39. Kh. Z. Brainina, N. Yu. Stozhko, G. Belysheva, O. Inzhevatova, L. Kolyadina, C. Cremisini, M. Galletti, *Anal. Chim. Acta* **514** (2004) 227
40. F. Al Nasir, A. Jiries, M. Batarseh, F. Beese, *Environ. Monit. Assess.* **66** (2001) 253
41. C. Reilly, *J. Sci. Food Agric.* **23** (1972) 1143.

Journal of the Serbian Chemical Society
JSCS-info@shd.org.rs • www.shd.org.rs/JSCS
J. Serb. Chem. Soc. *75* (12) 1711–1719 (2010)
JSCS–4090
UDC 678.744+661.8'078.2:542.913
Original scientific paper

Simplification of the synthesis of the reversible addition–fragmentation chain transfer agent 2-(2-cyanopropyl)-dithiobenzoate

MILOŠ B. MILOVANOVIĆ[1#], MILENA AVRAMOVIĆ[2], LYNNE KATSIKAS[2]* and IVANKA G. POPOVIĆ[2#]

[1]*Institute of Chemistry, Technology and Metallurgy, University of Belgrade, Belgrade and* [2]*Faculty of Technology and Metallurgy, University of Belgrade, Belgrade, Serbia*

(Received 30 June 2010)

Abstract: The general literature procedure for the preparation of the reversible addition–fragmentation chain transfer (RAFT) agent 2-(2-cyanopropyl)-dithiobenzoate (CPDB) was modified by omitting the recrystallisation of the intermediate di(thiobenzoyl)disulphide. The yield of the CPDB in the simplified synthesis was increased four times compared to the standard one. The behaviour of the CPDB obtained by the modified procedure and by the standard one in the polymerisation of methyl methacrylate was investigated. The CPDB synthesized by the simplified procedure showed itself to be a good RAFT agent, giving excellent control over the polymerisation of methyl methacrylate and it behaved in the same manner as the CPDB prepared by the literature method. The obtained poly(methyl methacrylate) had a narrow molecular weight distibution (PD = 1.1).

Keywords: 2-(2-cyanopropyl)-dithiobenzoate; preparation; reversible addition–fragmentation chain transfer; poly(methyl methacrylate).

INTRODUCTION

In recent years, much effort has been focused on the synthesis of polymers with controlled molar masses and very narrow molar mass distributions. With the development of several methods of controlled radical polymerisation, well-defined polymers with complex architectures, including block,[1,2] graft[3] and star[4,5] structures, could be prepared. The development of these methods was promoted by the growing need for truly living radical polymerisation systems that would offer all the benefits of ionic polymerisations without the serious disadvantages inherent to such systems. Among them, RAFT (reversible addition–fragmen-

* Corresponding author. E-mail: Lynne@tmf.bg.ac.rs
# Serbian Chemical Society member.
doi: 10.2298/JSC100628082M

tation chain transfer) polymerisation has proven itself to be the most versatile one, since it is applicable to a wide range of monomers and can be performed in a wide variety of solvents over a broad range of experimental conditions. RAFT polymerisations are now being used successfully by an ever-growing number of research groups around the world. The key to successful RAFT polymerisations is the presence of a highly efficient dithioester chain transfer agent. Among numerous RAFT agents, only a few are commercially available (carboxymethyl dithiobenzoate, for example). Regarding the importance of the synthesis of RAFT agents of different structures, a large number of procedures for the synthesis of dithioester compounds have been developed. As the syntheses of these RAFT agents are usually costly and require multi-step reactions, the loss of polymerisation mediator throughout the RAFT polymerisation process may be an issue when scaling-up the process. A simple reaction that leads to the full removal of the thiocarbonyl-thio end group from the polymeric chains and recovery of the chain transfer agent has already been reported.[6] In addition, simplifications of the syntheses of RAFT agents would promote scaling-up the RAFT polymerisation processes.

This study focused on the synthesis of 2-(2-cyanopropyl)-dithiobenzoate (CPDB) which, together with cumyl dithiobenzoate, is one of the most frequently employed RAFT agents. CPDB was reported to be an efficient RAFT agent in the polymerisation of a number of monomers.[7–10] 2-(2-Cyanopropyl)-dithiobenzoate can be synthesized in two ways. One method is a single-step procedure, by reaction of Davy reagent or P_4S_{10} with benzoic acid. The obtained CPDB was used to control *in situ* the free-radical polymerisation of styrene and alkyl (meth)acrylates.[11] The isolation of pure CPDB demands a multi-step procedure.[12] One of the steps in this preparation is the synthesis of dithiobenzoic acid. Dithiobenzoic acid is unstable and should be stored at low temperatures (< –20 °C)[13] or used immediately. For this reason, it is usually transferred into di(thiobenzoyl)disulphide. Di(thiobenzoyl)disulphide is used not only for the synthesis of CPDB, but also for the syntheses of many different RAFT agents.[14]

In the present study, the standard procedure for the preparation of CPDB was modified and simplified by omitting the intermediate step of the recrystallisation of di(thiobenzoyl)disulphide in order to avoid great loss of material in this step. The behaviour of the CPDB synthesized by the simplified procedure in the polymerisation of methyl methacrylate was investigated and compared with that of the CPDB synthesized by the standard method.

EXPERIMENTAL

Methyl methacrylate, MMA, (Fluka) was distilled under reduced pressure after removal of the inhibitor with a 10 % aqueous NaOH solution. Azobis(isobutyronitrile), AIBN, (Aldrich), was purified by recrystallisation from methanol. Benzene, thiophene free, (Fluka) was distilled before use.

The RAFT agent, 2-(2-cyanopropyl)-dithiobenzoate (CPDB), was prepared by a standard method described in the literature.[15] To a thoroughly dried, three-necked round-bottomed flask equipped with a magnetic bar, addition funnel, thermometer and condenser was added elemental sulphur (6.4 g, 0.20 mol), 25 % sodium methoxide solution in methanol (40 g) and anhydrous methanol (40 g). Benzyl chloride (12.6 g, 0.10 mol) was the added dropwise *via* an addition funnel over a period of 90 min at room temperature. The resulting violet-brown solution was then heated and allowed to reflux overnight. After cooling to room temperature, the mixture was filtered to remove the white solid (sodium chloride) which was formed as a by--product during the reaction. The methanol was removed by rotary evaporation at 40 °C. The resulting violet-brown solid was then re-dissolved in distilled water (100 ml) and transferred to a separation funnel. The crude sodium dithiobenzoate solution was washed with diethyl ether (3×50 ml). A final layer of ether (50 ml) was added to the solution and the two-phase mixture was then acidified with 32 % aqueous HCl until the aqueous layer lost its characteristic violet-brown colour and the top, ether, layer was deep purple. The ether layer containing dithiobenzoic acid was extracted. Deionized water (120 ml) and 1.0 M NaOH (240 ml) were added, and sodium dithiobenzoate was extracted into the aqueous layer. This washing process was repeated two times more to yield a final solution containing sodium dithiobenzoate (360 ml).

The next step was the synthesis of di(thiobenzoyl)disulphide. Potassium ferricyanide (13.17 g, 0.040 mol) was dissolved in deionized water (200 ml). Potassium ferricyanide solution (140 ml) was transferred to a conical flask equipped with a magnetic bar. Potassium ferricyanide solution was added dropwise to the sodium dithiobenzoate *via* an addition funnel over a period of 1 h under vigorous stirring. The red precipitate was filtered and washed with deionized water until the washings become colourless. The solid was dried under vacuum at room temperature. The product was recrystallized from anhydrous ethanol.

The target compound was prepared in the reaction of di(thiobenzoyl)disulphide with azobisisobutyronitrile (AIBN). A solution of AIBN (2.90 g, 0.018 mol) and di(thiobenzoyl)disulphide (3.60 g, 0.012 mol) in ethyl acetate (70 ml) was heated at reflux for 18 h. The ethyl acetate was removed under vacuum. The crude product, CPDB-1, was subjected to column chromatography on a 25×2.6 cm column filled with silica gel (Woelm mesh size 0.063–0.2 mm, ICN Pharmaceuticals, Germany) as the stationary phase and ethyl acetate: *n*-hexane (0.2:0.98) as the eluent, at a flow rate of 1.0 mL min^{-1}.

Due to the large loss of di(thiobenzoyl)disulphide in the recrystallisation step, the synthesis of di(thiobenzoyl)disulphide was repeated but this time it was used in the subsequent reaction without recrystallisation to yield CPDB-2.

The structure of the CPDB from the both synthesis was confirmed by ^{13}C-NMR spectroscopy using a Varian-Gemini-200 (200 MHz) instrument.

In order to determine whether CPDB-2 was equally effective as a RAFT agent as CPDB-1, methyl methacrylate was polymerised using both RAFT agents.

The polymerisations of methyl methacrylate, MMA, were performed in a three-necked round-bottomed flask equipped with a magnetic stirring bar, a condenser, a thermometer, an inlet for nitrogen and a rubber septum for removing samples. The flask was charged with MMA (30 ml, 0.28 mol), benzene (10 ml, 0.11 mol), AIBN (40 mg, 0.24 mmol) and CPDB (104 mg, 0.470 mmol). Nitrogen was bubbled through the reaction mixture for 15 min at room temperature before starting the polymerisation, while during the polymerisation the nitrogen stream was directed over the top of the condenser, thus keeping the reaction mixture under a nitrogen atmosphere. A preheated oil bath was employed to commence the polymerisations. The polymerisations were performed at 60 °C. Samples were removed from the flask every 2 h

via a needle and syringe and precipitated into methanol. The polymer samples were reprecipitated from chloroform solution into methanol and dried to constant mass at room temperature under vacuum.

The number and weight average molar masses, $\overline{M}_n$ and $\overline{M}_w$, respectively, and the polydispersity index, *PD*, of the obtained polymers were determined at 30 °C by gel permeation chromatography, SEC, using a Waters instrument fitted with four analytical columns (Waters HR 2, HR 3, HR 4 and HR 5E) and a refractive index detector. THF was used as the solvent at a flow rate of 1.0 ml min^{-1}. The obtained chromatograms were analyzed with Waters Breeze software using a calibration curve of narrow molar mass distribution PMMA standards (PSS Polymer Standards Service GmbH, Mainz, Germany).

RESULTS AND DISCUSSION

The RAFT agent, CPDB, was prepared in two syntheses which differed in the recrystallisation of the intermediate di(thiobenzoyl)disulphide. The final products (CPDB1 and CPDB2, with and without recrystallisation, respectively) from both syntheses were subjected to column chromatography with silica gel as the stationary phase and ethyl acetate:*n*-hexane (0.20:0.98) as eluent. The crude product made from the di(thiobenzoyl)disulphide recrystallized in ethanol gave seven fractions: green (which did not enter the column), yellow and pink which stayed on the column, and yellow (eluted first), pink, red and purple which eluted last. The main purple fraction gave 2-(2-cyanopropyl)-dithiobenzoate as a red--purple liquid after evaporation of the eluent. The yield of the CPDB-1 was extremely low when the pure substance was obtained (5 % of the theoretical yield).

The crude product from the second synthesis made from the di(thiobenzoyl)-disulphide without recrystallisation was reddish coloured, but after the column chromatography it gave the characteristic purple coloured fraction as the main product. The crude product from this synthesis gave four fractions: yellow and orange, which stayed on the column, and yellow and the main purple one, which eluted last. After evaporation of the eluent, the main purple fraction from the second synthesis gave CPDB-2 as a red-purple liquid.

The fact that more fractions were obtained during the column chromatography of CPDB-1 than during the chromatography of CPDB-2 indicates that during recrystallisation not only was di(thiobenzoyl)disulphide inherently lost, but also that it decomposed. It was observed that a resinous material was formed during the recrystallisation, which when removed was insoluble in ethanol. This could be the explanation of the green fraction which did not enter the column.

The ^{13}C-NMR spectrum and the numbering of the C atoms of the prepared CPDB-1 and CPDB-2 are shown in Figs. 1 and 2, respectively, from which it can be seen that all the expected peaks were present. One additional peak was found in the spectrum of the CPDB2 (at 23 ppm). This could arise by the recombination of primary radicals from the decomposition of AIBN, used in the last step of the synthesis. It was reported[12] that the highest level of impurity found in CPDB could be attributed to recombined radicals arising from the decomposition of

AIBN. This recombination compound was found to be difficult to remove from the RAFT agent, even after column chromatography, but it is inert to any radical reaction. The peak of the carbon atoms from the four equivalent CH_3 groups of such a compound is expected at 23 ppm in a ^{13}C-NMR spectrum. It is important to emphasise that the yield of the CPDB in the second synthesis was increased to 20 % of theoretical yield, which is four times more compared to the first one.

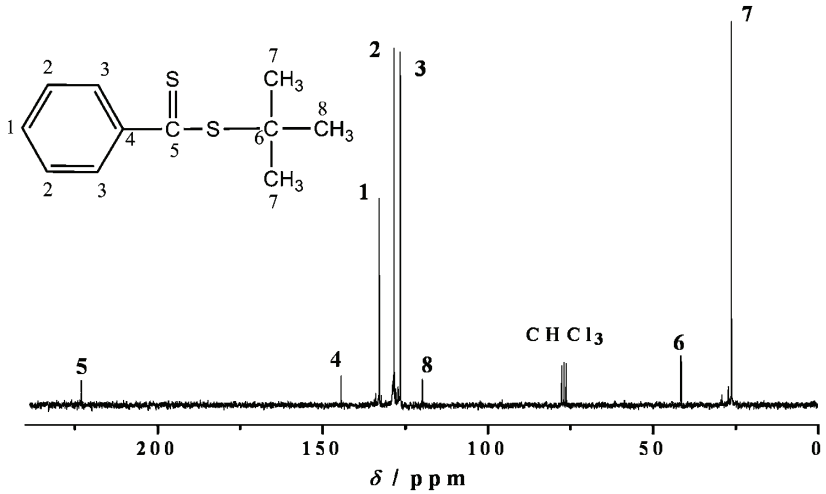

Fig. 1. ^{13}C-NMR Spectrum of CPDB-1 (inset: structure of CPDB with C atoms numbered).

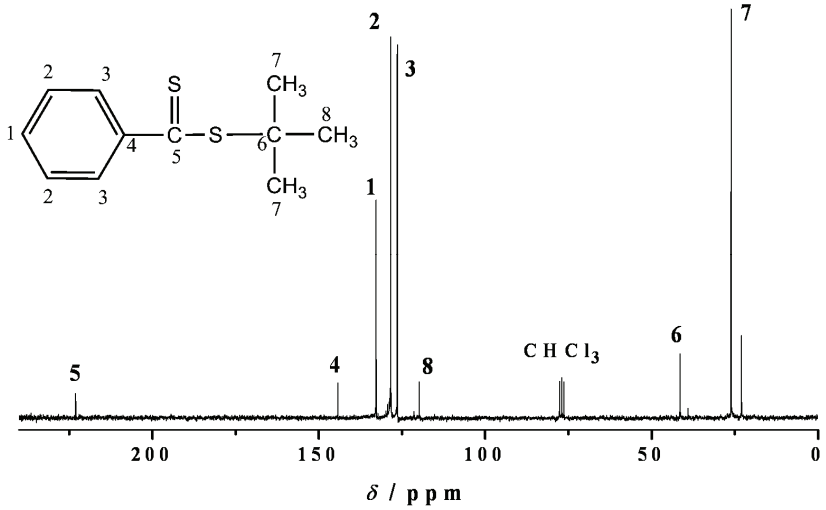

Fig. 2. ^{13}C-NMR Spectrum of CPDB-2 (inset structure of CPDB with C atoms numbered).

A change in the standard method of preparation of CPDB was previously reported in the literature.[16] The alteration concerned of the same step in the

procedure of CPDB synthesis to which attention was paid in this study. The purification di(thiobenzoyl)disulphide by the recrystallisation in ethanol was substituted by column chromatography using ethyl acetate/petroleum ether (1:1) as the eluent. The yield of CPDB was 50 % of the theoretical one, which is 2.5 times larger than one obtained in the present study. However, it must be emphasised that the purification di(thiobenzoyl)disulphide was completely avoided in synthesis procedure employed in this study, which is extremely important for laboratory or industrial scale-ups.

Two RAFT polymerisation of methyl methacrylate were performed using CPDB from the two different syntheses. Samples were taken from the reaction flask every 2 h. The polymer obtained after the RAFT polymerisation was pink due to the attachment of CPDB to the chain ends. Two series of PMMA samples were obtained: PMMA-1 from the polymerisation using the CPDB-1 and PMMA-2 from the polymerisation using the CPDB-2. The number and weight average molar masses, M_n and M_w, and the polydispersity index, *PD*, of the obtained polymers are given in Table I. The polymerisations mediated by CPDB-1 and CPDB-2 exhibited very similar kinetics, *i.e.*, the polymerisation rates were very similar (Fig. 3a).

TABLE I. Number and weight average molar mass and polydispersidity index, *PD*, of the PMMA-1 and PMMA-2 samples

Time, h	PMMA-1			PMMA-2		
	M_n / g mol^{-1}	M_w / g mol^{-1}	*PD*	M_n / g mol^{-1}	M_w / g mol^{-1}	*PD*
2	16625	18415	1.108	15161	16674	1.100
4	19481	21676	1.112	20872	23001	1.102
6	25126	27972	1.113	26071	28901	1.109
8	30436	34062	1.119	31958	35648	1.115
10	37271	41800	1.122	39412	44310	1.124

A comparison of $\overline{M}_w$ of PMMA-1 and PMMA-2 samples as a function of polymerisation time is shown in Fig. 3b, from which it can be seen that the molar mass increased with polymerisation time, as is to be expected for RAFT-controlled polymerisations, and that the rate of increases were very similar. The SEC chromatograms revealed good control of the CPDB-mediated polymerisations with narrow molar mass distributions. The comparison of An SEC chromatogram of a PMMA sample obtained using CPDB-2, is compared with that of the corresponding PMMA sample prepared using CPDB-1, in Fig. 4. As can be seen, the chromatograms are very similar.

The polydispersities of the PMMA samples from both series (Table I) were also very similar for the same polymerisation time, indicating that CPDB-1 and CPDB-2 affected the same polymerisations.

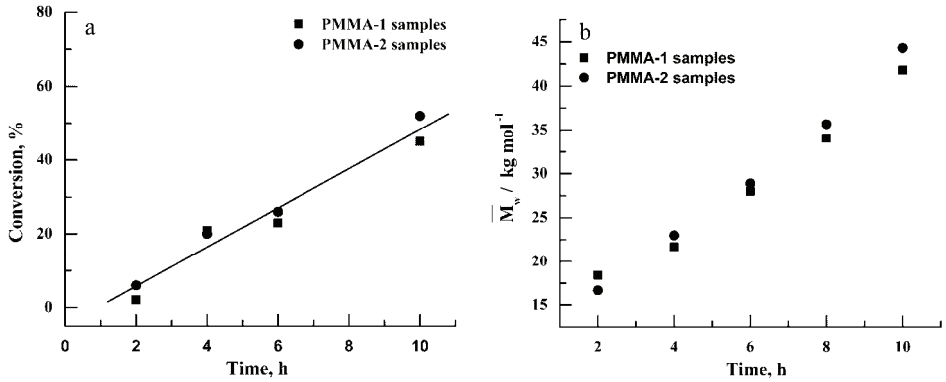

Fig. 3. a) MMA Conversion *vs.* polymerisation time in the presence of CPDB-1 and CPDB-2. b) Weight average molar mass of the PMMA-1 and PMMA-2 samples *vs.* polymerisation time.

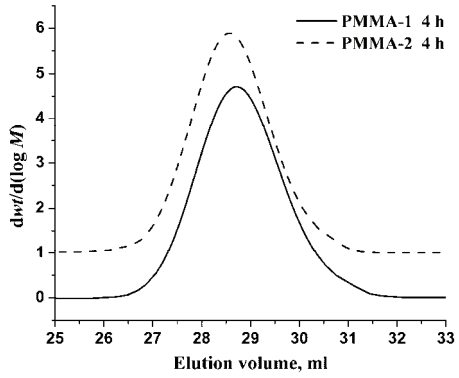

Fig. 4. SEC Chromatogram of PMMA samples obtained by polymerisation of MMA in the presence of CPDB-1 and in the presence of CPDB-2 for 4 h.

As can be seen, the CPDB obtained by the simplified procedure exerted the same effects in the polymerisation of PMMA as that obtained by the literature procedure.

CONCLUSIONS

The procedure of CPDB preparation was modified and simplified by omitting the recrystallisation of the intermediate di(thiobenzoyl)disulphide. The yield of the CPDB in the simplified synthesis was increased by a factor of four comparing to the literature method. The CPDB synthesized by the simplified procedure provided very good control of the polymerisation of methyl methacrylate, yielding PMMA samples with narrow molar mass distibutions, and behaved in the same manner as the CPDB prepared by the standard literature procedure. The simplification of the synthesis of CPDB introduced in this study is very important from the points of view of time, scale-up and amounts of solvents necessary.

Acknowledgement. This investigation was financed by the Ministry of Science and Technological Development of the Republic of Serbia, through Project No.142023.

И З В О Д

ПОЈЕДНОСТАВЉЕЊЕ ПОСТУПКА СИНТЕЗЕ RAFT АГЕНСА 2-(2-ЦИЈАНОПРОПИЛ)-ДИТИОБЕНЗОАТА

МИЛОШ Б. МИЛОВАНОВИЋ[1], МИЛЕНА АВРАМОВИЋ[2], LYNNE KATSIKAS[2] и ИВАНКА Г. ПОПОВИЋ[2]

[1]*Институт за хемију, технологију и металургију, Универзитет у Београду, Београд*
[2]*Технолошко-металуршки факултет, Универзитет у Београду, Београд*

Стандардни поступак синтезе 2-(2-цијанопропил)-дитиобензоата (CPDB) агенса из литературе за RAFT полимеризацију, односно за реверзибилну адиционо-фрагментациону трансфер полимеризацију, је модификован изостављањем прекристализације међупроизвода бис-(тиобензоил)дисулфида. Принос CPDB-а синтетисаног поједностављеним поступком је четири пута већи у односу на принос CPDB-а синтетисаног стандардним поступком. Испитано је понашање CPDB-а добијеног модификованим и оног добијеног стандардним поступком у полимеризацији метил метакрилата. CPDB добијен поједностављеним поступком показао се као добар RAFT агенс који успоставља одличну контролу полимеризације метил метакрилата и који се понаша на исти начин као CPDB синтетисан стандардним поступком. Добијени поли(метил метакрилат) има уску ширину расподеле молских маса (*PD* = 1.1).

(Примљено 30. јуна 2010)

REFERENCES

1. S. Kulkarni, C. Schilli, B. Grin, A. H. E. Muller, A. S. Hoffman, P. S. Stayton, *Biomacromolecules* **7** (2006) 2736
2. G. Moad, R. T. A. Mayadunne, E. Rizzardo, M. Skidmore, S. H. Thang, *Macromol. Symp.* **192** (2003) 1
3. H. Bottcher, M. L. Hallensleben, S. Nub, H. Wurm, *Polym. Bull.* **44** (2000) 223
4. A. Blencowe, J. F. Tan, T. K. Goh, G. G. Qiao, *Polymer* **50** (2009) 5
5. J. Bernard, X. Hao, T. P. Davis, C. Barner-Kowollik, M. H. Stenzel, *Biomacromolecules* **7** (2006) 232
6. S. Perrier, P. Takolpuckdee, C. A. Mars, *Macromolecules* **38** (2005) 2033
7. J. B. McLeary, F. M. Calitz, J. M. McKenzie, M. P. Tonge, R. D. Sanderson, B Klumperman, *Macromolecules* **37** (2004) 2383
8. M. Benaglia, E. Rizzardo, A. Alberti, M. Guerra, *Macromolecules* **38** (2005) 3129
9. L. Katsikas, M. Avramović, R. D. B. Cortes, M. B. Milovanović, M. T. Kalagasidis Krusić, I. G. Popović, *J. Serb. Chem. Soc.* **73** (2008) 915
10. J. B. McLeary, J. M. McKenzie, M. P. Tonge, R. D. Sandersona, B. Klumperman, *Chem. Commun.*(2004) 1950
11. A. Dureault, Y. Gnanou, D. Taton, M. Destarac, F. Leising, *Angew. Chem. Int. Ed.* **42** (2003) 2869
12. S. Perrier, C. Barner-Kowollik, J. F. Quinn, P. Vana, T. P. Davis, *Macromolecules* **35S** (2002) 30
13. Y. K. Chong, J. Krstina, Tam P. T. Le, G. Moad, Almar Postma, E. Rizzardo, S. H. Thang, *Macromolecules* **36** (2003) 2256

14. Y. Mitsukami, M. S. Donovan, A. B. Lowe, C. L. McCormick, *Macromolecules* **34** (2001) 2248
15. S. Perrier, C. Barner-Kowollik, J. F. Quinn, P. Vana, T. P. Davis, *Macromolecules* **35** (2002) 8300
16. Uma Adash, *PhD Thesis*, University of Canterbury, New Zealand, 2005, http:// //ir.canterbury.ac.nz/bitstream/10092/1282/1/thesis_fulltext.pdf (last accessed on 18.06.2010).

Journal of the Serbian Chemical Society
JSCS-info@shd.org.rs • www.shd.org.rs/JSCS
J. Serb. Chem. Soc. *75* (12) 1721–1732 (2010)
JSCS–4091
UDC 532.13:541.25:539.196
Original scientific paper

Studies of viscous antagonism, excess molar volumes, viscosity deviation and isentropic compressibility of ternary mixtures containing N,N-dimethylformamide, benzene and some ethers at 298.15 K

RIJU CHANDA, ASHIS BANERJEE and MAHENDRA NATH ROY*

Department of Chemistry, North Bengal University, Darjeeling-734013, India

(Received 6 August 2009, revised 27 August 2010)

Abstract: The densities (ρ) and viscosities (η) for ternary liquid mixtures of *N*,*N*-dimethylformamide + benzene + an ether were measured as a function of composition at 298.15 K. From experimental measurements, the excess molar volumes (V^E), viscosity deviation ($\Delta\eta$), antagonic interaction index (I_A) and Gibbs free energy of activation for viscous flow (ΔG^{*E}) were evaluated. The speeds of sound were also measured and excess isentropic compressibilities (K_s^E) were calculated at the experimental temperature. The results are discussed and interpreted in terms of molecular package and specific interaction predominated by hydrogen bonding.

Keywords: viscous antagonism; viscosity deviations; excess molar volumes; isentropic; compressibility; molecular interactions.

INTRODUCTION

The grouping of solvents into classes is often based on the nature of intermolecular forces because the manner in which solvent molecules are associated with each other has a marked effect on the resulting properties. Rheology is the branch of science[1] that studies material deformation and flow, and is increasingly applied to analyze the viscous behaviors of many pharmaceutical products,[2] and to establish their stability and even bio-availability, since it has been firmly established that viscosity influences the absorption rate of a drug in the body. The increasing use of the solvents: *N*,*N*-dimethylformamide (DMF), benzene, 1,3-dioxolane, 1,4-dioxane, tetrahydrofuran, 1,2-dimethoxyethane, di-isopropyl ether, diethyl ether, 2-methoxyethanol and 2-ethoxyethanol and their mixtures in many industrial processes, such as battery, pharmaceutical and cosmetics, has greatly stimulated the need for extensive information on their various properties. Hence,

* Corresponding author. E-mail: mahendraroy2002@yahoo.co.in
doi: 10.2298/JSC090806132C

the present study gives extensive information on the various properties when these ethers are taken with DMF and benzene as mixed solvent systems.[1–7] The determination of density, viscosity and speed of sound are valuable tools to learn about the liquid state[8,9] because of the close connection between liquid structure and macroscopic properties.

The viscosity and density of these ternary liquid mixtures were used to understand the molecular interactions between the components of the mixture to develop new theoretical models and also for engineering applications.[10,11] In systematic investigations, the viscosities, densities and speeds of sound of different solvents and their mixtures were reported in previous papers.[12–18]

The present work contributes and extends the study of density (ρ), viscosity deviations ($\Delta\eta$), viscous antagonism, excess molar volumes (V^E) and isentropic compressibility (K_S^E) to mixtures of DMF and benzene with some ethers, where DMF is represented as A, benzene as B and the ethers as C.

EXPERIMENTAL

DMF (C_3H_7NO) was obtained from Merck and LR, and further purified by standard methods.[19] Benzene (S. D. Fine Chemicals, purity > 99 %) was further purified by means of a simple distillation technique with the first and last 20 % of the distillate being discarded[20–22] and finally the density and viscosity value were compared with the literature.[23] The final purities of the obtained solvents were >99.5 %.

The experimental ethers, namely 1,3-dioxolane (1,3-DO), 1,4-dioxane (1,4-DO), tetrahydrofuran (THF), 1,2-dimethoxyethane(1,2-DME), di-isopropyl ether (DIE), diethyl ether (DEE), 2-methoxy ethanol (2-ME) and 2-ethoxyethanol (2-EE) were obtained from Merck and LR. These were further purified by standard methods.[24–27] The purities of the liquids was ascertained by GLC and also by comparing the experimental values of densities, viscosities and sound velocities with those reported in the literature,[24,27–35] as listed in Table I. The purities of the finally obtained solvents were >99 %.

TABLE I. Physical properties of the pure solvents at 298.15 K

Solvent	ρ / g cm^{-3}		η / mPa s		u / m s^{-1}	
	Experimental	Literature	Experimental	Literature	Experimental	Literature
DMF	0.94609	0.9447[27]	0.8586	0.802 [27]	1465.2	1465.0[27]
Benzene	0.8735	0.8735[23]	0.5920	0.5920 [23]	1252.7	--
1,3-Dioxolane	1.0577	1.0586[33]	0.5878	0.5873[21]	1338.2	1338.8[33]
1,4-Dioxane	1.0287	1.0279[33]	1.1779	1.196[25]	1344.4	1345.5[33]
Tetrahydrofuran	0.8807	0.8811[25]	0.463	0.460[25]	1292.2	1294.0[29]
1,2-Dimethoxy ethane	0.8615	0.8611[35]	0.4089	0.4089[35]	1146.2	–
Di-isopropyl ether	0.7250	0.7250[21]	0.379	0.3791[21]	1050.1	–
Diethyl ether	0.7134	0.7134[25]	0.224	0.22404[25]	1080.8	–
2-Methoxy ethanol	0.95979	0.9600[34]	1.543	1.5414 [34]	1339.4	–
2-Ethoxy ethanol	0.92497	0.9256[27]	1.8277	1.851 [27]	1308.0	1308.0[27]

Densities (ρ) were measured with an Ostwald–Sprengel type pycnometer having a bulb volume of 25 cm^3 and an internal diameter of the capillary of about 0.1 cm. The pycnometer was calibrated at the experimental temperature with triply distilled water and DMF. The measurements were realized in a thermostated water bath controlled to ±0.01 K.[2] The weighings were performed on a Mettler electronic balance (AG-285) with a precision of ±0.01 mg. The viscosities (η) were measured by means of a suspended Ubbelohde type viscometer[7], which was calibrated at the desired temperature with triply distilled water and purified methanol using density and viscosity values from the literature. The ultrasonic speeds (u) were determined using a single-crystal variable path ultrasonic interferometer (Mittal Enterprises, New Delhi) working at 5 MHz,[32,36] which was calibrated with water, methanol and benzene. The temperature stability was maintained within ±0.01 K by circulating thermostatic water around the cell with a circulating pump. The solutions were prepared by mixing known volumes of pure liquids in air-tight stoppered bottles at 298.15 K. The precisions of the speed of sound, density and viscosity measurements were ±0.2 m s^{-1}, ±3×10^{-4} g cm^{-3} and ±2×10^{-4} mPa s, respectively. The estimated uncertainty for the excess molar volume (V^E), viscosity deviation ($\Delta\eta$), antagonic interaction index (I_A) and excess isentropic compressibilities (K_s^E) were ±0.5×10^{-4} m^3 mol^{-1}, ±0.0004 mPa s, ±0.002 and ±0.2 Pa^{-1}, respectively.

RESULTS AND DISCUSSION

The measured density (ρ), viscosity (η) and the speeds of sound (u) data for mixtures of (DMF) (A), benzene (B), and the ethers (C), *i.e.*, 1,3-dioxolane, 1,4--dioxane, tetrahydrofuran, 1,2-dimethoxyethane, di-isopropyl ether, diethyl ether, 2-methoxy ethanol and 2-ethoxyethanol were used to calculate the excess molar volume (V^E), viscosity deviation ($\Delta\eta$) and excess isentropic compressibility (K_s^E).

Viscous antagonism is the term used in respect to the interaction between the components of a system that cause the total viscosity of the latter to be less than the sum of the viscosities of the individual components in the system. The method compares the viscosity of the system determined experimentally, η_{exp}, with that expected in the absence of interaction, η_{calcd}. Viscous antagonism is exists when, $\eta_{exp} < \eta_{calcd}$. This procedure is used when Newtonian fluids are involved.[37]

Quantitatively, as per the absolute reaction rates theory,[38] the deviations of viscosities from the ideal mixture values for a three-component system can be calculated as:

$$\Delta\eta = \eta - \sum_{i=1}^{3} x_i\eta_i \quad (1)$$

where η is the viscosity of the mixture, x_i and η_i are the mole fraction and viscosity of the pure components, respectively. The $\Delta\eta$ values for all the studied ternaries were found to be negative over the whole composition range at 298.15 K, as depicted by a representative plot in Fig. 1 as a function of the mole fraction of both DMF (x_A) and benzene (x_B). The $\Delta\eta$ values for the ternary mixtures (A) + (B) + 1,3-DO, 1,4-DO, THF, 1,2-DME, DIE, DEE, 2-ME and 2-EE (C) are plotted against the mole fraction of DMF (x_A) in Fig. 2, from which it can be

observed that $\Delta\eta$ increases as the mole fraction of DMF increases. The mixtures have a tendency of maximization, indicating a strong specific interaction between the unlike molecules. From the values of $\Delta\eta$, given in Table II, it can be concluded that the affinity of the molecules of the ethers towards benzene molecules in the presence of DMF is enhanced in the following order:

A + B + 2-EE > 2-ME > DEE > DIE > 1,2-DME > THF >1,4-DO > 1,3-DO

Here, dispersion and dipolar interactions between the DMF, benzene and 1,3-DO, 1,4-DO, THF, 1,2-DME, DIE, DEE, 2-ME and 2-EE molecules are operative, resulting in negative $\Delta\eta$ but with the increasing x_A, the dipolar interactions dominate giving rise to less negative values of $\Delta\eta$.[31]

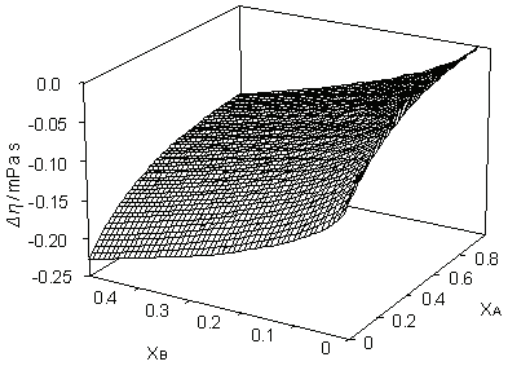

Fig. 1. 3D mesh plots of viscosity deviations ($\Delta\eta$) of DMF (A) + benzene (B) + 1,3-DO (C) mixtures with mole fraction of DMF (x_A) and benzene (x_B) at 298.15 K.

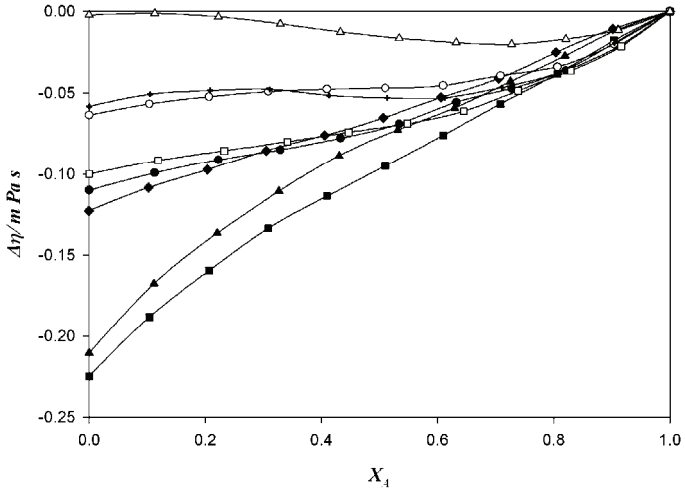

Fig. 2. Viscosity deviations ($\Delta\eta$) of: ■) DMF (A) + benzene (B) + 1,3-DO (C); ▲) DMF (A) + benzene (B) + 1,4-DO (C); ♦) DMF (A) + benzene (B) + THF (C); ●) DMF (A) + benzene (B) + 1,2-DME (C); □) DMF (A) + benzene (B) + DIE (C); ○) DMF (A) + benzene (B) + DEE (C); +) DMF (A) + benzene (B)+ 2-ME (C); Δ) DMF (A)+ benzene (B) + 2-EE (C) mixtures with mole fraction of DMF (x_A) at 298.15 K.

TABLE II. Experimental density (ρ), viscosity (η), viscosity deviations ($\Delta\eta$), antagonic interaction index (I_A), excess molar volumes (V^E), Gibbs energy of activation (ΔG^{*E}) of viscous flow, experimental sound velocities (u), isentropic compressibility (K_s) and excess isentropic compressibility (K_s^E) of *N*,*N*-dimethylformamide (A) + benzene (B) + 1,3-DO, 1,4-DO, THF, 1,2-DME, DIE, DEE, 2-ME and 2-EE (C) at 298.15 K

x_A	x_B	ρ / g cm^{-3}	η / mPa s	$\Delta\eta$ / mPa s	I_A	V^E / cm^3 mol^{-1}	ΔG^{*E} / J mol^{-1}	u / m s^{-1}	K_s / 10^{-12} Pa^{-1}	K_s^E / 10^{-12} Pa^{-1}
N,*N*-Dimethylformamide (A) + benzene (B) + 1,3-DO (C)										
0.0000	0.4868	0.9584	0.3650	–0.2248	0.38118	–0.1310	–1174.47	1302.1	615.4	340.2
0.1036	0.4363	0.9583	0.4296	–0.1881	0.30349	–0.2120	–871.83	1326.2	593.3	301.0
0.2064	0.3863	0.9578	0.4859	–0.1594	0.24506	–0.2630	–665.66	1336.7	584.3	275.0
0.3083	0.3367	0.9568	0.5393	–0.1334	0.19566	–0.2690	–504.20	1339.8	582.2	256.0
0.4095	0.2874	0.9557	0.5862	–0.1137	0.15942	–0.2600	–393.34	1339.8	583.0	240.0
0.5099	0.2386	0.9542	0.6320	–0.0949	0.12741	–0.2290	–301.30	1338.9	584.6	225.0
0.6094	0.1901	0.9527	0.6775	–0.0761	0.09797	–0.1890	–222.05	1344.1	581.0	205.0
0.7082	0.1420	0.9509	0.7235	–0.0567	0.07006	–0.1310	–151.39	1359.0	569.4	177.0
0.8062	0.0943	0.9492	0.7682	–0.0383	0.04552	–0.0840	–94.27	1387.0	547.6	139.0
0.9035	0.0470	0.9476	0.8148	–0.0179	0.02040	–0.0360	–39.35	1444.6	505.7	81.0
1.0000	0.0000	0.9461	0.8586	0.0000	0.00000	0.0000	0.00	1465.2	440.7	0.0
N,*N*-Dimethylformamide (A) + benzene (B) + 1,4-DO (C)										
0.0000	0.5301	0.9472	0.6569	–0.2104	0.25767	–0.2210	–548.86	1097.5	876.5	314.0
0.1118	0.4708	0.9479	0.6990	–0.1674	0.20782	–0.2770	–408.52	1130.9	824.9	276.0
0.2207	0.4131	0.9486	0.7290	–0.1364	0.17129	–0.3170	–317.23	1157.7	786.6	251.0
0.3268	0.3568	0.9487	0.7539	–0.1106	0.14044	–0.3130	–245.96	1181.8	754.7	232.0
0.4303	0.3020	0.9486	0.7750	–0.0886	0.11372	–0.2940	–189.09	1204.9	726.1	216.0
0.5311	0.2485	0.9484	0.7900	–0.0727	0.09381	–0.2540	–152.49	1226.6	700.8	203.0
0.6295	0.1964	0.9479	0.8027	–0.0591	0.07641	–0.2000	–123.44	1263.5	660.8	175.0
0.7255	0.1455	0.9474	0.8180	–0.0430	0.05598	–0.1430	–87.32	1301.5	623.1	149.0
0.8192	0.0958	0.9469	0.8329	–0.0273	0.03588	–0.0860	–53.23	1350.9	578.7	116.0
0.9107	0.0473	0.9464	0.8483	–0.0111	0.01500	–0.0380	–18.61	1435.8	512.6	61.0
1.0000	0.0000	0.9461	0.8586	0.0000	0.00000	0.0000	0.00	1465.2	440.7	0.0
N,*N*-Dimethylformamide (A) + benzene (B) + THF (C)										
0.0000	0.4800	0.8797	0.4022	–0.1227	0.23749	–0.2530	–645.90	1165.1	837.5	296
0.1023	0.4309	0.8868	0.4507	–0.1084	0.19612	–0.3150	–491.81	1210.0	770.1	268
0.2041	0.3820	0.8939	0.4957	–0.0973	0.16504	–0.3570	–382.37	1238.0	729.9	244
0.3054	0.3334	0.9009	0.5413	–0.0855	0.13641	–0.3840	–290.26	1263.2	695.7	226
0.4061	0.2851	0.9078	0.5843	–0.0761	0.11455	–0.3900	–225.66	1290.5	661.5	210
0.5064	0.2370	0.9145	0.6285	–0.0654	0.09315	–0.3790	–169.18	1322.2	625.4	190
0.6061	0.1891	0.9211	0.6744	–0.0528	0.07132	–0.3360	–117.21	1357.2	589.4	168
0.7053	0.1414	0.9276	0.7191	–0.0412	0.05294	–0.2860	–80.15	1392.0	556.4	140
0.8041	0.0941	0.9338	0.7681	–0.0251	0.03062	–0.2000	–37.14	1430.3	523.4	104
0.9023	0.0469	0.9400	0.8153	–0.0107	0.01235	–0.1090	–9.35	1484.8	482.5	58
1.0000	0.0000	0.9461	0.8586	0.0000	0.00000	0.0000	0.00	1465.2	440.7	0
N,*N*-Dimethylformamide (A) + benzene (B) + 1,2-DME (C)										
0.0000	0.5357	0.8702	0.3970	–0.1100	0.20674	–0.3050	–564.64	1137.8	887.7	285.0
0.1128	0.4752	0.8782	0.4473	–0.0994	0.16596	–0.3780	–418.36	1176.0	823.4	239.0
0.2225	0.4165	0.8862	0.4939	–0.0913	0.13661	–0.4290	–318.28	1203.8	778.6	212.0

TABLE II. Continued

x_A	x_B	ρ / g cm^{-3}	η / mPa s	$\Delta\eta$ / mPa s	I_A	V^E / cm^3 mol^{-1}	ΔG^{*E} / J mol^{-1}	u / m s^{-1}	K_s / 10^{-12} Pa^{-1}	K_s^E / 10^{-12} Pa^{-1}
N,*N*-Dimethylformamide (A) + benzene (B) + 1,2-DME (C)										
0.3291	0.3594	0.8943	0.5376	–0.0851	0.11561	–0.4650	–250.96	1228.2	741.3	192.0
0.4329	0.3038	0.9022	0.5813	–0.0779	0.09698	–0.4760	–196.86	1243.8	716.5	184.0
0.5338	0.2498	0.9100	0.6257	–0.0690	0.07926	–0.4690	–150.92	1264.5	687.2	171.0
0.6320	0.1971	0.9177	0.6735	–0.0557	0.05849	–0.4320	–101.41	1282.7	662.3	162.0
0.7276	0.1459	0.9251	0.7155	–0.0473	0.04743	–0.3600	–81.04	1319.6	620.8	136.0
0.8208	0.0960	0.9324	0.7593	–0.0363	0.03519	–0.2690	–60.68	1367.3	573.7	104.0
0.9115	0.0474	0.9395	0.8061	–0.0214	0.02029	–0.1600	–36.31	1437.6	515.0	60.0
1.0000	0.0000	0.9461	0.8586	0.0000	0.00000	0.0000	0.00	1465.2	440.7	0.0
N,*N*-Dimethylformamide (A) + benzene (B) + DIE (C)										
0.0000	0.5668	0.7958	0.3997	–0.1000	0.17669	–0.4880	–441.50	1219.2	845.3	261.0
0.1186	0.4995	0.8103	0.4506	–0.0917	0.13814	–0.6450	–306.30	1261.7	775.3	208.0
0.2324	0.4350	0.8248	0.4975	–0.0856	0.11174	–0.7330	–217.97	1287.0	732.0	181.0
0.3417	0.3731	0.8394	0.5424	–0.0800	0.09219	–0.7680	–157.51	1301.5	703.3	168.0
0.4467	0.3136	0.8541	0.5858	–0.0742	0.07703	–0.7550	–115.90	1305.3	687.2	167.0
0.5478	0.2563	0.8690	0.6274	–0.0689	0.06644	–0.7070	–92.30	1312.8	667.7	162.0
0.6450	0.2012	0.8840	0.6700	–0.0612	0.05550	–0.6140	–72.20	1326.7	642.7	151.0
0.7386	0.1481	0.8993	0.7161	–0.0487	0.04100	–0.5050	–47.43	1351.0	609.2	131.0
0.8289	0.0970	0.9145	0.7608	–0.0364	0.02957	–0.3430	–33.58	1394.5	562.3	97.0
0.9160	0.0476	0.9302	0.8069	–0.0215	0.01747	–0.1810	–21.97	1450.8	510.8	58.0
1.0000	0.0000	0.9461	0.8586	0.0000	0.00000	0.0000	0.00	1465.2	440.7	0.0
N,*N*-Dimethylformamide (A) + benzene(B) + DEE (C)										
0.0000	0.4869	0.7902	0.3396	–0.0636	0.16770	–0.5930	–149.83	1231.1	835.0	232.0
0.1036	0.4364	0.8051	0.3936	–0.0568	0.13130	–0.7240	–6.68	1273.2	766.2	180.0
0.2064	0.3864	0.8201	0.4449	–0.0523	0.10686	–0.8030	76.39	1292.9	729.5	160.0
0.3084	0.3367	0.8353	0.4944	–0.0492	0.08974	–0.8420	118.97	1308.8	698.9	146.0
0.4096	0.2875	0.8508	0.5420	–0.0477	0.07860	–0.8510	128.90	1321.0	673.5	137.0
0.5099	0.2386	0.8662	0.5884	–0.0470	0.07088	–0.7940	117.13	1321.3	661.2	141.0
0.6095	0.1901	0.8819	0.6353	–0.0455	0.06354	–0.7110	92.89	1332.0	639.1	135.0
0.7083	0.1420	0.8978	0.6863	–0.0394	0.05125	–0.5970	71.94	1347.9	613.0	125.0
0.8063	0.0943	0.9137	0.7364	–0.0340	0.04178	–0.4260	35.94	1377.1	577.1	105.0
0.9035	0.0470	0.9298	0.7947	–0.0200	0.02321	–0.2290	15.69	1433.5	523.4	67.0
1.0000	0.0000	0.9461	0.8586	0.0000	0.00000	0.0000	0.00	1465.2	440.7	0.0
N,*N*-Dimethylformamide (A) + benzene (B) + 2-ME (C)										
0.0000	0.4932	0.9229	1.0157	–0.0583	0.04851	–0.7550	116.78	1228.2	718.3	172.6
0.1048	0.4415	0.9269	1.0006	–0.0508	0.04393	–0.8290	107.22	1267.4	671.7	137.0
0.2085	0.3903	0.9306	0.9806	–0.0485	0.04400	–0.8770	84.83	1305.2	630.8	107.0
0.3111	0.3397	0.9343	0.9593	–0.0477	0.04532	–0.9170	57.87	1325.7	609.0	96.0
0.4127	0.2896	0.9375	0.9336	–0.0515	0.05114	–0.9120	18.99	1340.8	593.4	91.0
0.5131	0.2401	0.9402	0.9105	–0.0530	0.05459	–0.8690	–14.16	1349.7	583.8	92.0
0.6125	0.1911	0.9427	0.8891	–0.0530	0.05636	–0.8030	–43.84	1360.2	573.4	92.0
0.7109	0.1426	0.9444	0.8743	–0.0466	0.05101	–0.6720	–54.50	1376.2	559.0	88.0
0.8083	0.0946	0.9457	0.8623	–0.0376	0.04229	–0.5090	–57.14	1403.5	536.8	76.0
0.9046	0.0470	0.9462	0.8597	–0.0194	0.02245	–0.2770	–31.15	1460.1	495.7	45.0

TABLE II. Continued

x_A	x_B	ρ g cm^{-3}	η mPa s	$\Delta\eta$ mPa s	I_A	V^E cm^3 mol^{-1}	ΔG^{*E} J mol^{-1}	u m s^{-1}	K_s 10^{-12} Pa^{-1}	K_s^E 10^{-12} Pa^{-1}
N,*N*-Dimethylformamide (A) + benzene (B) + 2-ME (C)										
1.0000	0.0000	0.9461	0.8586	0.0000	0.00000	0.0000	0.00	1465.2	440.7	0.0
N,*N*-Dimethylformamide (A) + benzene (B) + 2-EE (C)										
0.0000	0.5354	0.9066	1.1640	–0.0022	0.03794	–0.8320	357.25	1280.9	672.3	123.1
0.1128	0.4750	0.9139	1.1302	–0.0013	0.03793	–1.0870	323.16	1315.6	632.2	95.2
0.2224	0.4163	0.9202	1.0944	–0.0033	0.03962	–1.2200	283.41	1342.6	602.9	77.8
0.3290	0.3592	0.9252	1.0574	–0.0076	0.04265	–1.2330	238.98	1362.6	582.1	68.6
0.4327	0.3037	0.9297	1.0205	–0.0126	0.04571	–1.1800	191.86	1371.6	571.8	69.5
0.5336	0.2497	0.9331	0.9855	–0.0165	0.04707	–1.0320	147.35	1383.5	559.9	68.6
0.6318	0.1971	0.9361	0.9526	–0.0192	0.04651	–0.8560	104.14	1394.6	549.2	68.6
0.7275	0.1459	0.9390	0.9222	–0.0202	0.04333	–0.6680	63.44	1415.4	531.6	61.3
0.8207	0.0960	0.9414	0.8968	–0.0170	0.03456	–0.4490	33.23	1441.3	511.4	51.2
0.9115	0.0474	0.9437	0.8744	–0.0114	0.02160	–0.2200	8.82	1483.6	481.4	31.1
1.0000	0.0000	0.9461	0.8586	0.0000	0.00000	0.0000	0.00	1465.2	440.7	0.0

In order to secure more comparable viscous antagonic results, the so called antagonic interaction index (I_A), introduced by Howell,[37] was taken into account:

$$I_A = (\eta_{cal} - \eta_{exp}) / \eta_{cal} \quad (2)$$

The antagonic interaction index (I_A) values at 298.15 K for the ternary mixtures (A) + (B)+ 1,3-DO, 1,4-DO, THF, 1,2-DME, DIE, DEE, 2-ME and 2-EE (C) are plotted against x_A in Fig. 3. It was found that each mixture had a maxi-

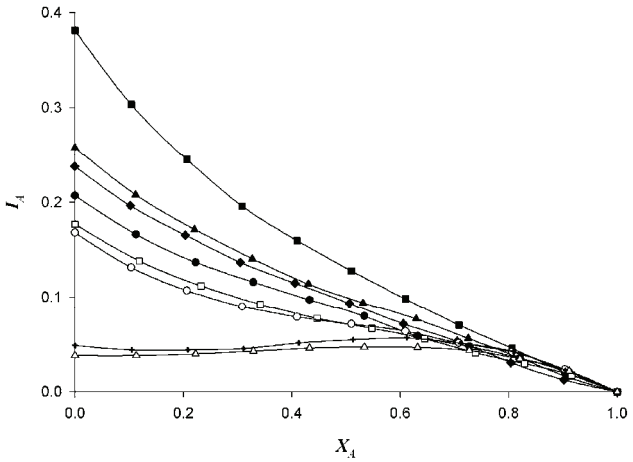

Fig. 3. Antagonic Index (I_A) of: ■) DMF (A) + benzene (B) + 1,3-DO (C); ▲) DMF (A) + benzene (B) + 1,4-DO (C); ♦) DMF (A) + benzene (B) + THF (C); ●) DMF (A) + benzene (B) + 1,2-DME (C); □) DMF (A) + benzene (B) + DIE (C); ○) DMF (A) + benzene (B) + DEE (C); +) DMF (A) + benzene (B) + 2-ME (C); Δ) DMF (A) + benzene (B)+ 2-EE (C) mixtures with mole fraction of DMF (x_A) at 298.15 K.

mum at x_A = 0.0, which then decreased with increasing x_A. A perusal of Table II shows that the experimentally determined viscosities, η_{exp} for all mixtures for various mole fractions at the experimental temperature are lower than those of their calculated values, η_{calcd}, which demonstrates viscous antagonism in the eight mixtures studied herein. The explanation of this behavior is based on the known phenomenon of molecular dissociation, as a consequence of the weakening of the non-covalent bonding formed between the molecules, causing a decrease in the size of the molecular package, which logically implies an increase in I_A.[1,12] The maxima observed indicate strong specific interaction between the unlike molecules, which is predominated by non-covalent interaction. Thus, the molecular package increases gradually with the addition of DMF to the mixtures, which implies a decrease in I_A.

The excess molar volumes, V^E were calculated from the density data according to the following equation:[39]

$$V^E = \sum_{i=1}^{3} x_i M_i \left(1/\rho - 1/\rho_i\right) \quad (3)$$

where M_i, and ρ_i are the molar mass and density of the pure components, respectively, and ρ is the density of the mixture. For the ternary systems, in general, the V^E values were found to be negative over the whole composition range under study at 298.15 K, which is depicted as a representative plot in Fig. 4 as a function of the mole fraction of both DMF (x_A) and benzene (x_B). The V^E values for the eight ternary mixtures under examination are presented in Fig. 5. The values at first decreases to minima and then increase with increasing x_A. The eight ternary mixtures show minima at the same point, *i.e.*, at x_A = 0.3. The trend is:

(A)+(B)+1,3-DO > 1,4-DO > THF >1,2-DME > DIE > DEE > 2-ME > 2-EE

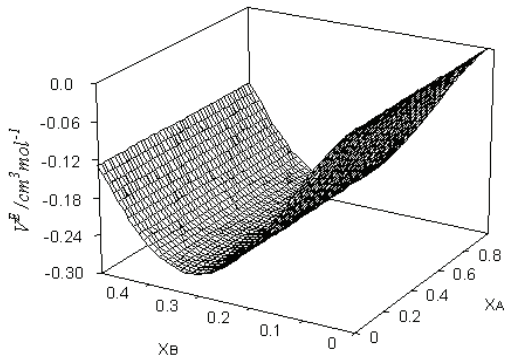

Fig. 4. 3D mesh plots of excess molar volumes (V^E) of: DMF (A) + benzene (B) + 1,3-DO (C) mixtures with mole fraction of DMF (x_A) and benzene (x_B) at 298.15 K.

The negative values of V^E indicate the presence of strong molecular interaction between the components of the mixture. Volume changes for a mixed system result from changes in the free volume of the liquids, since the bond

lengths and bond distances in the molecules themselves do not change. The optimum packing condition is directly related to differences in molecular sizes and intermolecular attractions, in particular when hydrogen bonding occurs between unlike molecules creating association complexes, as well as being effected by the breaking of interactions between like molecules.[32] Several effects contribute to the value of V^E, such as: dipolar interaction, interstitial accommodation and possible hydrogen bonded interactions between unlike molecules.[40] The actual volume change would, therefore, depend on the relative strength of these three effects. Similar results have been reported earlier.[41,42]

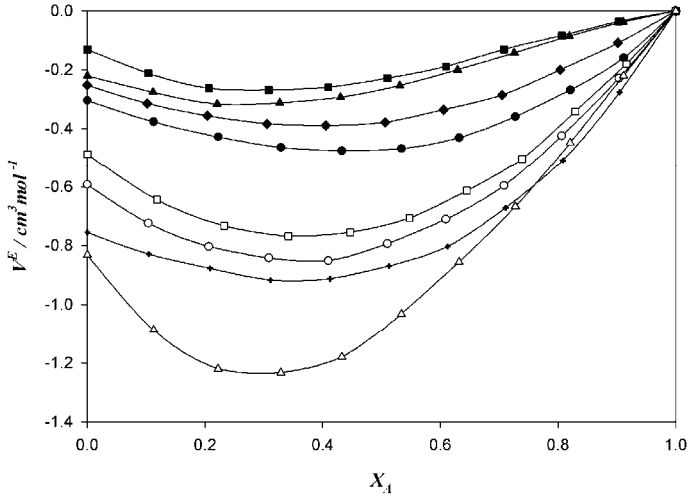

Fig. 5. Excess molar volumes (V^E) of: ■) DMF (A) + benzene (B) + 1,3-DO (C); ▲) DMF (A) + benzene (B) + 1,4-DO (C); ♦) DMF (A) + benzene (B) + THF (C); ●) DMF (A) + benzene (B) + 1,2-DME (C); □) DMF (A) + benzene (B) + DIE (C); ○) DMF (A) + benzene (B) + DEE (C); (+), DMF (A) + benzene (B) + 2-ME (C); Δ) DMF (A) + benzene (B) + 2-EE (C) mixtures with mole fraction of DMF (x_A) at 298.15 K.

Based on the theory of absolute reaction rates,[38] the excess Gibbs energy, ΔG^{*E}, of viscous flow for a ternary system was calculated from:

$$\Delta G^{*E} = RT \ln(\eta M/\rho) - RT \sum_{i=1}^{3} x_i \ln(\eta_i M_i/\rho_i) \quad (4)$$

where M and M_i are the molar mass of the mixture and of the pure components i. According to the literature, positive ΔG^{*E} values indicate specific interactions, while negative values indicate the dominance of dispersion forces.[43,44] From the ΔG^{*E} values recorded in Table II, it can be seen that for all the ternary mixtures, these values are negative or positive keeping similarity with the $\Delta\eta$ values and thereby supports the conclusion drawn from the V^E and $\Delta\eta$ considerations.

Table II contains the sound velocity (u), the isentropic compressibility (K_s) and excess isentropic compressibility (K_s^E) data for the observed mixtures, which were calculated using the following equations: [45]

$$K_s = \left(u^2 \rho_{exp}\right)^{-1} \quad (5)$$

$$K_s^E = K_s - \sum_{i=1}^{3} x_i K_{s,i} \quad (6)$$

where, $K_{s,i}$ gives the isentropic compressibility for the pure components of the mixture.

Figure 6 predicts the curves for the ternary mixtures of K_s^E. The values are positive in all the cases and decreases as the mole fraction of DMF increases. There is a parallel in the qualitative behavior of the K_s^E and V^E curves. The K_s^E values follow the sequence:

(A)+(B)+1,3-DO > 1,4-DO > THF >1,2-DME > DIE > DEE > 2-ME > 2-EE

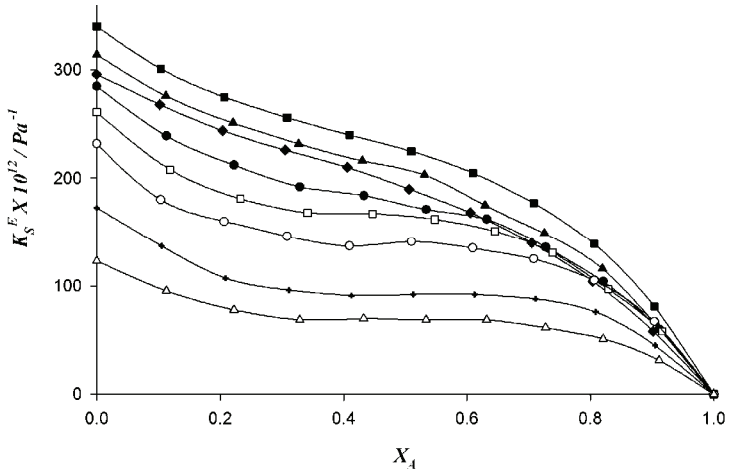

Fig. 6. Excess isentropic compressibility (Ks^E) of: ■) DMF (A) + benzene (B) + 1,3-DO (C); ▲) DMF (A) + benzene (B) + 1,4-DO (C); ♦) DMF (A) + benzene (B) + THF (C); ●) DMF (A) + benzene (B) + 1,2-DME (C); □) DMF (A) + benzene (B) + DIE (C); ○) DMF (A) + benzene (B) + DEE (C); (+), DMF (A) + benzene (B) + 2-ME (C); Δ) DMF (A) + benzene (B) + 2-EE (C) mixtures with mole fraction of DMF (X_A) at 298.15 K.

The positive K_s^E values are due to the breaking of interactions and the corresponding disruption of molecular order in the pure components.[24] The donor–acceptor interaction between the component molecule plays an important part for the mixtures containing open chain ethers, especially those having a hydroxyl group, where there is strong specific interaction between the component molecules leading to lower value of K_s^E. Interactions between the molecules of DMF,

benzene or ethers are broken in the mixing process; the breaking leads to positive K_S^E values for the mixture containing cyclic ethers as compared to the open chain ethers. Similar results were reported earlier by some authors.[24,32]

CONCLUSIONS

After a thorough study of the behavior of ethers in *N*,*N*-dimethylformamide + benzene mixtures, a clear idea about the type and amount of molecular interactions between them was obtained and an idea about antagonism was given. The similarity in the working formula of the antagonic interaction index and viscosity deviation would probably indicate that the two properties are similar but a close comparison between these two parameters gave a clear distinction.

Acknowledgments. The authors are thankful to the Departmental Special Assistance Scheme under the University Grants Commission, New Delhi (No. 540/6/DRS/2007, SAP-1) and Department of Chemistry, North Bengal University for the instrumental and financial assistance.

И З В О Д

ИСПИТИВАЊЕ ВИСКОЗНОСТИ, ДОПУНСКЕ МОЛАРНЕ ЗАПРЕМИНЕ, ПРОМЕНЕ ВИСКОЗНОСТИ И ИЗЕНТРОПСКЕ КОМПРЕСИБИЛНОСТИ ТЕРНЕРНИХ СИСТЕМА *N*,*N*-ДИМЕТИЛФОРМАМИДА, БЕНЗЕНА И ЕТАРА НА 298,15 K

RIJU CHANDA, ASHIS BANERJEE и MAHENDRA NATH ROY

Department of Chemistry, North Bengal University,Darjeeling-734013, India

Извршена су мерења густина (ρ) и вискозности (η) тернерних смеша *N*,*N*-диметилформамид + бензен + етар, у функцији састава и на температури од 298,15 K. Из експерименталних података су израчунате вредности допунске моларне запремине (V^E), промене вискозности ($\Delta\eta$), интеракциони индекс (I_A) и Гибсову слободну енергију активације (ΔG^{*E}). Такође, на температури на којој су извршени експерименти, мерене су и брзине звука и израчунате допунске изентропске компресибилности (K_s^E). Добијени резултати су анализирани у функцији молекулског паковања и специфичних интеракција проузрокаваних присуством водоничних веза.

(Примљено 6. августа 2009, ревидирано 27. августа 2010)

REFERENCES

1. J. V. Herraez, R. Belda, *J. Solution Chem.* **33** (2004) 117
2. R. Belda, J. V. Herraez, O. Diez, *Phys. Chem. Liquids*. **42** (2004) 467
3. S. L. Oswal, H. S. Desai, *Fluid Phase Equilib*. **161** (1999) 191
4. S. L. Oswal, H. S. Desai, *Fluid Phase Equilib*. **186** (2001) 81
5. P. Dimitrios, P. Constantinos, *J. Chem. Eng. Data* **40** (1995) 202
6. G. Czechowski, B. Zywucki, J. Jadzyn, *J. Chem. Eng. Data* **33** (1998) 55
7. R. Belda, J. V. Herraez, O. Diez, *Phys. Chem. Liquids* **43** (2005) 91
8. M. N. Roy, D. K. Hazra. *North Bengal Univ. Rev*. **8** (1997) 54
9. C. R. Reid, B. E. Poling, *The Properties of Gases and Liquids*., Ch. 1, McGraw-Hill, New York, 1998

10. C. Lafuente, B. Ginar, A. Villares, I. Gascon, P. Cea, *Int. J. Thermophys*. **25** (2004) 1735
11. P. S. Nikam, L. N. Shirsat, M. Hasan, *J. Ind. Chem. Soc*. **77** (2000) 244
12. M. N. Roy, A. Choudhury, A. Sinha, *J. Teach. Res. Chem.* **11** (2004) 12
13. D. K. Hazra, M. N. Roy, B. Das, *Ind. J. Chem. Technol*. **1** (1994) 93
14. M. N. Roy, A. Jha, R. Dey, *J. Chem. Eng. Data* **46** (2001)1327
15. M. N. Roy, A. Sinha, B. Sinha, *J. Sol. Chem.* **34** (2005) 1319
16. M. N. Roy, S. R. Choudhury, A. Jha, *J. Ind. Chem. Soc*. **79** (2002) 623
17. M. N. Roy, A. Jha, A. Choudhury, *J. Chem. Eng. Data* **49** (2004) 291
18. M. N. Roy, B. B. Gurung, A. Choudhury, *J. Ind. Chem. Soc*. **81** (2004)1
19. D. D. Perrin, W. L. F. Armarego. *Purification of Laboratory Chemicals*, 3rd ed., Pergamon, Oxford, 1988
20. A. Vogel, *Practical Organic Chemistry*, 4th ed., Longman, London, 1978
21. J. A. Riddick, W. B. Bunger, T. K. Sokano, *Organic Solvents: Physical Properties and Methods of Purifications*, Vol. 2, 4th ed., Wiley-Interscience, New York, 1986
22. S. J. Kharat, P. S. Nikam, *J. Chem. Eng. Data* **48** (2003) 1202
23. H. Casas, L. Segade, C. Franjo, E. Jiménez, *J. Chem. Eng. Data* **43** (1998) 756
24. T. M. Aminabhavi, B. Gopalkrishna, *J. Chem. Eng. Data* **40** (1995) 856
25. A. K. Covington, T. Dickinson, *Physical Chemistry of Organic Solvent Systems*, Plenum, New York, 1973
26. M. N. Roy, A. Sinha, B. Sinha, *J. Solution Chem.* **34** (2005) 1319
27. I. Johnson, M. Kalidoss, R. Srinivasamoorthy, *J. Chem. Eng. Data* **47** (2002) 1388
28. *TRC Tables*, *Selected Values of Properties of Chemical Compounds*, Thermodynamic Research Center, A & M University, College Station, TX, 1974
29. T. M. Aminabhavi, V. B. Patil, *J. Chem. Eng. Data* **43** (1998) 497
30. D. R. Lide, *CSIR Handbook of Chemistry and Physics*, 7th ed., 1990–1991
31. M. N. Roy, B. Sinha, *J. Mol. Liq.* **133** (2007) 89
32. M. N. Roy, M. Das, *Phys. Chem. Liq*. **44** (2006) 663
33. I. Gascón, S. Martín, P. Cea, M. C. López, F. M. Royo, *J. Sol. Chem.* **31** (2002) 905
34. D. K. Hazra, B. Das, *J. Phys. Chem*. **99** (1995) 269
35. J. Barthel, R. Neueder, H. Roch, *J. Chem. Eng. Data* **45** (2000) 1007
36. M. N. Roy, A. Jha, A. Choudhury, *J. Chem. Eng. Data* **49** (2004) 291
37. N. K. Howell, in *Proceedings of the 7th International Conference*, Wales, 1993
38. S. Glasstone, K. J. Laidler, H. Eyring, *The Theory of Rate Process*, McGraw-Hill, New York, 1941, p. 514
39. B. Djordjević, I. Radović, M. Kijevčanin, A. Tasić, S. Šerbanović, *J. Serb. Chem*. Soc. **74** (2009) 477
40. P. S. Nikam, S. J. Kharat, *J. Chem. Eng. Data* **50** (2005) 455
41. P. Brocos, E. Calvo, A. Pineiro, R. Bravo, A. Amigo, *J. Chem. Eng. Data* **44** (1999) 1341
42. A. Amigo, R. Bravo, M. Pintos, *J. Chem. Eng. Data* **38** (1993) 141
43. T. M. Reed, T. E. Taylor, *J. Phys. Chem*. **63** (1959) 58
44. R. Meyer, M. Meyer, J. Metzer, A. Peneloux, *Chem. Phys*. **62** (1971) 406
45. C. Lafuente, B. Giner, A. Villares, I. Gascon, P. Cea, *Int. J. Thermophys*. **25** (2004) 1735.

Journal of the Serbian Chemical Society
JSCS-info@shd.org.rs • www.shd.org.rs/JSCS
J. Serb. Chem. Soc. *75* (12) 1733–1741 (2010)
JSCS–4092
UDC 669.3+669.187.25:504.75:615.9
Original scientific paper

The possibilities of the utilization of the polymetallic concentrate Čoka Marin

LIDIJA D. GOMIDŽELOVIĆ*#, EMINA D. POŽEGA# and VLASTIMIR K. TRUJIĆ

Mining and Metallurgy Institute, Zeleni bulevar 33, 19210 Bor, Serbia

(Received 14 July 2009, revised 30 June 2010)

Abstract: This paper presents the results of calculations of the composition of composite concentrates used as the charge in the Copper Smelter in Bor, from the aspect of the behavior of zinc, lead, arsenic, cadmium and mercury. These elements have extremely harmful effects on the environment and human health; hence it is crucial to comply with legal values of their emission into the environment.

Keywords: copper smelting; impurities; concentrate; ecology; distribution.

INTRODUCTION

Zinc, lead, arsenic, cadmium and mercury are toxic for most living organisms on the Earth. Even very small concentrations of these elements (expressed in ppm) have serious toxic effects.[1] The behavior and distribution of harmful elements in the production process in the Copper Smelter in Bor, have been observed for many years by the experts of Copper Institute (now Mining and Metallurgy Institute Bor).[1] These elements are major pollutants in the environment and have negative effect on the quality of the produced copper and sulfuric acid, which necessitates the continuous monitoring of their content in the starting raw materials. Based on previous studies in the Copper Smelter from the reverberatory furnace, with the gas phase, more than 50 % arsenic, 40–50 % lead and 41 % zinc present in starting charge are emitted into the atmosphere, while the rest is deposited in the slag.[2] During smelter treatment of concentrate, 48.7 % of the mercury is emitted with gases during roasting, and 47.3 % into the gases during smelting.[2]

Marin with a lot of impurities presents a demanding charge that could be treated using the existing technology in the reverberatory furnace only if the allowed limits of any harmful elements in starting mixture are not exceed. In this way, the risk of environmental accidents would be reduced to a minimum.

* Corresponding author. E-mail: lgomidzelovic@yahoo.com
# Serbian Chemical Society member.
doi: 10.2298/JSC090714085G

The increased industrialization has been followed all over the world by the extraction and redistribution of mineral substances from their natural deposits. Passing through the processes of treatment and use, the mineral raw materials arrive *via* waste water, gases, dust and waste dumps into the air, water and land, and, thus, indirectly into the food chain.[3]

Lead is a typical accumulative poison. It causes the prevention of hemoglobin synthesis, neurological problems (aggressive and destructive behavior), kidney damage and even permanent brain damage.[4]

Zinc is one of the micro-elements necessary for the proper functioning of the body functioning, but in excessive doses can lead to problems in growth and reproduction.[1]

Arsenic, a metalloid that can enter into the body through the lungs and gastrointestinal tract, has negative influence on the process of protein coagulation, and could form complex compounds with co-enzymes.[5]

Cadmium is also an accumulative toxin that adversely affects important enzymes; causes bone disease and kidney damage. Inhalation of dust and gases containing cadmium leads to lung failure due to the accumulation of water in them.[6–8]

Mercury enters into the body by ingestion and inhalation and transfers *via* the blood to the brain where could pass through the blood–brain barrier and causes insomnia, depression and irritability. It also leads to kidney damage.[9] It is only temporarily deposited in the body and a large part is eliminated through the digestive system.

The sampling method for copper concentrates is defined by the SRPS Standard BG-3:451.

The technological analysis of a concentrate includes the determination of content the required elements for process optimization and technological process management, while the environmental analysis involves the determination of the contents of Pb, Zn, As, Sb, Cd, Se, Hg and Cl, which are used to perform an environmental assessment of the concentrate.

Lead and zinc are usually present in the copper ore in the form of PbS and ZnS, arsenic is present in the form of Cu_3AsS_4, FeAsS and Cu_3AsS_4 minerals,[10] while mercury is present in the form of HgS and cadmium in the form of CdS.

The associated elements in a copper concentrate are distributed during smelting according to their physico–chemical properties and are concentrated in the intermediates and products of the pyrometallurgical treatment. The behavior of each element depends on several factors, the most important of which are: the form in which they are present in the raw materials, the technological parameters of the applied process, their inter-relationship with other elements, the concentration of certain elements, *etc*. The parameters of the distribution each element can only be reliably determined by raw material treatment using the specific technology.[11]

A block diagram of copper concentrate treatment, including treatment of the off-gases and sulfuric acid production, is given in Fig. 1.

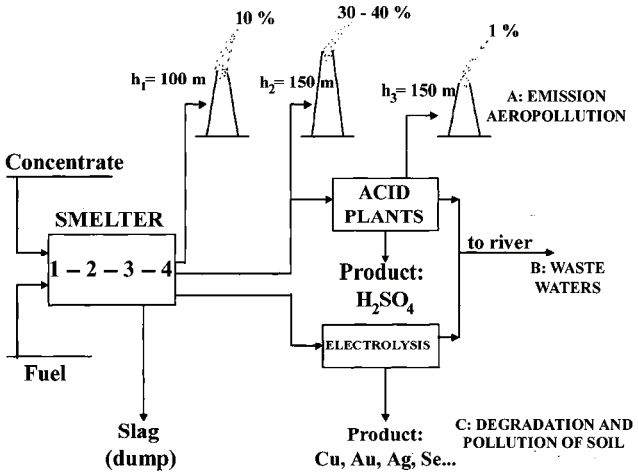

Fig. 1. Block diagram of copper concentrate treatment with pollution sources (1 – roasting; 2 – smelting; 3 – converting; 4 – flame refinement).

The distributions of zinc, lead and arsenic in the output products (anode copper, slag, sludge and water, gas) were calculated based on their emission in the period from 1991 to 1997.[12]

For the cadmium and mercury distribution, there are no available data about their emission, hence a critical analysis of the available data on their distribution through the output products of the copper concentrate treatment[2,3,13] was performed. The obtained distributions of Zn, Pb, As, Cd and Hg, determined as given above, are presented in Table I.

TABLE I. Distribution of Pb, Zn, Hg, Cd and As in the reverberatory furnace in %

Phase	Pb	Zn	Hg	Cd	As
Batch	100	100	100	100	100
Anode copper	1.95	0.05	0	1.37	2.44
Slag	63.76	54.39	5	8.45	12.06
Sludge and water	4.73	4.49	31.6	5.18	34.31
Gas	29.63	41.08	63.4	85	51.19

RESULTS AND DISCUSSION

Monitoring of the contents of impurities in the raw mixture

Using the polymetallic ore from the deposit “Čoka Marin”, the collective concentrate (7.92 % Cu, 26 g t^{-1} Au, 127.2 g t^{-1} Ag, 3.92 % Zn, 1.1 % Pb, 0.98 % As, 0.0011 % Cd, 12.1 g t^{-1} Hg) is produced. This concentrate should be

combined with the already used concentrates for the preparation the mixture in reverberatory furnace (the composition in relation to the contents of the impurities is given in Table II), in such a way that the composition of obtained concentrate mixture meets the allowed limits for the content of zinc, lead, arsenic, cadmium and mercury. The compositions of used imported concentrates (1--ASSAREL and 2-ELATZITE) are given in Table III. The allowed limits for the contents of zinc, lead, arsenic, cadmium and mercury, estimated based on the prescribed contents of these metals in the output gases of Copper Smelter, are listed in Table IV, from which it is possible to conclude that these impurities in the composite concentrate have to be significantly lower than in the concentrates delivered in the reverberatory furnace and used for the preparation of the mixture.

TABLE II. Input contents of impurities in the copper concentrate formed from the mixture (the amount of concentrate Čoka Marin was varied within the limits of 0–10 wt. %)

Concentrate	Weight (dmt)	Content, %				
		Zn	Pb	As	Cd	Hg
Bor	36050	0.68	0.15	0.19	0.0025	0.000104
Krivelj	86265	0.06	0.009	0.012	0.0027	0.000018
Majdanpek	47510	0.52	0.16	0.01	0.0026	0.000023
Import	30000	0.03	0.2	0.02	0.0025	0.00008
Čoka Marin	–	3.92	1.1	0.98	0.011	0.00121

TABLE III Composition of the used import concentrates (ratio 1:1)

Concentrate	Content, %				
	Zn	Pb	As	Cd	Hg
1	0.04	0.4	0.009	0.0025	0.00006
2	0.02	0.03	0.03	0.0025	0.0001

TABLE IV Allowed limits of the contents of heavy metals (Zn, Pb, As, Cd and Hg; internal limits applied in the Copper Smelter in Bor, based on the allowed values of these elements in the output gases)

Element	Individual concentrate, %	Composite concentrate, %
Zn+Pb	3	1.5
As	0.2	0.1
Cd	0.01	0.0025
Hg	0.0005	0.0002

Using the percentage amounts and the weight of the concentrates from Table II, the calculation was realized based on the obtained data for the contents of Zn, As, Pb, Cd and Hg in the domestic and imported concentrates. A detailed analysis of the results is shown in Figs. 2a–2d.

The changes in the contents of zinc and lead in the concentrate mixture containing varying amounts of Čoka Marin concentrate, within the limits 0–10 %, are presented in Fig. 2a. Analyzing this figure, it is possible to conclude that the

combined contents of these two metals did not exceed the allowed limit of 1.5 % (Zn+Pb), even when the maximum 10 % of Čoka Marin concentrate was present in the mixture.

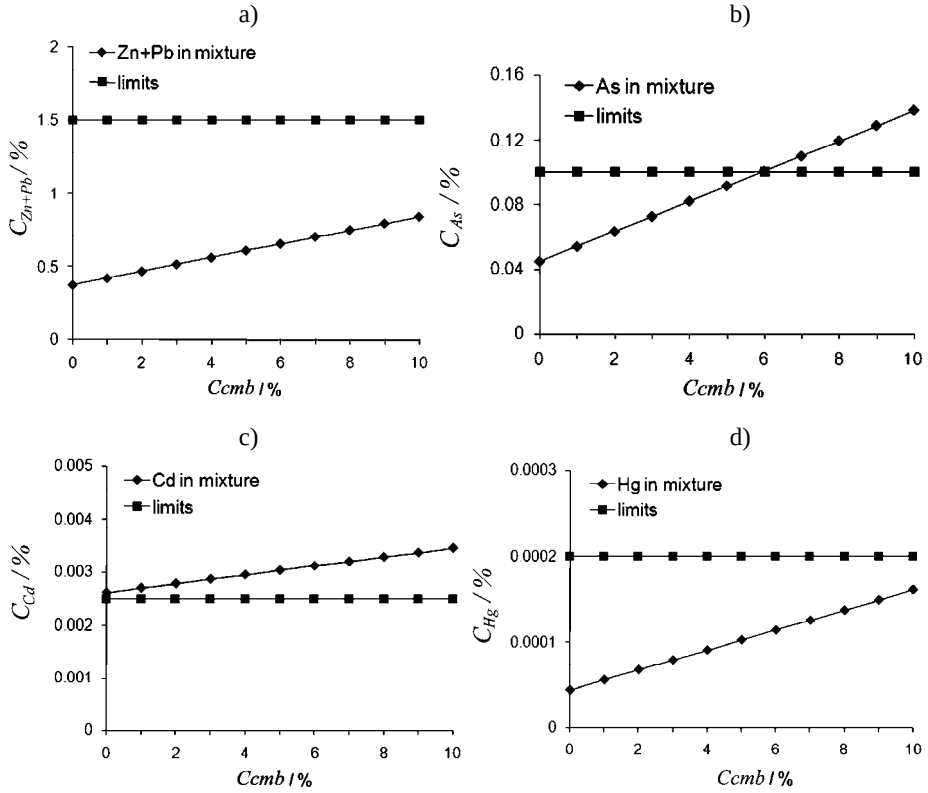

Fig. 2. Change of impurities content in the concentrate mixture depending on the varying contents of Čoka Marin concentrate (a – Zn+Pb; b – As; c – Cd and d – Hg); *Ccmb* – percentage of concentrate Čoka Marin in batch; C_{Zn+Pb} – percentage of zinc and lead in concentrate mixture; C_{As} – percentage of arsenic in concentrate mixture; C_{Cd} – percentage of cadmium in concentrate mixture; C_{Hg} – percentage of mercury in concentrate mixture.

The change in the content of arsenic in the concentrate mixture containing varying amounts of Čoka Marin concentrate, within the limits 0–10 % is shown in Fig. 2b. Analyzing this figure, it is possible to conclude that the content of this element exceeds the prescribed limit of 0.1 % when the amount of Čoka Marin concentrate in the mixture exceeded about 6 %.

The change in the content of cadmium in the concentrate mixture containing varying amounts of Čoka Marin concentrate, within the limits 0–10 %, is presented in Fig. 2c. Analyzing this figure, it is possible to conclude that content of this metal is above the allowed limit of 0.0025 % Cd when more than 2 % of

Čoka Marin concentrate was added to the mixture. Concentrate mixtures containing less than 2.5 % Čoka Marin concentrate met the given ecological conditions for their use.

The change of the content mercury in the concentrate mixture containing varying amounts of Čoka Marin concentrate, within the limits 0–10 %, is shown in Fig. 2d. Analyzing this figure, it is possible to conclude that content of this metal in the mixture did not exceed the allowed limit of 0.0002 % Hg, even when the amount of Čoka Marin concentrate was the maximum of 10 %.

Monitoring the content of impurities through the anode copper and pollution sources

Taking into account the data listed in Table I, which considers only the content of impurities in the mixture, the original calculations are extended. Additionally, the obtained results included a distribution of impurities between the anode copper and the by-products (slag, sludge and water and gas) from the smelting of the copper concentrate, which cause different types of pollution. These are shown in Fig. 3.

The distribution of zinc between the anode copper and the by-products (slag, sludge and water, gas) obtained during the processing of mixtures composed of the copper concentrates listed in Table II is presented in Fig. 3a. Analyzing this Figure, it is possible to conclude that the largest amount of zinc from the process is contained in the slag and, in second place, in the gas phase. The anode copper contains a negligible quantity of zinc.

The distribution of arsenic between the anode copper and the by-products (slag, sludge and water, gas) obtained during the processing of mixtures composed of the copper concentrates listed in Table II is presented in Fig. 3b. Maximum amount of arsenic from process exits in the gas phase and the rest mostly in waste water, while the slag bonds a small amount of this element. The anode copper contains 2.44 % As (Table I).

The distribution of cadmium between the anode copper and the by-products (slag, sludge and water, gas) obtained during the processing of mixtures composed of the copper concentrates listed in Table II is shown in Fig. 3c. The largest part of cadmium from the process exits in the gas phase, while the other by products contain smaller amounts of this element; about 1 %. remains in the anode copper.

The distribution of mercury between the anode copper and the by-products (slag, sludge and water, gas) obtained during the processing of mixtures composed of the copper concentrates listed in Table II is shown in Fig. 3d. Mercury is completely removed from the anode copper and the largest part of this element exits with the gases and waste water.

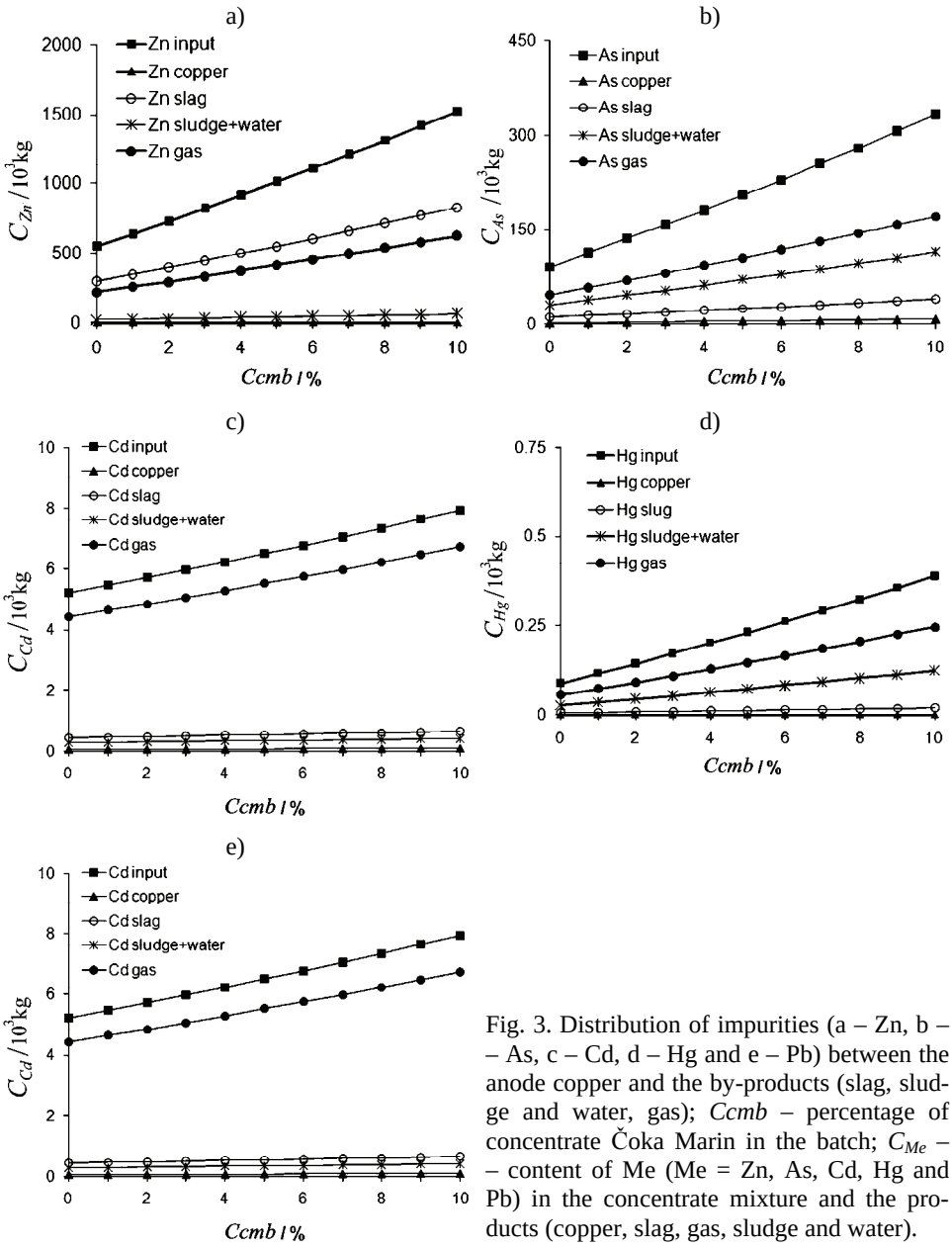

Fig. 3. Distribution of impurities (a – Zn, b – – As, c – Cd, d – Hg and e – Pb) between the anode copper and the by-products (slag, sludge and water, gas); *Ccmb* – percentage of concentrate Čoka Marin in the batch; C_{Me} – – content of Me (Me = Zn, As, Cd, Hg and Pb) in the concentrate mixture and the products (copper, slag, gas, sludge and water).

The distribution of lead between the anode copper and the by-products (slag, sludge and water, gas) obtained during the processing of mixtures composed of the copper concentrates listed in Table II is presented in Fig. 3e. For the most

part, lead remains in the slag, but a significant portion exits in the gas phase, while about 2 % is contained in the anode copper.

Based on the calculation results in the first part of this study, it can be seen that the content of cadmium is the main problem, if the set limits for the contents of impurities are to be met. The use of 0 to 10 % Čoka Marin concentrate in the mixture is not limited by the emission of zinc, lead or mercury into the atmosphere.

Arsenic allows the use of Čoka Marin concentrate up to about 6 % in the mixture.

The cadmium in the Čoka Marin concentrate allows the participation of this concentrate in the mixture only up to about 2.5 %, which limits its practical use and does not allow the high profitability its gold content to be expressed.

The use of Čoka Marin concentrate in the existing process is also limited by the cumulative increase of the content of impurities in the atmosphere during the exploitation. This indicates that the use of this concentrate in other modern processes may be possible under strict control.

Based on the results obtained in this part of the work, the distribution of the impurities (As, Pb, Zn, Cd and Hg) can be monitored through the anode copper and the by-products (slag, sludge and water, gas).

Based on the obtained results, it could be concluded that significant amounts of Zn, As, Cd, Hg and Pb exits with gases and for this reason, special attention should be to paid to the process of capture and purification of the gases and also to the provision of a hermetic gas line.

The waste water carries significant amounts of As and Hg, which necessitates the employment of suitable procedures for its purification.

With the slag, larger quantities of Zn and Pb are removed that necessitates the determination of the form in which these elements exist and that regulations are adhered to for the postponement of such material, to reduce soil degradation.

CONCLUSIONS

Taking into account all the mentioned influences of zinc, lead, arsenic, cadmium and mercury and their content in possible mixtures for smelting in the reverberatory furnace, such a solution cannot be recommended. For the health reasons, it would be better to export this type of concentrate to allow it to be smelted now using appropriate contemporary technology, or to wait for the installation of new technology in the RTB Bor Smelter Plant.

ИЗВОД

МОГУЋНОСТ КОРИШЋЕЊА ПОЛИМЕТАЛИЧНОГ КОНЦЕНТРАТА ЧОКА МАРИН СА АСПЕКТА УТИЦАЈА САДРЖАЈА ШТЕТНИХ ЕЛЕМЕНАТА НА ОКОЛИНУ

ЛИДИЈА Д. ГОМИЦЕЛОВИЋ, ЕМИНА Д. ПОЖЕГА и ВЛАСТИМИР К. ТРУЈИЋ

Институт за рударство и металургију, Зелени булевар 33, 19210 Бор

У раду су изложени резултати прорачуна састава композитних концентрата који се користе као шаржа у Топионици бакра у Бору са аспекта понашања штетних елемената: цинка, олова, арсена, кадмијума и живе. Ови елементи показују веома штетно дејство на околину и здравље људи, тако да је од изузетне важности да се испоштују законом порписане вредности њихове емисије у околину.

(Примљено 14. јула 2009, ревидирано 30. јуна 2010)

REFERENCES

1. M. D. Dimitrijević, A. I. Kostov, V. M. Tasić, N. M. Milošević, *J. Hazard. Mater*. **164** (2009) 892
2. N. T. Mitevska, Ž. D. Živković, in *Proceedings of Sulfide Smelting*, Seattle, NY, 2002, p. 547
3. D. M. Vučurović, Č. N. Knežević, in *Copper Metallurgy*, Copper Institute, Bor, 2000, p. 250 (in Serbian)
4. R. R. Jones, *Lancet* **16** (1989) 669
5. J. Maslowska, M. Ahmadi, *Przemysl Spozywczy* **45** (1991) 201 (in Polish)
6. F. Gazza, Ann. della Facolta di Med. Vet. **10** (1990) 171
7. J. P. Groten, E. J. Sinkeldam, J. B. Luten, P. J. Van Bladeren, *Food Chem. Toxicol*. **28** (1990) 435
8. A. O. Igwegbe, H. M. Belhaj, T. M. Hassan, A. S. Gibali, *J. Food Safety* **13** (1992) 7
9. W. L. Chang, *Biomed. Environ. Sci. Res*. **3** (1990) 125
10. N. T. Mitevska, Ž. D. Živković, *J. Min. Metall. B* **38** (2002) 93
11. C. R. Fountain, M. D. Coulter, J. S. Edwards, *Minor Element Distribution in the Copper Isasmelt Process*, *Copper*, *91*, Volume IV, Pegamon Press, New York, 1991, p. 359
12. V. M. Tasić, D. R. Milivojević, N. M. Milošević, D. V. Karabašević, in *Proceedings of 36th IOC on Mining and Metallurgy*, (2004), Bor Lake, Serbia, 2004, p. 371 (in Serbian)
13. I. N. Mihajlović, N. D. Štrbac, Ž. D. Živkovic, R. M. Kovačević, M. M. Šteharnik, *Miner. Eng.* **20** (2007) 26
14. E. D. Požega, L. D. Gomidželović, V. K. Trujić, M. M. Ćirković, in *Proceedings of Ecological Truth*, (2009), Kladovo, Serbia, (2009), p. 108 (in Serbian).

Journal of the Serbian Chemical Society
JSCS@tmf.bg.ac.rs • www.shd.org.rs/JSCS
J. Serb. Chem. Soc. 75 (12) 1743–1754 (2010)

Contents of Volume 75

NUMBER 1

NUMBER 2

NUMBER 3

NUMBER 4

NUMBER 5

NUMBER 7

NUMBER 8

NUMBER 10

NUMBER 11

NUMBER 12

J. Serb. Chem. Soc. 75 (12) 1755–1762 (2010)

Author index

Subject Index of Vol. **75** and *List of Referees* in the year *2010* are given at the Internet address of the Journal of the Serbian Chemical Society (http:// //www.shd.org.rs/jscs/).

End of Volume 75.

Journal of the Serbian Chemical Society
JSCS-info@shd.org.rs • www.shd.org.rs/JSCS
Volume *75* (2010)

Subject index

Journal of the Serbian Chemical Society
JSCS-info@shd.org.rs • www.shd.org.rs/JSCS
Volume 75 (2010)

2010 List of referees

Editorial Board of the Journal is grateful to the following referees for reviewing the manuscripts during 2010:

Bakr F. Abdel-Wahab, *Applied Organic Chemistry Department, National Research Center, Dokki, Giza, Egypt*
Biljana Abramović, *Faculty of Sciences, University of Novi Sad, Novi Sad, Serbia*
Hazem M. Abu Shawish, *Faculty of Science, Research Center, Al-Aqsa University, Gaza, Palestine*
M. Adharvana Chari, *Department of Applied Chemistry, Kyung Hee University, Suwon, Yongin-si, South Korea*
Mara Aleksić, *Faculty of Pharmacy, University of Belgrade, Serbia*
Ahmet Alim, *Public Health Laboratory, Sivas Directorate of Health, Sivas, Turkey*
Ivana Aljančić, *Institute of Chemistry, Technology and Metallurgy, University of Belgrade, Serbia*
Mohammad Amir, *Faculty of Pharmacy, Hamdard University, New Delhi , India*
Aldo Andreani, *Dipartimento di Scienze Farmaceutiche, Università di Bologna, Bologna Italy*
Deana Andrić, *Faculty of Chemistry, University of Belgrade, Serbia*
Katarina Anđelkovič, *Faculty of Chemistry, University of Belgrade, Serbia*
Goran Angelovski, *Max Planck Institute for Biological Cybernetics, Tübingen, Germany*
Mališa Antić, *Faculty of Agriculture, University of Belgrade, Serbia*
Vesna Antić, *Faculty of Agriculture, University of Belgrade, Serbia*
Dušan Antonović, *Faculty of Technology and Metallurgy, University of Belgrade, Serbia*
Farooq Anwar, *University of Agriculture, Faisalabad, Pakistan*
Item J. Atangwho, *Depatment of Biochemistry, University of Calabar, Nigeria*
Amir Azam, *Department of Chemistry, Jamia Millia Islamia, New Delhi, India*
Milka Avramov Ivić, *Institute of Chemistry, Technology and Metallurgy, University of Belgrade, Serbia*
Nada Babovič, *Faculty of Applied Ecology, Belgrade, Serbia*
Petr Babula, *ÚPL - University of Veterinary and Pharmaceutical Sciences, Brno, Czech Republic*
Alessia Bacchi, *Dipartimento di Chimica Generale ed Inorganica, University of Parma, Parma, Italy*
Goran Bačić, *Faculty of Physical Chemistry, University of Belgrade, Serbia*

Veronica S. Chedea, *University of Agricultural Sciences and Veterinary Medicine, Cluj-Napoca, Romania*
Božidar Cekić, *Vinča Institute of Nuclear Sciences, Belgrade, Serbia*
Veronica S. Chedea, *University of Agricultural Sciences and Veterinary Medicine, Cluj-Napoca, Romania*
Yuru Chen, *College of Life Science, Nanjing Normal University, Nanjing, China*
Chinpiao Chen, *Department of Chemistry, National Dong Hwa University, Shoufeng, Taiwan, Republic of China*
Fanica Cimpoesu, *Institute of Physical-Chemistry, Bucharest, Romania*
Gianni Ciofani, *Italian Institute of Technology, Smart Materials Lab, Center for Micro-BioRobotic, Pontedera (Pisa), Italy*
Francesco Crea, *Dipartimento di Chimica Inorganica, Università di Messina, Messina, Italy*
Janos Csanadi, *Faculty of Sciences, University of Novi Sad, Novi Sad, Serbia*
Janoš Čanadi, *Faculty of Sciences, University of Novi Sad, Novi Sad, Serbia*
Valerija I. Češljević, *Faculty of Sciences, University of Novi Sad, Novi Sad, Serbia*
Željko Čupić, *Institute of Chemistry, Technology and Metallurgy, University of Belgrade, Serbia*
Gordana Ćirić Marjanović, *Faculty of Physical Chemistry, University of Belgrade, Serbia*
Tanja Ćirković Veličković, *Faculty of Chemistry, University of Belgrade, Serbia*
Aleksandra Daković, *Institute for Technology of Nuclear and other Raw Materials, Belgrade, Serbia*
Ljiljana Damjanović, *Faculty of Physical Chemistry, University of Belgrade, Serbia*
José S. Dambolena, *Instituto Multidisciplinario de Biología Vegetal (CONICET-UNC), Córdoba, Argentina*
Inês da Silva, *Technical University of Denmark, Lyngby, Denmark*
Andrés de Blas, *Facultad de Ciencias, Universidade da Coruna, Coruna, Spain*
Henrique Guilhon de Castro, *Universidade Federal do Tocantins, Gurupi-TO, Brasil*
Silvia Dei, *Dipartimento di Scienze Farmaceutiche, Università di Firenze, Sesto Fiorentino (FI), Italy*
Aleksandar Dekanski, *Institute of Chemistry, Technology and Metallurgy, University of Belgrade, Serbia*
Dragana Dekanski, *Biomedical Research, R&D Institute, Galenika a.d., Belgrade, Serbia*
Thereza Christina Monteiro De Lima, *Department of Pharmacology, Center of Biological Science (CCB), Universidade Federal de Santa Catarina, Brazil*
Ahmet Demirbas, *Department of Chemistry, Karadeniz Technical University, Trabzon, Turkey*
Brás Heleno de Oliveira, *Universidade Federal do Paraná, Parana, Brazil*
Sergio Paulo Severo de Souza Diniz, *Department of Biochemistry, University of Maringa, Parana, Brazil*
Concetta De Stefano, *Dipartimento di Chimica Inorganica,Università di Messina, Messina (Vill. S. Agata), Italy*
Radovan Dimitrijević, *Faculty of Mining and Geology, University of Belgrade, Serbia*
Benoit Divol, *Institute for Wine Biotechnology, Stellenbosch University, Matieland, South Africa*

Deepak Ganjewala, *Amity Institute of Biotechnology, Noida, India*
Ali Gargouri, *Laboratoire de Génétique Moléculaire des Eucaryotes, Centre de Biotechnologie de Sfax, Sfax, Tunisia*
Renata Gašparová, *University of Ss. Cyril and Methodius in Trnava, Trnava, Slovakia*
Katya Georgieva, *M. Popov Institute of Plant Physiology, Bulgarian Academy of Sciences, Sofia, Bulgaria*
Athina Geronikaki, S*chool of Pharmacy, University of Thessaloniki, Thessaloniki, Greece*
Charansingh Gill, *Dr. Babasaheb Ambedkar Marathwada University, Aurangabad, Maharashtra, India*
Shanmugam Girija, *Department Of Biotechnology, Bharathiar University, Coimbatore, Tamil Nadu, India*
Dejan Gođevac, *Institute of Chemistry, Technology and Metallurgy, University of Belgrade, Serbia*
Gordana Gojgić-Cvijović, *Institute of Chemistry, Technology and Metallurgy, University of Belgrade, Serbia*
Sandra Cristina Gonçalves Gouveia, *Centro de Química da Madeira, Universidade da Madeira, Portugal*
Malgorzata Grabarczyk, *Faculty of Chemistry, Maria Curie-Sklodowska University, Lublin, Poland*
Branimir Grgur, *Faculty of Technology and Metallurgy, University of Belgrade, Serbia*
Sanja Grgurić-Šipka, *Faculty of Chemistry, University of Belgrade, Serbia*
Laurence Grimaud, *Laboratoire Chimie et Procédés,Ecole Nationale Supérieure de Techniques Avancées, Paris, France*
Dragoljub Grubišić, *Institute for Biological Research Siniša Stanković, University of Belgrade, Beograd*
žAlisa Gruden-Movsesijan, *Institute for the Application of Nuclear Energy - INEP, Beograd-Zemun, Serbia*
Ivan Gržetić, *Faculty of Chemistry, University of Belgrade, Serbia*
Ivan Gutman, *Department of Chemistry, Faculty of Science, University of Kragujevac, Serbia*
Valeria Guzsvany, *Department of Chemistry, Biochemistry and Environmental Protection, Faculty of Sciences, University of Novi Sad, Serbia*
Béla Gyurcsik, *Department of Inorganic and Analytical Chemistry, University of Szeged, Szeged, Hungary*
Milica Gvozdenović, *Faculty of Technology and Metallurgy, University of Belgrade, Serbia*
Abraha Habtemariam, *Department of Chemistry, University of Warwick, Coventry, U.K.*
Sajjad Haider, *Department of Chemical Engineering, College of Engineering, King Saud University, Riyadh, Saudi Arabia*
Reza Hajian, *College of Science, Islamic Azad University Branch of Gachsaran, Gachsaran, Iran*
Hans-Jürgen Hamann, *Institut für Chemie, Humboldt-Universität zu Berlin, Berlin, Germany*
Bingfang He, *College of Biotechnology and Pharmaceutical Engineering, Nanjing University of Technology, Nanjing, China*

Emiko Kaneko, *Tohoku University, Japan*
Ivanka Karadžić, *Department of Chemistry, School of Medicine, University of Belgrade, Serbia*
Ioannis Karapanagiotis, *Ormylia Art Diagnosis Center, Sacred Convent of the Annunciation, Ormylia, Greece*
Fikret Karcı, *Pamukkale University, Faculty of Science and Arts, Denizli, Turkey*
Fatma Karipcin, *Science and Arts Faculty, Süleyman Demirel University, Isparta-Turkey*
Petr Kaspar, *CTU FEE, Technical University, Praha, Czech Republic*
Arvind M. Kayastha, *School of Biotechnology, Banaras Hindu University, Varanasi, India*
Alan Kelly, *Graduate Studies and School of Food and Nutritional Sciences, University College Cork, Cork, Ireland*
Shane Kendell, *School of Science and Technology, University of New England, Armidale, Australia*
Hanan Mohammed Khairy Moustafa, *National Institute of Oceanography and Fisheries, Alexandria, Egypt*
Nadeem Khan, *Department of Diagnostic Radiology, Dartmouth Medical School, Hanover, USA*
Mirjana Kijevčanin, *Faculty of Technology and Metallurgy, University of Belgrade, Serbia*
Edward Cameron Kirby, *Resource Use Institute, Kinglassie, Fife, Scotland*
Goran Klobučar, *Department of Zoology, Faculty of Science, University of Zagreb, Croatia*
Koffi Koba, *Ecole Supérieure d'Agronomie, Université de Lomé, Lomé, Togo*
Ljljana Kolar Anić, *Faculty of Physical Chemistry, University of Belgrade, Serbia*
Ulrich Kortz, *School of Engineering and Science, International UniVersity Bremen, Bremen, Germany*
Velizar Kostadinov Gochev, *Biological Faculty, "Paisii Hilendarski" University of Plovdiv, Plovdiv, Bulgaria*
Nenad M. Kostić, *Chemistry Department, Texas A & M University-Commerce, Texas, USA*
Aleksandar Kremenović, *Faculty of Mining and Geology, University of Belgrade, Serbia*
Antoniana U. Krettli, *Centro de Pesquisas René Rachou, Fiocruz & Universidade Federal de Minas Gerais (UFMG), Belo Horizonte, Brazil*
Svjetlana Krištafor, *Department of Organic Chemistry, Faculty of Chemical Engineering and Technology, University of Zagreb, Croatia*
Nedeljko Krstajić, *Faculty of Technology and Metallurgy, University of Belgrade, Serbia*
Turibio Kuiate Tabopda, *Faculté de Pharmacie, Université de Bourgogne, Dijon Cedex, France*
Zeynel Kılıç, *Department of Chemistry, Ankara University, Ankara, Turkey*
Vesna Kuntić, *Faculty of Pharmacy, University of Belgrade, Serbia*
Marc Lamshöft, *Institute of Environmental Research (INFU) of the Faculty of Chemistry, TU Dortmund, Germany*
Eduardo A. Castro, *Facultad de Ciencias Exactas de la Universidad Nacional de La Plata, La Plata, Argentina*
Peter Langer, *Institut für Chemie, Universitat Rostock, Rostock, Germany*

Liping Meng, *Department of Chemistry, University of California, Davis, California, USA*
Slavko Mentus, *Faculty of Physical Chemistry, University of Belgrade, Serbia*
Katalin Mészáros Szécsényi, *Department of Chemistry, Faculty of Sciences, University of Novi Sad, Novi Sad, Serbia*
Anne S Meyer, *Technical University of Denmark, Lyngby, Denmark*
Slawomir Mielcarek, *Faculty of Physics, Adam Mickiewicz University, Poznan, Poland*
Nevena Mihailović, *Institute for the Application of Nuclear Energy - INEP, Beograd-Zemun, Serbia*
Spiro Mihaylov Konstantinov, *Faculty of Pharmacy, Medical University of Sofia, Sofia, Bulgaria*
Dušan Mijin, *Faculty of Technology and Metallurgy, University of Belgrade, Serbia*
Miloš Milčić, *Faculty of Chemistry, University of Belgrade, Serbia*
Šćepan Miljanić, *Faculty of Physical Chemistry, University of Belgrade, Serbia*
Nenad Milosavić, *Institute of Chemistry, Technology and Metallurgy, University of Belgrade, Serbia*
Slobodan Milosavljevicć, *Faculty of Chemistry, University of Belgrade, Serbia*
Neda Mimica-Dukić, *Faculty of Sciences, University of Novi Sad, Serbia*
Ubavka Mioč, *Faculty of Physical Chemistry, University of Belgrade, Serbia*
Valentin Mirčeski, *Institute of Chemistry, UKIM, Skopje, R. Macedonia*
Tsutomu Miyasaka, *Toin University of Yokohama, Yokohama, Japan*
Kristina Mladenovska, *Institute of Pharmaceutical Technology, Faculty of Pharmacy, Skopje, Macedonia*
Mosaad S. Mohamed, *Faculty of Pharmacy, Helwan University, Helwan, Egypt*
Vesna Mrvić, *Institute of Soil Science, Belgrade, Serbia*
Mahmoud Nasrollahzadeh, *Laboratory of Organic Chemistry, Moshashimi Company, Babol, Iran*
Olgica Nedić, *Institute for the Application of Nuclear Energy - INEP, Beograd-Zemun, Serbia*
Éva Németh-Zámbori, *Corvinus University of Budapest, Department of Medicinal and Aromatic Plants, Budapest , Hungary*
Emily D. Niemeyer, *Department of Chemistry and Biochemistry, Southwestern University, Georgetown, USA*
Svetozar Niketić, *Faculty of Chemistry, University of Belgrade, Serbia*
Aleksandra Nikolić, *Institute of Chemistry, Technology and Metallurgy, University of Belgrade, Serbia*
Branislav Nikolić, *Serbian Chemical Society, Belgrade, Serbia*
Li Niu, *Changchun Institute of Applied Chemistry, Chinese Academy of Sciences, Changchun, China*
Jasmina Novaković, *Apotex Inc, Toronto, Canada*
Maciej J. Nowak, *Institute of Physics, Polish Academy of Sciences, Warsaw, Poland*
Maja Obradović, *Institute of Chemistry, Technology and Metallurgy, University of Belgrade, Serbia*
Isiaka A. Ogunwande, *Natural Product Research Unit, Lagos State University, Ojo, Lagos, Nigeria*
Krishan G. Ojha, *Department of Chemistry, M.D.S. University, Ajmer (Raj.), India*

Natalija Polović, *Faculty of Chemistry, University of Belgrade, Serbia*
Angelina Popova, *Department of Physical Chemistry, University of Chemical Technology and Metallurgy, Sofia, Bulgaria*
Mirjana Popsavin, *Department of Chemistry, Faculty of Sciences, University of Novi Sad, Serbia*
Velimir Popsavin, *Department of Chemistry, Biochemistry and Environmental Protection, Faculty of Sciences, University of Novi Sad, Serbia*
Lenuta Profire, *Faculty of Pharmacy, "Gr. T. Popa" Medicine and Pharmacy University, Romania*
Maria Prokopova Geneva, *Acad. M. Popov Institute of Plant Physiology, Bulgarian Academy of Sciences, Bulgaria*
Susana Puntarulo, *Physical Chemistry-PRALIB, University of Buenos Aires-CONICET, Argentina*
Ain Raal, *Department of Pharmacy, University on Tartu, Tartu, Estonia*
Dušanka Radanović, *Institute of Chemistry, Technology and Metallurgy, University of Belgrade, Serbia*
Bojan Radak, *Vinča Institute of Nuclear Sciences, Belgrade, Serbia*
Ivona Radović, *Faculty of Technology and Metallurgy, University of Belgrade, Serbia*
Niko Radulović, *Department of Chemistry, Faculty of Science, University of Niš, Serbia*
Siniša Radulović, *Institute for Oncology and Radiology of Serbia, Belgrade, Serbia*
Velimir Radmilović, *Lawrence Berkeley National Laboratory, University of California, Berkeley, USA*
Raghavachary Raghunathan, *Department of Organic Chemistry, University of Madras, Madras, India*
Karlo Raić, *Faculty of Technology and Metallurgy, University of Belgrade, Serbia*
Pravin Ramchandra Puranik *School of Life Sciences, North Maharashtra University, Jalgaon, MS, India*
Natarajan Raman, *Department of Chemistry, VHNSN College, Virudhunagar, India*
Nevenka Rajić, *Faculty of Technology and Metallurgy, University of Belgrade, Serbia*
Vesna Rakić, *Faculty of Agriculture, University of Belgrade Serbia*
Slavica Ražić, *Faculty of Pharmacy, University of Belgrade, Serbia*
C. Devendranath Reddy, *Department of Chemistry, Sri Venkateswara University, Tirupati, Andhra Pradesh, India*
Daniela Rigano, *Department of Chemistry of Natural Compounds, University Federico II, Napoli, Italy*
Mihailo Ristić,*Institute for Medicinal Plant Research "Dr. Josif Pančić", Belgrade, Serbia*
Goran Roglić, *Faculty of Pharmacy, University of Belgrade, Serbia*
Marin Roje, *Ruđer Bošković Institute, Zagreb, Croatia*
Romeo Romagnoli, *Dipartimento di Scienze Farmaceutiche, Université di Ferrara, Ferrara, Italy*
Josep Ros, *Departament de Química, Universitat Autònoma de Barcelona, Barcelona, Spain*
Tudor Rosu, *University of Bucharest, Chemistry Faculty, Bucharest, Romania*
Sergio Rosselli, *Department of Organic Chemistry, University of Palermo, Palermo, Italy*

Vladimir Šukalović, *Institute of Chemistry, Technology and Metallurgy, University of Belgrade, Serbia*
Manish Tadhani, *Sardar Patel University, Gujarat, India*
Hassan Tajik, *Department of Chemistry, Guilan University, Rasht, Iran*
Hamdi Temel, *Department of Chemistry,, Faculty of Education, Dicle University, Diyarbakir, Turkey*
Vesna Tepavčević, *Department of Pharmacy, Faculty of Medicine, University of Novi Sad, Serbia*
Vele Tešević, *Faculty of Chemistry, University of Belgrade, Serbia*
Živoslav Tešić, *Faculty of Chemistry, University of Belgrade, Serbia*
Demetrius G. Themelis, *Department of Chemistry , Aristotle University of Thessaloniki, Greece*
Nina Todorović, *Institute of Chemistry, Technology and Metallurgy, University of Belgrade, Serbia*
Vera Todorović, *School of Dentistry, Pančevo, University Business Academy, Novi Sad, Serbia*
Xinli Tong, *Department of Chemistry, Tianjin University, Tianjin, PR China*
Snežana Trifunović, *Faculty of Chemistry, University of Belgrade, Serbia*
Vessela Tsakova, *Institute of Physical Chemistry, Bulgarian Academy of Sciences, Sofia, Bulgaria*
Sachiko Tsukamoto, *Kumamoto University, Kumamoto, Japan*
Srećko Trifunović, *Department of Chemistry, Faculty of Science, University of Kragujevac, Serbia*
Nenad Trinajstić, *Ruđer Bošković Institute, Zagreb, Croatia*
Lemi Turker, *Middle East Technical University, Ankara, Turkey*
Ljerka Tušek-Božić , *Division of Physical Chemistry, Ruđer Bošković Institute, Zagreb, Croatia*
Mustafa Tuzen, *Gaziosmanpasa University, Tokat, Turkey*
Paraskevas Tzanavaras, *Department of Chemistry , Aristotle University of Thessaloniki, Greece*
Aysel Ugur, *Department of Biology, Faculty of Arts and Sciences, Mugla University, Mugla, Turkey*
Gordana Uščumlić, *Faculty of Technology and Metallurgy, University of Belgrade, Serbia*
Suresh B. Waghmode, *Department of Chemistry, Ganeshkhind, University of Pune, India*
Karon Waldron, *Department of Chemistry, University of Montréal, Montréal, Canada*
Dun-Jia Wang, *Department of Chemistry and Environmental Engineering, Hubei Normal University, PR China*
Bradley G. Williams, *Department of Chemistry, University of Johannesburg, South Africa*
Jill K. Winkler-Moser, *USDA/ARS Research Cemist, Functional Foods Research, Peoria, IL, USA*
Dorota Woźniak, *University of Medicine, Department of Biology and Botany, Wrocław, Poland*
Longhou Wu, *Institute of Molecular Medicine, Huaqiao University, China*
Wu Xu, *Pacific Northwest National Laboratory, USA*
Shi Ping Yan, *Nankai University, Nankai , China*

Muhammad Zia-ur-Rehman, *Pakistan Council of Scientific & Industrial Research Laboratories Complex, Lahore, Pakistan.*
Jiri Zima, *Department of Analytical Chemistry, UNESCO Laboratory of Enviromental Electrochemistry, Charles University in Prague, Czech Republic*
Mario Zlatović, *Faculty of Chemistry, University of Belgrade, Serbia*
Liu Zuliang, *School of Chemical Engineering, Nanjing University of Science & Technology, Nanjing, China*
Branka Žarković, *Faculty of Agriculture, University of Belgrade, Serbia*
Emila Živković, *Faculty of Technology and Metallurgy, University of Belgrade, Serbia*
Jelena Živković, *Medical Faculty of Niš, Department of Pharmacy, Niš, Serbia*